Deformation, emplacement and tectonic inferences: the great tonalite sill, southeast Alaska, U.S.A.

Gary M. Ingram

DEFORMATION, EMPLACEMENT AND TECTONIC INFERENCES: THE GREAT TONALITE SILL, SOUTHEAST ALASKA, U.S.A.

by

Gary M. Ingram

A thesis submitted in partial fulfilment of the degree of Doctor of Philosophy at the Department of Geological Sciences, University of Durham,

1992.

To Mum and Dad

COPYRIGHT

ACKNOWLEDGEMENTS

Firstly I would like to thank Donny Hutton for introducing me to the Great Tonalite Sill and making me go to such a wonderful place as southeast Alaska (remember the Marine Bar, Ketchikan?), and for having constant enthusiasm throughout the past three years.

Secondly I thank Dave Brew of the USGS (Alaskan Division) Menlo Park, California, for smoothing the way for the project to take place and for his support during its tenure. The financial support and the use of facilities granted by the USGS in general is gratefully acknowledged.

Thanks to Geoff Meek for being my field assistant and expert boat handler during the 1990 field season. Also thanks to Mark "Spod" Gibbs for assisting me in 1991, especially for the Camp 17 walk-out: "Russian roulette 1991". I am most grateful to Doug Bogden for his companionship and for the use of his monster 350 cubic inch V8 1976 Chevrolet pickup truck during the 1991 season. Thanks to Joe and Dave Grady, Genia Smith, Harold "Nanook of the North" Pilcher, Greg Norman, Mark, Malcolm Goepfert, and the rest of the bunch at the University of Alaska Southeast for their company in 1990 and 1991. Thanks to Jim Wilson and Bruce ("is he the cleaner?") of Coastal Helicopters, Juneau, for delivering us safely to our destinations. Much gratitude goes to Kent Fagerstrom of Nordic Tugs, for supplying the Sea Dory in 1991 and to Dick Emberton for his company and hospitality at the "Annex Hilton" in Taku Inlet, 1990. Thanks to Linc Hollister, Weecha, Jim Drinkwater, Pat Goerlitz, Lonnie Spencer and McKelvey's Bar.

Constant inspiration has been gained from many people in Durham, starting with the oldies: Great-Grandpops Thuggy; Grandpops Chris Jones, Steve Jolley and Ken McCaffrey; Grandma Richard England; Gerald, Dave, Ivan, Chezza, Ian, etc... Special thanks to Mike "women are all mental" Curtis for his constant banter and general Welshness. Thanks to Nilpf and Sally for their help and company over the past 6 years. Cheers to Jipper, Andy, Dunstan, Filth, Mossy, Jane, Tim, Chris, Paul, Jon, John Bole, Parky, Mark, Miles, Zoe.

Special thanks go to Ruth for putting up with me since 1990 and proposing to do so on a long-term basis.

Thanks to Dave Asbery, Carole Blair, Lynne Gilchrist, Karen Atkinson, Dave Schofield, Alan Carr and Gerry Dresser for photos, Ron Lambert and George Randall for thin sections, and George Ruth.

The generous financial support of the Shell International Petroleum Company is gratefully acknowledged. Thanks also to Michelle Martin, Sharon Munro, Rick Preston, Griff Cordey and John McKinnell (of Shell International/Expro). Cheers to the Shell students: Martijn, Jenny, Bastiaan, Dan, Jonathan, Stuart and the rest.

ABSTRACT

The unique late Cretaceous to early Tertiary Great Tonalite Sill (GTS) of SE Alaska and British Columbia is a very long (c.1000km) and thin (<25km), orogen-parallel, composite batholith, which may separate two major superterranes in the western Cordillera: the Insular superterrane (including the Alexander and Wrangellia terranes) from the Intermontane superterrane (including the Stikine and Cache Creek terranes).

The steeply NE dipping, sheet-like plutons of the Great Tonalite Sill are dominated by NW-SE striking concordant fabrics with steep lineations, which formed within a country rock shear zone of similar dimensions - the Great Tonalite Sill shear zone - prior to the complete crystallization of the calc-alkaline tonalitic magmas. The steep, multiple dyke like nature of this composite body and its emplacement during orogenic contraction, imply that ascent and emplacement have been achieved by dyke wedging mechanisms along the deep reaching, probably crustal scale, shear zone. The remarkable narrowness and yet persistence of the Great Tonalite Sill, is probably the result of petrogenesis associated with a very localised zone of crustal thickening, produced by the associated narrow shear zone extending along the orogen length.

Deformation in the Great Tonalite Sill shear zone is dominated by NE-SW directed contraction orthogonal to the orogenic strike associated with a component of NE over SW high angle shear. Such a shear zone of late Cretaceous to early Tertiary age, lying along 800 km of the boundary between the Insular and Intermontane superterranes, strongly implies that it represents the actual boundary between them. That being the case, then terrane accretion during this interval was orthogonal and not obliquely dextral as in some current interpretations of paleomagnetic data. NE side up tilting of mid Cretaceous plutons may therefore be responsible for much of the anomalous palaeomagnetic data determined for these intrusions.

"The thing is, helicopters are different from planes. An airplane by its nature wants to fly, and if not interfered with too strongly by unusual events or by a deliberately incompetent pilot, it will fly. A helicopter does not want to fly. It is maintained in the air by a variety of forces and controls working in opposition to each other, and if there is any disturbance in this delicate balance the helicopter stops flying, immediately and disastrously. There is no such thing as a gliding helicopter."

Commentary: Harry Reasoner, February 16, 1971.

"Geology departments are like helicopters."

Gary M. Ingram, 25 November 1992.

FOREWORD

The fieldwork described in this thesis was carried out on foot, but many locations were inaccessible and demanded boat and helicopter support. In the Juneau area, the work was carried out mainly on foot, but inaccessible ridge sections were reached by helicopter and the detailed Taku Inlet section, the author worked from a small skiff which could be beached. The fieldwork between Port Snettisham and Walker Cove was carried out using a 22' Sea Dory cabin cruiser and landings were facilitated by means of a 5' dinghy. This latter sea borne study lasted four weeks. The total time spent in the field over two successive field seasons was five months.

CONTENTS

CHAPTER 1

GRANITOID ASCENT, EMPLACEMENT, DEFORMATION AND ANALYSIS

1.1 Introduction

A relationship has been established between zones of tectonic activity and the occurrence of granitic rocks. In nearly all plate tectonic environments, granitic rock may be found, but the vast majority is located in orogenic regions, specifically subduction-related, orogenic continental margins and continent-continent orogenic belts. In addition, large inter-continental transcurrent shear zones have been shown to localise granitoids (Reavy 1989, Sylvester 1988, Hutton & Reavy 1992). Granitic magma may occur in other settings such as ocean basins and island arcs, but the greatest volume is produced in areas underlain by continental crust. In essence, granites and associated rocks are formed in large volumes whenever continental crust is heated by rising hot mantle or thickened by collision processes (Fyfe 1988).

Collision. In the subduction-related western Cordilleras of North and South America, prolonged periods of granite magmatism, giving rise to great batholiths, have taken place throughout the Mesozoic and Cainozoic. Examples of these vast batholiths are the Coast Plutonic Complex of Alaska and British Columbia (Roddick 1974), the Peninsular Ranges Batholith of Baja California (Silver & Chappell 1988) and the Coastal Batholith of Peru (Pitcher 1978), which are related to the subduction of oceanic crust under a continental margin. Tonalite and granodiorite are the most abundant rocks in these batholiths, which commonly contain mafic enclaves and carry a chemical component with a mantle signature. The much more leucocratic Himalayan

granites, which are related to continent-continent collision, plot within the true graite field and contain a sedimentary chemical signature (France-lanard & LeFort 1988). These examples indicate that the prevailing plate tectonic regime may have an influence on the source and chemistry of the granitic rocks produced.

Emplacement. The emplacement of granitoids was a problem tackled in the 'Granite Series': an hypothesis in which Read (1957) and Buddington (1959) related the emplacement style of granitoid batholiths to the crustal level into which they were emplaced. In this approach, the Cordilleran batholiths, termed 'magmatic intrusive' or 'epizonal', were interpreted to have formed at relatively high levels in the crust. At low levels in the crust, 'autochthonous' or 'catazonal' plutons, typical of migmatitic belts of granite with sedimentary affinities, were proposed to have formed. Covering the ground inbetween these two types were the 'parautochthonous' or 'mesozonal' granitoid plutons, which formed at intermediate depths. However, work by Pitcher & Berger (1972) on the Donegal Batholith, Ireland, indicated that all the emplacement styles included in the Granite Series were present at the same crustal level. Furthermore, Pitcher (1978, 1979) considered that the granite type and the emplacement style could be related to the tectonic regime dominant during its emplacement. This threw into disarray the Granite Series theory and opened the way for a new, tectonics-based approach, which was explored by Hutton (1982) in the Main Donegal Granite, NW Ireland. He concluded that the emplacement of the pluton was syntectonic and had been accommodated along a sinistral shear zone. Furthermore, Hutton (1988a) suggested that "in general, space for magma can be created by the combination of tectonically-created cavities and internal magma related buoyancy". Further developments indicated that granitic plutons may be emplaced into tectonic regimes dominated by the following end-members: transcurrent shear, extensional shear and reverse (contractional) shear (e.g. Hutton 1988b, McCaffrey 1989, Hutton et al. 1990, Hutton 1992, Hutton & Ingram 1992, McCaffrey 1992, Hutton & Reavy 1992). On the other hand, if rising magma is not affected by tectonic

forces and is allowed to rise diapirically due to its own internal buoyancy, the resulting plutons may emplace as simple balloons (Marsh 1982, Mahon et al. 1988, Courrioux 1987, Cruden 1990, England 1990, England 1992). It follows that the emplacement of granitic plutons may be controlled by combinations of the tectonic end-members and the internal buoyancy forces associated with the rising pluton. It is the combination of all these factors which dictates the form of a particular pluton at emplacement level.

Petrogenesis. Work by Chappell & White (1974, 1984), White & Chappell (1988) and Chappell & Stephens (1988) on the Caledonian granites of the Lachlan Fold Belt, southeast Australia, shed light on the problem of source rocks for the genesis of granitic melts. They indicated that there were two contrasting types of granites: S-type granite, that is granites with properties which show that they were derived from a sedimentary source; I-type granites, that is granites derived from a purely or dominantly igneous source. Subduction-related, Cordilleran I-type granitoids are interpreted to have formed from the partial melting of basaltic to andesitic source rocks and continental collision-related S-type granitoids, e.g. the Himalayan Leucogranites, from the partial anatexis of metasedimentary gneisses (Chappell & Stephens 1988, France-Lanord & Le Fort 1988, Fyfe 1988, Silver & Chappell 1988). The next question which must be answered is: how does the concentration and ascent of such melts from the source rock to the final emplacement level take place? Inferences can be made from the field study of exposed deep crustal granites and by the use of physical models. It is becoming clear that granitic magma petrogenesis, ascent and emplacement are all related to tectonic activity affecting the continental lithosphere (Karlstrom 1989, McCaffrey 1989, Patterson 1989, Reavy 1989, Hutton & Reavy 1992).

Fundamentally, the following work seeks to reveal the ascent and emplacement mechanisms, plus aspects of the petrogenesis, of a tonalitic, Cordilleran batholith and to relate this to the plate tectonic regime prevalent during its emplacement. The

methods employed are dominantly field-orientated. They embrace detailed field observation of the geometry of structures and emplacement features, which formed during emplacement and crystallization of granitic magma and are now recorded in the many individual plutons composing the batholith. The work has been followed up with microstructural analysis, the application of available experimental data plus mathematical and physical models, in the laboratory.

1.2 Granitoid rheology

Rheology is the science of deformation and flow; the critical study of elasticity, viscosity and plasticity (flow); the relationship between stress strain and strain rate. The rheology of a magma is dependent on several parameters: crystal content, degree of interaction of the crystals, temperature, pressure and the amount and nature of volatiles e.g. water, flourine (Spera 1980). These parameters are all important in governing the relationship between shear stress and strain rate in a magma. Materials in general can exhibit three main properties when exposed to external stresses:

(i) ***Elasticity:*** For an elastic material, the applied stress is proportional to the strain and is described by Hooke's Law:

$$\delta \alpha \varepsilon \qquad [1.1]$$

δ = stress, ε = strain

When the stress is released, the strain is recovered and the material returns to its original shape.

(ii) ***Yield Point:*** At the yield point, a substantial, sudden amount of plastic deformation (flow) takes place under a constant load termed the Yield Stress (δ_O).

(iii) ***Viscous Flow:*** In a liquid exhibiting *Newtonian Flow* (fig. 1.1), the shear stress is directly proportional to the strain rate. The constant of proportionality is the Newtonian viscosity.

$$\tau \alpha \varepsilon' \qquad [1.2]$$

$$\tau = \eta\varepsilon' \qquad [1.3]$$

τ = shear stress, ε' = strain rate, η = viscosity

Certain substances when sheared show little or no tendency to flow until a certain shear stress is reached, when the flow rate increases sharply e.g. modelling clay. This behaviour is termed *Bingham Flow* (fig.1.1). Substances such as modelling clay, blood and paste behave in a *non-Newtonian manner.* They may be modelled as compound liquids or solid particles suspended as a fluid. In suggesting the term "magma", Scrope (1872) stressed its analogy to such compounds.

Silicate melt has been modelled as both a Newtonian fluid, the viscosity of which depends on the viscosity of the melt and on the fraction of suspended solids (Shaw 1965, Arzi 1978), and as a Bingham fluid, having a finite yield strength (e.g. Shaw et al 1968, Shaw 1969, Murase & McBirney 1973, Sparks et al 1977) which is dependent on the melt fraction. Experimental work by Van der Molen & Paterson (1979) suggests that granitic magma exhibits a range of rheological properties during crystallization. Completely molten rock behaves as an ideal Newtonian fluid, the viscosity of which depends on the chemical composition of the melt and on the temperature (e.g. Bottinga & Weill 1972). In the range of high melt fractions in excess of 50%, the magma may exhibit the properties of a Bingham fluid, however, it has not been established if the yield strength is a function of the crystallizing melt or a property of the viscous magma. At low melt fractions, grain to grain interactions become more dominant, until solid-like behaviour is exhibited at a sufficiently low level. The onset of

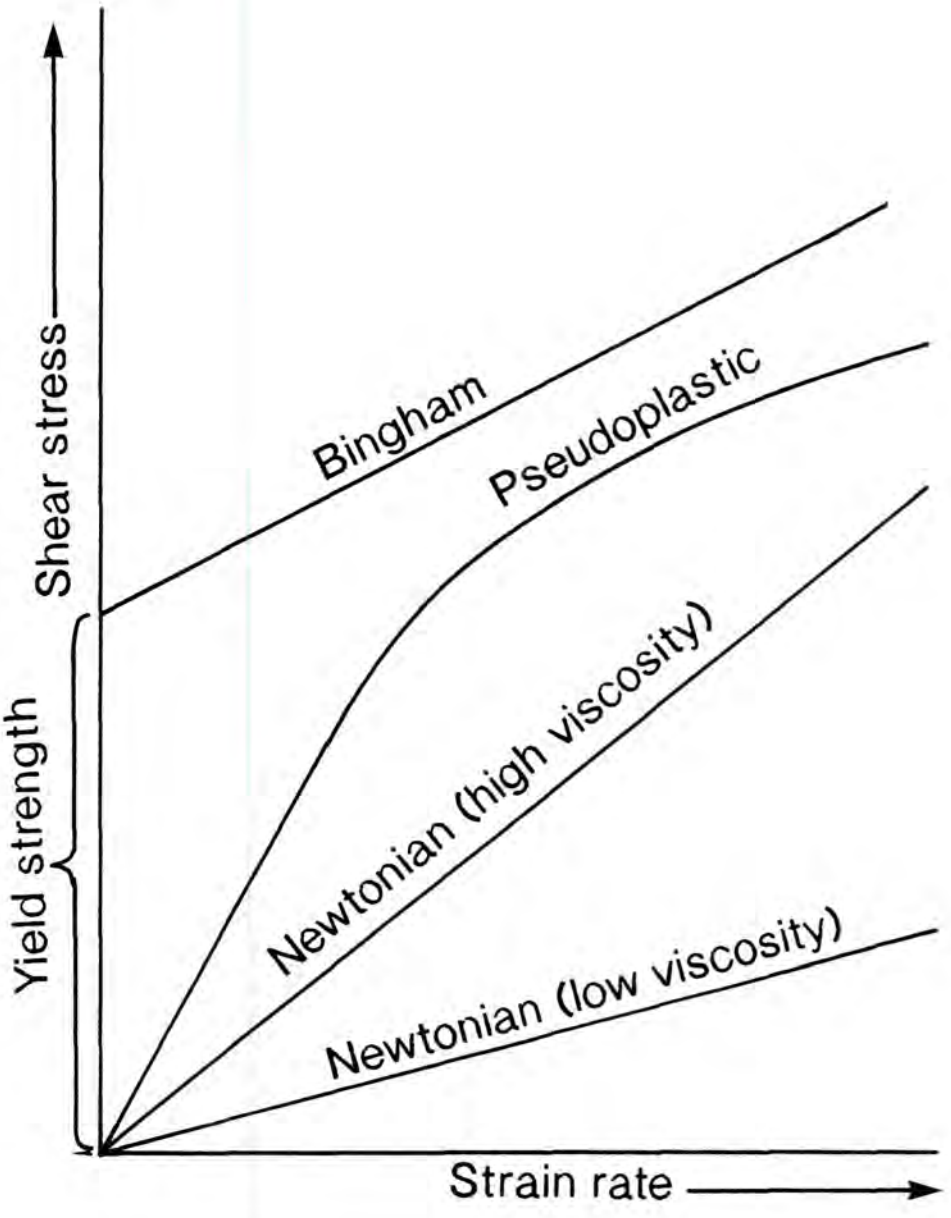

Figure 1.1 Graphs of shear stress versus strain rate for various rheologies.

solid-like behaviour ("lock-up") will occur at a critical melt fraction (CMF) or rheological critical melt percentage (RCMP, Arzi 1978). Values for the critical melt fraction quoted by Arzi (1978) and Van der Molen & Paterson (1979) are 20±10% and 30-35% respectively. The curve of relative velocity versus melt percentage remaining (fig. 1.2, Arzi 1978) illustrates the changes in viscosity for a suspension of rigid spheres in a Newtonian viscous melt, according to Roscoe's formula:

$$\eta_r = (1.35C - 0.35)^{-2.5} \qquad [1.4]$$

η_r = relative viscosity, C = melt percentage

It indicates a critical melt fraction at 26% melt, the value coincident with the minimum porosity for closely packed identical spheres. A distribution of non-equal sizes of spheres or grain sizes will tend to move the curve to the left and hence the critical melt fraction to lower values (Roscoe 1952, Van der Molen & Paterson 1979).

McCaffrey (1989) stresses that experimental work has been carried out only for true granites and not for a range of granitic compositions such as tonalites and granodiorites. However, field studies and modelling indicate that magmas with tonalitic or granodioritic compositions may have viscosities orders of magnitude less than those of true granites (Hutton 1992, this study).

1.3 Structural development in granitoids

The analysis of structures which developed within granitoids and their wall rocks during deformation, is the main method for modelling the tectonic regime prevalent during granitoid emplacement and subsequent crystallization. The implications of rheological models constitute a useful framework, in which granitic structures can be viewed in relation to the crystallization state of the original intrusive magma.

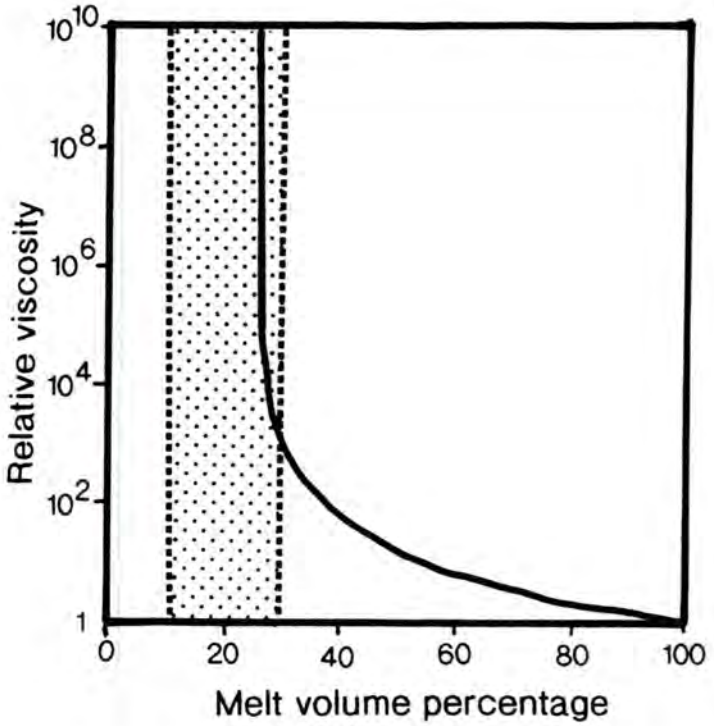

Figure 1.2 Curve showing relative viscosity versus melt percentage for a Newtonian melt according to Roscoe's formula. A rheological critical melt percentage (RCMP) is indicated at 26% (Arzi 1978)

With respect to this study, the following subsections describe the structures with the most important implications for granitoid structural development.

1.3.1 *Pre-full crystallization deformation - the magmatic state*

This type of deformation occurs before all of the phases in a granitic magma have crystallized i.e. when the amount of melt present is well in excess of the critical melt percentage. In such situations, early formed euhedral phases (most commonly feldspar and mafic phenocrysts) and rigid xenoliths rotate into alignment, at right angles to the principal contractional stress, when exposed to a stress field (Gay 1968, Hutton 1988a, fig. 1.3). This alignment, composed of internally undeformed, euhedral phenocrysts, surrounded by internally undeformed late interstitial crystals (typically quartz), is termed a "pre-full crystallization" (PFC, Hutton 1988a) fabric and is to an extent equivalent to the "magmatic state" and "magmatic flow" fabrics of Blumenfeld & Bouchez (1988) and Paterson et al. (1989), respectively. However, the term "PFC fabric" is preferred to the terms "magmatic state" and "magmatic flow" in this thesis.

The absence of internal deformation in quartz is the main criterion in separating a PFC fabric from that which is formed by post-full crystallization deformation, as it is usually the first phase to exhibit signs of strain. However, it must be assumed, when using this criterion, that the quartz has not been recrystallized and that most post-full crystallization deformation takes place at temperatures below the solidus (e.g. McCaffrey 1989).

1.3.2 *Crystallization lock-up deformation - the magma/solid transition*

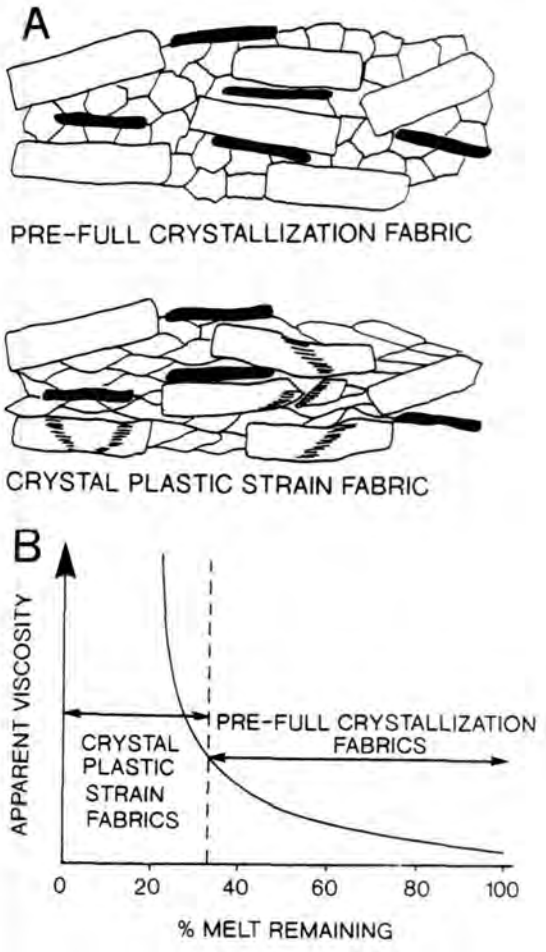

Figure 1.3 Time of deformation relative to crystallization state in granitoids: A. Pre-full crystallization and crystal plastic strain fabrics (rectangular crystals = feldspar, black crystals = hornblende/micas); B. Fabric types in relation to Arzi type diagram.

At lower melt percentages (30-35%), the phenocryst phases will start to interact and initiate the formation of a solid framework, capable of transmitting stress. Qualitative field studies indicate that, before the onset of plastic flow behaviour, strain is partitioned into discrete deformation zones, rather than homogenously transmitted throughout the deforming magma and these discrete zones have been termed "pre-full crystallization lock-up" shears (Hutton & Ingram 1992). If deformation ceases after the formation of these structures, the phenocrysts and matrix will be preserved in an internally undeformed state. Pre-full crystallization (PFC) lock-up shears may therefore mark the transition between the pre- and post-full crystallization states, probably indicating that the granitoids in which they are preserved, contained a melt fraction on or below the critical fraction.

1.3.3 *Crystal plastic deformation - the solid state*

Deformation of a granitoid, at or below the solidus temperature of its constituent mineral phases, will produce strain in those minerals, dominantly by the process of dislocation creep. As mentioned above, variation in temperature and strain may control the the proportions of weak and more resistant fractions (e.g. quartz and feldspar), and the characteristics of the shear structures produced. If there is enough heat in the granitoid system during deformation, homogenous crystal alignment may occur by ductile plastic mechanisms and the aligned crystals will show evidence of internal plastic deformation, especially quartz. The type of fabric produced has been termed a "crystal plastic strain" fabric (Hutton 1988a, fig. 1.3) and "solid state deformation" by Blumenfeld & Bouchez (1988).

The types of shear structures present in a deformed granitoid may act as mechanical and thermal indicators. As the temperature in a granitoid falls and approaches, or corresponds to, the 500°C mechanical interface in wet granites, the bulk strength increases rapidly (Gapais 1989). At the grain scale, this is the point corresponding to the brittle-ductile transition in feldspars and is similar in some ways

to the type of behaviour displayed in magmas as the melt percentage drops towards, or to, the critical melt percentage and a similar increase in bulk strength occurs. At both these points, homogenous strain becomes partitioned into discrete zones of shear. In both examples, the magma or solid can be described as a mixture of weak and more resistant fractions, whose proportions vary with temperature or strain, or both, and which control production of structures during deformation.

1.3.4 *Cloosian structural development in granitoids.*

Hans Cloos' (Balk 1937) classification of granitic structures for many years formed the basic analytical approach for igneous rocks (see also Marre 1986). Two types of structures were thought to occur: (i) *Primary structures.* These were formed in response to "flow" in the crystallizing magma, which aligned the platy crystals, implying the operation of "magmatic currents" moving against the wall rocks, in a manner analogous to water flowing in a stream. Joints were also formed at this time, in response to further elongation of the magma; (ii) *Secondary structures.* These formed in the solid state as metamorphic structures e.g. cross-cutting foliations and boudinage structures.

Berger & Pitcher (1970), Pitcher & Berger (1972) and Hutton (1988a) all critisized this approach, with a common argument that silicate melts do not behave in a manner analogous to flowing water, but as a viscous magma and a deformable material. Hutton (1988a), in particular, opposed the view that the term "deformation" was apparently reserved for the later, metamorphic structures, and not for the primary structures. Öertel (1955), however, had not considered the possibility that a fluid magma could transmit strain. Here is a quotation (translated from German by the British Geological Survey) from his work on the granite at Loch Doon, Scotland:

"The lack of clear linear elements along these [foliation] planes shows that we are dealing with a crystallization formation i.e. the foliation does not result from the [shear] movement itself..."

He went on to state that the granite could not be regarded as a fluid when it was deformed, as fluids were incapable of transmitting shear strain. In other words, the view at the time was that magmatic state/pre-full crystallization fabrics were formed by crystallization processes (e.g. marginal crystallization), not deformation. This is a purely historical note, but it is enlightening nonetheless.

Hutton (1988a) proposed that the Cloosian system be abandoned in favour of a less genetic system, in which the deformation history, modelled in terms of external tectonically-imposed strains combined with internal buoyancy-related strains, is related to the changing rheology of the magma. In addition, Berger & Pitcher (1970) argued that joints were of limited use in relation to tectonic models of granitoids, because later, uplift-related joints could be confused with the "primary" joints of Cloos.

1.4 Strain analysis.

The analysis of strain in deformed granitoids and their wall rocks should ultimately produce, or strive to produce, a three-dimensional representation of the strain ellipsoid for each sample point. The strain ellipsoid, with reference to the terminology of Flinn (1965. fig. 1.4), describes the amounts of relative deformation, along three mutually perpendicular principal axes, of an initially spherical object. The X-axis, the Y-axis and the Z-axis represent the values corresponding to the maximum stretching direction, the intermediate stretching direction and the minimum, or negative, stretching direction, respectively. These values may be related by the equations:

$$X/Y = (Y/Z)^k \qquad [1.5]$$

therefore

$$\mathrm{Log}_{10}(X/Y) = k\ \mathrm{log}_{10}(Y/Z) \qquad [1.6]$$

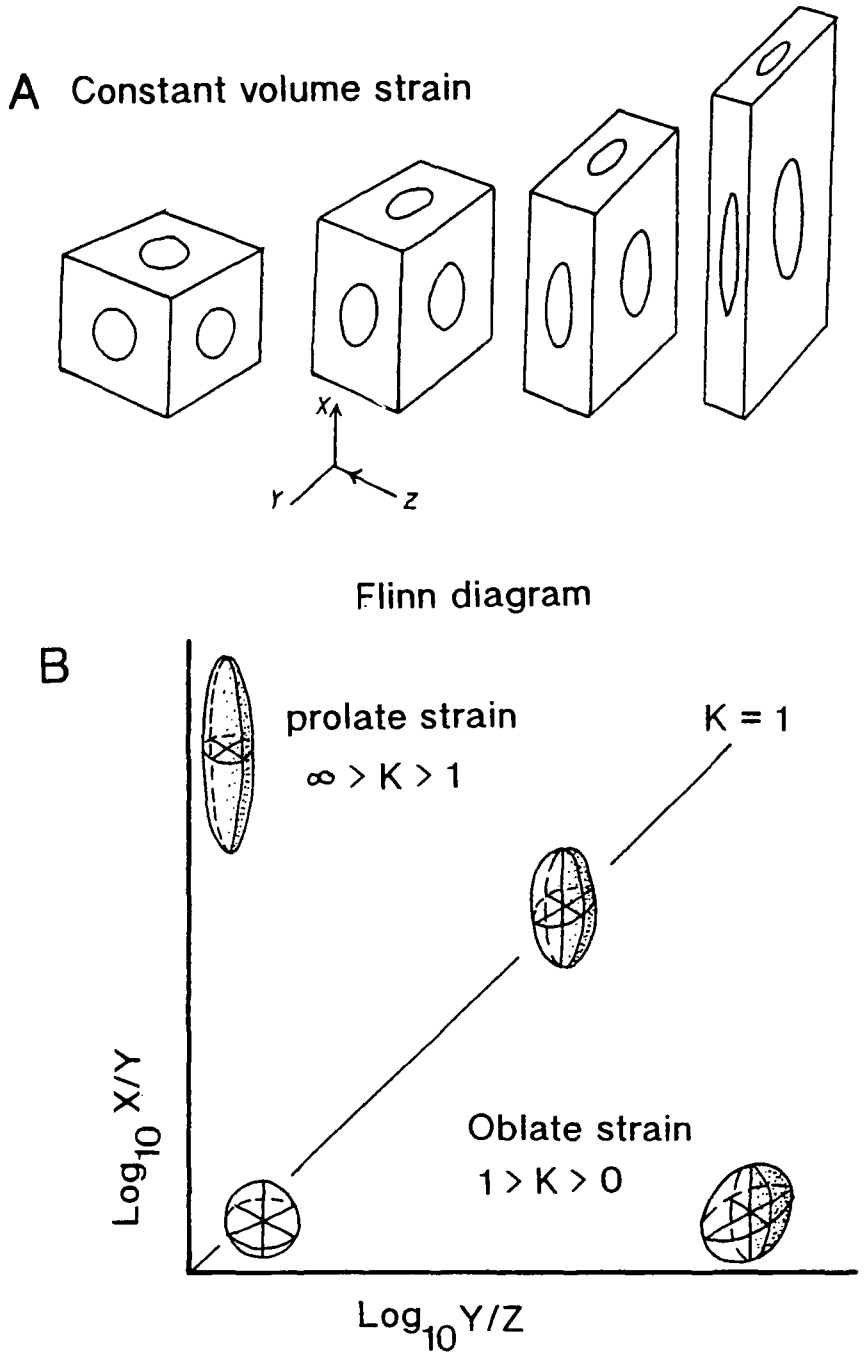

Figure 1.4 Calculation of strain in granitoids: A. This sequence of strain increments shows progressive K = 1 strain (constant volume) in a rock containing initially spherical markers e.g. mafic enclaves. B. Flinn diagram: measurements of initially spherical enclaves can be used to calculate K-values which describe the shape of the strain ellipsoid, as discussed in the text. (modified from Ramsay & Huber 1983).

The k-value describes the shape of the ellipsoid and is represented by the gradient in the graph of $Log_{10}(X/Y)$ versus $Log_{10}(Y/Z)$ (fig. 1.4).

1.4.1 *Methodology*

Quantitative estimates of strain in granitoid rocks may be gained from the analysis of the mean shapes of populations of microgranitoid enclaves (Vernon 1983), which are also known as mafic xenoliths, mafic enclaves or autoliths. These are commonly composed of microdiorite, microgranodiorite and microtonalite (e.g. Sabine 1963). The variation in the mean shapes of such enclave populations, as an estimate of internal strain variations throughout granitoid plutons, has been well documented (Holder 1979, Hutton 1982, Courrioux 1987, Hutton 1988b) and is used extensively in this thesis. Vernon (1983) reviewed much of the literature concerning microgranitoid enclaves and concluded that the existence of the enclaves is best explained by mingling and quenching of globules of more mafic magma in the host granitoid magma. Some mixing may take place in certain circumstances, but mingling is consistent with the characteristic blob-like appearance and microstructure of the enclaves. In addition to the mafic enclaves, lava pillows and pillow breccias are examples of other originally elliptical objects, which can be used to estimate strain in deformed rocks. For the purpose of strain analysis, these enclaves, lava pillows and pillow breccias are assumed to have:

(1) a negligible viscosity contrast with their host rock

(2) an originally spherical, or subspherical shape shape.

Assumptions and errors. In order to interpret the results from the field measurements, it is first of all necessary to make some general assumptions about the strain markers:

(1) the strain markers were originally spherical or had a high sphericity;

(2) the strain markers had a negligible viscosity contrast with their host;

(3) the results obtained from different types of strain markers are directly comparable.

However, it is unlikely that all of the strain markers were originally spherical all of the time and therefore corrections must be applied to assumption (1) to correct for their initial shapes. Lava pillows, for example, are rarely spherical when they are first extruded. They commonly show a subhorizontal elongation, due to gravity spreading and the style of extrusion, when viewed in an undeformed state. However, a further assumption about the three-dimensional shape of lava pillows must be made. In this thesis it is assumed that they are mushroom-shaped (i.e. oblate) when in an undeformed state. This, of course, is an oversimplification as pillows may vary in shape due to variations in initial viscosity and the possibility that they may be interconnected as a series of lava tubes, rather than discrete entities (Cas & Wright 1987). However, careful obsevation in the field, especially at three-dimensional outcrops, can distinguish between the tube type and the types in which the pillows are more discrete bodies.

In addition to these aforementioned considerations, the initial orientation of the long axes of the strain markers, with respect to the interpreted compressional palaeostress direction, is very important. If the long axis is initially parallel to the principal compressional stress direction, the resulting strained shape will be an underestimate of the finite strain ellipsoid. If the long axis is perpendicular to the principal compressional stress direction, the recorded strain will be an overestimate. The palaeohorizontal within pillow lava sequences may be estimated by observing the direction in which the upper pillows drape into the cavities between pillows below. Thus the tongues of the drapes point in the direction of younging, at 90° to the palaeohorizontal.

Statistical analysis may also indicate if groups of strain markers have an initial, preferred shape. Figure 1.5 shows a skewed frequency distribution of the x/z ratios of some deformed mafic enclaves, indicating that the rock contained an initial alignment of non-equidimensional mafic enclaves. The distribution is skewed to the left, towards the lower values, indicating that the initial long axes of the enclaves were orientated

parallel to the principal compressional stress direction, resulting in the production of a few high to very high values and many values at the lower end of the scale. The resulting calculation of strain will therefore be an underestimate of the actual finite strain. Without making corrections for different initial shapes and preferred alignment, for different strain markers, assumption (2) breaks down.

Much of the deformation recorded by deformed mafic enclaves is interpreted to have been incurred in the magmatic state i.e. they have a negligible viscosity contrast with their host. In support of this view, Vernon (1983) cites microstructural evidence for PFC fabrics of plagioclase laths within deformed enclaves, which show no evidence of grain deformation or recrystallization. However, it is likely that the host granitoid magma and the mafic enclaves do not reach the critical melt fraction simultaneously, therefore, due to their more mafic composition, the enclaves probably have a higher viscosity at some point during the crystallization interval of a pluton. This means that assumption (2) is not strictly true and the mean shapes of populations of mafic enclaves probably underestimate slightly the magmatic state deformation.

Quantitative strain calculation. A quantitative estimate of the shape of the strain ellipsoid can be made by measuring the X/Z, Y/Z and, where possible, X/Y ratios of mafic enclaves, lava pillows, pillow breccias and other such strain markers, in the field. These can then be encorporated on a Flinn (1965) plot (fig. 1.4) and the k-value describing the shape of the strain ellipsoid may be calculated. The most commonly exposed surfaces, available for the measurement of strain markers, are those (a) perpendicular to the foliation, but parallel to the lineation (X/Z) and (b) perpendicular to both the foliation and the lineation (Y/Z). On each of these surfaces, during this study, as many measurements of the enclaves' long and short axes, as possible, were measured. The author attempted to record the dimensions of at least 30 -34 enclaves on each surface, in order that the sample would be statistically representative of the population at each locality.

Once the data have been collected, it is important to choose the most accurate method for calculating the mean value of each of the axial ratios, as the initial distribution of values is often skewed. Following Lisle (1977), the mean used in this thesis is the harmonic mean, as it effectively normalises a skewed distribution and gives good estimates of the true mean:

$$\textit{The Harmonic Mean: } H = n / \Sigma(1/R_f) \qquad [1.7]$$

where n = total number of measurments, R_f = final axial ratio of the deformed enclave. The arithmetic mean of these measurements is of little value and will consistently give innaccurate results if the distribution is skewed (fig. 1.6). Where the paucity of mafic enclaves precludes quantitative estimates of strain, one can make qualitative observations based on the intensities of PFC and CPS fabrics relative to those in the areas in which enclaves are abundant (e.g. Hutton 1988b).

1.4.2 *Removing strain from deformed rocks*

It is possible to calculate the original width (W_o) of the strained sheet-like plutons by calculating a conversion factor (F) and applying it to the present, strained width (W_Z), which is parallel to the Z-axis in the strain ellipsoid:

$$W_o = F\, W_Z \qquad [1.8]$$

F may be calculated from the radius of the original unstrained spheroid (A) and the present value of the Z-axis of the strain ellipsoid (Z):

$$F = A/Z \qquad [1.9]$$

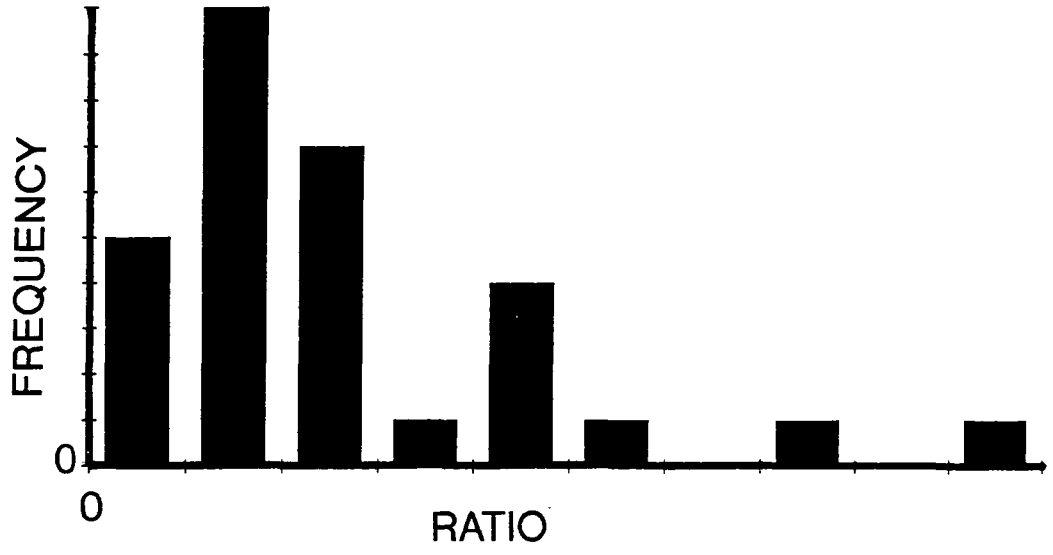

Figure 1.5 Example of a skewed frequency distribution (see text for details).

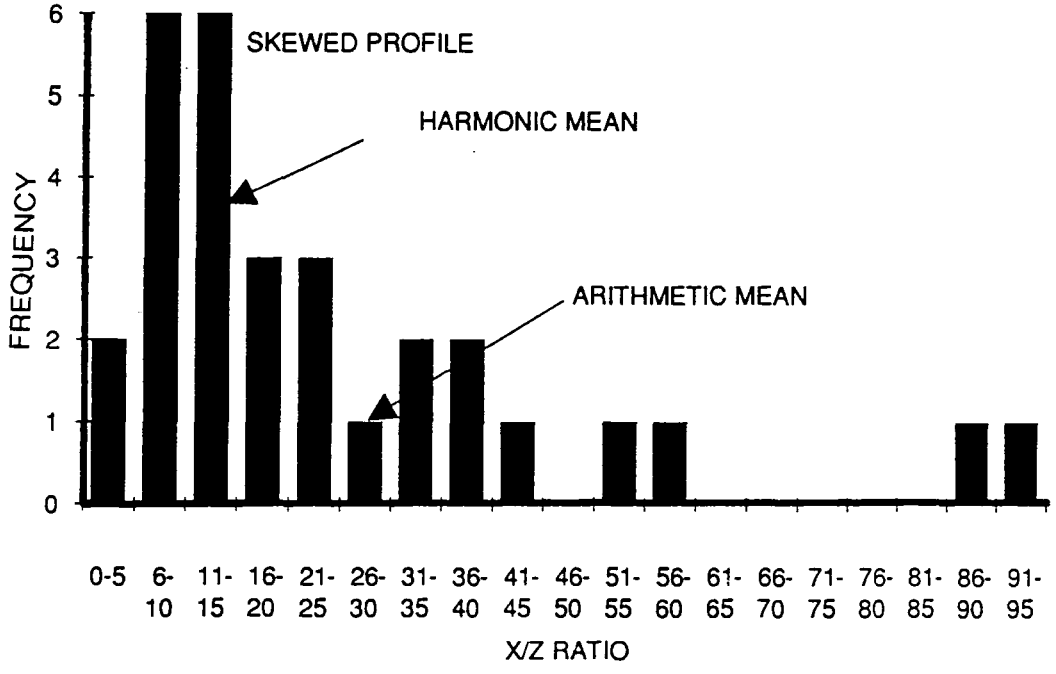

Figure 1.6 Harmonic and arithmetic means in a skewed frequency distribution. An harmonic mean effectively normalises the distribution and gives a "modal" average.

A may be calculated from the relative lengths of the X, Y and Z axes and the K-value of the strain ellipsoid. Using the equation from the Flinn (1965) nomenclature:

$$X/Y = (Y/Z)^K$$

Rearranging: $X = Y\,(Y/Z)^K$ [1.10]

Assuming that volume is conserved during deformation, and A is the radius of the undeformed strain spheroid, the following approximation is true:

$$XYZ = A^3$$

Rearranging: $X = A^3/YZ$ [1.11]

Writing [1.10] and [1.11] as simultaneous equations:

Thus: $X^2 = A^3(Y/Z)^K/Z$

Rearranging: $A^3 = X^2Z/(Y/Z)^K$

Let Z = 1: $A^3 = X^2Y^{-K}$

$$A = (X^2Y^{-K})^{-3}$$ [1.12]

Substitute $Z = 1$ into equation [1.9]:

The conversion factor $F = A$ [1.13]

Therefore: $F = (X^2Y^{-K})^{-3}$ [1.14]

Substitute F into equation [1.8]:

Thus the original width of the pluton, $W_o = (X^2Y^{-K})^{-3}\,W_Z$ [1.14]

1.5 Shear sense.

Simple shear is is an example of non-coaxial deformation, which leads to the development of asymmetries in deformation structures. These asymmetric structures, which usually occur on a mesoscopic or microscopic scale, are termed "shear sense indicators" and, as the term implies, the indicators provide information about the sense of movement, or kinematics, of a particular deformation. In order to determine the sense of shear, the indicators must be viewed in a plane that is parallel to the transport lineation and perpendicular to the foliation with which they are associated. Shear sense indicators can develop in both the magmatic and solid states and there is a number of types which can be used and have been documented in literature.

If a magma contains a melt percentage well in excess of its rheological critical melt percentage (RCMP, Arzi 1978, fig. 1.2) i.e. greater than 45% melt (Blumenfeld & Bouchez 1988), then the free rotation of the constituent phenocrysts is permitted. As has been stated by Hutton (1988), the deformation of such a magma will induce the formation of PFC fabrics or magmatic state fabrics, due to the rotation of the elongate laths into parallelism with the principal strain axis. Sense of shear may be deduced from the relationships of individual rotated grains to one another, or the relative obliqity of fabrics. Blumenfeld & Bouchez (1988) describe shear sense indicators for magmatic state deformation, two of which are used in this thesis (fig. 1.7). (1) The sense of obliquity between the planar foliation, described by the alignment of early formed phenocrysts, and the walls of the deforming shear zone, will provide a sense of shear; (2) The sense of imbrication, or *tiling,* of megacrysts, which have rotated into contact in a viscous matrix, will give the sense of shear. Statistical counting of populations of tiling orientations will demonstrate that the larger population will give the sense of shear.

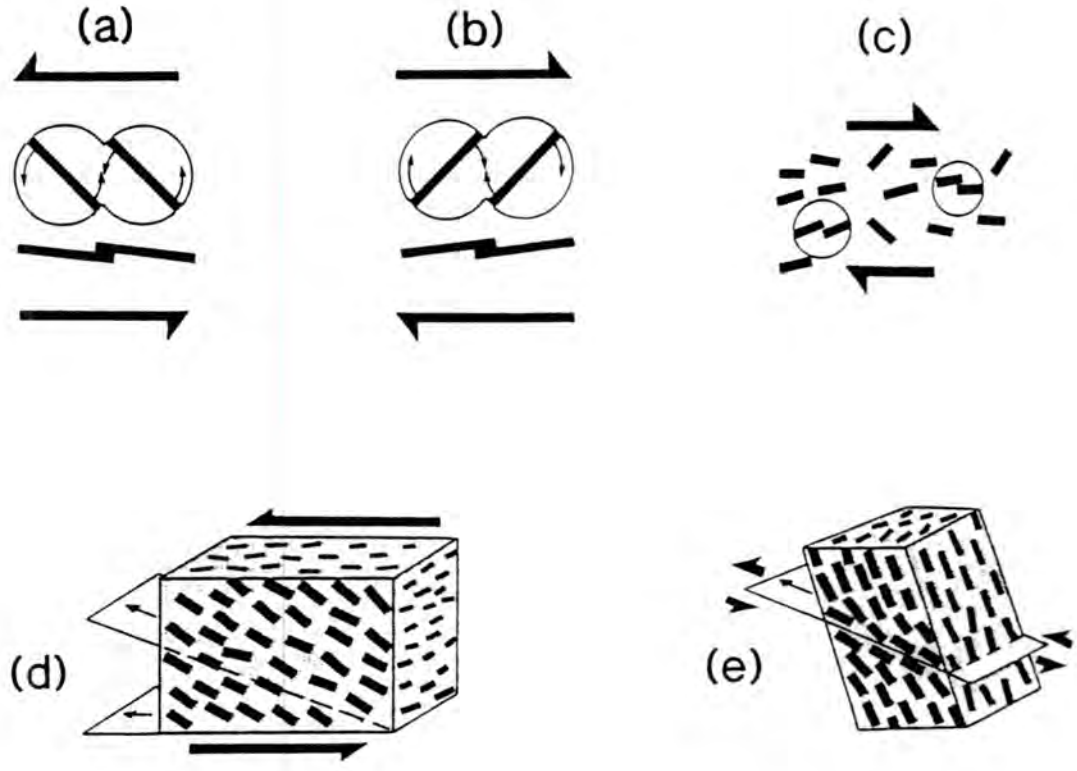

Figure 1.7 Magmatic state/PFC shear sense indicators: a., b. & c. show tiling of early formed phenocrysts, which rotate into into contact in response to simple shear; d. Fabric/wall rock obliquity gives shear top-to-the-left shear sense in this case (a, b, c & d from Blumenfeld & Bouchez 1988); e. Discrete PFC lock-up shear cutting the main fabric shows top-to-the-left shear sense (see also fig 1.8, Ingram & Hutton in prep).

PFC lock-up shears. Shear sense indicators may also develop in the transition period between the fully magmatic (PFC) state and the fully crystallized state. This is the time interval during which "pre-full crystallization lock-up" (PFC lock-up, Ingram & Hutton 1992) takes place i.e. the crystallized phases are increasingly forced into contact as the melt percentage decreases. During this interval, the relative viscosity of the magma increases dramatically (Arzi 1978, van der Molen & Patterson 1979) and strain, instead of dispersing into a more intense homogenous PFC fabric, partitions into discrete zones of shear, termed PFC lock-up shears (Hutton & Ingram 1992). The shear band axes contain internally undeformed laths of (commonly) plagioclase and the sense of shear can be deduced by observing the sense of rotation of the PFC fabric into the shear (fig. 1.8).

Shear sense indicators may also occur in the solid state. These indicators develop in the wall-rocks of plutons during deformation and, if the deformation continues after full crystallization of a pluton, they may develop in the intrusive rocks. The application of shear sense indicators to granitic rocks was initially made by Berthé et al. (1979), who applied the term S-C mylonite in their description of the shear sense indicators in an orthogneiss, in the South Armorican Shear Zone, France. Publications since then have applied these S-C indicators to metamorphic rocks e.g. Lister & Snoke (1984). The 'S' and 'C' terms refer to two sorts of foliation: (1) The 'S', or schistosité, surfaces are related to the accumulation of finite strain parallel to the XY flattening plane and are parallel to the shear zone walls; (2) the 'C', which stands for 'cisaillement' or shear, surfaces are related to localized high shear strains, and these cut through the pre-existing schistosities. The C-planes initiate at about 45° or less from the shear zone walls, with a sense of shear which is synthetic to the overall shear sense in the wall rocks (fig. 1.9).

Simpson & Schmid (1983) cite numerous other shear sense indicators including asymmetric augen, or porphyroclast, structures, which developed in mylonitic gneisses (fig. 1.9). The augen are composed of relatively flow-resistant grains (commonly feldspar) within a ductile and more fine-grained matrix. Other types are asymmetric

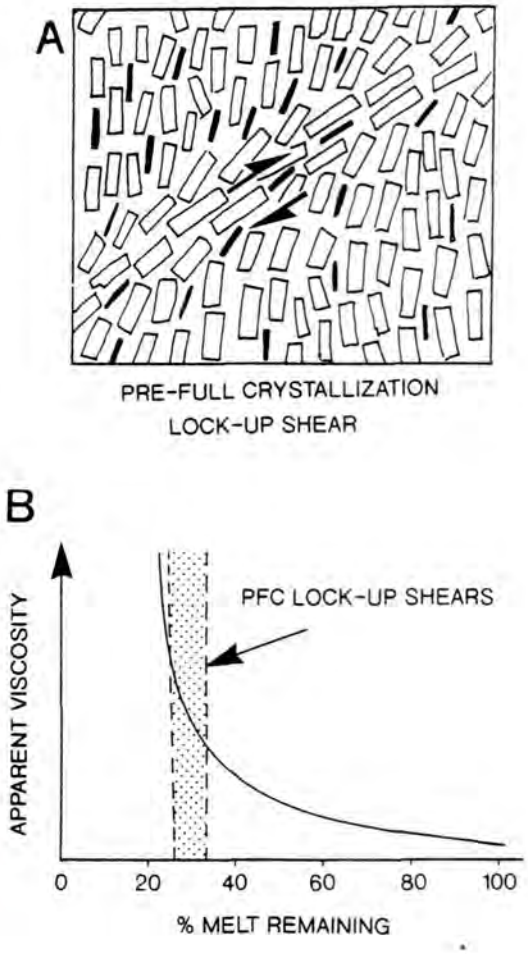

Figure 1.8 Development of pre-full crystallization lock-up shears in relation to crystallization state in granitoids. A. A top-to-the-right PFC lock-up shear in profile. Rectangular crystals are feldspar phenocrysts and thin black crystals are mafics. B. Occurrence of PFC lock-up shears in relation to melt percentage present. Graph is similar to that used by Arzi (1978) and van der Molen & Paterson (1979).

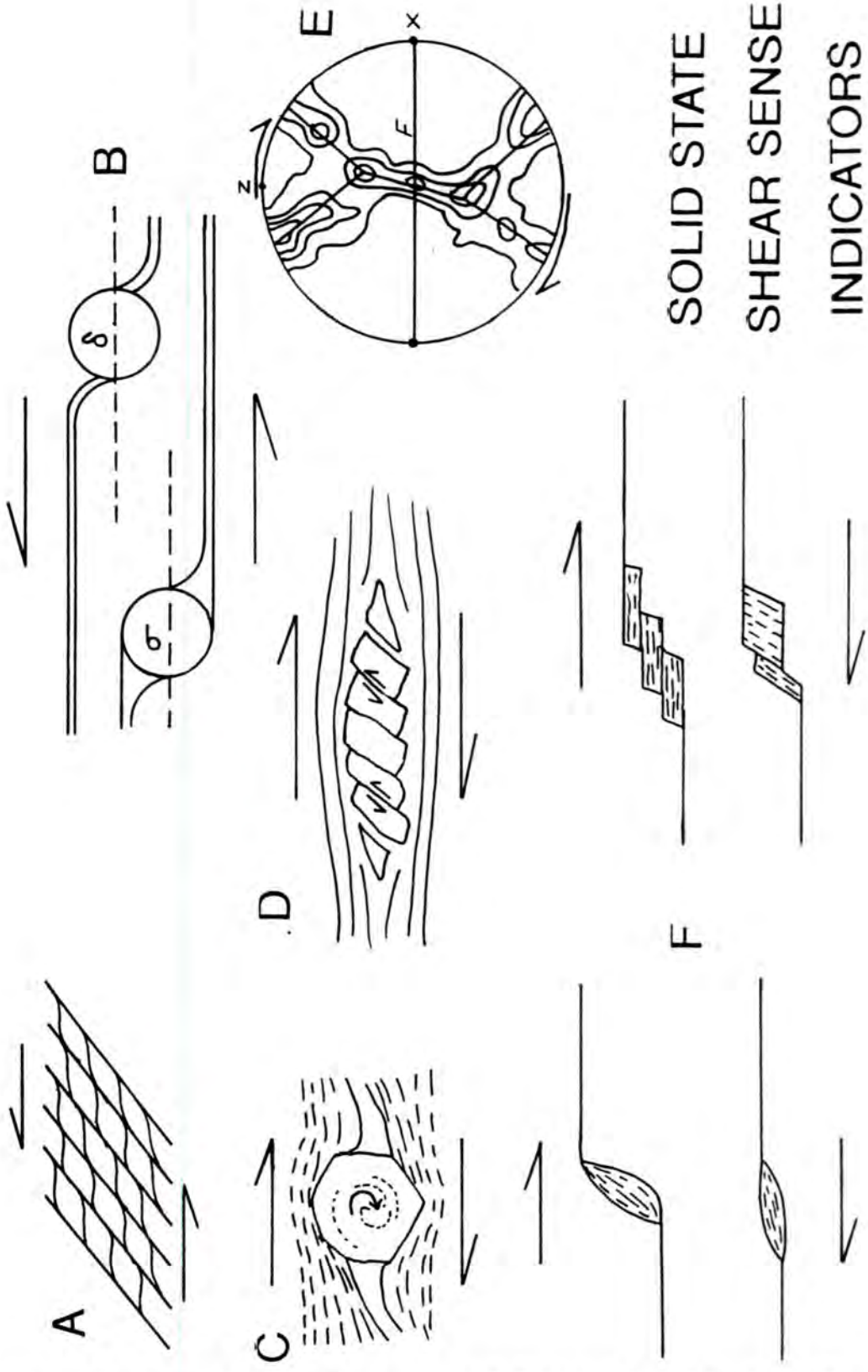

Figure 1.9 Solid state shear sense indicators: A. S-C fabric (Lister & Snoke 1984); B. Sigma and delta porphyroblasts (Passchier & Simpson 1986); C. Rotated garnet porphyroblast and associated pressure shadows (Powell & Vernon 1979); D. Broken and displaced hard grains in a ductile matrix (Simpson & Schmid 1983); E Optically measured C-axis fabric with asymmetric central girdle with respect to the foliation (F) (Behrmann & Platt 1982); F. Examples of mica "fish" (Lister & Snoke 1984).

pressure shadows on porphyroclasts (fig. 1.9), which have a high ductility contrast to their matrix and are themselves rotated with the same sense as the external shear component. Passcier & Simpson (1986) classified the porphyroclast systems into a σ–type porphyroclast system and a δ-type porphyroclast system (fig. 1.9). Porphyroblasts e.g. garnets may contain curved inclusion trails due to the growth of the mineral during shearing. Broken and displaced grains may also be useful shear sense indicators and in the sheared stack of cards model, the sense of slip on the displaced grains will be antithetic to the overall shear sense (fig. 1.9 Etchecopar 1977). Crystallographic fabrics developing along a rotational strain path are asymmetric with respect to foliation and stretching lineation, and evidence for such asymmetries reflects the sense of shear (e.g. Lister & Hobbs 1980). Mica "fish" (Lister & Snoke 1984) in S-C mylonites also produce shear sense information, and occur where pre-existing large white mica grains are boudinaged by a combination of brittle and crystal-plastc processes (fig. 1.9).

White et al. (1986) summarize many of the shear sense indicators in common use in the following list. Rotation of: (1) a pre-existing or generated foliation, (2) deformed markers, (3) fragments owing to shear fractures, (4) fragments owing to tensile fractures; Asymmetry of: (5) intrafolial folds, (6) trails growing around rotating clasts, (7) trails growing around non-rotating clasts, (8) elongate recrystallized quartz grains, (9) dragged-out mica porphyroblasts, (10) quartz c-axis fabrics; (11) microshears or shear bands; (12) shear bands or S-bands; (13) sheared porphyroblasts.

It is important to build up a consistent data base when making shear sense interpretations. McCaffrey (1989) stressed that shear sense indicators should not be used in isolation due to the presence of zones of antithetic shear, which are common in deformed terrains. Consistent shear sense data collected in the field is the best evidence on which to base kinematic interpretations, and microstructural evidence should not be used without comparison with this.

1.6 Emplacement and ascent mechanisms

1.6.1 *Forceful ascent and emplacement*

Granite diapirism has long been recognised as a magma ascent mechanism. It is largely driven by buoyancy and the rising diapirs' capacity to reduce the viscosity of, and push aside, their wall rocks. The final emplacement mechanism of magma, resulting from diapiric uprise, is often regarded as the ballooning diapir. Such plutons may be recognised by (i) sub-circular pluton shapes; (ii) well-developed concentric internal foliations; (iii) concentric folding of country rocks near the contact; (iv) horizontal lineations associated with, and tangential to, the crestal regions of the body; (v) strong oblate strains at the margin (vi) steep lineations and prolate strains associated with the diapir tail; (vii) vertical uplift of country rocks in excess of the vertical thickness of the pluton (Marsh 1982, Courrioux 1987, Mahon et al. 1988, Cruden 1990, England 1990, England 1992). Examples include the Northern Arran Granite (England 1992) and Ardara, Donegal (Pitcher & Berger 1972).

However, as stated by Marsh (1982), unless the diapiric bodies are unusually large (radius > 10km), they will solidify at depth without a great deal of penetration through the crust. Repeated ascent along the same path is necessary for successful ascent by diapirism.

1.6.2 *Passive emplacement*

During passive emplacement, mechanisms take place in order that space may be created, into which magma may be emplaced. Stoping of large blocks of crustal rocks, during the uprise of magma, creates space, and this was the mechanism favoured by Daly (1933) to account for many of the large plutons in the Sierra Nevada. Pitcher & Berger (1972) and Pitcher (1978,1979) also cited examples of stoped plutons in

Donegal (e.g. Fanad and Thorr plutons). The formation of ring dykes by cauldron subsidence is an example of passive emplacement, in which a central plug of crust collapses, allowing magma to flood into the sub-circular fracture array thus formed (e.g. Clough et al. 1909)

1.6.3 *Emplacement and tectonics*

Among the first workers to investigate the relationship between granite emplacement and tectonics were Pitcher & Read (1960) and Pitcher & Berger (1972). Their work on the Donegal plutons, especially the Main Donegal Granite, established that the deformation in the aureole rocks was broadly coeval with emplacement of the plutons. Uncertainties about the exact relationship between certain late, tectonic folds and cleavages, trending parallel to the margins of the Main Donegal Granite, and the emplacement mechanism, was investigated by Hutton (1977). He established a chronological sequence of seven deformation phases in the aureole, D1 - D7, of which D4 is broadly coeval with the emplacement of the Main Donegal Granite. By applying the structural techniques previously discussed, Hutton (1982) was able to demonstrate that emplacement and deformation were more or less synchronous. Other studies (e.g. Hanmer 1981, Hutton 1988a, 1988b, Hutton et al. 1990, McCaffrey 1989, 1992, Reavy 1989), indicate that granites may be related to, or controlled by, deformational features such as active major faults and shear zones. These synkinematic plutons may be recognised by (i) elongate shapes whose long axes coincide with linear belts of deformation and metamorphism (shear zones); (ii) PFC and CPS fabrics and lineations which are parallel to and continuous with fabrics the shear zone; (iii) PFC fabrics in the pluton which exist alongside CPS fabrics in the wall rocks and indicate a drop in the crystal plastic strain magnitude between wall rocks and pluton; (iv) the synkinematic growth of metamorphic minerals in the wall rocks; (v) the presence of structures indicative of deformation close to the Critical Melt Fraction (van der Molen and Paterson 1979) i.e. before full crystallization; (vi) small scale structures which

developed at similar times to emplacement (e.g. melt-filled shears) (e.g. Pitcher & Russell 1977, Leake 1978, Hutton 1982, Hollister & Crawford 1986, Reavy 1989, Hutton et al. 1990, McCaffrey 1992, this study).

With this framework, it is possible to separate tectonics-related from buoyancy-related emplacement deformation. This ability to distinguish between the two is extremely important, as the kinematics of deformational events, which have controlled the emplacement of plutons, may be accurately dated using their published crystallization ages.

1.6.4. *Comment on ascent mechanisms*

As mentioned previously, granitoid magma may ascend through the crust in the form of diapirs. These are interpreted to ascend due to their internal buoyancy and ability to thermally soften and push aside the country rock through which they are travelling. As mentioned by Hutton (1988a) they may interact with extensional or transcurrent fault systems, which reach to varying levels in the lithosphere. The final arrest of diapirs takes place at the point of density equilibration and/or the point at which insufficient heat energy is available for thermal softening.

Experimental modelling of magma transport by Whitehead & Helfrich (1990) indicates that, for a continuous melt source, the first fluid to rise forms spherical pockets (diapirs) and a conduit trailing behind the diapir transports upwelling material through steady Pouseille flow. These conduits support solitary waves, which behave nearly like solitons (solitary waves that are conserved upon collision with any other waves) and it has been shown theoretically that these waves have closed streamlines, and hence directly transport unmixed material upwards. It is thought that waves such as these may convey material form very large distances within the earth, to the brittle regions of the crust.

The occurrence of mid crustal plutons, which are constructed from many coalesced sheets, provides evidence for magma ascent in the form of dykes (e.g. Brew

& Ford 1981, Ingram & Hutton 1992 in prep, Hutton 1992, Hutton & Ingram 1992, McCaffrey 1992). However, Marsh (1982) concluded that dykes were not responsible for the transfer of magma from the Benioff zone to the surface, in island arc systems. In his view, the orientation of dykes was controlled by the orientation of the regional principal stresses, and this limited their inclination to ± 20° fom the horizontal. Since there was no pattern of seismicity in support of such inclined dykes, he precluded their presence. More recent work suggests that zones of weakness (e.g. large shear zones), rather than the orientation of the principal stresses, may have the major control on the orientation of sheets in syntectonic plutons (Hutton 1992, Hutton & Ingram 1992). Evidence suggests that these component sheets were emplaced oblique to and often at high angles to the principal stresses, in comparison to the Andersonian (Anderson 1951) dyke model. A dyking ascent mechanism would allow rapid propogation and transport of magma from the mantle into the crust with minimal heat loss (e.g. Pollard & Johnston 1973), thus solving the problem posed by the energy-inefficient diapiric ascent model. This discussion will be expanded in chapter five.

1.7 Granitoid dating techniques

The following formulae summarise the fundamental laws governing radiometric geochronological techniques.

The fundamental decay law for radioactive elements is:

$$A = A_0 \varepsilon^{-\lambda t} \qquad [1.15]$$

where A is the amount of parent isotope left, A_0 is the initial amount of parent isotope, λ is the decay constant and time is t. The decay constant λ has the dimensions T^{-1} and the half-life of a radioactive isotope is $\log_\varepsilon 2/\lambda = 0.693/\lambda$.

From [1.15] one can derive: $A_0 - A = A(\varepsilon^{\lambda t} - 1)$ [1.16]

For each atom of the parent which has decayed ($A - A_0$) one daughter atom is produced, so equation [1.16] can be written as:

$$D = P(\varepsilon^{\lambda t} - 1) \qquad [1.17]$$

where D = number of daughter atoms now and P = number of parent atoms now.

There are several modern techniques for dating the crystallization and, by implication, the emplacement of igneous rocks. However it must be taken into account when utilising such techniques that later deformational and metamorphic events may reset the ages gained from certain techniques e.g. ^{40}K-^{40}Ar. In general, U-Pb (zircon) dating is regarded as the technique with the best resolution for obtaining magmatic dates and the least affected by metamorphic and deformational effects. This technique has been extensively used in dating intrusive rocks in the western Cordillera e.g. Gehrels (1990).

1.7.1 *U-Pb (zircon) dating.*

The results from U-Pb (zircon) analytical techniques are used in dating the crystallization of intrusive bodies (usually felsic) which contain accessory zircon. There are a number of techniques available to extract age dates from U-Pb systematics, but most of the dates quoted from other workers in this thesis were calculated following a technique similar to that described by Gehrels (1990): The zircons are initially separated from their host rocks by crushing and then separating in heavy liquids. Next they are washed in acid (3N HNO_3), purified in a vibrator, passed through heavy liquids and seived to separate different size fractions. Final selections of grains are made under the microscope. The selected zircons are dissolved in HF>>HNO_3 for 30

hours at 240°C, evaporated to dryness and then redissolved in 6N HCl at 215°C for 12 hours. The resulting solution is then spiked with a known $^{208}Pb/^{235}U$ tracer. After chemical separation (outlined by Krogh 1973) the samples are run in a thermal ionization mass spectrometer. From the results, the age calculations and error analyses are made. The errors are assumed to be random and include those from (1) measured isotopic ratios, (2) mass-dependent correction factors, (3) $^{208}Pb/^{235}U$ of the spike and (4) composition of the initial Pb.

From equation [7] one can calculate the expected variation with time in the values of both Pb^{206}/U^{238} and Pb^{207}/U^{235}. A graph of Pb^{206}/U^{238} versus Pb^{207}/U^{235}, with respect to time, constructed from these predicted values defines the curve known as the "concordia". A specimen having isotopic ratios which plot exactly onto the curve has a concordant age which can be read straight off the graph. More commonly, suites of samples plot onto a straight line which intersects the concordia at two points. This is a discordia line, and is usually the result of Pb loss/U gain or U loss/Pb gain i.e. the system was not closed (see fig. 1.10). The upper intercept (τ_0) on the concordia is usually interpreted as the age of the zircon sample and, depending on the particular sample pattern, the lower one (τ) may be interpreted as the time elapsed since the system was opened. Interpretations such as these, in addition to impure samples (grains with different geological histories) grains with old, relic, cores may introduce errors into the dating technique. However, improved techniques for purification of single grains can avoid the difficulties posed by interpretations of large populations.

1.7.2 *K-Ar dating*

In this system, 11% of K^{40} yields Ar^{40} and the remaining 89% yields Ca^{40}. Their half lives are 11,850 Ma and 1,470 Ma respectively. The K^{40}-Ca^{40} system is difficult to use because non-radiogenic Ca is so abundant under normal circumstances and so it is the K^{40}-Ar^{40} system that is used. The minerals most suitable for K-Ar

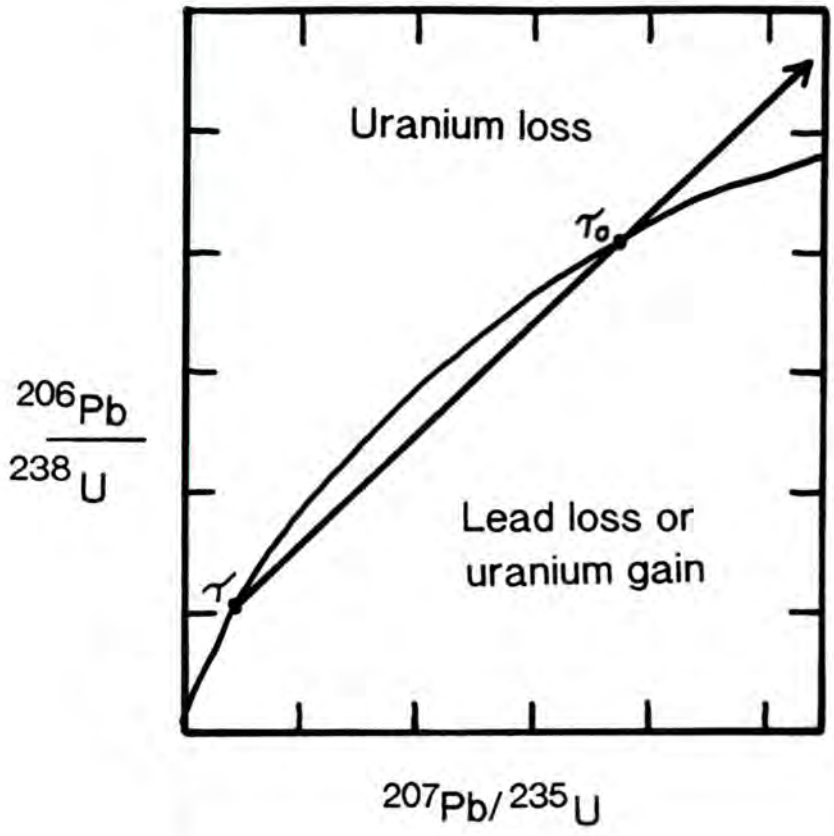

Figure 1.10 Concordia diagram illustrating the effects of Pb loss and U gain or loss on U-Pb systems (see text) (Faure 1986).

dating include biotite, muscovite and hornblende from plutonic rocks and high grade metamorphic rocks and feldspar from volcanic rocks.

The following assumptions are made when attempting to calculate the absolute age of a mineral: (1) No ^{40}Ar produced by ^{40}K has escaped, (2) The mineral was closed to ^{40}Ar and ^{40}K throughout its lifetime, (3) No outside ^{40}Ar was incorporated into the mineral, (4) An appropriate correction for atmospheric ^{40}Ar is made, (5) The isotopic composition of K in the mineral is normal and was unchanged except by decay of ^{40}K, (6) The decay constants of ^{40}K are known accurately, (7) ^{40}Ar and K concentrations are determined accurately.

This system yields good results, but the above assumptions may be invalidated by reheating events such as metamorphism (i.e. burial), which cause the release of the argon gas. This effectively resets the age or gives an anomalously young age if the data is not interpreted properly. The blocking temperature, above which the argon is released, varies for different minerals, but is approximately 250°C for phyllosilicates and 500°C for hornblende (Harrison 1981). The regional variation in K-Ar dates of a specific mineral provides information about the time of cooling, related to uplift, through this blocking temperature isotherm. By dating minerals with different blocking temperatures, the cooling rates of uplifted crust can be determined (Faure 1986).

In the western USA, this method has been used to date the uplift of parts of metamorphic belts, to ascertain the amount of crustal tilt, and to correlate, over large areas, periods of major uplift. It is important to stress that the dates obtained using the K-Ar system are not interpreted to represent the crystallization of plutons.

1.7.3 *$^{40}Ar/^{39}Ar$ dating*

The $^{40}Ar/^{39}Ar$ method of dating, first described in detail by Merrihue & Turner (1966), can overcome some of the limitations of the K-Ar method, which are caused by the loss of argon. In principle, the method is based on the formation of ^{39}Ar from ^{39}K by the irradiation of K-bearing samples with thermal and fast neutrons in a nuclear

reactor. The method requires irradiation of a sample of known age (flux monitor) and corrections for interfering nuclear reactions with isotopes of Ca, K, Ar and Cl. After release of all gases the measured $^{40}Ar/^{39}Ar$ dates are comparable to conventional K-Ar dates, but are based solely on measurements of isotopic ratios of argon.

Stepwise heating of irradiated samples provides a range of dates from the $^{40}Ar/^{39}Ar$ ratio from each outgassed fraction. A plateau may be formed due to the release of argon by the more retentive minerals in the sample and this may be equal to, or slightly less than the date of crystallization. However, a uniform distribution of excess ^{40}Ar in the sample will produce a plateau which gives anomalously old dates. Anomalously old dates are also caused by the measurement of minerals with excess ^{40}Ar at low temperatures and by the undetected loss of ^{39}Ar during the incremental heating process. A correction for atmospheric ^{40}Ar is also needed, based on the assumption that ^{36}Ar is of atmospheric origin and that the $^{40}Ar/^{36}Ar$ ratio (atmospheric) is 295.5. This atmospheric error may be avoided by using an argon isotope correlation diagram, in which the measured $^{40}Ar/^{36}Ar$ and $^{39}Ar/^{36}Ar$ ratios from the outgassed fractions are plotted together, ideally forming a straight-line isochron. The slopes of the isochrons are equal to the $^{40}Ar/^{39}Ar$ ratio, from which the age of the sample can be calculated. In most cases, the intercept gives the atmospheric $^{40}Ar/^{36}Ar$ ratio.

The data, collected during the stepwise outgassing procedure, can be used to derive the temperature at the time recorded by the plateau date. This enables the construction of cooling curves for rocks that contain several K-bearing minerals with different argon blocking temperatures (from Faure 1986). This facet of the method has been used to compare the relative cooling rates for different parts of metamorphic belts, e.g. southeast Alaska (Wood et al. 1991), and the implications of this will be discussed later in the thesis.

1.8 Palaeomagnetic analysis

Palaeomagnetic analysis has been used extensively in the western Cordillera of North America, in order to determine the relative movements between different crustal fragments or terranes and the continental margin. In fundamental terms, the palaeomagnetism of a rock provides data about the inclination and azimuth of the earth's magnetic field at the time of its formation. The azimuth of the field indicates the direction of the palaeomagnetic north pole and the inclination indicates the lattitude at which the rock formed. Equipped with this information, it is possible to locate the exact position of the apparent palaeopole.

For a dipole field, at all parts on the magnetic equator, the magnetic inclination is zero and the magnetic field is horizontal. In the northern magnetic hemisphere, the magnetic lattitude and the magnetic inclination are positive. In the southern hemisphere they are negative and the magnetic field is inclined above the horizontal. The relationship between the magnetic lattitude λ and the magnetic inclination I (fig. 1.11) is:

$$I = \tan^{-1}(2\tan\lambda) \qquad [1.18]$$

An important feature of the dipole field is that it has complete rotational symmetry about its axis. This means that the field vectors along any circle of longitude can be superimposed upon those of any other circle by rotation about this axis. However, it is possible to derive a unique magnetic lattitude because each magnetic inclination defines a unique distance from the magnetic equator. In other words, palaeomagnetic data can determine palaeolattitude uniquely, but not palaeolongitude.

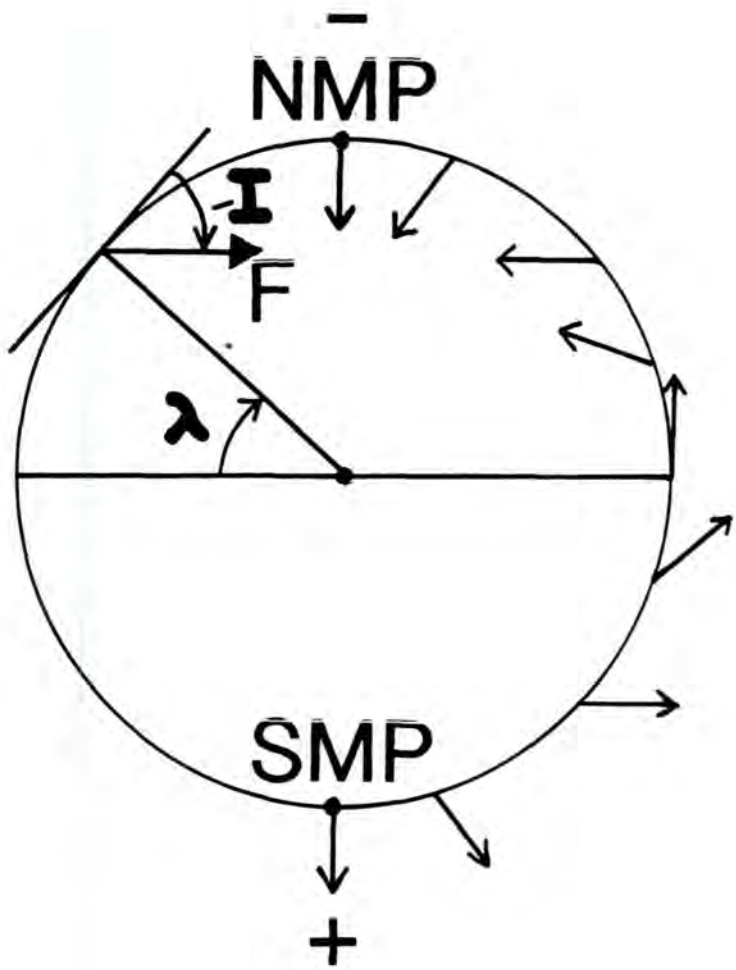

Figure 1.11 Magnetic dipole M at the centre of circle produces fields F shown along the circle. I = magnetic inclination or plunge beneath horizontal. λ = magnetic latitude. NMP = north magnetic pole. SMP = south magnetic pole. (Cox & Hart 1986).

1.8.1 *Rock magnetization*

Some rocks have good magnetic memories and yield good palaeomagnetic data, but others do not. Igneous rocks which were hot when they were intruded, extruded or deposited, retain a record of the ambient magnetic field as they cool. This is called Thermoremanent Magnetization (TRM). The temperature below which the magnetic memory is retained is known as the Curie temperature and for the mineral magnetite, it is characteristically at 580°C. Sediments may also record the earth's magnetic field as they are deposited. This memory is known as Depositional Remanent Magnetization (DRM). Commonly, sediments contain one strongly magnetic grain in every thousand grains (Cox & Hart 1986), which acts like a tiny compass needle as it passes through the water column. Small grains are least affected by water turbulence and as a consequence, rocks like siltstones are good recorders, whereas sandstones are not.

1.8.2 *Sample selection*

Only certain types of rocks are suitable for palaeomagnetic analysis. According to Cox & Hart (1986), extrusive rocks are excellent magnetic recorders provided that they were above the Curie temperature when extruded or deposited. Such volcanic formations cool quickly and instantaneously record the palaeofield. In special circumstances, sediments may record DRM . However, in sediments there is a greater scope for error and this may depend on the depositional environment and other factors such as compaction. Sediments may acquire a palaeomagnetic direction that is shallower than the ambient field, if deposited in quiet conditions or if they were compacted after deposition. This inclination shallowing error can complicate palaeolattitudinal interpretations by implying northward movements that did not take place. Red beds are also commonly used, but error is inherited by a paucity of fossils for dating and difficulties in determining when they became magnetized. Limestones

are fossiliferous and hence datable, but their DRM may be destroyed by recrystallization. In the view of Cox & Hart (1986), the rock formations of last resort for sampling are plutons because it is rarely possible to determine how much a pluton has been tilted.

1.8.3 *Measurement*

In the laboratory, initial analysis in a magnetometer provides data which describes the magnetic moment of the specimen: the inclination, the declination and a scalar number which gives the length of the vector. Further steps are taken to eradicate "soft" magnetization which may have overprinted the primary magnetization. This is called magnetic cleaning and may involve heating and/or exposure to a varying alternating magnetic field. Both these techniques strive to randomize the magnetic moments of the grains bearing the "soft" remanent magnetization, in order to reveal the real, "hard" magnetization.

1.8.4 *Applications to tectonic models*

Obviously, if a rock has been tilted, or or has undergone a major translation, or if the constituent magnetic particles, e.g. silt grains in an unlithified sediment and magnetized crystals in a cooling intrusive body, have been irreversibly tectonically disturbed, the resultant palaeomagnetic vector will not correspond to the expected vector for the time period in which it developed. It is important therefore to have a good database of the positions of true palaeopoles throughout the geological timescale. The position of the magnetic palaeopole changes through geological time and therefore using this kind of database, it is possible to construct time sequences of palaeomagnetic poles, or apparent polar wander (APW) paths, for particular crustal fragments. In the western Cordillera of North America, the palaeopoles of allochthonous or suspect terranes are compared with the APW path for continental

North America and therefore models of the relative movement of terranes along the continental margin can be constructed (e.g. Umhoefer et al. 1989). As more data is collected from field studies, the APW path for North America is constantly revised (e.g. Butler et al. 1991) and new interpretations must be made.

One of the major problems with the palaeomagnetic analysis of allochthonous or suspect terranes, in the western Cordillera and elsewhere, is that if anomalous results are gained from samples, they can be explained by two end-member processes or a combination of both: (1) Translation of the terrane, without disturbing its palaeohorizontal, with respect to North America, (2) Tilting of the terrane such that the palaeohorizontal is disturbed, without movement relative to North America. There are two main schools of thought concerning the anomalous palaeomagnetic results which have been gained from the terranes which make up the western Cordillera. Workers in one school, such as Umhoefer et al. (1989), advocate up to 2400km of northward translation and a component of rotation of terranes with respect to the North American Margin, but workers in the other "fixist" school suggest that the same terranes have not moved significantly, and that tilting to the SW was a dominant factor in creating the anomalous palaeopoles (e.g. Butler et al. 1991). In both cases the interpretations were based on samples which yielded anomalously shallow magnetic vectors, indicative of low apparent palaeolattitudes with respect to North America.

This is an ongoing argument which will be addressed and discussed later in this thesis. It is important to stress that one must be able to verify palaeomagnetic results with geological data in the field. If the palaeomagnetic arguments are not corroborated with hard geological evidence, arguments such as those stated above may never be reconciled.

CHAPTER 2
THE COAST MOUNTAINS OF SOUTHEAST ALASKA

2.1 Geological setting of southeast Alaska and British Columbia

2.1.1 *Introduction*

Southeast Alaska and British Columbia are composed largely of a collage of tectonic belts and tectonostratigraphic terranes, which were accreted to the North American margin during subduction of oceanic crust eastwards under the North American craton. The geology has been divided into five main domains: (from east to west) the Foreland belt, the Omenica belt, the Intermontane belt, the Coast belt and the Insular belt (Wheeler et al. 1991, fig. 2.1). Of these, the Foreland and Omenica belts represent ancient North American cratonic rocks and pericratonic rocks (deposited upon the craton), respectively. The Insular and Intermontane belts, which are termed "superterranes", represent younger displaced terranes accreted to the ancient continental margin, and these are separated by the Coast belt, which is composed largely of the Coast Plutonic Complex.

Ancestral North America. In more detail, the ancestral Foreland belt is composed of middle Proterozoic to Carboniferous passive and offshelf continental margin sediments, Devonian to Carboniferous clastic wedges, upper Carboniferous to Jurassic passive margin sediments and Permian clastics. The Omenica belt is formed from a complex of continental margin and related rocks: middle Proterozoic to Jurassic passive and offshelf continental margin sediments, cratonic metasediments overlying

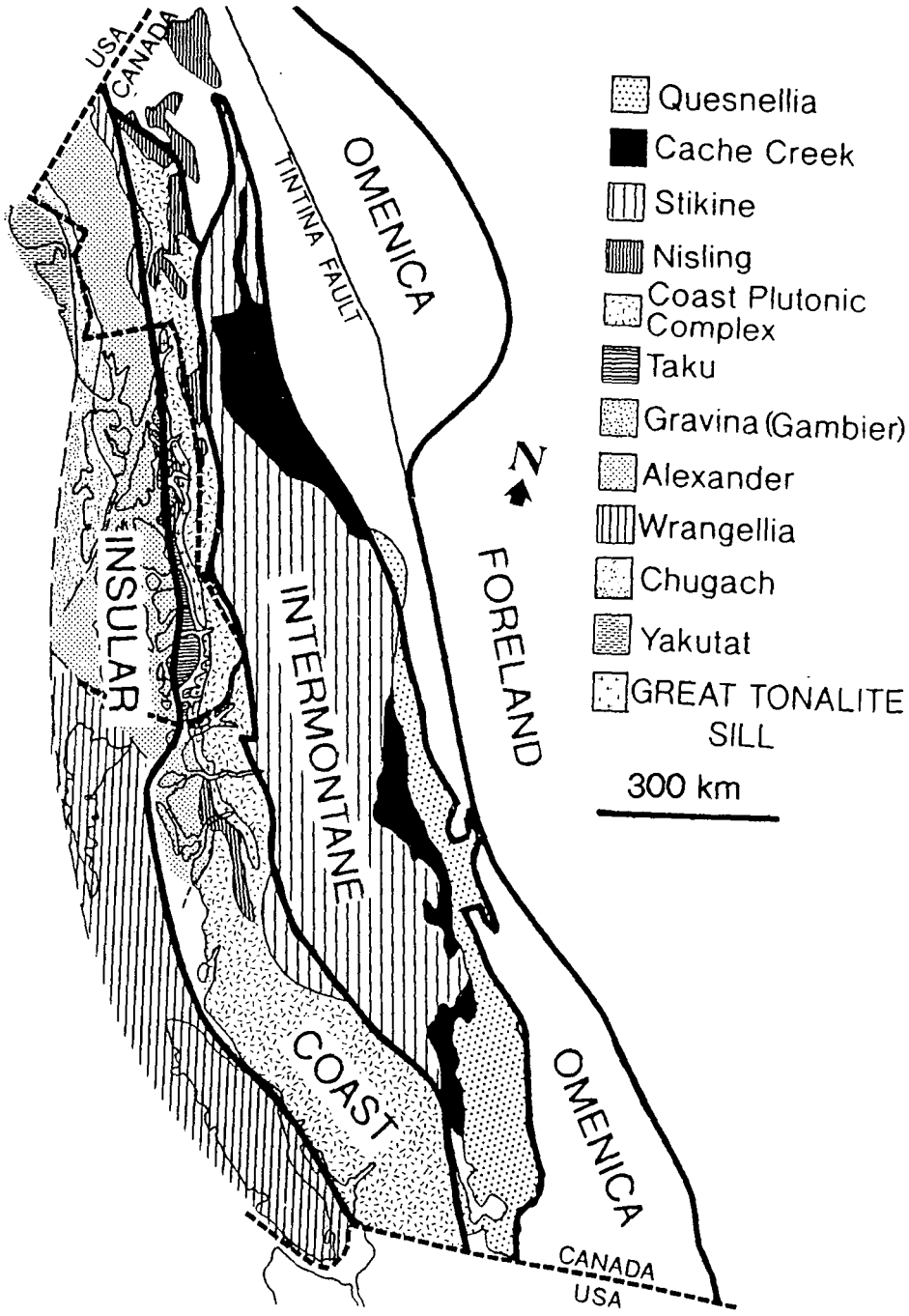

Figure 2.1 The distribution of the main recognised terranes in the Coast Mountains of the western Cordillera (compiled by Wheeler et al. 1991).

lower Proterozoic basement gneiss and Devonian to late Triassic oceanic marginal basin volcanics and sediments, and intruded by Jurassic and Cretaceous plutons.

The Coast Mountains of southeast Alaska. The terranes which accreted to the ancient North American continental margin are those which form the Coast Mountains today. The majority of these terranes belong to the Intermontane and Insular superterranes (Rubin et al., 1990), which correspond to composite terranes I and II respectively, of Monger et al. (1982) (fig. 2.2). The terranes making up the Intermontane superterrane are thought to have amalgamated by latest Triassic time and accreted to ancestral North America in the Jurassic. By the late Jurassic, the terranes of the Insular superterrane amalgamated and are believed to have accreted to the continental margin in Cretaceous time (e.g. Rubin et al. 1990). The Coast plutonic Complex, which lies between the two superterranes, is composed chiefly of Cretaceous to Tertiary granitoid plutons, which are not included in a terrane classification. However, there are sedimentary and volcanic sequences defining component terranes throughout the Coast belt.

2.1.2 *Tectonostratigraphic terranes*

The **Intermontane superterrane** is composed of Devonian to Jurassic rocks of the Stikinia, Cache Creek, Yukon-Tanana and Quesnellia terranes, which are composed as follows (from Wheeler et al. 1991, Mortensen 1992):

Stikinia. This terrane represents an ancient island arc and Devonian to Permian arc volcanics and platform carbonates dominate. Triassic and Jurassic arc volcanics, volcaniclastics, chert and arc-derived clastics, intruded by cogenetic intrusions, are also typical. Its basement is not exposed, but it may be underlain by rocks correlative with the Yukon-Tanana terrane (see below)

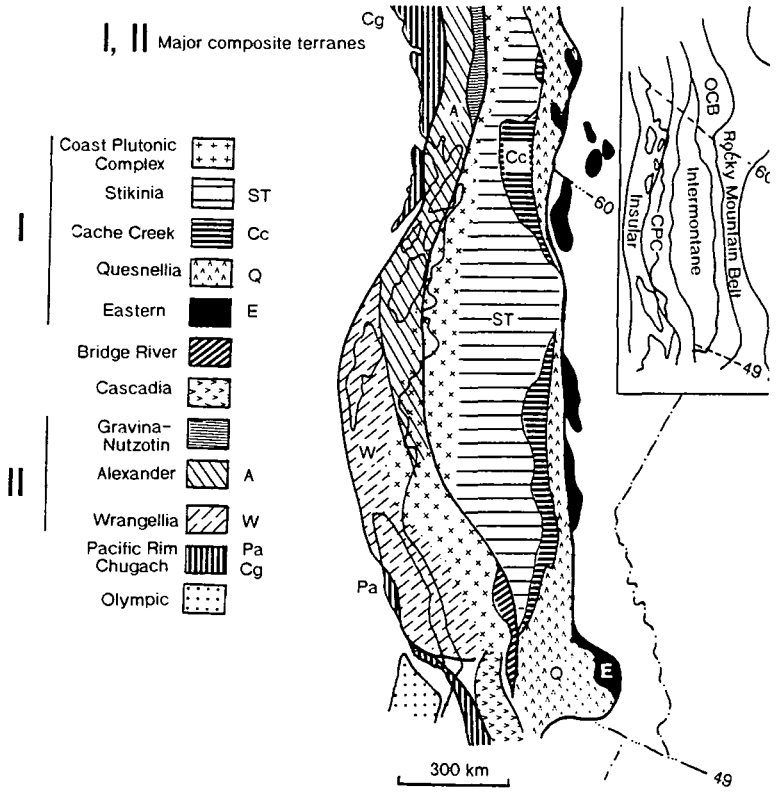

Figure 2.2 Terranes I and II of Monger et al (1982), which correspond to the Intermontane and Insular superterranes respectively.

Cache Creek. In basic terms, the Cache Creek terrane typifies an accretionary wedge/subduction complex. It is composed of lower Carboniferous to lower Jurassic oceanic volcanics and sediments, upper Triassic island-arc volcanics and local accretionary melange. Rock types include radiolarian chert, argillite, basalt, carbonates and Alpine type ultramafics.

Yukon-Tanana. This is one of the largest and most enigmatic of the Cordilleran terranes and is composed of polydeformed metamorphic rocks derived from a variety of igneous and sedimentary protoliths. Much of it is a product of episodic continental arc magmatism, with three main pulses in (a) late Devonian - early Carboniferous, (b) mid Permian, and (c) late Triassic - early Jurassic time. Parts of this terrane may also be referred to as the Nisling terrane.

Quesnellia. This is essentially an island arc complex and is composed of upper Triassic and lower Jurassic arc volcanics and cogenetic intrusives, overlain by Jurassic arc-derived clastics.

The **Coast belt** is composed mostly of Cretaceous to Tertiary plutons, but contains recognisable terranes:

Taku: Again, this is regarded as an island arc complex, composed of: Upper Palaeozoic basaltic volcanics; Permian marble, phyllites and felsic metatuff; Middle and Upper Triassic limestone, shale, phyllite and basaltic breccia; possible Jurassic to Lower Cretaceous flysch and metatuff. However, Gehrels et al (1991b) suggest that much of the Taku terrane belongs to the *Yukon-Tanana* terrane, which is also correlative with the *Nisling* terrane (e.g. Wheeler et al. 1991) found in the Omenica belt.

Gravina-Nutzotin belt: This arc is composed of upper Jurassic and Lower Cretaceous overlap assemblage of flysch and volcanics (Monger & Berg 1987). It has been correlated with the Gambier overlap arc assemblage, which also stratigraphically overlies parts of the Insular and Intermontane superterranes (Wheeler et al. 1991).

Coast Plutonic Complex: The mainly Cretaceous to Early Tertiary granitic intrusions of the Coast Plutonic Complex (Fig. 2.1) intruded the SW part of the Intermontane Superterrane in southeastern Alaska and British Columbia, and form six major belts (Brew & Morrell 1983).

The **Insular superterrane** lies outboard to the W and is essentially made up from rocks of the Alexander and Wrangellia terranes (Wheeler et al. 1991):

Alexander. This island arc complex is composed of Upper Proterozoic to Triassic volcanics and sediments deposited in e.g. ocean arc, back arc, platform, rift, trough and offshelf settings, intruded by magmas probably with similar sources to the volcanics.

Wrangellia. Again, this is an ancient island arc. Its basement is composed of Devonian to Permian arc volcanics, clastics and platform carbonates. This is overlain by Triassic oceanic rift tholeiitic basalts and carbonates plus Jurassic arc volcanics, and intruded by plutons of cogenetic origin. In addition, the Alexander and Wrangellia terranes are overlain by the ***Gravina-Nutzotin Belt.***

Outer terranes. These lie to the west of the Alexander and Wrangellia terranes, but are still considered as part of the Insular belt, and include:

Chugach terrane. This is composed of Cretaceous greywackes and argillites and a lower Cretaceous melange of upper Triassic to lower Cretaceous blocks, which form the inner part of an accretionary prism.

Yakutat terrane. Constituents include upper Cretaceous turbidite and melange (containing upper Triassic to lower Cretaceous blocks), lower Tertiary tholeiitic volcanics and marine clastics from the outer part of an accretionary prism.

2.1.3 *Palaeomagnetic work*

Palaeomagnetic data from western North America, specifically southeastern Alaska and British Columbia, suggest that rocks of the Chugach, Wrangellia, Alexander, and Stikine terranes, the Coast Plutonic Complex, and possibly part of the Omenica belt were located around 2000km south, around the latitude of Baja California, in early late Cretaceous time (e.g. Monger & Irving 1980, Umhoefer 1987). It has been envisaged that relative northward translation of these terranes, to their present positions, took place in the late Cretaceous to early Tertiary interval (e.g. Thrupp & Coe 1986).

More recently, however, emphasis has been placed on the uncertainties involved in the interpretation of palaeomagnetic results from the western Cordillera. The so-called "Baja British Columbia" hypothesis (Umhoefer 1987) has created much controversy over the perceived origin of the discordant palaeomagnetic inclinations, essentially leading to two schools of thought: (1) those who suggest that the terranes moved thousands of kilometres northwards (e.g. Gabrielse 1985, Irving et al. 1985, Umhoefer 1987, Umhoefer 1989, Beck 1991) and (2) those in favour of in-situ tilting of the terranes to explain the palaeopole inclinations (e.g. Butler et al. 1989, Butler et al. 1991). Both schools of thought explain the data satisfactorily, but available structural and metamorphic field data is not sufficient to support either (1) or (2) alone. More field data is needed to contribute to this argument, in order to establish

which school is essentially correct. A more thorough discussion of this controversy, in the light of the implications from the work contained herein, is continued in chapter 6, section 6.4.

2.1.4 *Terrane transport models and field geology*

Perhaps the most important implications arising from calculations of the movements of allochthonous terranes and the determinations of relative plate motions, are the restrictions which they place upon each another. It is clear that determinations for the motions of the plates should correspond to those made for the terranes which they have carried, and form a coherent hypothesis.

Debiche et al. (1987) developed a computer program in order to simulate the position of terranes, as a function of time, as they were driven by the oceanic plates. The main variables which define the trajectories are: 1) the stage poles describing the motion of oceanic plates with respect to the continent, 2) the sequence of plates carrying the terrane (one plate can be divided by propagating ridges to form several others), 3) the time of docking of the terrane, 4) the co-ordinates of the point of docking. The plate model of Engebretson et al. (1985) was used in the analysis and the terrane trajectory was calculated by back modelling, using the stage poles. However, there are many uncertainties inherent in this type of modelling and in the case of Engebretson et al. (1985), these were weighted in favour of rapid northward relative movement of the Kula and Farallon plates, with respect to North America, in order to fit in with the late Cretaceous dextral strike slip models. The uncertainties concerning interpretations of the palaeomagnetic data, leading to reconstructions and estimates of apparent displacements, have already been stated (section 1.8.4).

If one accepts the perspective outlined above, the usefulness of applied field geology becomes clear. Certain kinematic models are supported by modelling such as that above and the rocks in the field can provide data with which they can be tested. The most likely areas to collect useful data are at terrane boundaries, where the

majority of deformation has taken place during transport and docking. Syntectonic plutons, which were emplaced at or near a terrane boundary, are especially useful as they may record the ambient tectonics at a specific time indicated by their radiometric dates.

2.2 The Great Tonalite Sill

2.2.1 *Granitoid rocks in southeast Alaska*

About thirty percent of the 175,000 km^2 area of southeastern Alaska is underlain by intrusive igneous rocks and these have been divided up into six major and other minor plutonic belts (Brew & Morell 1983, see map fig 2.3). The major plutonic belts are related to the above terrane classification as follows:

(1) ***Fairweather-Baranof belt.*** This early to mid-Tertiary belt of granodiorite is associated with the Insular superterrane (Alexander, Wrangellia and Chugach terranes).

(2) ***Muir-Chichagof belt.*** The host for the mid-Cretaceous tonalite and granodiorite of this belt is the Insular superterrane, more specifically the Alexander and Wrangell terranes.

(3) ***Admiralty-Revillagigedo belt.*** The Cretaceous porphyritic granodiorite, quartz diorite and diorite of this belt occur in the Gravina and Taku terranes (i.e. NE edge of Insular superterrane and SW edge of Coast belt).

(4) ***Klukwan-Duke belt.*** These mid-Cretaceous "Alaskan type" ultramafic-mafic plutons occur within the Admiralty-Revillagigedo belt.

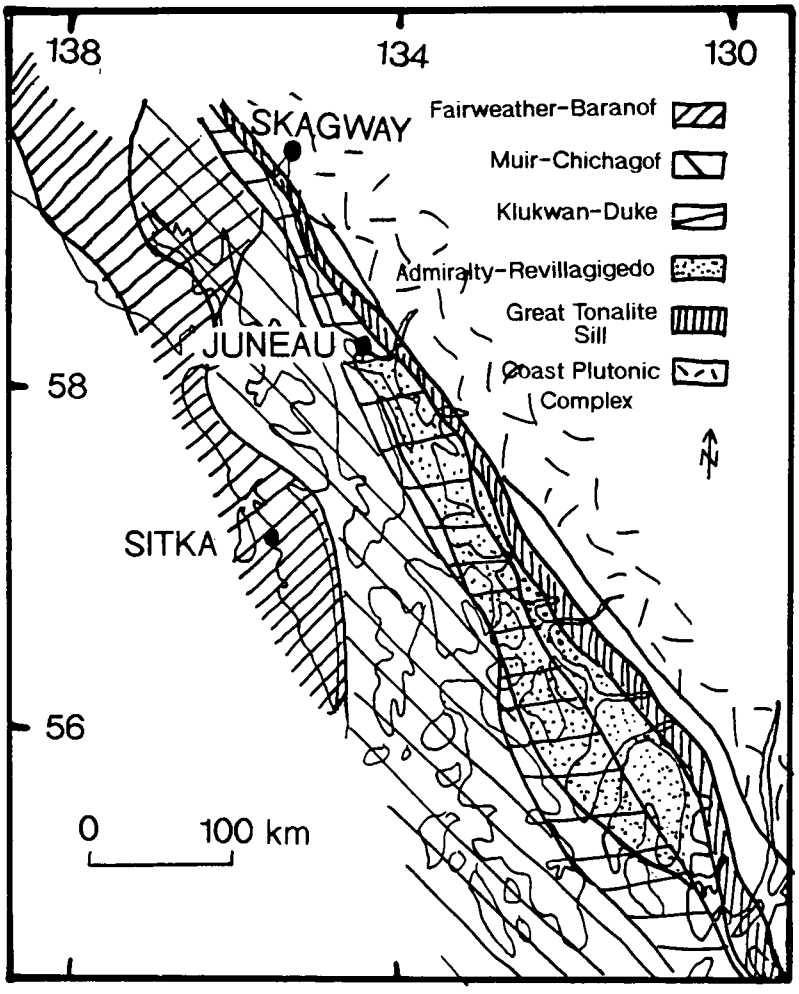

Figure 2.3 Plutonic belts of southeast Alaska. Modified from Brew & Morrell (1983).

(5) ***Great Tonalite Sill belt.*** This is an extensive belt of tonalitic plutons, dating form late Cretaceous to early Tertiary, which lies at or near the SW edge of the Coast belt (Coast plutonic Complex).

(6) ***Coast Plutonic Complex.*** The Coast belt is dominated by these early to mid Tertiary granodiorite and quartz monzonite plutons, which have intruded the SW part of the Intermontane superterrane (e.g. Stikine terrane). The Coast Plutonic Complex has also been referred to as the Coast Range Batholith by Barker & Arth (1984).

2.2.2 *Introduction: The Great Tonalite Sill*

The Great Tonalite Sill of Southeast Alaska and British Columbia is one of the world's most remarkable intrusive bodies. It extends for more than 800km along strike, but yet is only 25km or less in width. The Great Tonalite Sill consists of a belt of elongate, coalesced, dominantly tonalitic plutons, themselves composed of many coalesced, tonalitic sheets, striking NW-SE and dipping steeply to the NE, which was emplaced at depths corresponding to pressures of around 7.5kb, between the Late Cretaceous to the Early Tertiary (Brew & Ford, 1981, Gehrels et al. 1984, Gehrels et al. 1991; Himmelberg et al. 1991, McClelland et al. 1991a). The rocks of the Great Tonalite Sill are heterogeneous but a medium to coarse grained hornblende-biotite tonalite is dominant, with garnet and sphene commonly occurring as accessory phases (Hutton & Ingram 1992). Granodiorites, medium grained diorites, plentiful synplutonic dykes and microdioritic enclaves are also found. Early, coarse, euhedral-hornblende-bearing rocks of dominantly ultramafic composition found near pluton contacts are thought to represent the precursors of the main tonalitic intrusions.

Strong deformation is a common feature of the Great Tonalite Sill and especially its SW wall rocks. This zone of deformation can be correlated over long distances and has been referred to in places as the ***Coast shear zone*** Crawford &

Crawford 1991, McClelland et al. 1992). It is thought that the Great Tonalite Sill and its associated shear zone may together mark, or lie close to, the effective boundary between the Intermontane and Insular superterranes. The plutons were emplaced during regional deformation associated with this major shear zone (The Great Tonalite Sill shear zone - further discussion in chapter 3) and therefore hold a record of the kinematics prevalent during the emplacement and crystallization interval.

Kinematics. Work by Crawford and Hollister (1982) suggested that the rocks to the east of the Sill in southern British Columbia were uplifted relative to the west by around 15 km between 60Ma and 50Ma. This is consistent with the dominant shear sense of top-to-the-SW, which has been observed in this study. In agreement with this, Crawford et al. (1987), Brew et al. (1989) and Stowell & Hooper (1990) have all suggested that most kinematic indicators record E-side-up displacement, although Gehrels & McClelland (1988), Crawford et al. (1989) and McClelland et al. (1992) locally recorded E-side-down indicators.

2.2.3 *Previous research*

Brew & Ford (1977 & 1978) first recognised that there existed a remarkably long and narrow belt of "prominent foliated granitic sills" lying along an extensive part of the western edge of the Coast Plutonic Complex. They commented on the remarkable linearity of these large-scale sills and implied that they had been intruded along a hypothetical plate boundary. In addition, the Coast Range Megalineament, a persistent structural zone of joints, foliation, compositional layering and small faults, is parallel to the sill trend, lending weight to their suggested link between emplacement, regional structure and deformation (i.e. syntectonic and synmetamorphic emplacement). They suggested that it was emplaced during middle or late Cretaceous time. Later, Brew & Morrell (1980) and Brew & Ford (1981) referred to this intrusive entity as the **Coast Plutonic Complex sill**, or simply "the sill", and again suggested

that it was emplaced along a structural discontinuity representing some kind of plate boundary. Brew & Ford (1984) referred to the "tonalite sill belt" in their paper and cited work by Crawford & Hollister (1982), which indicated the presence in British Columbia of a similar belt of plutons and associated metamorphic rocks. This confirmed that the tonalite sill stretched from at least Haines in Alaska to Prince Rupert, British Columbia.

Great Tonalite Sill. Brew et al. (1989) described the western part of the Coast plutonic-metamorphic complex (synonym: Coast Plutonic Complex) and noted the increase in the degree of deformation and the grade of metamorphism, culminating at, or close to the SW edge of the steeply NE dipping "great tonalite sill". The name "**great tonalite sill**" is the latest in a line of names for the originally-named Coast Plutonic Complex sill (Brew & Ford 1981) and serves to emphasise the nature of the batholith, which is of plate tectonic dimensions. However, it should be stressed here that the word "sill" refers to an extremely long and dense series of steeply NE inclined to vertical tabular tonalite bodies, rather than a flat lying one which the word may suggest. Brew & Ford (1981) called the batholith a sill, rather than a "dyke", as the tabular plutons from which it is formed are concordant to the steeply dipping shear zone fabrics in their wall rocks. The batholith as a whole is, in the author's view, more like a collection of "dykes", although in this thesis it is called the "**Great Tonalite Sill**", the "**Tonalite Sill**" or simply, the "**Sill**", in order to maintain continuity in the nomenclature.

2.2.4 *Dating*

The best available dating of the crystallization ages of the Great Tonalite Sill plutons has been carried out by Gehrels et al. (1991a), using conventional U-Pb techniques on zircons (see Gehrels 1990). Their work indicates that they were emplaced between c.83 Ma and c.57 Ma (possibly c.55 Ma) i.e. late Cretaceous to

early Tertiary. General trends in ages from their work suggest that the elongate tonalitic bodies become younger southeastward and northeastward.

Less elongate tonalitic-granodioritic intrusions located in the central portions of the Coast Plutonic Complex yield ages of 59-58 Ma and these are, in places, coeval with younger phases of the elongate Great Tonalite Sill bodies. In the more eastern parts of the Coast Plutonic Complex, U-Pb dating of large granite-granodiorite intrusions indicates that they were emplaced at 51-48 Ma.

Work by Barker & Arth (1984) on the often migmatitic Central Gneiss Complex of the Coast Plutonic Complex, located east of Ketchikan in Boca de Quadra, southeast Alaska, suggested that it is the oldest unit of the Coast Plutonic Complex, with U-Pb dates of 128-140 Ma, and that it may represent the roots of a high-K, calc-alkaline arc. More recently, Gehrels et al. (1991b) obtained zircon fractions from similar rocks, again in Boca de Quadra and also to the north in Burroughs Bay. The U-Pb date for crystallization of rocks in the former was tentatively placed at 336 ± 34 Ma (mid-Palaeozoic) and for the latter was 215 ± 15 Ma (late Triassic). They also state that inherited zircon components within some of the Eocene plutons e.g. Turner Lake pluton (Drinkwater et al. 1990) yield dates which are indicative of mid-Palaeozoic to early Proterozoic, probably reflecting assimilation of continental rocks during ascent of these plutons. The dates acquired from individual plutons, and their implications, are discussed in more detail in chapter three.

2.2.5 *Thermobarometry*

Geothermometry carried out on samples from southeast Alaska has been based on the garnet-biotite Fe-Mg exchange equilibrium, calculated using the preferred calibrations of Ferry & Spear (1978), Hodges & Spear (1982) and Ganguly & Saxena (1984). Geobarometry was based on (1) the garnet-aluminosilicate-quartz-plagioclase equilibrium (e.g. Newton & Haselton 1981), (2) the garnet-muscovite-plagioclase-biotite equilibrium originally proposed by Ghent & Stout (1981) and, in addition,

McClelland et al. (1991a) used (3) garnet-rutile-ilmenite-plagioclase-quartz equilibrium (Bohlen & Liotta 1986), and (4) garnet-rutile-aluminosilicate-quartz-ilmenite equilibrium (Bohlen et al. 1983) (e.g. Stowell 1989, McClelland et al. 1991a, Himmelberg et al. 1991).

In general, data from southeast Alaska indicate that the Great Tonalite Sill was emplaced at depths corresponding to pressures of c.5 kb - c.8 kb with peak temperatures of around 750°C during emplacement. Taking the Quottoon pluton of British Columbia as a particular example, Hollister (1982) calculated that the country rocks of the Central Gneiss Complex, adjacent to the intrusives, were at about 5 kb pressure and a temperature of about 750°C during tonalite emplacement.

Uplift. On the basis of data by Harrison et al. (1979), which indicated that these rocks cooled rapidly (from 700°C to 400°C in 3 Ma), Hollister (1982) suggested that there had been rapid uplift of the Central Gneiss Complex and the Quottoon pluton between 62 Ma and 48 Ma, beginning at 35km and terminating at 5km depth. This represented an uplift rate of 2mm/yr.

Stowell (1989) indicated that the emplacement of tonalite at Endicott Arm took place at a pressure of 5.1 ±0.3 kb and at a temperature of around 670°C. More recent data, from the Petersburg region of southeast Alaska (McClelland et al 1991a), suggests that rocks to the west of the Coast Plutonic Complex (Taku terrane, Gravina belt) were at temperatures of 465 - 890°C and pressures of 7.1 - 11.8 ±1 kb during the middle Cretaceous. They imply that the Gravina and Yukon-Tanana terranes (to the west) were juxtaposed at depths in excess of 7 kb and that the Great Tonalite Sill was emplaced, during a period marked by retrogression of the western wall rocks, at pressures of 7.5 - 7.7 ±1 kb, in the late Cretaceous. However, their data also shows that, up to 500 m from the intrusive contacts, pressures and temperatures may have been in excess of 9 kb and 750°C. Further implications of these data are discussed in chapter 6.

2.2.6 *The Great Tonalite Sill*

In order to outline the questions and problems which the following work seeks to address, it is first necessary to make some brief statements concerning the Great Tonalite Sill and its associated rocks. The Great Tonalite Sill of southeast Alaska and British Columbia is the longest and narrowest composite batholith in the western Cordillera and, in addition, is associated with an extensive contractional shear zone, known in places as the Coast Shear Zone (e.g. Crawford & Crawford 1991), but which is here called the Great Tonalite Sill shear zone. Previous work has shown that the Great Tonalite Sill was emplaced syntectonically into this shear zone during the late Cretaceous to early Tertiary and that these features lie approximately at the boundary between two superterranes, which collided sometime in the mid Cretaceous period. The collision was in response to easterly subduction of the oceanic crust, which carried the terranes, beneath the ancient North American craton. Palaeomagnetic work implies that a kinematic regime dominated by dextral strike slip was in operation during the great Tonalite Sill emplacement phase. The deformational structures, metamorphic and emplacement data now preserved, both in the Great Tonalite Sill plutons and its associated shear zone, supply evidence from which inferences pertaining to kinematics, metamorphism and emplacement, may be made.

In chapters four, five and six, the following major questions and their implications are addressed:

(1) What information do the structures contained in the Great Tonalite Sill plutons and their country rocks impart concerning the tectonic regime prevalent during pluton emplacement?

(2) What were the main mechanisms for the genesis ascent and emplacement of the Great Tonalite Sill plutons and what were the main controlling influences?

(3) What important implications do the timing and kinematics of the deformed, sill-like plutons and their wall rocks have for (i) the larger-scale plate tectonic regime? (ii) kinematic models based on palaeomagnetic data?

General methodology. This thesis presents data from detailed traverses, which were carried out on 9 fjord sections in southeast Alaska between Taku Inlet, to the north, and Walker Cove, to the south, together with detailed mapping in the Juneau area (Fig. 2.4). Other data (described in Ingram & Hutton, in prep), which extend the geographical scope of the thesis work to Haines, in the north, and Skeena River, to the south (British Columbia), are also presented in order to give a fuller picture. The data collected are voluminous and are concerned mainly with detailed structural studies i.e. fabric chronologies and geometries, transport lineation orientations, sense of shear indicators, strain studies and relative fabric intensities, metamorphic minerals and their time of formation relative to structural events. This has been combined with a special study of the timing of fabric formation relative to crystallization state in the sill rocks (magmatic-state/Pre-Full Crystallization and solid state/Crystal Plastic Strain: PFC & CPS respectively, Hutton 1988), together with evidence of intrusion processes, on various scales, to produce an account of the deformation history and kinematics, and a model for the emplacement mechanism of the Sill. It should be emphasised that, unlike previous studies, these features have been examined over most of the known length of the Great Tonalite Sill. There appears to be a remarkable consistency in these features throughout the belt, emphasising that the processes leading to their formation were on a fundamental, plate tectonic scale.

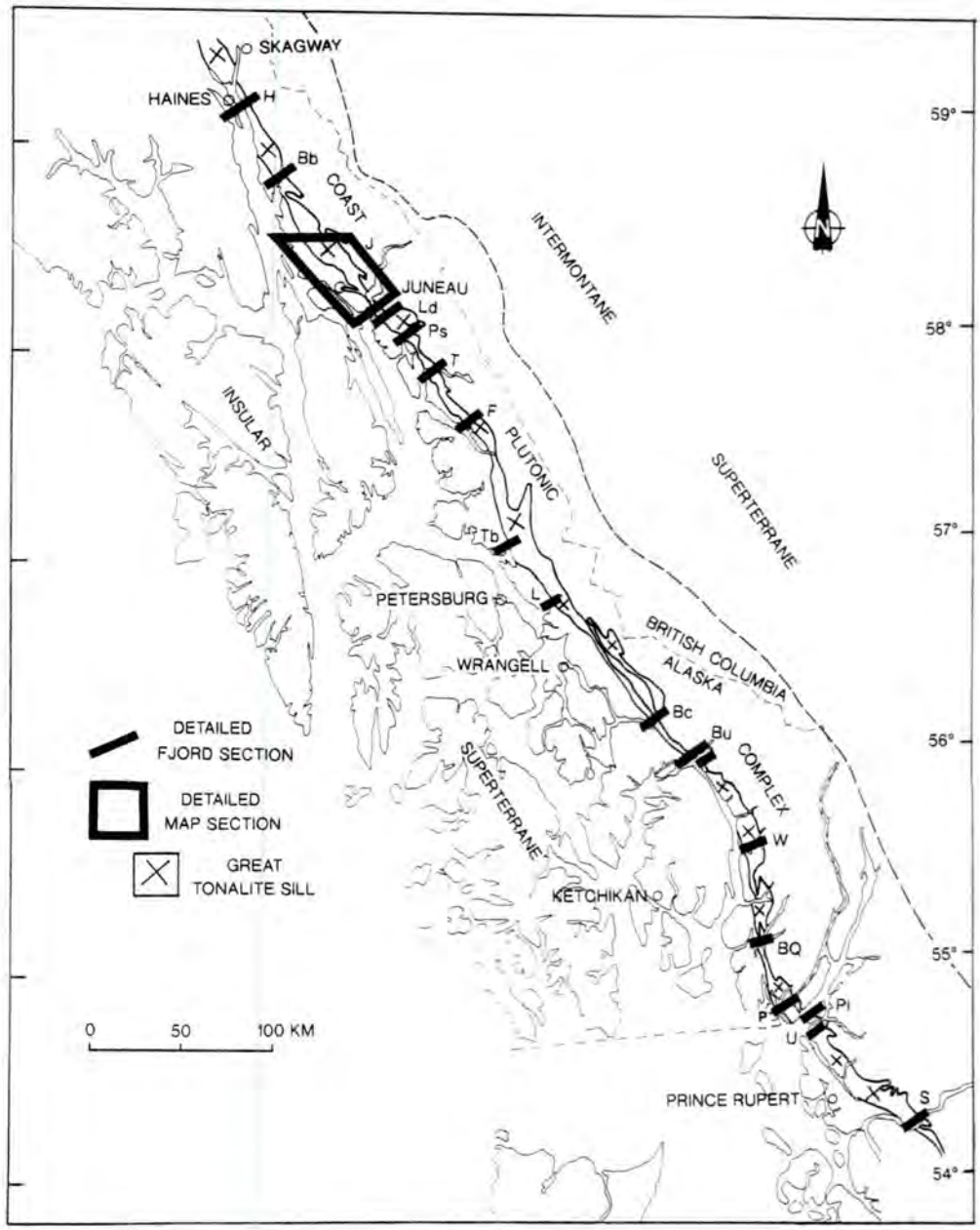

Figure 2.4 Field areas and fjord transects visited during the this study. H=Haines, Bb=Berners Bay, J=Juneau area (includes Taku Inlet), Ld=Lake Dorothy, Ps=Port Snettisham, T=Tracy Arm, F=Ford's Terror, Tb=Thomas Bay, L=LeConte Bay, Bc=Bradfield Canal, Bu=Burroughs Bay, W=Walker Cove, BQ=Boca de Quadra, P=Pearse Canal, Pi=Portland Inlet, U=Union Inlet, S=Skeena River.

CHAPTER 3
THE GREAT TONALITE SILL: STRUCTURE AND DEFORMATION

The following sections include structural and petrographical descriptions of individual traverses through the rocks of the Great Tonalite Sill, carried out by the author over 420 km of strike, between Herbert Glacier, Juneau, to Walker Cove, adjacent to the Behm Canal, near Ketchikan. Additional work, summarised in Hutton & Ingram (1992) and Ingram & Hutton (in prep.), extends the coverage of the Great Tonalite Sill rocks to Haines, in the north, and the Skeena River, British Columbia. The traverses took place mostly along the well-exposed flanks of glaciers and along the shorelines of fjords, but additionally the mountain ridges above the dense belts of Sitka Spruce forests provided good access to the rocks.

Juneau, and its environs (fig. 3.1), is the area in which a large amount of the field data acquisition took place. Excellent exposures of the Great Tonalite Sill occur, and were studied, along the flanks of Herbert, Mendenhall and Lemon Creek glaciers; on Mount Juneau, its flanks and adjacent valleys; along Vesper Peak ridge; and along the shores of Taku Inlet.

3.1 Juneau area: Taku Inlet

3.1.1 *Overview*

The most detailed work in this study was carried out at Taku Inlet (SE of Juneau), which traverses 30km across the well exposed, composite plutons of the

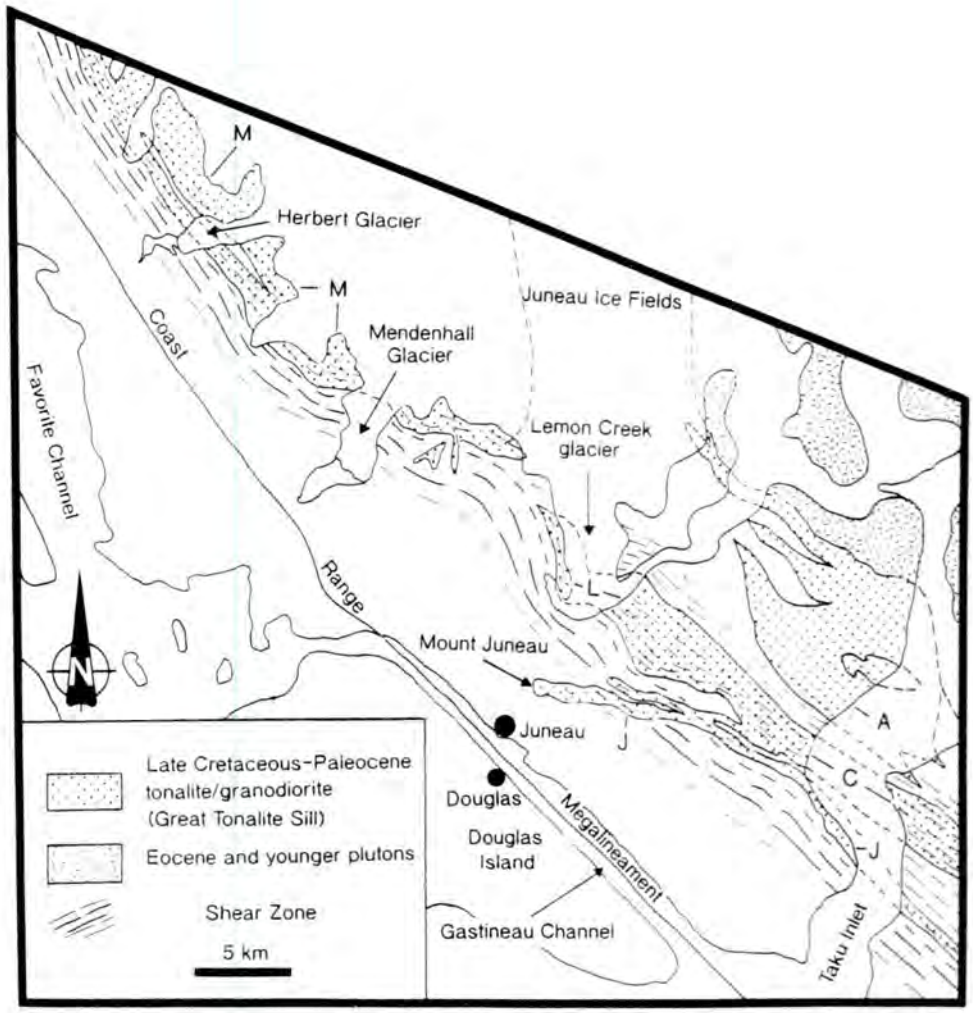

Figure 3.1 General geology map of the Juneau area: M=Mendenhall Glacier pluton, L=Lemon Creek Glacier pluton, J=Mount Juneau pluton, C=Carlson Creek pluton, A=Annex Lakes pluton.

Great Tonalite Sill belt (fig. 3.2 - fold out map at the end of section 3.1). These comprise (from SW to NE; all dating by conventional U-Pb method on zircon size fractions): The **Mount Juneau pluton**, dated at 81Ma (Wooden, written communication to Brew, 1990) and 72Ma (Gehrels et al. 1991a). This is a strongly foliated, garnet-bearing, hornblende-biotite tonalite body, with a maximum width of c.1km, which is composed of at least 11 steeply NE-inclined sheets separated by metasediment screens. The **Carlson Creek pluton**, dated at 66Ma (E part) and 67Ma (W part, Gehrels et al. 1991) is a similar, garnet-bearing, hornblende-biotite and biotite-hornblende tonalite, which is c.2.5km wide and is separated from the Mount Juneau pluton by a c.0.6km wide psammite gneiss screen. To the NE of this, the **Annex Lakes pluton** (59Ma, Gehrels et al. 1991a), which is c.8.5km wide at its widest point and separated from the Carlson Creek pluton by a 0.5-1.0km wide quartz-biotite-hornblende schist and migmatite screen, is a sphene-bearing, hornblende-biotite granodiorite. Emplaced within this is a possibly different unit, the Flat Point pluton (Drinkwater et al. 1990). To the NE, this late Cretaceous Tonalite Sill belt is cut by other Tertiary units, including the Turner Lake and Taku Cabin plutons.

For reference, figure 3.3 provides petrographical results from the modal analysis of various samples from the plutons in Taku Inlet, calculated from point counting thin sections. The quartz, plagioclase and alkali feldspar components have been normalised to 100% and then plotted on a Streckeisen (1973) diagram. This diagram is a convenient method of classifying granitic rocks and results from the work of Drinkwater et al. (1990) are illustrated in this plot.

Fabrics. These plutons and the immediate country rocks to the southwest are variably deformed by a steeply NE-inclined main foliation with a remarkably consistent down-dip (nearly 90° pitch angle) mineral stretching lineation. The earliest deformation in each pluton is represented by a Pre-Full Crystallization (PFC) or magmatic state fabric, which is defined by a planar and, within the foliation, a linear alignment of euhedral laths of plagioclase and amphibole. After crystallization, Crystal Plastic Strain

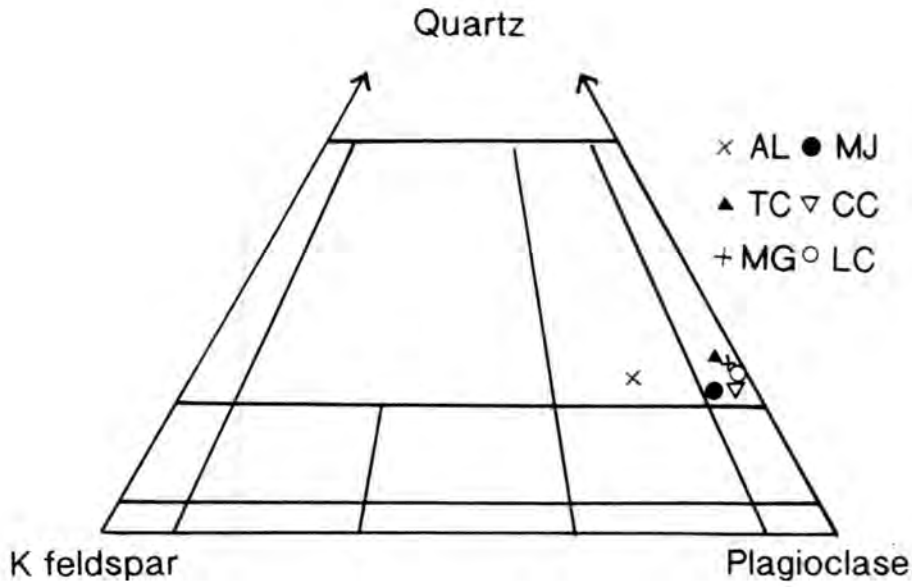

Figure 3.3 Streckeisen (1973) petrological classification diagram showing the average modal compositions of the main plutons in Taku Inlet (based on point counting thin sections): AL=Annex Lakes pluton, TC=Taku Cabin pluton, MG=Mendenhall Glacier pluton, MJ=Mount Juneau pluton, CC=Carlson Creek pluton, LC=Lemon Creek Glacier pluton (from Drinkwater et al. 1990).

(CPS) or solid state fabrics developed and overprinted the PFC fabrics to varying degrees (see section 1.3).

Fabric types vary from pluton to pluton, with the strongest solid state CPS foliations located in the Mount Juneau pluton, which include locally porphyroclastic mylonites. Pervasive CPS fabrics and structures are less important in the Carlson Creek pluton and the main fabrics are of the PFC type, but strains close to its southwest contact are high. The youngest of the three, the Annex Lakes granodiorite, is the least deformed pluton and exhibits PFC/magmatic state fabrics and shears, with minor CPS deformation from time to time. Within the country rocks, especially to the SW of the Sill rocks, strong fabrics and stretching lineations, identical to those in the plutons, are developed. The lineations are often defined by high grade metamorphic minerals e.g. sillimanite.

Shear sense. Foliation parallel shear sense indicators, associated with the steep CPS fabrics and lineations, are well developed both in the plutons and adjacent (particularly to the SW) country rocks. These include: crystal pressure shadows (sigma porphyroclasts/blasts), extensional crenulation cleavages, discrete ductile shears and asymmetric boudins, and show a consistent top-to-the-SW movement. This is especially the case with the most pervasive, grain scale, features (fig. 3.4). These structures are overprinted by a set of larger, conjugate, reverse ductile shears dipping both NE and SW. Also seen are less frequent N-S trending dextral and approximately E-W trending sinistral shears, which appear penecontemporaneous with the conjugate reverse structures.

PFC lock-up shears. Shear sense in the magmatic state is provided by discrete shears defined by euhedral laths of amphibole and plagioclase, which swing into parallelism with the shear plane. The shears are between 10cm and 1 m long and the width of the zone of deflection is 2-3cm. The euhedral laths in the medial shear plane are in general not affected by CPS strains, although, due to interaction between grains,

gure 3.4 Deformed appinitic country rock exhibiting top-to-the-SW (right) shear sense, from the southwest of Mendenhall Glacier pluton, west of Mendenhall Glacier. Field = 18 mm.

there is a minor amount of subgraining and quartz with strained extinction (see section 4.2 for further microstructural descriptions). As most of the deflection of these crystals is achieved by free rotation, with only this very minor solid state deformation, they are considered to have formed in the magmatic state at, or close to, the rheological critical melt percentage (RCMP, Arzi 1978; 30-35% melt, van der Molen & Paterson 1979; fig. 3.5). These types of structures have been defined as "lock-up shears" (Ingram & Hutton, in prep). They occur when, because of increasing crystal content, the deformation may suddenly switch from pervasive aligning of crystal laths to the development of discrete planar shear zones at an angle to the main crystal alignment. Further deformational aspects of these structures are discussed in sections 3.12 and 3.13.

Strain. Qualitatively, the intensity of the deformation associated with this intrusive event is low in the country rocks and higher in the Great Tonalite Sill belt, especially at its SW edge. This is borne out by strain analysis of the deformed shapes of lava pillows and pillow breccia, in the country rocks, and cogenetic mafic enclaves in the plutons. A more detailed interpretation of these data is presented in section 3.1.2, later in this chapter.

The following subsections offer detailed descriptions of each individual pluton in Taku Inlet, concentrating on contacts, intrusive relationships, fabrics, shears, shear sense and qualitative aspects of strain in each case. Each of the plutons will be described in a manner designed to stress the spatial distribution of the features. Two traverses of Taku Inlet, on the west and east shores, were carried out in order to obtain two representative sections through each of the plutons. Each pluton - traceable from shore to shore across the inlet - was accessible by virtue of continuous shoreline exposures between spring high and low water marks. In the following descriptions, features which can be correlated between traverses will be discussed together. To aid understanding of the accounts, reference should be made to figure 3.2, which

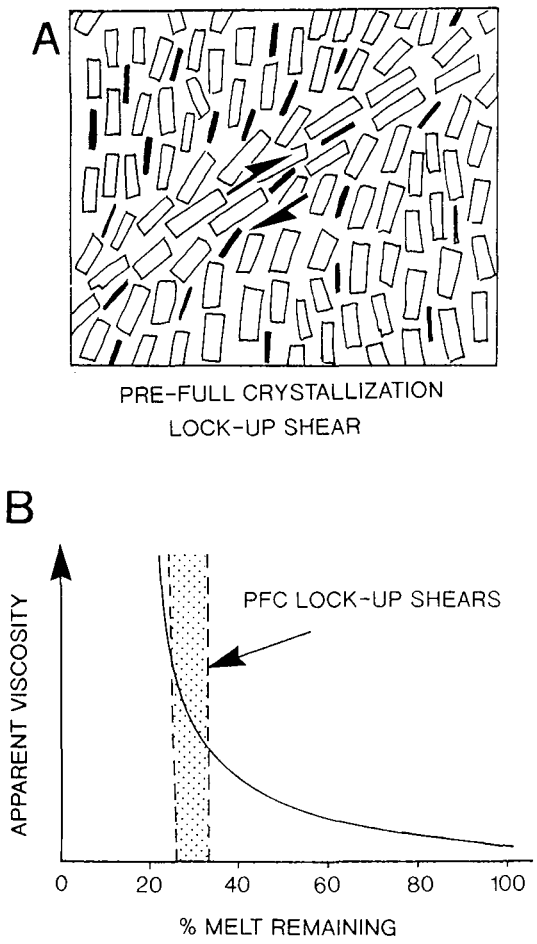

Figure 3.5 Development of pre-full crystallization lock-up shears in relation to crystallization state in granitoids. A. A top-to-the-right PFC lock-up shear in profile. Rectangular crystals are feldspar phenocrysts and thin black crystals are mafics. B. Occurrence of PFC lock-up shears in relation to melt percentage present. Graph is similar to that used by Arzi (1978) and van der Molen & Paterson (1979).

illustrates the various locations referred to in the text by means of a fold-out map at the end of this section (section 3.1). More detailed maps illustrating the most important structural data are also enclosed for reference, and these may be found in the back pocket of this thesis (maps 1 - 5).

3.1.2 *Mount Juneau Pluton.*

Country rocks. One kilometre to the southwest of the contact with the Mount Juneau pluton, at location 98, the quartz-biotite schists and pelites, of the middle to late Triassic Taku assemblage, contain steep NE-dipping cleavages, which are axial planar to tight, short wavelength, southwest vergent folds, whose hinges plunge to the south. These steep cleavages overprint and transpose shallower fabrics dominating in the areas to the west and representing earlier ?D_1 deformation increments, which were incurred during the same deformation interval. Therefore the steeply NE dipping fabrics essentially represent D_2 deformation, which can be seen to cut the D1 fabric in an S-C relationship, indicating top-to-the-SW shear sense. Bands of amphibolite (cogenetic with the tonalite) occur parallel to the steep D_2 foliation, and these become more common on approaching the southwest edge of the pluton. Adjacent to the pluton's southwestern contact, folds plunge steeply eastwards, in places subparallel to the strong stretching lineation (e.g. locations 104-106). This is interpreted as fold axis rotation due to the high strains in the rocks immediately west of the sill.

Intrusive rocks. Figure 3.6 shows the contact between the country rocks and the tonalite at location 106. The contact is concordant with the steeply NE dipping CPS foliation, the development of which is strong and, locally, mylonitic. It is extremely difficult to detect relict PFC fabrics within this pluton as they are so strongly overprinted by the later CPS fabrics. Figure 3.7 shows the highly deformed tonalite in the field, at location 195, emphasising the strong, 90° pitching, stretching lineation.

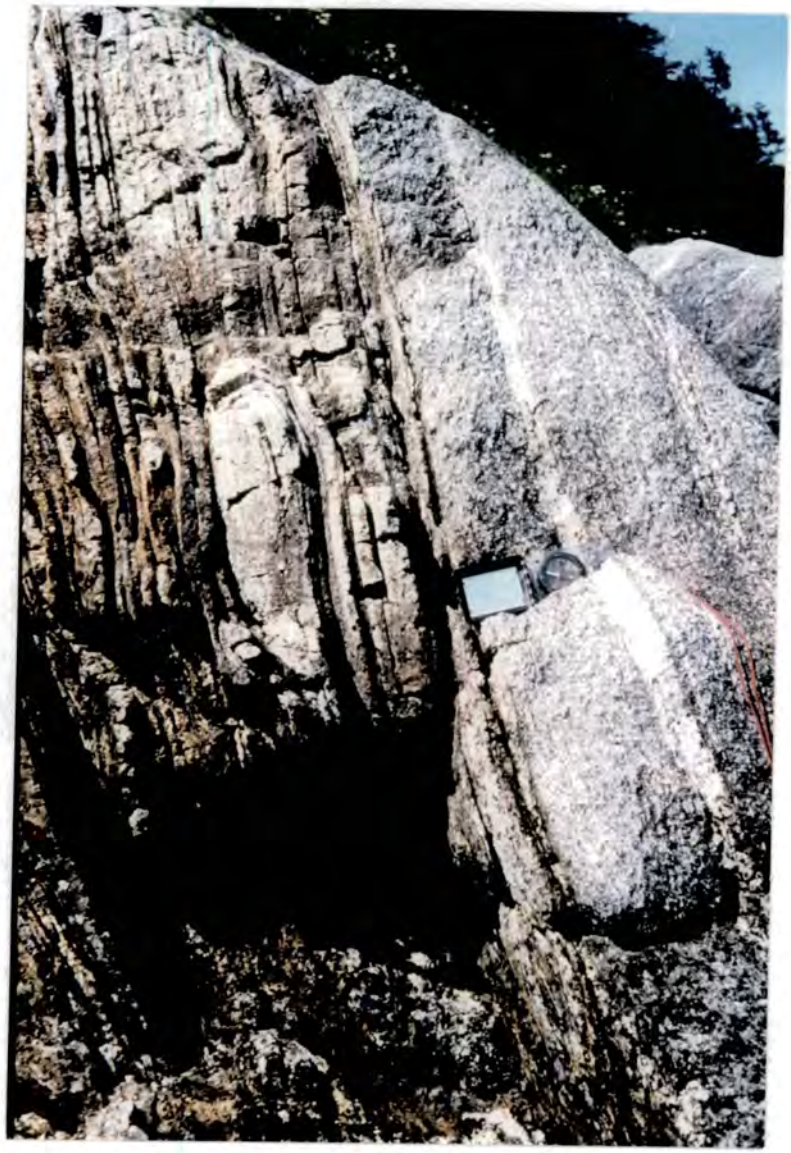

Figure 3.6 Contact between the Mount Juneau pluton, to the NE, and the country rock psammites, to the SW. Location 106, Taku Inlet.

Figure 3.7 Deformed tonalite from the Mount Juneau pluton, exhibiting an almost 90° pitching CPS stretching lineation. Location 195, Taku Inlet.

Synplutonic dykes within the tonalite near the contact have been folded into tight folds, which have hinges plunging subparallel to the stretching lineation.

Sheeting. Considering first the western shoreline traverse, the pluton contains numerous screens of metasediment at its southwestern and northeastern contacts, indicating an emplacement style dominated by sheeting. However, on the eastern shores of Taku Inlet, a complete xz profile section of the Mount Juneau pluton is spectacularly exposed and a total of eleven, clearly discernible, tonalite sheets and associated metasediment screens, together extending in profile for 350 metres, were recorded. Figure 3.8 illustrates these sheets and screens by means of a line drawing taken from a collage of photographs. Measurements taken from this tracing indicate that the pluton is composed of 84% tonalite sheets and 16% country rock screens, by width. Clearly, this exposure is thinner and has a more sheeted nature than that seen on the western shore, implying that the pluton probably tapers to the southeast, eventually forming a lateral termination. In addition, the pluton here is pervasively deformed by much stronger CPS to porphyroclastic mylonitic fabrics.

Shear sense. The most reliable, pervasive, shear sense indicators in all the plutons occur at the grain scale e.g. σ porphyroblasts. However, at and adjacent to the southwest contact of the Mount Juneau pluton, there are good examples of discrete, late stage, CPS/solid state shears, which are in agreement with the crystal scale shear sense of top-to-the-SW. Also adjacent to the contact, are highly deformed quartz-biotite-hornblende-garnet schists, surrounding asymmetric boudins of amphibolite with top-to-the-SW shear sense, and NW-SE trending sinistral shears. Location 116 is also adjacent to the contact, but here there are NW-SE trending dextral shears, which have been intruded by late melt (fig. 3.9), interpreted here to have a cogenetic relationship to the Mount Juneau pluton tonalite. This interpretation is based on the following: 1) the melts lying along the shears are granitic/granodioritic, and commonly approach minimum granitic melt compositions, 2) anatexis of the country rocks and mixing and

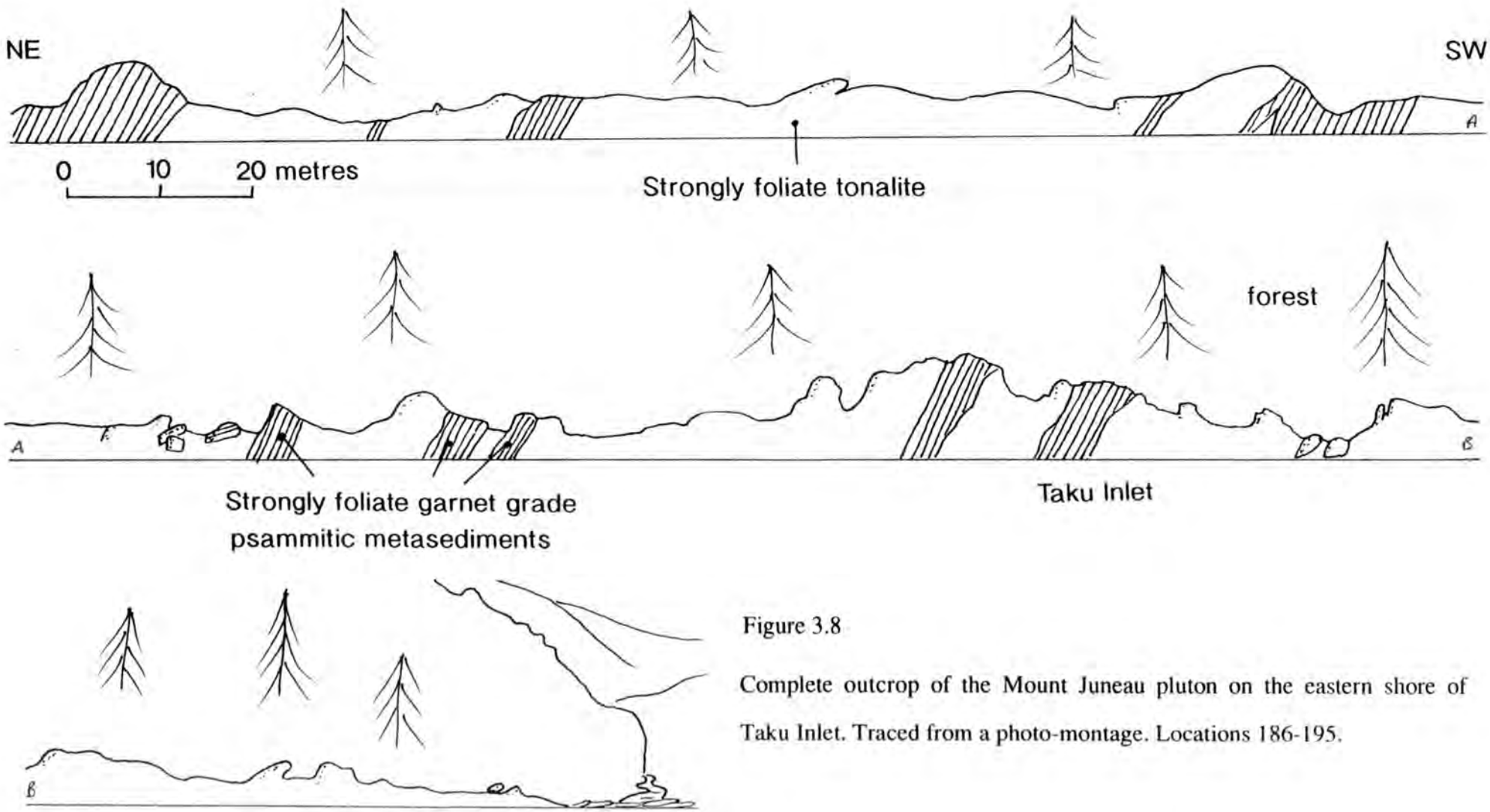

Figure 3.8

Complete outcrop of the Mount Juneau pluton on the eastern shore of Taku Inlet. Traced from a photo-montage. Locations 186-195.

mingling of such melts with the invading tonalite would be likely to create such compositions, 3) the melts are not deformed to the same degree as their wall rocks and commonly exhibit PFC/magmatic state fabrics, and 4) the shears hosting the melts are arranged in conjugate sets, which indicate NE-SW orientated shortening (see later discussion). This scenario is similar to that indicated by the D_2 foliation associated with the emplacement of the great tonalite Sill.

Further to the northeast, away from the contact, large (up to 3 m wide) boudins of tonalite, themselves enclosed by tonalite, occur at location 110, which again indicate top-to-the-SW shear. However, reverse, top-to-the-NE, discrete CPS shears are also present, the best example of which, measuring 15 metres long and dipping steeply southwest, was observed at location 113.

3.1.3 *Carlson Creek pluton.*

Country rock. The pluton is separated from the Mount Juneau pluton on the western shore by a 0.6 km wide screen of metasedimentary country rock and on the eastern shore by a 1.6 km wide "migmatite" zone of partially melted country rocks and irregular foliation parallel sheets of tonalitic/granodioritic composition. The metasediments on the western shore, observed at locations 120 and 121, are interbanded quartz-biotite schists, hornblende schists and quartzites. On the eastern shore, the country rock (locations 182, 183, 185) is distinctly migmatitic in appearance: a matrix of dominantly granodioritic rock, whose appearance indicates that it was not fully crystallized during deformation, encloses various blocks of country rock, ranging from folded, garnetiferous metasediments to irregular blocks of banded gneiss. The rock at location 183 in fact resembles the tonalite seen farther north within the boundary of the Carlson Creek pluton, previously mapped by Brew & Ford (1977), and in addition contains mafic enclaves. Also contained within this migmatitic separation zone are large rafts of metasediment, composed of quartz-biotite-

hornblende schists, which contain folded diopsidic layers probably representing metamorphosed calc-silicate bands.

Intrusive rocks. On approaching the southwestern contact with the Carlson Creek pluton, thin, concordant, centimetre thick sills and concordant veins of tonalite become evident, and these increase in density until the main contact is reached. The contact is sharp and concordant with the steep NE dipping CPS foliation and no discordant intrusive features are in evidence. The Carlson Creek pluton itself measures approximately 2.5 km wide and is composed of hornblende biotite tonalite (see fig. 3.10) with a relatively homogenous composition, which encloses many rafts of metasediment. At the southwest contact, the tonalite is weakly deformed by crystal plastic strains. This weak component is generally exhibited by elongated quartz crystals and slightly rounded, aligned, feldspars, which define the main foliation. The foliation dips steeply northeast throughout the pluton and in many places this is strongly emphasised by the alignment of elongate mafic enclaves and metasedimentary xenoliths. Northeast from the contact area, the crystal plastic strain (CPS) component diminishes and the foliation and weak down-dip lineation are marked mainly by the PFC alignment of internally undeformed plagioclase and amphibole laths (e.g. locations 122 and 181). In this area, structures indicative of magmatic sedimentation (see fig. 3.11, location 176) exist in addition to partially melted metasedimentary xenoliths, which were sheared and deformed contemporaneously with PFC fabric development. Xenocrysts of plagioclase occur within some of the more highly melted and deformed metasedimentary xenoliths, indicating magma mingling.

In the centre of the pluton CPS strains again become more important. Here the coarse tonalite contains a CPS foliation marked by elongated quartz and biotite crystals, and an alignment of rounded off feldspar laths (e.g. locations 180, 123). The NE-dipping foliation is strongly developed and within this is a pronounced down-dip lineation. Metasedimentary rafts and xenoliths are common and mixing between partial melts from these and the the dominant tonalite has, locally, resulted in a highly

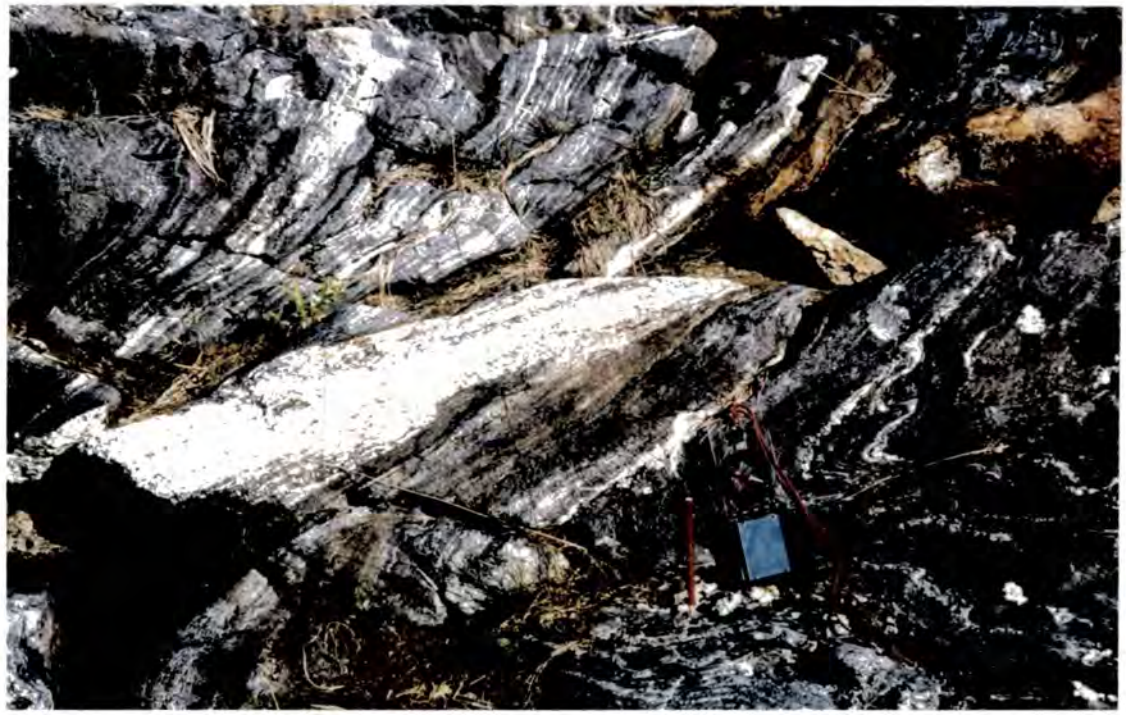

Figure 3.9 Melt filled dextral shear in psammites. Location 116, Taku Inlet.

Figure 3.10 Homogenous hornblende-biotite tonalite of the Carlson Creek pluton. A sheared mafic enclave has its long axis parallel to the main foliation, to the right of the picture. Location 124, Taku Inlet.

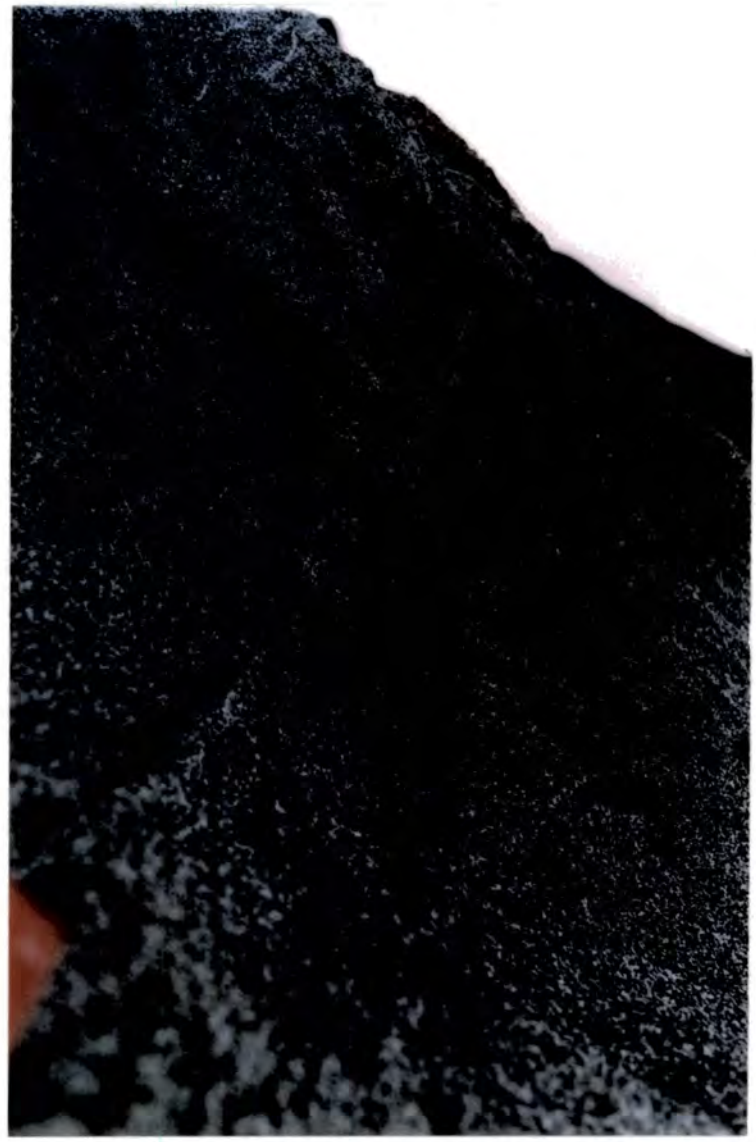

Figure 3.11 Magmatic sedimentation (scour channel) structure, trending top right to bottom left. Carlson Creek pluton, location 176, Taku Inlet.

garnetiferous, hybrid quartz-biotite-plagioclase-garnet rock. Within the larger rafts of metasediment, very large poikiloblastic garnets measuring up to 7 cm in diameter occur. At location 123, the tonalite has a banded appearance due to the abundance of streaked out xenoliths of mafic and metasedimentary composition. Here, and elsewhere in the pluton, many thick, shallow-dipping, cogenetic, granite pegmatite sheets occur, which cut across all the previous structures. Generally, they dip very gently eastwards and at location 175 these are particularly abundant, constituting more than 25% of the outcrop in vertical section. The high density in number, as well as their compositional uniformity, implies that these sheets were emplaced during a period of vertical extension, probably related to rapid uplift, late in the history of the Great Tonalite Sill. Moving towards the northeast, away from these locations for 100 m and more, the mask of crystal plastic strain is once again removed from the original PFC fabrics. The orientations of the relict PFC fabrics indicate that they are coplanar with the overprinting CPS fabrics.

Sheeting/emplacement features. Although the northeastern and southwestern contacts of the Carlson Creek pluton both exhibit sheeting, the northeastern contact is characterised by the presence of xenoliths, large metasediment rafts, mafic enclaves, dense vein networks, deformed tonalite sheets and boudins. The conctact zone exposed on the western shore (locations 125,126) contains a dense network of granitic veins, which have isolated many small blocks (average 0.5 - 1.0 m diameter) of Carlson Creek tonalite to form xenoliths. In addition, many xenoliths of metasediment have been created. It is possible that the granitic melt which intruded along these veins represents a partial melt, derived from the adjacent metasediments during intrusion of the Carlson Creek pluton, which re-intruded the tonalites.

Shear sense. In the southwestern contact area, solid state/CPS shears cut the foliation and these include top-to-the-NE and -SW reverse shears, and NW-SE trending dextral and WNW-ESE trending sinistral shears. The significance of these

conjugates will be discussed in section 3.1.5. In central parts of the body, asymmetric tails on deformed metasedimentary xenoliths indicate both reverse top-to-the-SW and a component of sinistral shear sense, within a plane subparallel to the foliation. Other shears include a steep top-to-the-NE reverse CPS shear, intruded by late but cogenetic melt, and ESE-WNW trending sinistral CPS shears. The presence of symmetrical boudins of sheeted tonalite at the northeastern contact, indicates that a pure shear component is dominant in this area and the lack of clear shear sense indicators corroborates this. Vertical extension is also important as strains are high enough at the contact to rotate fold axes, preserved in the rafts of metasediment, into parallelism with the main down-dip stretching lineation.

3.1.4 *Annex Lakes pluton.*

The Annex Lakes pluton lies to the northeast of the Carlson Creek pluton, and is separated from it by a 0.5 - 1 km wide zone of metasedimentary gneiss and migmatite. From the map (fig. 3.2) it can be seen that the Annex Lakes pluton is very well exposed on the western shore of Taku Inlet, whereas the eastern shoreline contains only two patches of granodiorite, which have been correlated with the main body by Brew & Ford (1977). In the following descriptions, the western traverse through the pluton will be dealt with first, followed by a detailed description of the eastern traverse through the host migmatites.

(1) Western traverse

Country rocks. The region between the Annex Lakes and Carlson Creek plutons is occupied by partially mobilised or migmatitic country rocks, enclosing rafts of hornblende-biotite-quartz schist. There is abundant evidence for deformation whilst these rocks were still in a partially molten state, especially near the southwest contact, in the form of attenuated "stringers" of mobilised mafic material, interpreted to have

originated from synplutonic dykes (see fig. 3.12, location 127). In addition, other more competent layers of banded mafic rock have been boudinaged and irregularly disrupted within a less competent, flowing, "mobilised" matrix of felsic, partially melted country rock.

Intrusives. The southwestern contact (locations 128,129) is highly veined and sheeted (fig. 3.13) and there is a dense population of metasediment sheets and rafts, which are concordant and lie parallel to the weak NE dipping foliation and down dip lineation. However, 100 m to the northeast the fabrics become more pronounced, before diminishing in strength again northeastwards (from location 130 to 132), where they are defined mainly by WNW-ESE striking and steeply NE dipping, non-lineated, PFC fabrics and the long axes of elongate mafic enclaves. This area is also characterised by the abundance of foliation-parallel, metasedimentary screens, dominantly composed of quartz-biotite-hornblende schists and quartzites, and centimetre to metre scale granodiorite sheets. The rafts and screens of metasediment formed more competent septa and at intervals have been offset by shears at intervals and deformed into asymmetric boudins. In addition to the metasedimentary screens, the sheeting features in the pluton at location 108 involve: (1) relatively thick (50 - 60 cm) bands of dioritic composition and (2) screens of interbanded medium grained tonalite and diorite, running parallel to the foliation.

Flat Point Pluton. A finer grained, more felsic variety of granodiorite occurs on approaching the Flat Point pluton (location 132): a body which Brew & Ford (1977) Drinkwater et al. (1990) regarded as a more homogenous, weakly foliated core zone to the Annex Lakes pluton. At the boundary to this core zone (as interpreted by Brew & Ford 1977), there is an abundance of more mafic bands alternating with granodiorite. Coarse dioritic enclaves, metasedimentary rafts, many shallow-dipping granite sheets and pegmatite veins also concentrate in this area. Within the boundary of the core zone, coarse grained, porphyritic biotite granodiorite is the characteristic rock

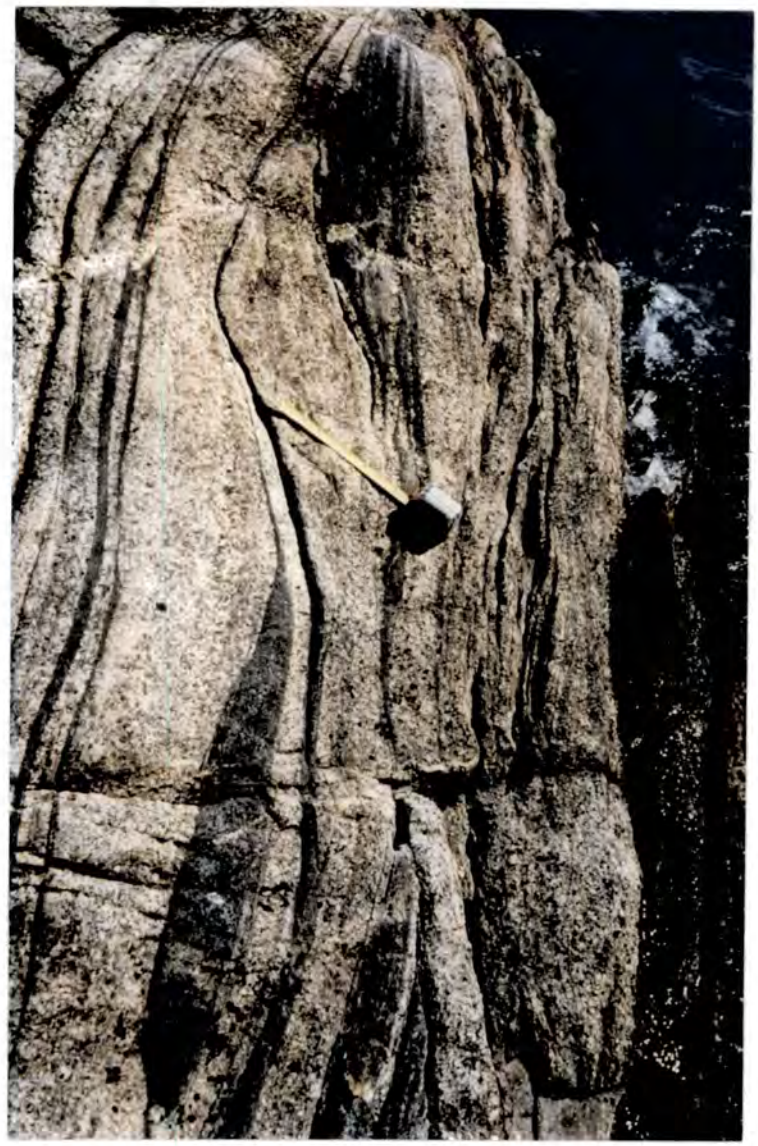

Figure 3.12 Attenuated synplutonic dyke material. Annex Lakes pluton. Location 127, Taku Inlet.

Figure 3.13 Foliation-parallel metasediment septa (dark) and granodiorite sheets. Location 131, Annex Lakes pluton, Taku Inlet.

type of the Flat Point pluton "facies". The foliation is marked by a weak, almost vertical NW-SE striking PFC fabric commonly emphasised by elongate mafic enclaves. In general, the core zone is weakly deformed, containing only PFC fabrics and, locally, undulose irregular banding caused by more mafic alternations within the granodiorite. A glimpse of the possible pre-emplacement structural trend is provided by large raft of quartzite (location 135), which exhibits a relict cleavage dipping steeply SW. The central part of the core zone exhibits complex relationships between: (1) felsic metasedimentary gneiss, which hosts (2) angular blocks of coarse grained diorites, and (3) Flat Point pluton facies granodiorite, which hosts (4) coarse grained granodiorite typical of the SW part of the Annex Lakes pluton. In addition, a large, 10-15 m diameter, locally pegmatitic, appinite xenolith occurs in this area (location 144) which may represent initial intrusives in the Great Tonalite Sill belt.

A traverse across the NE boundary of the Flat Point body, as mapped by Brew & Ford (1977), indicated that a gradational contact exists between coarse grained biotite granodiorite, to the northeast, and porphyritic medium-coarse grained biotite granodiorite within the core zone. Additionally, there is an abundance of metasedimentary rafts, xenoliths and thin irregular, discordant granitic veins in the vicinity of the contact, indicating that it, like the southwestern contact, may mark the location of a country rock septum separating large granodiorite sheets.

The remainder of the Annex Lakes pluton, from the Flat Point pluton to the northeastern contact, is composed of non-porphyritic, coarse grained, biotite granodiorite, which is more mafic compared to the granodiorite of the southwestern part of the pluton. Locally, however, granite occurs e.g. locations 149 and 150, in which a strong CPS foliation is evident. The section is, in general, dominated by the presence of many metasedimentary rafts and large xenoliths, which include quartz-biotite schists, calc-silicates and marbles and are either (1) angular and resemble stoped blocks, or (2) intruded by granodiorite sheets to form foliation parallel screens.

Shallow dipping, cross-cutting, pegmatite sheets (fig. 3.14), although common throughout the whole Annex Lakes pluton, are abundant in the NE area.

Shear sense. At the pluton's southwest contact, asymmetric boudins which cut the main foliation, indicate dominant top-to-the-SW reverse shear. Implied components of E-W and NW-SE orientated sinistral shear occur here, in the form of sheared metasedimentary xenoliths and discrete CPS shears, but the vergence of some tight folds in a metasediment raft also suggests a component of dextral shear in a zone trending NNW-SSE. Many late subhorizontal or shallowly NE dipping coarse granite sheets at the contact cut across the earlier features, and the walls of these commonly indicate either extensional- or reverse-top-to-the-SW shear. In the area southwest of the Flat Point pluton, boudinaged rafts and screens of metasediment, and more competent dioritic and tonalitic bands, within the granodiorite, have been dextrally offset. At location 108 this has occurred in a spectacular domino fashion, associated with PFC lock-up shears (fig. 3.15). In addition to the transcurrent shears, both top-to-the-SW and -NE reverse shears affect the banding in this general area. The remainder of the Annex Lakes pluton, to the northeast of the core zone, contains CPS shears and structures generally indicative of subhorizontal, NE-SW orientated, pure shear, most importantly: (1) discrete, conjugate reverse shears (closely spaced) directed to the southwest and the northeast (fig. 3.16 & 3.17), (2) small wavelength, upright, CPS folds affecting the foliation, with implied southwest vergence, although this is on a small scale (fig. 3.18).

(2) Eastern traverse.

The eastern traverse exposes two mappable fingers of the Annex Lakes pluton granodiorite (fig. 3.2). The country rock into which the Annex Lakes rocks are intruded is older, more deformed, Cretaceous to Tertiary tonalitic gneiss. The former is represented by porphyritic granodiorite typical of the main Annex Lakes pluton and

Figure 3.14 Shallow-dipping granite pegmatite sheets cutting the main foliation. Location 108, Annex Lakes pluton, Taku Inlet.

Figure 3.15 PFC/magmatic state domino style deformation of a foliation-parallel dioritic band. Location 108, Annex Lakes pluton, Taku Inlet.

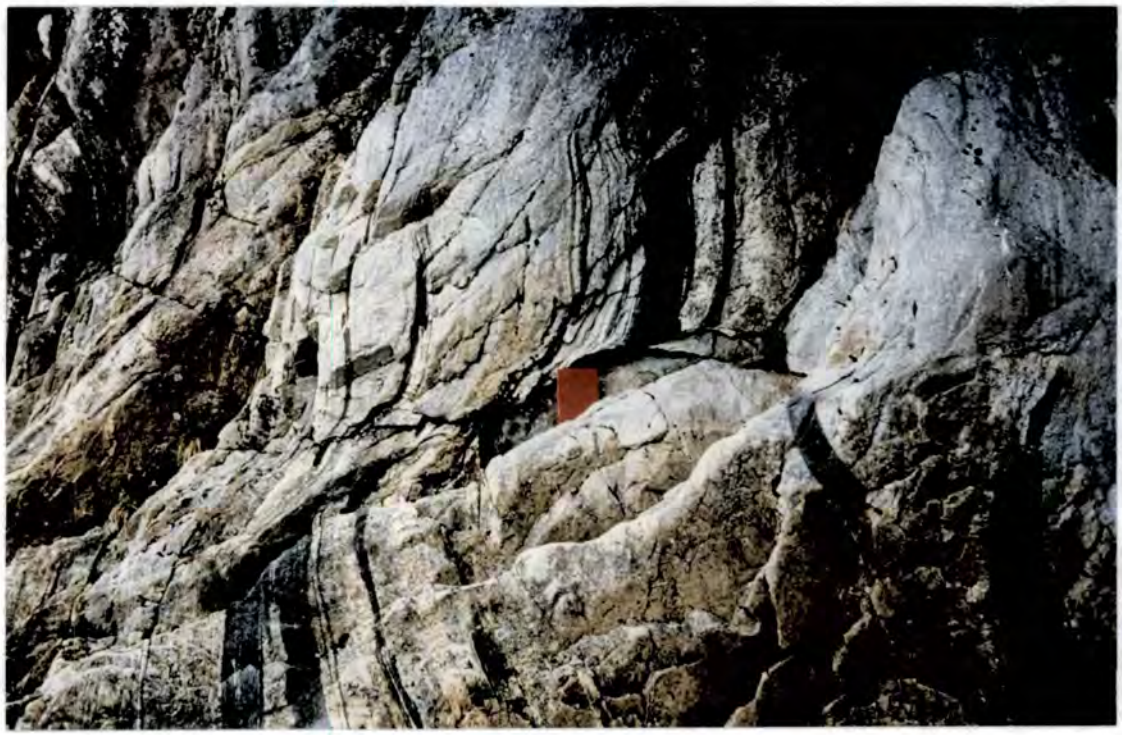

Figure 3.16 Shallow top-to-the-NE (right) ductile shear. Location 128, Annex Lakes pluton, Taku Inlet.

Figure 3.17 Conjugate reverse ductile shears. Rock face trends NE-SW. Annex Lakes pluton, location 151, Taku Inlet.

records only PFC deformational fabrics. Fabrics in both the country rocks and intrusives dip steeply northeast and are coplanar. Transport lineations in the tonalitic gneisses, when taken together with the evidence for dominant top-to-the-SW shear sense in the area, indicate a slight dextral component of movement. Screens of metasediment e.g. quartz-biotite-hornblende schists and blocks of older mafic material and synplutonic dykes occur throughout, giving the intrusives a very heterogenous and sheeted appearance (fig 3.19). Throughout this complete section, thick, subhorizontal sheets of granite and granite pegmatite cut across all previous features.

3.1.5 *Discrete CPS shears*

Figure 3.20 shows a summary equal angle stereonet of the shears from Taku Inlet. From this it can be seen that four dominant orientations of shears occur: top-to-the-NE and -SW reverse, NNW-SSE trending dextral and E-W trending sinistral. Taken together, the four dominant orientations of CPS shears recorded in Taku Inlet define a ***quadrimodal*** set (Woodcock & Underhill 1987, Underhill & Woodcock 1987) impling a $0<K<1$ strain (K defined by Flinn 1965) with NE-SW contraction (e.g. Hancock 1985, Underhill & Woodcock 1987). Timing of these late features is constrained by (a) the intrusion of a thin microdiorite (synplutonic) dyke along one such shear at location 170 (fig. 3.21) and (b) the more common occurrence of late stage, but related, granitic veins along the shears.

CPS shears are most abundant within the Annex Lakes body (e.g. fig 3.22) and its associated country rocks, where all four sets are equally represented. The Mount Juneau pluton does not have an abundance of shears, but two conjugate reverse sets are dominant, with top-to-the-SW shears in the majority. The Carlson Creek pluton has very few CPS shears. This distribution indicates that the quadromadal pattern of four conjugates, and therefore flattening strain, is dominant in the Annex Lakes pluton, whereas in the Mount Juneau pluton the pattern implies the increasing importance of a simple shear component.

Figure 3.18 Folded foliation. Location 151, Annex Lakes pluton, Taku Inlet.

Figure 3.19 Sheared intrusives and migmatitic host rocks from the eastern traverse through the Annex Lakes pluton and host gneisses. Location 170, Taku Inlet.

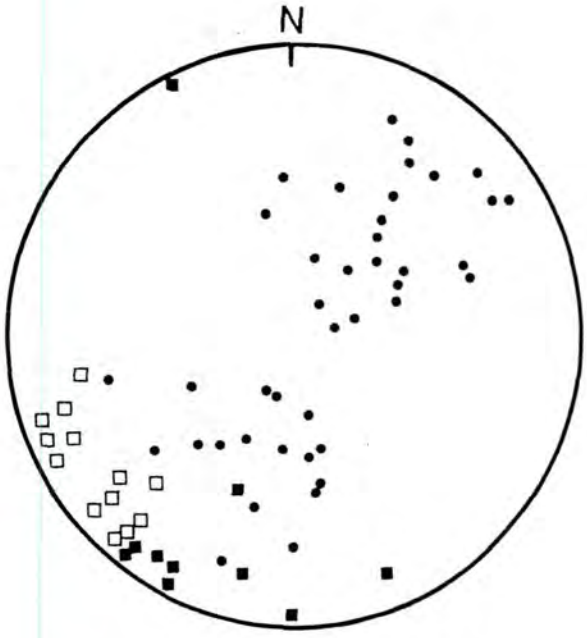

Figure 3.20 Equal area stereonet of the CPS shears from Taku Inlet: quadrimodal distribution implying 0<K<1 shear and NE-SW contraction. Solid circles = reverse shears, open squares = dextral shears, solid squares = sinistral shears (n = 65).

Figure 3.21 Mafic dyke emplaced along an E-W trending sinistral CPS shear. Location 170, Taku Inlet.

Figure 3.22 An example of N-S trending dextral shears cutting the main foliation. Location 168, Annex Lakes pluton, Taku Inlet.

3.1.6 *Taku Inlet: strain analysis*

At 25 locations along the Taku Inlet traverses (fig. 3.23), estimates of strain were made from the shapes of deformed objects (see section 1.4.1 for methodology), such as strained lava pillows, volcanic bombs (in the country rocks, fig. 3.24), and cogenetic mafic enclaves (in the plutons). Measurements for strain analysis were taken where possible, but at some locations strain markers were not present in high enough quantities to form a representative population, or the available rock faces were not at high enough angles to the main foliation and lineation, to permit accurate measurements. In these cases, qualitative estimates of strain were made, based mainly on fabric intensities, with reference to the fabric intensities in areas where strain markers were abundant. With these data it has been possible to construct a strain profile through the Great Tonalite Sill at Taku Inlet, starting from the country rocks near the Coast Range Megalineament (Gastineau Channel), to the southwest, and terminating within the younger Tertiary plutons, in the northeast.

As stated earlier, strain is higher, qualitatively, in the Great Tonalite Sill plutons than in the country rocks to the southwest. As the Sill is approached from the southwest, the country rock fabrics intensify northeastwards, culminating in a zone containing sub-mylonitic fabrics and steep transport lineations, at the southwest edge of the Mount Juneau pluton. Fabric intensities throughout the Taku Inlet section indicate that, in general, strains are concentrated along the flanks of plutons and their component sheets, indicating (1) a strong control imposed by rheological boundaries, and (2) that overall strain decreases towards the northeast, from a peak in the Mount Juneau pluton. Other qualitative data, such as the presence of magmatic sedimentation structures at location 176 (Carlson Creek pluton, see fig. 3.11) indicates that low strains may be present away from the rheological boundaries.

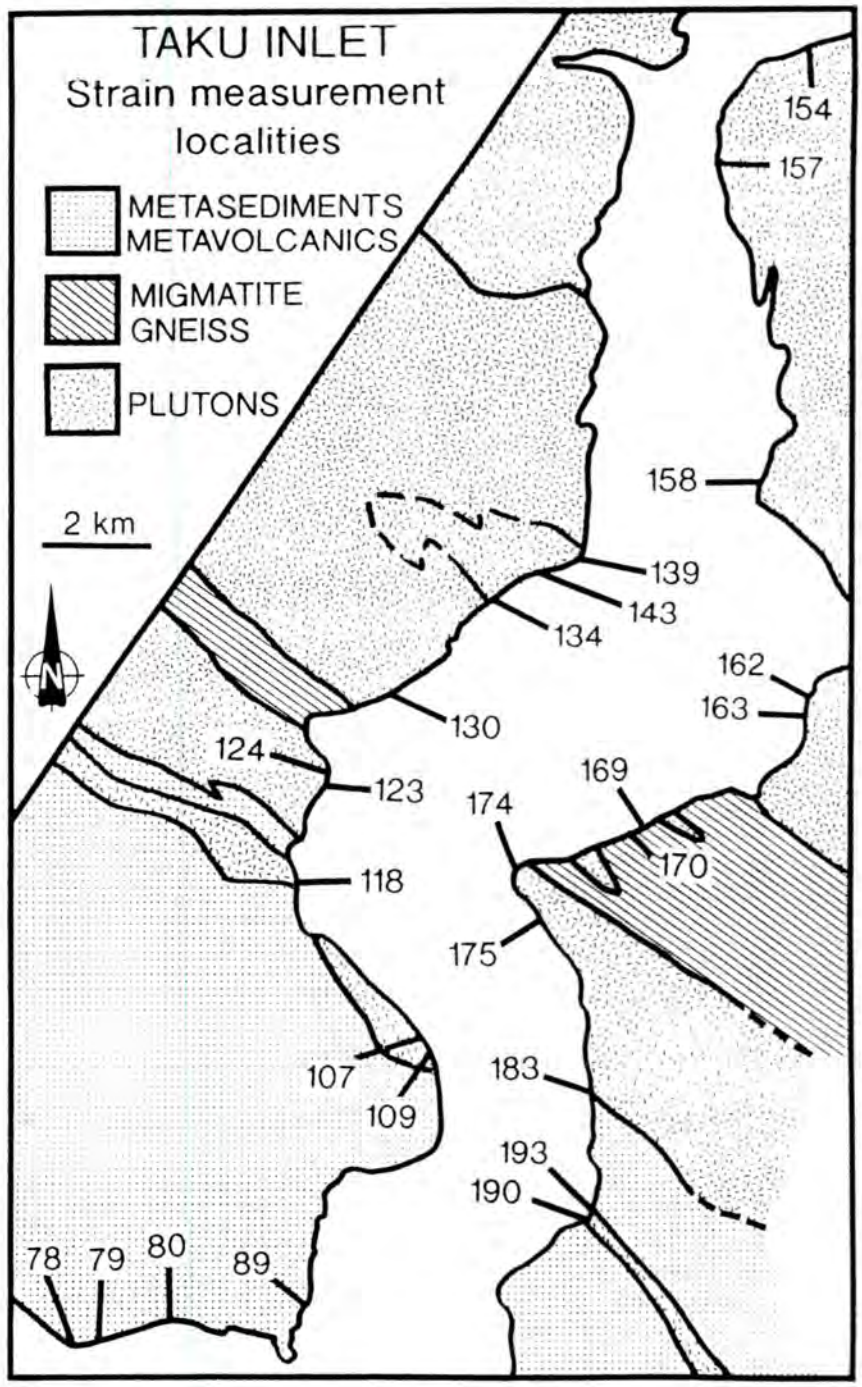

Figure 3.23 Strain measurement localities in Taku Inlet.

Results. Without taking into account likely differences in the initial shapes of the various strain markers used in this section, a profile of strain determinations has been obtained (fig. 3.25) across strike for some 20km and more. Section 1.4.1, in chapter 1, provided detailed information concerning the acquisition and methodology used by the author when studying populations of strain markers, such as deformed mafic enclaves in the plutons and deformed lava pillows and pillow breccias in the country rocks. Problems associated with the comparison of different sorts of strain markers were also discussed and it was concluded that, if the inferred initial shapes and initial alignments of the lava pillows in the country rocks are taken into account qualitatively, the x/z values for the country rocks probably represent overestimates of the strain. In addition, it was concluded that the harmonic means of the mafic enclave populations (commonly n = 30-34) in the plutons provided underestimates of strain. These conclusions therefore emphasise further the considerable difference between the very high strains in the plutons and the low strains in the country rocks.

In general terms, the strain profile shows low strains in the country rocks (around x/z = 4), which increase dramatically into the Mount Juneau and Carlson Creek plutons (values in the region of x/z = 14 - 25) and then diminish more gradually to the NE. Such a bell-shaped, asymmetric strain profile across the Great Tonalite Sill and its country rocks is typical of many shear zones (Ramsay & Graham 1970, Kligfield et al. 1981, Ramsay & Huber 1987). The x/z profile is complemented by K-values (K defined by Flinn 1965), which are very low (K ≅ 0.1 - 0.2) in the country rocks (probably reflecting oblate pre-tectonic initial shapes in the lava pillows and compactional strains in the volcaniclastics), which increase sharply towards 1 in the Mount Juneau pluton and then further NE decrease to lower values in the other plutons (K ≅ 0.05 – 0.35). The K≅1 strain component has been interpreted as a simple shear strain component concentrated and focused at the SW edge of the tonalite sill belt. This interpretation is based largely on the fact that in the Mount Juneau pluton, which lies at the SW edge of the Great Tonalite Sill belt, the K ≅ 1 component correlates with an abundance of top-to-the-SW reverse shears and pervasive, foliation

Figure 3.24 An horizontal section (XY) through lava pillows near Point Salisbury, Taku Inlet. These were used for the calculation of strain estimates.

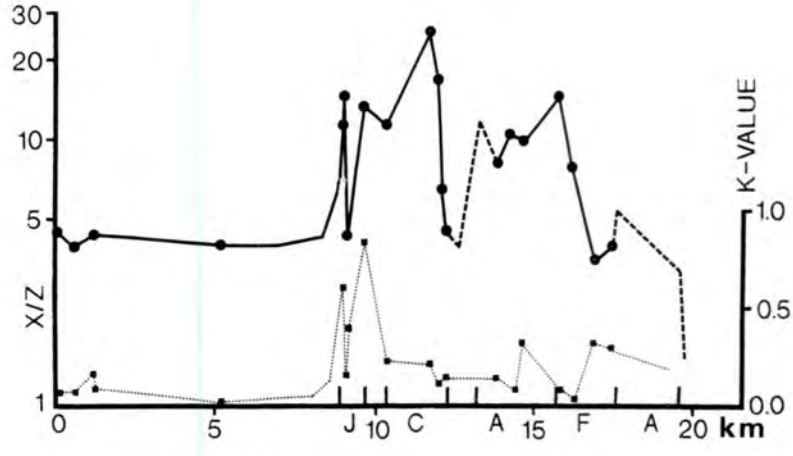

Figure 3.25 Taku Inlet: Superimposed plots of strain and k values versus distance, constructed using data from strained mafic enclaves, basalt pillows and volcanic bombs. J=Mount Juneau Pluton, C=Carlson Creek Pluton, A=Annex Lakes Pluton, F=Flat Point Pluton. Solid circles=X/Z values; solid squares=k-values.

parallel, reverse slip (simple shear) indicators. The plutons lying to the NE (Carlson Creek, Annex Lakes, Turner Lake), however, do not contain such unambiguous shear sense and commonly show features consistent with a pure shear regime, especially the Annex Lakes pluton (e.g. conjugate PFC lock-up shears, low K-values, CPS shears). The reduction in K-values to the NE of the Mount Juneau pluton is associated with an overall northeastward reduction in x/z strain (fig. 3.25). Expanding on this, it is clear from the strain profile in the NE area that strains increase at pluton internal and country rock contacts, although the K-values remain low. These particular flattening strain components are interpreted here to be associated with, and caused by, pluton intrusive wedging processes: replenishment of plutons in their central zone will cause deformation of the existing crystallizing magma outside and adjacent to these zones. At the pluton contacts, PFC strains are thus concentrated. However, there is also a tectonic flattening strain superimposed upon the whole system. Although in the early, synmagmatic stages it is difficult to differentiate between strain caused by wedging and that caused by the superimposed contractional flattening effects, the later CPS/solid state structures record only the tectonic component. These CPS shears are distributed in quadrimodal sets which have thus recorded $0<K<1$ strains. This component was probably incurred progressively throughout the complete emplacement and crystallization interval of the Great Tonalite Sill plutons in Taku Inlet.

This model implies spatial strain partitioning in a contractional, thrust sense, regime thus:

(1) NE over SW simple shear strain at the southwest edge of the Great Tonalite Sill,
(2) Flattening in the NE part of the Great Tonalite Sill, dying off to the NE.

In more detail, the profile provides information about strain distributions through the individual plutons. The ***Mount Juneau pluton*** profile (based on five strain determination localities, see fig 3.23) indicates that high strains are located at the pluton boundaries (x/z = 11 to 14.5) and that the cental portion is characterised by low

strains (x/z = 4.3). This implies that strain is concentrated at the rheological boundaries between the country rocks and the plutonic rocks. In addition, K values are higher here than anywhere else in the Taku Inlet section, implying that the strongest simple shear (plane strain) overprinting of the initial, oblate strains (due to stresses associated with sheet emplacement), and therefore the main axis of the Great Tonalite Sill shear zone, is situated here. The ***Carlson Creek pluton*** does not have such a clear profile because there is a bias towards sampling localities located in the northeastern third of the intrusion. However, the profile obtained (based on five localities) indicates that there are high strains, but in this case they are not exclusively located at the pluton margins. There appears to be a strain "high" within the Carlson Creek pluton, 0.5km from the NE contact (locations 123, 175: x/z = 25.3, 16.7), which may coincide with an internal boundary separating two component tonalitic sheets. Interestingly, Gehrels et al. (1991) calculated different dates for the east and west parts of this intrusion and this data may support the presence of different component sheets. Considering the ***Annex Lakes pluton,*** strain is generally lower than in the Carlson Creek body (x/z = 3.5 to 9.9), but one strain measurement (from the five available) of x/z = 14.6 (location 134, fig. 3.23) has been recorded in the contact zone between the Annex Lakes pluton and the SW edge of the Flat Point pluton. The contacts of the younger Flat Point pluton were originally defined on the basis of general differences in petrography and state of deformation (Brew & Ford 1977, Drinkwater et al., 1990), but workers were uncertain whether the Flat Point pluton represented a differentiated phase of the Annex Lakes body, or a separate intrusion altogether. This strain datum implies that, indeed, there is a boundary at this point and this, coupled with local evidence for intrusion of the Flat Point pluton into the Annex Lake pluton (section 3.1.3), suggests that the former represents a cogenetic intrusive phase into the latter and not an in-situ differentiated core. Northeastwards, into the Turner Lake pluton, strains drop to increasingly lower values and, at location 154, this is represented by a flattening strain with an x/z value of only 1.64.

Both the Carlson Creek and Annex Lakes plutons are characterised by oblate ($K < 0.33$) strains. These strains are interpreted to be the results of deformation during sheet emplacement (see section 4.3), coupled with NE-SW orientated, subhorizontal, shortening. The quadrimodal ductile shear data, discussed earlier (section 3.1.5), indicates that this tectonic shortening continued after the intrusions crystallized fully, with the principal strain axes remaining in a similar orientation. It is not clear how much of the $K \cong 1$ component in the Mount Juneau pluton was incurred in the magmatic state, but it is certain that simple shear continued into the crystal plastic regime, well after the pluton had fully crystallised. The final stages of the shear zone movement resulted in the formation of the porphyroclastic mylonites now exposed.

Un-straining the plutons. The strain data can also be used to perform a quantitative unstraining exercise, the results of which emphasise that the Great Tonalite Sill was originally quite long and thin. This correlates well with the preservation within some of these units e.g. Carlson Creek, of original magmatic sedimentation features, indicative of low strains. Using the method described in section 1.4.2., the plutons in Taku Inlet (Mount Juneau, Carlson Creek, Annex Lakes) were un-strained and the un-straining factor (F) was calculated for each pluton as follows: 3.12 (Mount Juneau), 4.73 (Carlson Creek), 3.51 (Annex Lakes). These results show that although the plutons record strains in excess of $X/Z = 15$ or 20 in places, their original widths were not in excess of 5 times greater than their present widths.

Assuming that this result is typical for the Great Tonalite Sill belt as a whole and estimating that the average length and breadth of the belt are 1000 km and 10 km respectively, the original, undeformed belt would have measured approximately 1000 km × 50 km. Therefore the present long, thin geometries of the individual plutons making up the Great Tonalite Sill probably reflect, to a very large extent their original intrusive geometries.

3.1.7 *Summary of the Taku Inlet section*

(1) Petrography. In general, the plutons are composed of biotite-hornblende and hornblende-biotite tonalite, biotite granodiorite, granodiorite and minor granite. Often, the plutons have a banded appearance due to the presence of attenuated layers of metasedimentary gneiss, synplutonic mafic dykes and cogenetic appinite. Important accessory minerals include garnet, epidote and sphene.

(2) Deformation fabrics. Both CPS and PFC deformation fabrics strike NW - SE and dip steeply NE. CPS fabrics are associated with a consistent down dip (nearly 90° pitching) mineral stretching lineation and PFC fabrics may have, within the foliation plane, a down dip linear alignment of plagioclase and amphibole laths. These deformation features are present in a zone at least 10 km across strike. The strongest CPS fabrics are located at the SW boundary of the Great Tonalite Sill and at individual pluton contacts. The stereonets on figure 3.26 illustrate that the orientations of the PFC and CPS fabrics cannot be separated and are therefore parallel, indicating that the orientations of the principal strain axes did not change significantly throughout the crystallization interval.

(3) Shear sense. The dominant shear sense is reverse top-to-the-southwest. Discrete shears are also abundant, but these define four conjugate sets (collectively a quadrimodal set) which indicate a large component of NE - SW directed, subhorizontal, pure shear. PFC lock-up shears attest to syn-emplacement deformation in a similar regime.

(4) Strain. Qualitatively, strain is low in the country rocks and high in the intrusives. A quantitative strain profile shows that the highest strains occur at the SW edge of the Great Tonalite Sill (Mount Juneau pluton) and here the K - values approach 1, indicating the presence of a large simple shear component. It is this area of the traverse

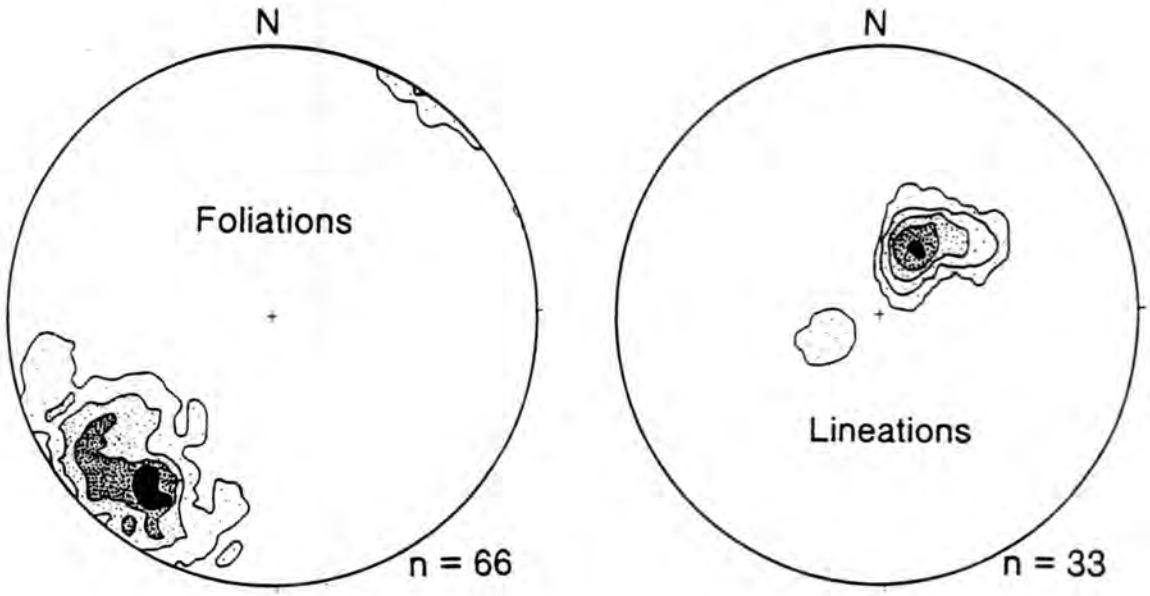

Figure 3.26 Lambert equal area stereonet of foliation and lineation data from Taku Inlet. Contour intervals are 1, 5, 11, 15 percent.

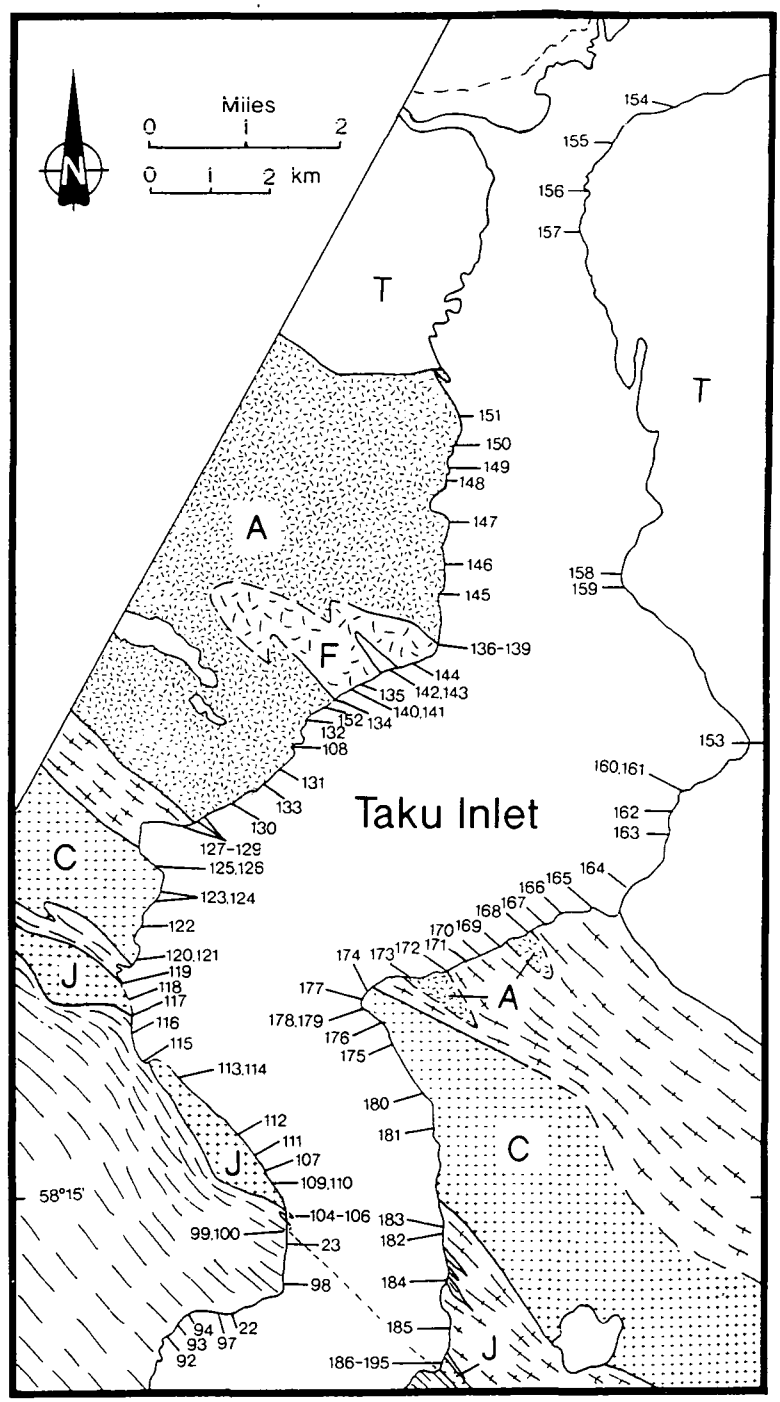

Figure 3.2 Lithology and location map of the Great Tonalite Sill plutons at Taku Inlet: J=Mount Juneau pluton, C=Carlson Creek pluton, A=Annex Lakes pluton, F=Flat Point pluton, T=Turner Lake pluton (including Taku Cabin pluton of Drinkwater et al (1990). Parallel dashes = shear zone fabric. Dashes with ticks = gneissose fabric in country rock.

which is correlated with the medial plane of the Great Tonalite Sill shear zone. Strain magnitudes decrease towards the NE and in this area, K = 0 (flattening) strains dominate, which may be related to pluton intrusive wedging and spatial strain partitioning. High strains are also concentrated at individual pluton or sheet boundaries. Calculations based on the strain profile indicate that the Tonalite Sill plutons in Taku Inlet were originally less than five times their original thickness. The *quadrimodal* set (Woodcock & Underhill 1987, Underhill & Woodcock 1987) of discrete shears implies a $0<K<1$ strain with NE-SW contraction (e.g. Hancock 1985, Underhill & Woodcock 1987) in the post-crystallization interval.

(5) ***Emplacement.*** Observations indicate that the component plutons of the Great Tonalite Sill in Taku Inlet were dominantly emplaced by foliation-parallel sheeting mechanisms, which occurred during regional defomation associated with the Great Tonalite Sill shear zone. Evidence for the stoping of blocks and emplacement of melt along shear bands has also been observed, but these processes were observed on a smaller scale.

3.2 Juneau area: glacier and ridge sections

As well as the Taku Inlet fjord section, several well-exposed sections through the Great Tonalite Sill intrusions occur above sea level in the Juneau area (fig 3.1): the **Mendenhall Glacier pluton** (62Ma, Gehrels et al. 1991), the **Lemon Creek Glacier pluton** and the **Mount Juneau pluton.** The main igneous rock types are biotite-hornblende or hornblende-biotite tonalite. The country rocks to the W, which belong to the western metamorphic belt (Crawford et al 1987, Brew et al. 1989, 1992; Wood et al. 1992), are mainly volcaniclastics, pelites and psammites, with minor amounts of calc-silicate and marble. These rocks have been affected by the Great Tonalite Sill

shear zone, which has been traced all the way from Taku Inlet NW to the Herbert Glacier and beyond.

3.2.1 *Herbert Glacier section.*

The *Mendenhall Glacier pluton* at Herbert glacier is a garnetiferous, sphene-bearing, hornblende-biotite tonalite, which, in its SW part, is made up of at least three steeply NE-inclined tonalite sheets, each in excess of 500m wide, separated by metasediment screens (fig. 3.27). At the southwestern edge of the most southerly sheet (sheet 1, measuring 650 m wide), strongly developed, NE inclined, ductile SC fabrics (Lister & Snoke 1984) occur in the intrusives, with a shear sense of top-to-the-SW. The metamorphosed greywackes and siltstones of the western country rocks also contain discrete shears, indicating top-to-the-SW shear sense. The steeply NE-dipping, intense, CPS fabrics in the southwestern "footwall" area have down-dip lineations and are concentrated in a zone measuring 2km wide from the southwestern pluton contact, and at individual sheet contacts. CPS fabric intensities are high at the country rock rheological boundaries, but decrease towards the centre of individual sheets, where the original PFC fabrics and zoning of feldspars may be discerned, and also towards the northeast parts of the sheets and of the pluton as a whole. The CPS and PFC fabrics are coplanar and the stereonet in figure 3.28 illustrates this.

Shear sense indicators, including S-C fabrics and sigma porphyroclasts, in the CPS fabrics, and magmatic tiling structures (Blumenfeld & Bouchez 1988), within the PFC fabrics, all indicate dominant top-to-the-SW movement (fig. 3.29). Thin screens of plastically deformed country rock, which include some calc-silicates, commonly surround asymmetric boudins of tonalite with a shear sense of top-to-the-SW. Conjugate shears, which in some cases are filled with late but cogenetic melt, record dextral, sinistral and reverse movement. These conjugates indicate that NE - SW directed pure shear was also important during the latter stages of the crystallization interval.

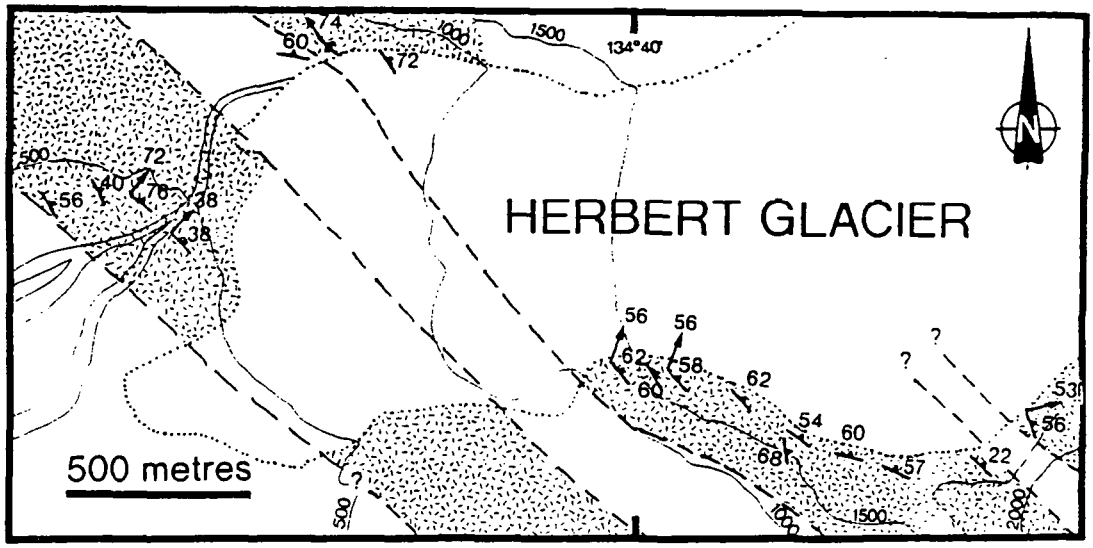

Figure 3.27 Foliation map of the Mendenhall Glacier section at Herbert Glacier. Random pattern = intrusives.

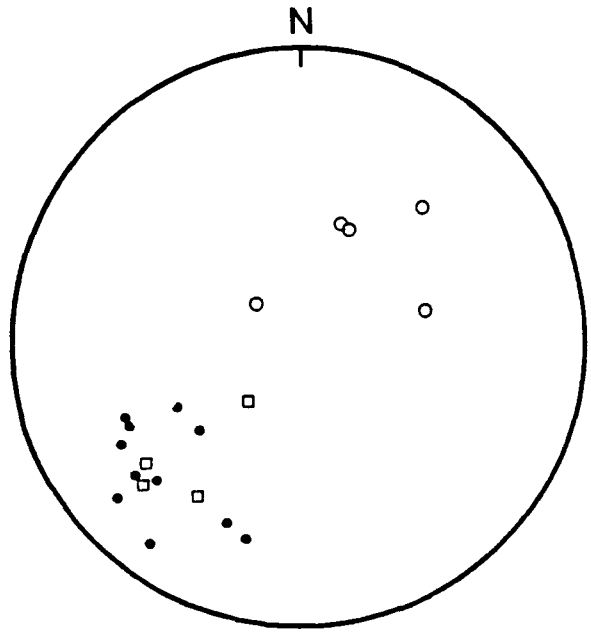

Figure 3.28 Combined PFC and CPS foliation and lineation data from Herbert Glacier. Solid circle = CPS fabric, open square = PFC fabric, open circle = lineation. (Lambert equal area stereonet, n = 22).

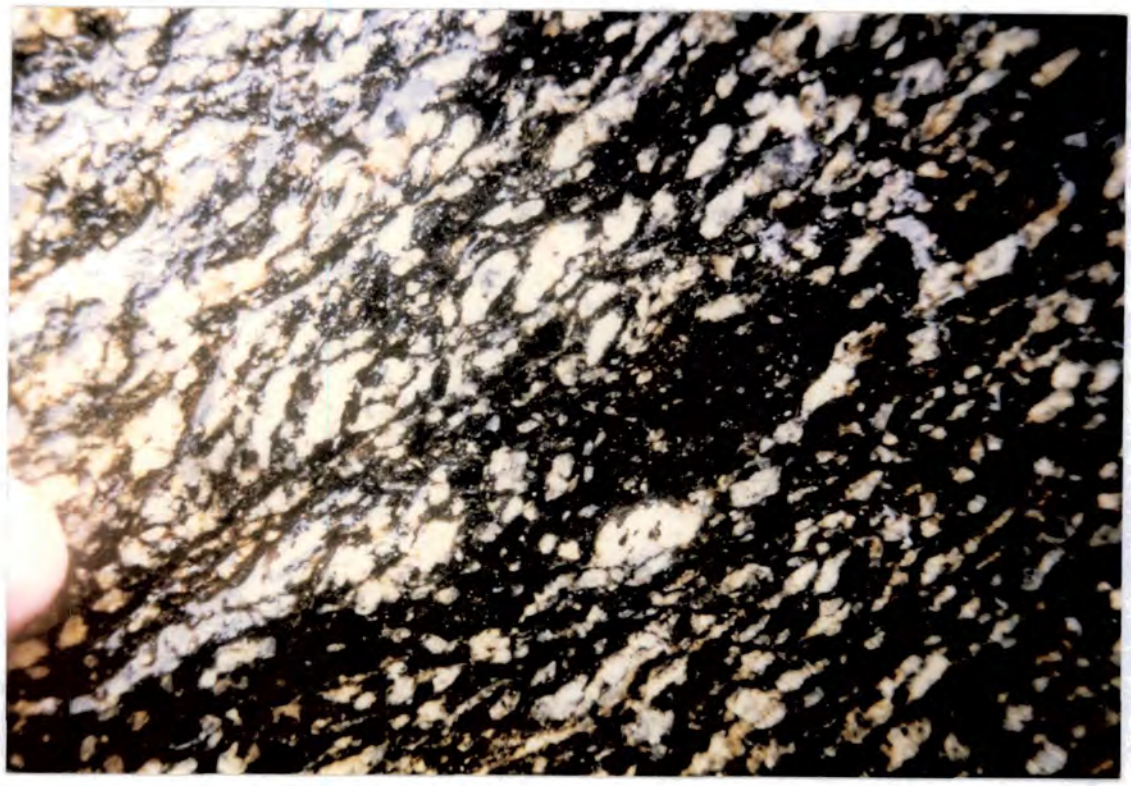

Figure 3.29 Tiling of plagioclase laths indicates top-to-the-SW (right) shear sense. Southern flank of Herbert glacier.

Strain estimates calculated from mafic enclaves show that, at the southwestern edge of the second, 600 m wide, tonalitic sheet, x/z = 11.3 and K = 0.64. If this is compared with the Taku Inlet strain profile (fig. 3.25), then this K approaching 1 component may also be interpreted as a simple shear component. A strain profile was unobtainable, however, due to the paucity of suitable enclaves and the lack of correctly orientated three-dimensional exposure. Qualitatively, strains decrease towards the northeast.

The nature of the pluton implies that emplacement took place dominantly by sheeting and dyking. The sheets of tonalite and screens of metasediment, seen at the present exposure level, are concordant to the regional (D_2) foliation trend, impling that the sheets exploited foliation-parallel weaknesses. Although it is possible that such large country rock screens (650m wide) and tonalite sheets (>500m wide) may have been rotated into parallelism with the regional foliation, the author interprets, on the basis of field relationships, that this was not a dominant mechanism.

3.2.2 *Mendenhall Glacier section.*

At this location (see fig. 3.1 and also the Mendenhall Glacier pluton structural map in the back pocket of the thesis), the rock of the Mendenhall glacier pluton section is mainly a sphene-bearing, biotite-hornblende tonalite. Its southwest edge is dominated by the presence of intrusive sheets on many scales, measuring from fractions of a metre to map scale sheets in excess of 100 metres thick, which are separated by metasediment screens up to 600 metres wide (fig 3.30).

A zone of pervasive CPS foliation with top-to-the-SW shear is also concentrated at the southwest edge (fig. 3.31) and into the volcaniclastics to the southwest. The intense deformation has resulted in the steep, pervasive foliation surfaces illustrated in figure 3.32. Figure 3.33 shows a close-up of the foliation surface, with its nearly-90° pitching lineation marked by the long axes of small, stretched out volcanic bombs. Shear sense in the country rocks is consistently top-to-the-southwest

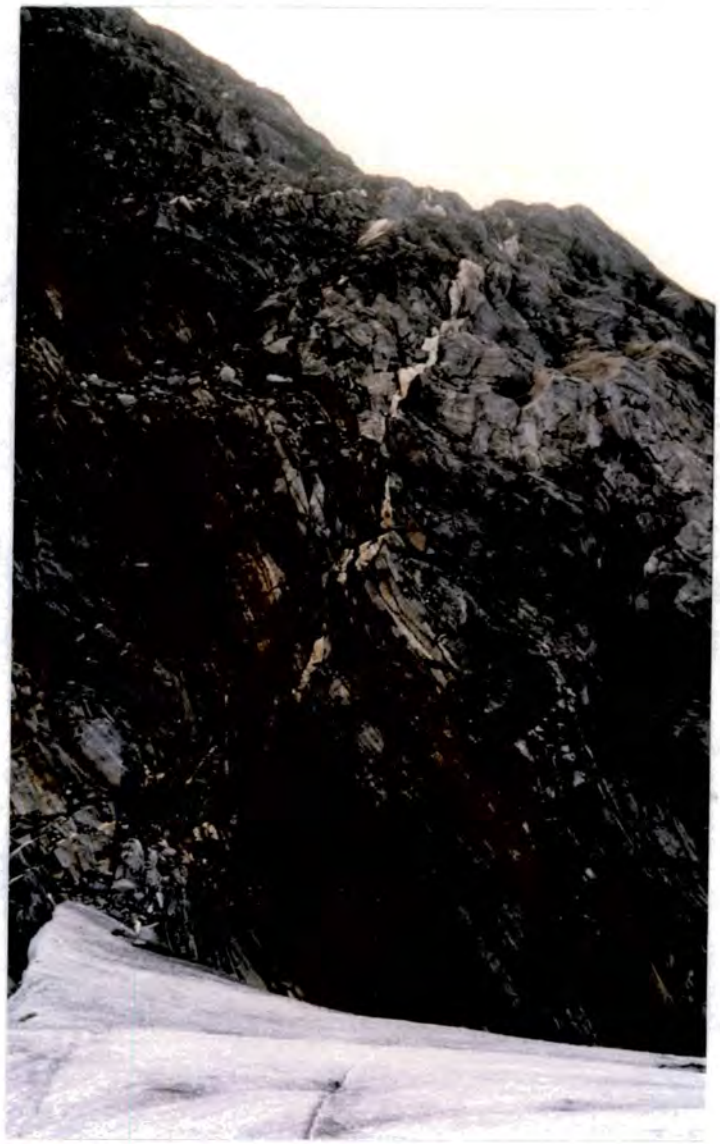

Figure 3.30 Steeply NE dipping screen of metasediment enclosed by tonalite: Mendenhall Glacier pluton. Field assistant for scale (bottom left).

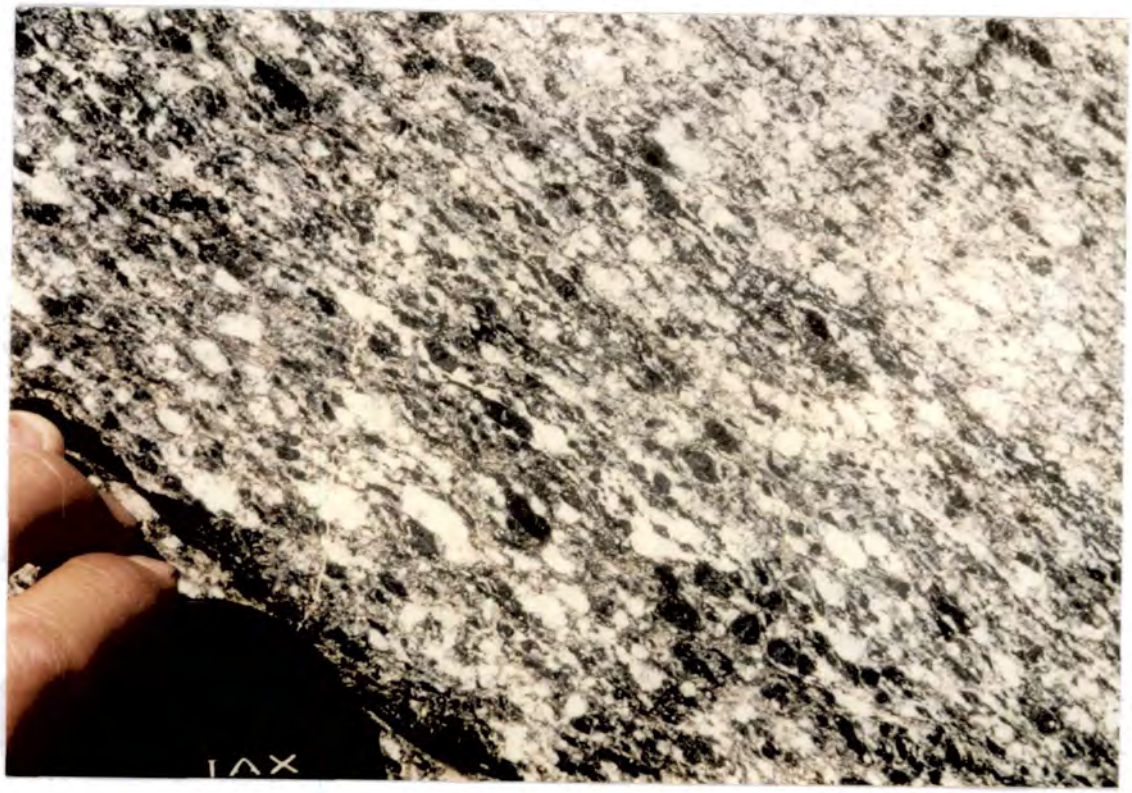

Figure 3.31 Tonalite with crystal plastic SC fabric indicating top-to-the-SW (left) shear: SW edge of the Mendenhall Glacier pluton.

Figure 3.32 Steep pervasive foliation in volcaniclastic rocks SW of the Great tonalite Sill on the east flank of Mendenhall Glacier.

and is exhibited most commonly by thin, asymmetrically boudined, fine grained volcaniclastic bands (fig. 3.34). Within the main tonalite body, the width of this zone, measured from the main tonalite contact to its full extent northeastwards, is 500 - 600 m, and measured from the most southerly intrusive sheet, including the intervening country rock screens, is 1.5 km. To the NE of this zone, there are well-developed, coplanar, PFC fabrics and PFC shears with variable orientation: reverse top-to-the-NE and -SW, and extensional top-to-the-SW. Other syn-emplacement features, apart from the obvious PFC lock-up shears, include discrete, low angle reverse, ductile shears which have late, but cogenetic melt intruded along them. Similar melt was detected in some boudin necks and in a high temperature kink band, again implying that deformation was coeval with melt availability. Late deformational structures include discrete cataclastic/mylonitic, thin shear bands, which, in places, are grouped together in anastomosing networks. Dextral and sinistral (fig. 3.35) shears are both represented: the dextral shears are orientated NNW-SSE and the sinistral shears are orientated ESE-WNW, implying that they represent two conjugate sets, which formed in response to NE-SW directed subhorizontal shortening.

Estimates of strain, derived from the shapes of deformed mafic enclaves, in this area indicate that $x/z = 8.4$ and $K = 0.29$. Estimates of strain from similar deformed enclaves, but this time in porphyroclastically mylonitized tonalite at the extreme SW edge of this pluton, give average values of $x/z = 80$. Many of the deformed enclaves at this location are stretched to such a degree that measurement becomes impossible. K values were not obtained in connection with this extreme case, but other estimates nearby indicate $x/z = 27$ to 29 and K values between 0.27 and 0.33 i.e. mostly flattening strains.

3.2.3 *Lemon Creek Glacier section (including camp 17)*

Foot of Lemon Creek Glacier. The hornblende-biotite tonalite of the NNW-SSE trending *Lemon Creek Glacier pluton* contains at its SW margin a relatively large

Figure 3.33 Detail of the rocks in figure 3.32: strong nearly 90° pitching lineationon the foliation surface. Three dimensional observations confirmed a K>1 strain component here.

Figure 3.34 Fine to medium grained banded volcaniclastic rocks exposed close to figures 3.32 and 3.33. This XZ profile shows small asymmetric boudins with top-to-the-SW (left) shear sense.

Figure 3.35 Late, discrete, cataclastic/mylonitic shear bands sinistrally offset a late granite pegmatite vein: eastern traverse of Mendenhall Glacier.

number (>20) of individual sheets, each between c.1m and 100m thick. This is especially evident in the exposures located at the foot of Lemon Creek Glacier, which are close to the interpreted northwestern lateral termination of the pluton (fig. 3.36). The tonalitic sheets are separated by numerous screens of metasediments (commonly calcareous, see figs. 3.37A & B) and minor amounts of deformed and disrupted microdioritic synplutonic dykes. Strong, NE dipping, CPS fabrics with down-dip transport lineations (fig. 3.38) are developed throughout this section and analyses of crystal pressure shadows, asymmetric boudins (fig. 3.39) and melt filled shears indicate reverse top-to-the-SW movement. Commonly, the lineation varies in plunge to indicate a minor dextral oblique sense of movement coupled to the reverse shear sense. However, E-W trending sinistral CPS shears and zones of sinistrally verging folds also occur (fig. 3.40), but dextral conjugates for these, common in many other sections, were not recorded.

In summary, this section represents a highly sheeted lateral part of the Lemon Creek Glacier pluton, in which reverse to-to-the-SW shear sense is dominant.

Camp 17 ridge section. Country rocks in the southwest of the section are composed of quartz-biotite-garnet schists, biotite-hornblende schists, psammites and quartzites, which contain ptygmatically folded leucocratic veins. The fold hinges are parallel to the moderately plunging transport lineation, which lies within the plane of the moderately NE inclined schistosity. At the contact on Vesper Peak, the intrusive tonalite has a high mafic content (mostly hornblende) and contains garnets, which, along with plastically deformed amphibole and plagioclase crystals, indicate foliation parallel, reverse, top-to-the-SW shear sense. The intensity of the strong CPS fabric near the contact is heterogenous and thin, highly deformed, bands occur at intervals, with similar shear sense. The overall fabric intensity decreases northeastwards and at approximately 300m NE from the contact relict, coplanar, PFC fabrics can be identified. The transport lineation in the complete section plunges generally to the northeast with a pitch angle of around 70° to 80° SE (fig. 3.41). Taken together with

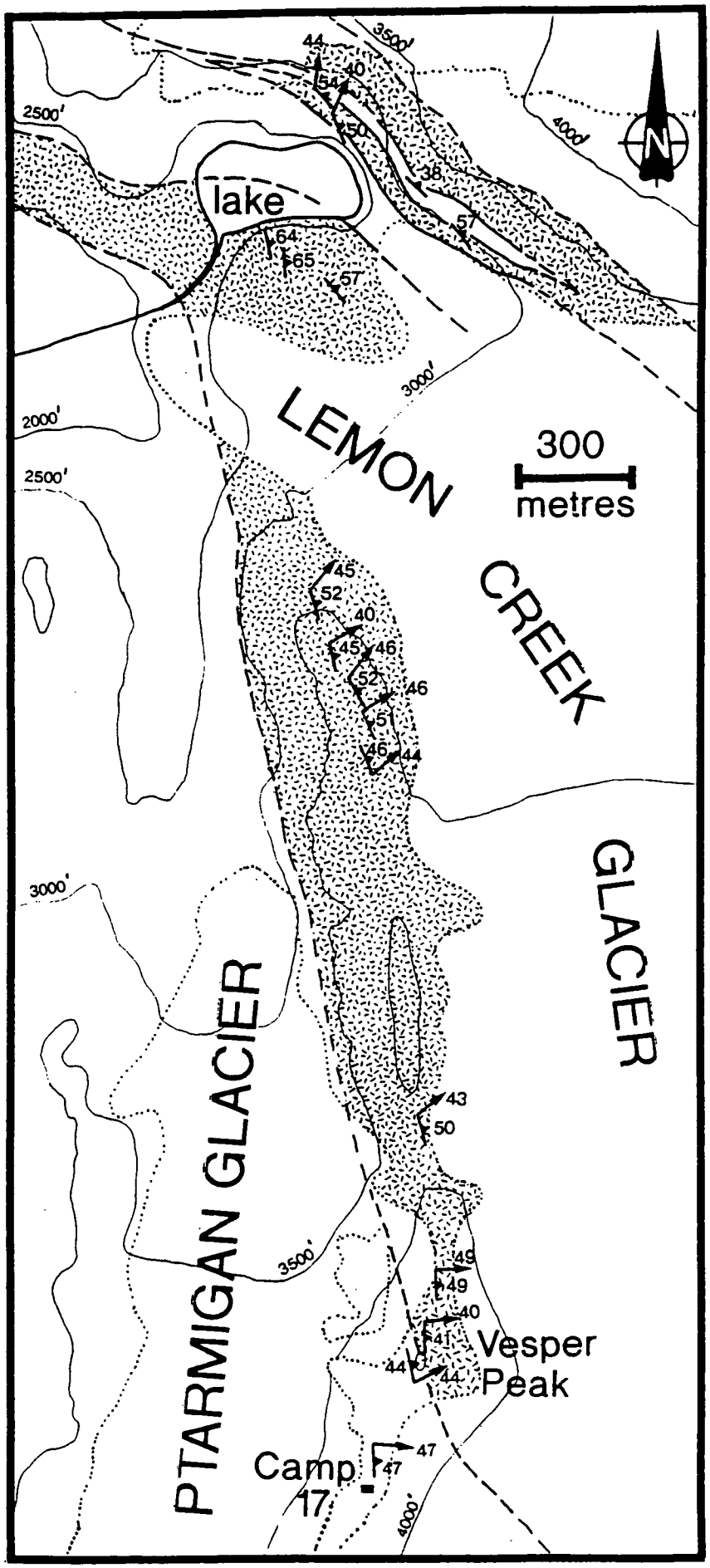

Figure 3.36 Foliation and lithology map of the Lemon Creek Glacier pluton, near Juneau. Random pattern = intrusives.

A

B

Figures 3.37A & B Metasediment screens (commonly calcareous) separating foliation parallel sheets of intrusive tonalite: Lemon Creek Glacier pluton.

Figure 3.38 Steep stretching lineation on steeply NE dipping foliation: Lemon Creek Glacier pluton.

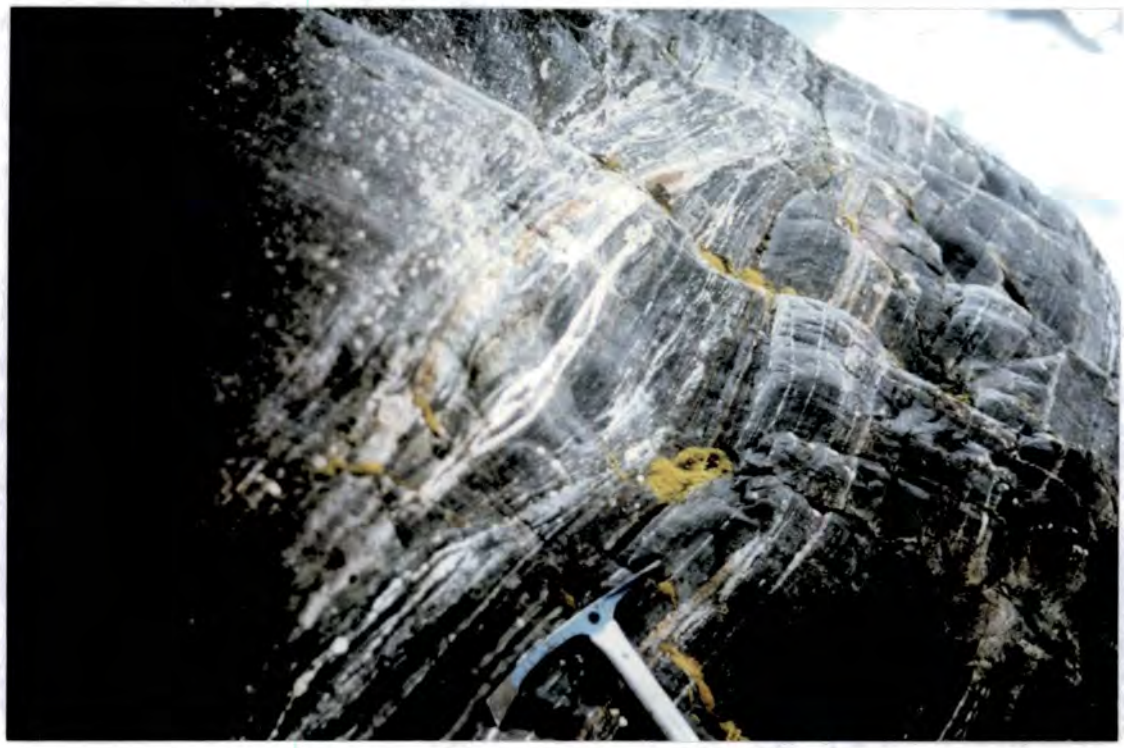

Figure 3.39 Asymmetric boudin indicating top-to-the-SW shear: Lemon Creek Glacier pluton.

Figure 3.40 Sinistrally verging folds within a calcareous foliation parallel screen: Lemon Creek Glacier pluton.

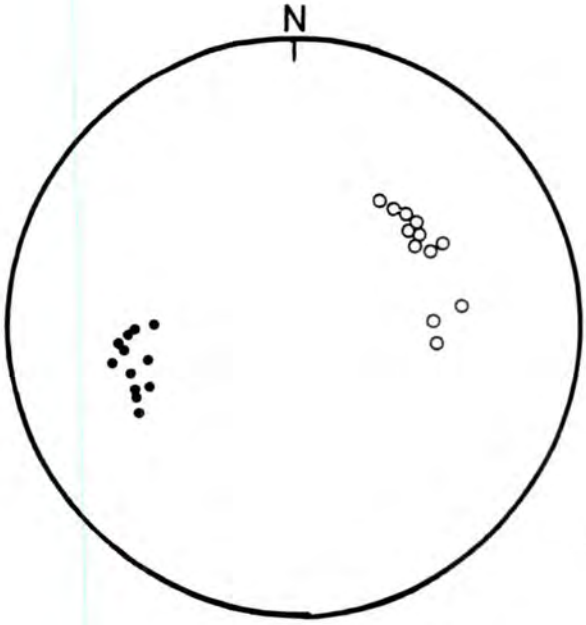

Figure 3.41 Fabrics and lineations: Lemon Creek Glacier pluton (Camp 17 ridge section). Solid circle = foliation, open circle = lineation (n = 24).

the dominant top-to-the-SW shear sense, this lineation data indicates a slight dextral component of movement. The main foliation is also axial planar to west vergent folds of a leucocratric vein, indicating that vein emplacement took place before deformation and foliation development.

Many screens and schlieren of metasediment, cogenetic mafic bands and tonalite sheets occur throughout the ridge section, parallel to the main NE dipping foliation (figs. 3.42 & 3.43). These features are interpreted here to indicate that emplacement of the tonalite took place mainly by a sheeting process, although it is possible that they may have been deformed from originally non-planar geometries. In places, angular xenoliths of mafic to ultramafic material have been recorded. One such xenolith is exceptionally large, measuring 15m by 20m. This material probably represents the precursor to the main tonalitic intrusive phase (fig. 3.44).

Measurements from the shapes of mafic enclaves indicate that the average x/z values in the inner area, 300m from the contact, are approximately 18, with low K-values (0.23) indicative of flattening strains. Qualitatively, strains increase towards the southwestern contact, but insufficient populations of suitable enclaves precluded a quantitative estimate of strain in the contact area.

In summary, both sections show: (1) remarkably consistent top-to-the-SW shear sense, (2) steeply NE-inclined CPS foliations, (3) down-dip lineations with high pitch angles, indicating a slight dextral kinematic component and (4) abundant foliation-parallel tonalite sheets on all scales, indicating a sheeting emplacement mechanism.

3.2.4 *Mount Juneau and Granite Basin sections.*

On a map, the sphene and garnet-bearing, biotite-hornblende tonalite of the ***Mount Juneau pluton*** appears to truncate the Great Tonalite Sill shear zone fabrics and metamorphic isograds of the western metamorphic belt (SW of the Sill, Ford & Brew 1977, fig. 3.2). Remapping of this pluton during this study reveals that the

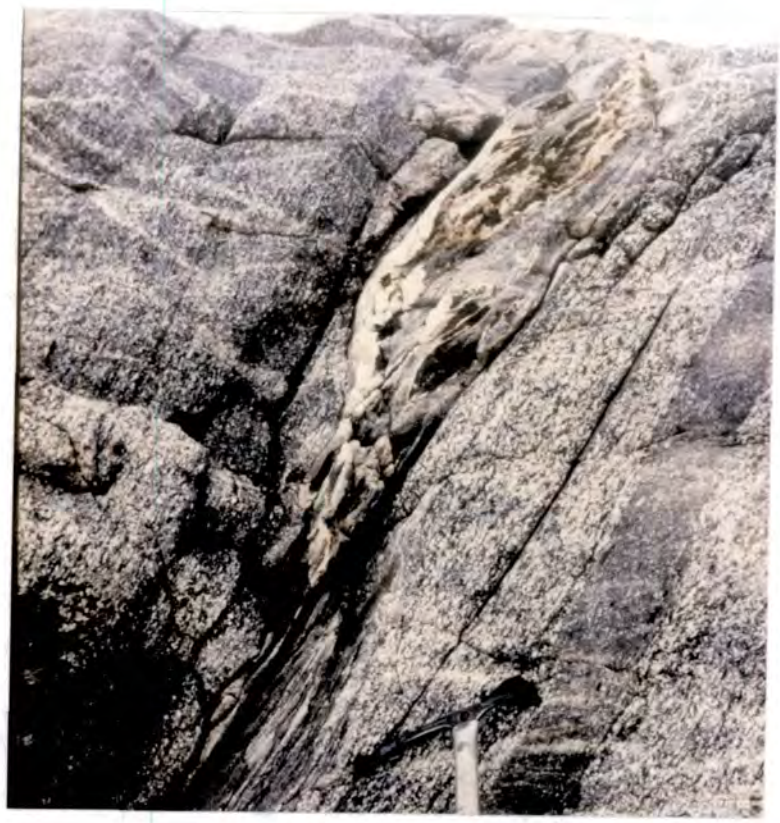

Figure 3.42 Foliation parallel, NE dipping metasediment screen: Lemon Creek Glacier pluton.

Figure 3.43 Foliation parallel, NE dipping layer of cogenetic mafic rock: Lemon Creek Glacier pluton.

Figure 3.44 Large xenolithic mass of appinitic rock within the Lemon Creek Glacier pluton at the Camp 17 ridge section.

intrusion is steeply NE-inclined at Taku Inlet and also to the NW, up to the Granite Basin (500m altitude). Above this on Mount Juneau itself (1060m) the pluton becomes gently NE-inclined (c.30° dip). The map pattern at this level is produced by erosion of a shallow dipping sheet and the truncation of underlying features is more apparent than real. The following subsections describe the nature of the Mount Juneau pluton in the Granite Basin/Granite Creek area (steep zone) and on Mount Juneau itself (shallow zone).

Granite Basin. Foliations in the country rocks and intrusives, in the Granite Basin area (fig. 3.45), dip steeply northeast and are coplanar with the contacts of the steeply dipping tonalitic sheets (figs. 3.46 & 3.47). Two main map scale intrusive tonalite sheets occur in the area and many other minor sheets, including appinitic varieties, occur within the country rocks near their contacts. The tonalite has intruded country rocks composed of alternating psammites, quartzites, pelites, fine grained volcaniclastics and crystal tuffs. However, in the northeast of the area, psammitic schists are dominant. Both PFC and CPS fabrics can be discerned in the tonalites and, in general, the steep PFC fabrics are cut by shallower CPS fabrics in an SC type relationship. The shear sense derived from this relationship indicates top-to-the-SW, reverse, shear and this is corroborated by independent shear sense indicators throughout the section: sigma porphyroblasts and asymmetric boudins. In places the transport lineation on the CPS foliation surface, when coupled with the shear sense data, indicates a component of sinistral shear, which is substantiated by the presence of sinistrally sheared boudins. At the head of Granite Creek, psammitic schists rich in kyanite exhibit a down dip lineation defined by the alignment of undeformed kyanite crystals in the steeply northeast dipping foliation plane (fig. 3.48). This indicates that kyanite growth, during prograde metamorphism, was coeval with active deformation and tonalite sheet emplacement.

The intensity of fabrics, and therefore the strain intensity, varies throughout the section. Cogenetic mafic enclaves were not in abundance, but qualitative estimates of

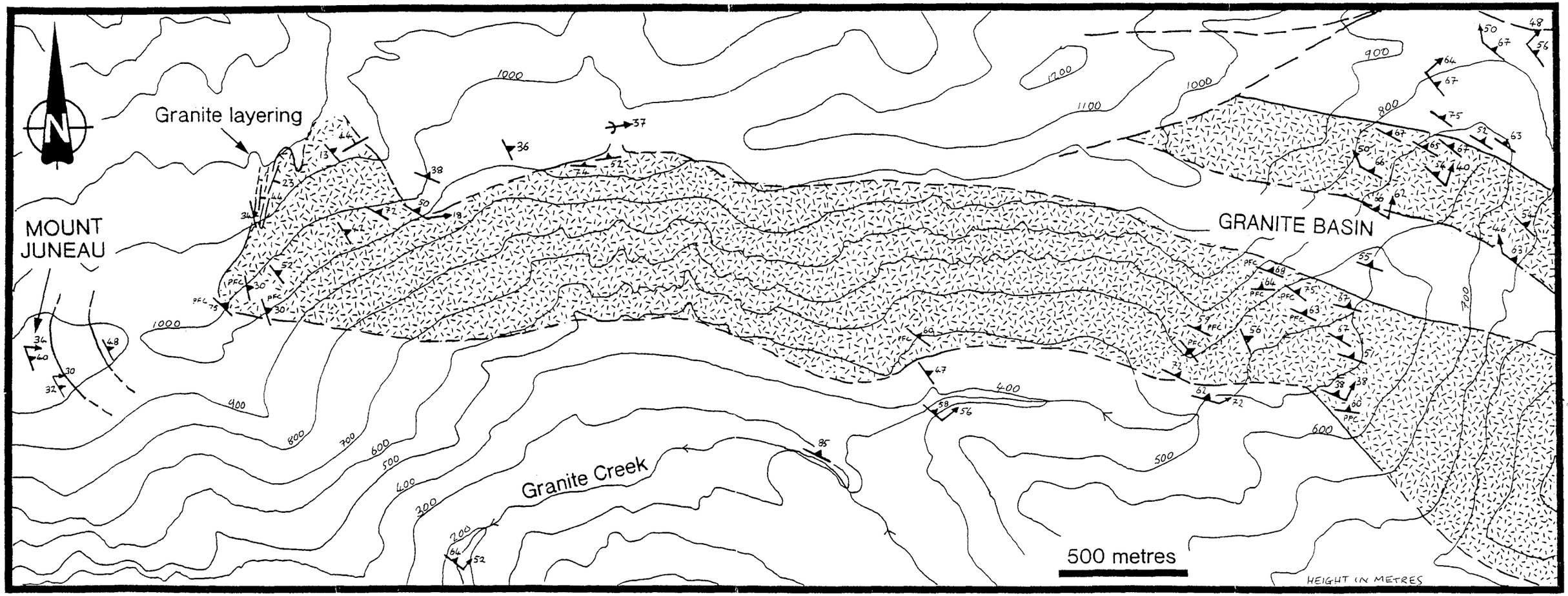

Figure 3.45 Lithology and foliation map of the Granite Creek/Granite Basin area, including the Mount Juneau ridge section, NE of Juneau. Random pattern = intrusives.

Figure 3.46 The SE flank of the Granite Basin showing the steeply NE dipping, grey, tonalite sheets and the country rock screens to the SW (right) of the picture. Height of the outcrop in this figure is approximately 200 metres.

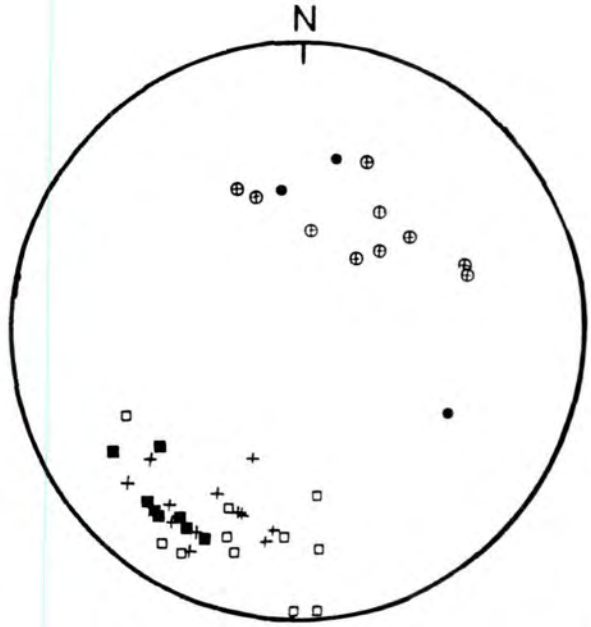

Figure 3.47 Structural data from the Granite basin area. Open square = PFC fabric, solid square = CPS fabric, cross = country rock foliation, Solid circle = CPS lineation, Circle with cross = country rock lineation (Lambert equal area stereonet, n = 58).

strain indicate that high strains are concentrated at or near the contacts of the large intrusive sheets i.e. at rheological boundaries. A quantitative measurement of strain near the northeast contact of the northeastern sheet, indicates that Y/Z = 8.4. In the central parts of the individual sheets, relict PFC fabrics become important and it is here that their relationships to the later CPS overprint can be seen. On a larger scale, strain dies off to the southwest, into the metasediments and metavolcanics, which underlie the tonalitic sheets. The intrusives therefore lie within a high strain, top-to-the-SW, reverse, shear zone and this has been correlated with the shear zone seen at Taku Inlet (fig. 3.1).

Mount Juneau ridge section. The most striking difference between the rocks in this section (fig. 3.45) and those in the Granite Basin section, which lies 4 km to the east and 400 to 500 m lower in altitude, is the very low state of strain. The attitudes of the foliations and sheet contacts are significantly shallower here than in the Granite Basin and PFC fabrics dominate in the tonalites.

The country rocks to the west, on the summit of Mount Juneau, are mainly chloritic pelites, slates and metavolcanic rocks including crystal tuffs, of the Taku terrane. They have moderately northeast dipping D_2 foliations with down dip lineations and contain asymmetric quartz boudins, indicating consistent top-to-the-SW reverse shear. 800m northeast of the summit occurs the contact with the garnet-bearing, hornblende-biotite tonalite. The rock contains a well developed PFC fabric, with a moderate northeast dip. Strains are not high at the contact, but the metamorphic grade increases to amphibolite facies.

Exposure on the northern flank of the main ridge gives a sectional view of the intrusion and it is here that the internal sheeted structure of the pluton is very well developed (fig. 3.49). The sheets are tonalitic in composition and vary between 30 cm and 1 m wide (modally 0.5 m wide), with individual sheets traceable for up to 30 m in length. The sheets at first glance resemble compositional igneous layering, such as that described by Harry & Emeleus (1960) in SW Greenland. These authors described

Figure 3.48 Aligned kyanite crystals on the foliation plane of a metasediment septum: Granite Basin.

Figure 3.49 View, looking SW, of tonalite layering near the roof of the Mount Juneau pluton, with chilling towards the top of each sheet. Field of view = 5 metres.

granitic layering formed essentially by the alternation of mafic bands with granite. The mafic bands (a few cm thick) commonly graded upwards into granitic bands (10-40 cm thick) with a similar grain size, and both were interpreted to have formed due to repeated in situ differentiation of an unusually fluid, volatile rich, magma. On closer inspection, the sheets within the Mount Juneau pluton, unlike the SW Greenland granites (Harry & Emeleus 1960) are graded from top to bottom according to crystal grain size. There is an apparent compositional grading effect seen in outcrop, caused by the change in grain size, which alters the overall colour of the rock throughout a single sheet: the finer crystalline portions within any single sheet create a darker rock colour compared to that exhibited by the coarser ones. Inspection at thin section scale, however, indicated that the relative proportions of different minerals are roughly constant throughout each sheet, from coarse to fine crystal size.

Chilled margins. The polarity of this crystal size grading changes systematically throughout the pluton, which suggests that it may have formed as a consequence of granite sheets chilling against their wall rocks. The sheets remain remarkably parallel and planar, over distances of at least 30 metres, and lack the sedimentary style undulations and disturbances described by the above authors in the Greenland examples. Thus it is interpreted that the sheets possess chilled margins, which appear to be located on one side only: at their bases in the bottom half of the body (figs. 3.50 & 3.51) and along their tops in the upper portion of the sill (fig. 3.52). This field relationship is consistent throughout the pluton and therefore this model indicates that the intrusion on Mount Juneau represents a kind of granitic sheeted dyke complex, with repeated intrusion in the central zone. PFC fabrics lie parallel to the shallow dipping walls of these sheets, but at intervals CPS fabrics, in steeper orientations, cut through with a shear sense of top-to-the-SW. There is no particular zone of high strain in this traverse and it appears that the sheet intrusion on Mount Juneau lies essentially to the southwest of the Great Tonalite Sill shear zone (fig. 3.1).

Figure 3.50 Close up of a tonalite layer boundary at the base of the Mount Juneau pluton. Note grain size reduction towards the base.

Figure 3.51 Hand specimen from the same locality as 5.50, again showing grain size reduction towards the base. Note also the presence of equant, magmatic garnets. Scale in centimetres.

Figure 3.52 Outcrop of tonalite sheets near the roof of the Mount Juneau pluton: note chilling towards the top of each sheet.

Emplacement into a thrust flat. The pluton on Mount Juneau may have formed in a thrust flat, which was dilational in a generally contractional environment (fig. 3.53). This is similar to the emplacement mechanism previously described by Rykkelid (1987), who indicated that the gabbro and granodiorite of the Sunnhordland Batholith, west Norway, had been emplaced into such a releasing bend (fig. 3.54). However, in his model the magma intruded as sills or sheets, which retained both their chilled margins. The model proposed for the Mount Juneau pluton involves the rapid propagation of sheets into the dilational area. The high wedging stresses that such sheets possessed probably aided the opening of the thrust flat.

3.2.5 *Lake Dorothy.*

This poorly accessible section was visited by helicopter in 1985 by D.H.W. Hutton and W. Nelson (USGS). The following material is summarised from a report written by Hutton and submitted to the USGS. Data is summarised in Ingram & Hutton (in prep).

To the southeast of Lake Dorothy, a ridge section running from SW to NE exposes tonalite and high grade country rocks to the NE (fig. 3.55). The traverse basically cuts across the southeastern continuation of the Carlson Creek tonalite, 2.5 km southeast of Taku Inlet, and therefore provides additional information about this pluton. The metasedimentary rocks to the SW of the pluton, include biotite-sillimanite-garnet schists and quartzites, plus minor calc-silicate layers. Early coarse to medium-grained, layered amphibolite and hornblende-plagioclase rocks generally form rafts or large xenoliths within the younger tonalite. The rafts and screens are aligned parallel to the foliation in the surrounding tonalite and diorite. The main rock type is medium to coarse grained hornblende-biotite tonalite and it contains abundant mafic enclaves. Using these enclaves as strain indicators, an harmonic mean of $x/z = 15$ was determined at one locality. Early deformation is represented by PFC fabrics which strike NW-SE, dip steeply NE and contain steeply-plunging hornblende mineral

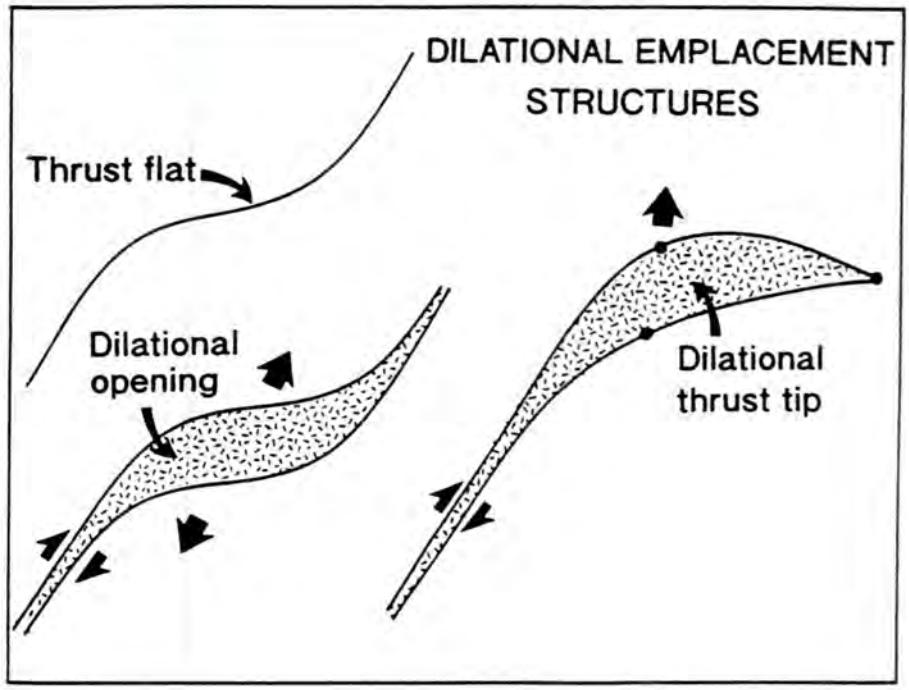

Figure 3.53 Cross sectional view of two possible dilational structures within an overall contractional regime.

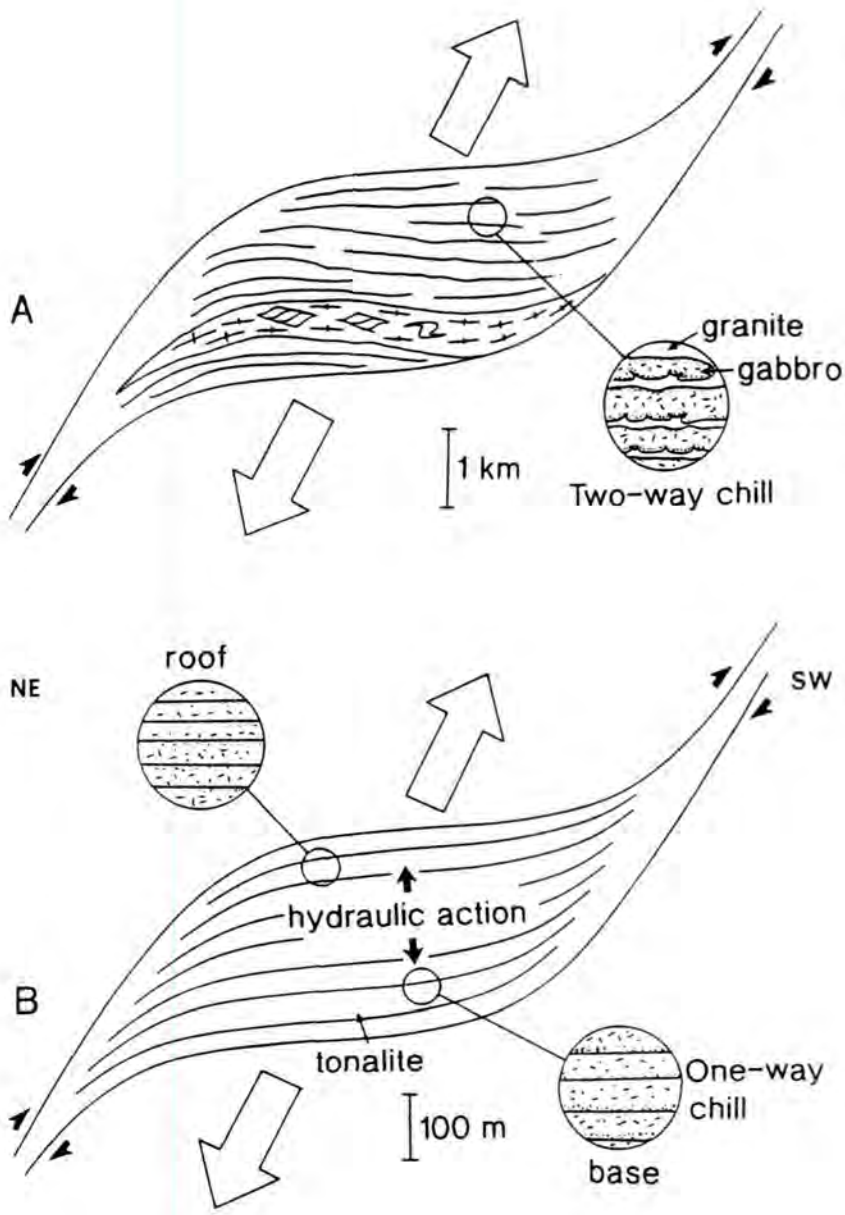

Figure 3.54 Models for granitoid emplacement into a thrust flat: (A) Stolmen gabbro, Norway, passively emplaced into thrust releasing bend (modified from Rykkelid 1987). Chilling occurs on both sides of the intruding sheets. (B) Mount Juneau Pluton, emplaced by wedging and sheeting into a dilational thrust flat. Chilling occurs on one side only of the intruding sheets.

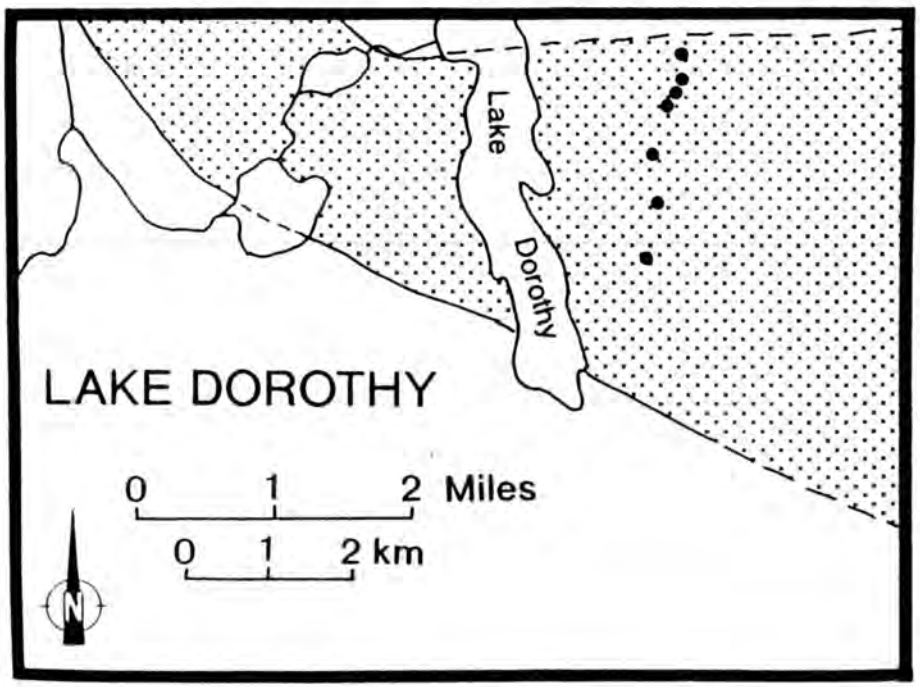

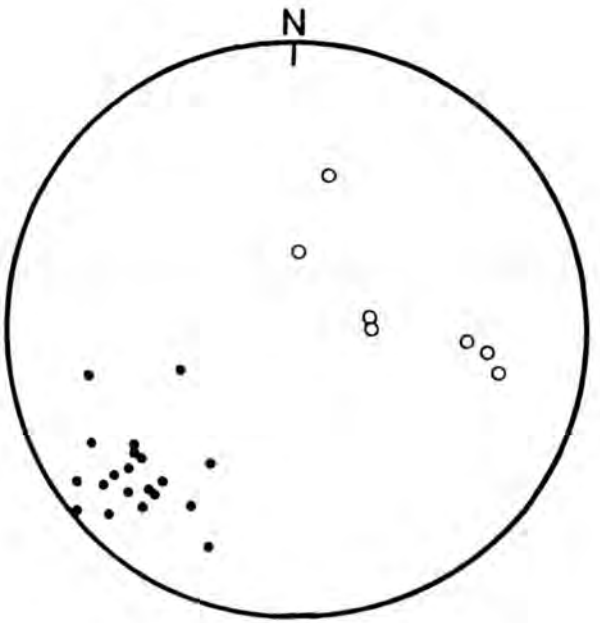

Figure 3.55 Lithology an location map of Lake Dorothy, near Taku Inlet. Black dots = structural localities. Shading = intrusives (Carlson Creek pluton). Lambert equal area stereonet of structural data from Lake Dorothy ridge section. Solid circle = foliation, open circle = lineation (n = 29).

lineations. Later, down-temperature, parallel, CPS fabrics overprint this and indicate similar transport directions. In general top-to-the-SW shear sense dominates in the SW part of the pluton and the transport lineation is close to 90°, but conjugate sets of discrete reverse shears also occur, which suggest a large pure shear component. However, towards the northeast part of the pluton, the lineation reduces in plunge to the SE and a component of sinistral shear along the main foliation is indicated (fig. 3.55). Rocks in the NE contact zone resemble a migmatite, in which hornblendite and other phases are boudined and enclosed by granodiorite. The granodiorite appears to have flowed around the boudins before it had fully crystallized. Observations indicate that the tonalite and associated diorite were emplaced during active deformation associated with the Coast shear zone. This deformation outlived the emplacement phase and although it mainly kept to the same kinematic pattern, it may have switched from contractional (reverse) tectonics in the SW to oblique sinistral tectonics in the NE. The orientation of kinematic indicators and their implied shear sense, in both the pre- and post-crystalline states remained constant, implying that the geometry of the principal stress axes did not change in geometry significantly during the crystallization interval of the pluton.

In the late stages of intrusion, cross-cutting veins of microdiorite developed and post-dating these are 20-30m thick, steeply-inclined, strike-parallel sheets of biotite-granodiorite. The latest event is the intrusion of thin, planar, flat-lying, pegmatite-aplogranite sheets, representing the final granitic melt.

3.2.6 *Summary of the Juneau area.*

In addition to the introductory overview in section 3.1, the following salient points are stressed:

(1) The main intrusive rock types are biotite-hornblende- and hornblende-biotite tonalite (± garnet, sphene).

(2) The country rocks are mainly (arc-related) volcaniclastics, pelites, psammites, minor calc silicate and marble.

(3) The shear zone associated with the Great Tonalite Sill has been traced from the SW contact of the Mount Juneau pluton, in Taku Inlet, to the SW contact of the Mendenhall Glacier pluton at Herbert Glacier. Shear sense associated with this is dominantly reverse, top-to-the-SW and associated foliations dip steeply NE and have down-dip lineations (fig. 3.56).

(4) Kyanite crystals in a large metasedimentary screen within the Sill, aligned parallel to the main lineation, indicate that deformation and metamorphism were coeval.

(5) Strain estimates indicate that the SW edge of the Great Tonalite Sill represents the axis of a major shear zone. A simple shear component is associated with its SW edge and this dies off northeastwards, into an area dominated by flattening strains, which decrease in magnitude to the northeast. High strains are also localised at intrusive sheet and pluton boundaries i.e. at rheological boudaries.

(6) Emplacement probably took place by the propagation of sheets of tonalite magma along foliation-parallel weaknesses, during active shear zone deformation.

(7) The tonalite on Mount Juneau may have been emplaced into a dilational thrust flat, by a sheeting mechanism analogous to a sheeted dyke complex. The apparent truncation of regional metamorphic isograds and foliations by this intrusion is caused solely by erosion of a relatively flat sheet. The pluton is otherwise concordant.

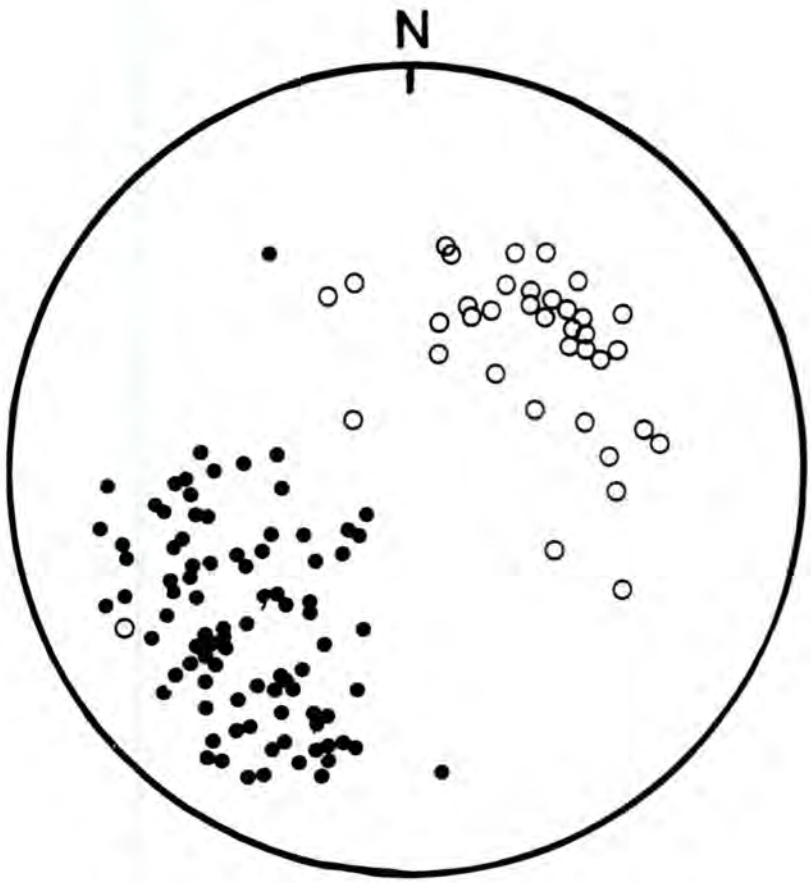

Figure 5.56 Summary of structural data from the Juneau area. Solid circle = foliation, open circle = lineation. (Lambert equal area stereonet, n = 129).

In the preceeding sections, detailed geological accounts of the Juneau area rocks have been presented. The main purpose of these accounts has been to characterise a traverse through the Great Tonalite Sill, which may be regarded as a type section. In what follows, the author presents further detailed descriptions of traverses through the Sill, at intervals along a strike section of approximately 800 km length. Thus the Juneau type section may be compared with these additional sections in order to asses its applicability, as a general model, over an extensive length of the Great Tonalite Sill.

In the following sections, accounts of these additional across strike fjord transects begin first of all at Port Snettisham, south of Taku Inlet, and move southwards to Tracy Arm, Ford's Terror, Thomas Bay, LeConte Bay, Bradfield Canal, Burroughs Bay, and finally to Walker Cove (see fig. 2.3). Sections to the south of Walker Cove to the Skeena River (B.C.) and north of Juneau (to Haines) extend the scope of the study and are described in the final section (mapping by D.H.W. Hutton; taken from Ingram & Hutton, in prep.).

3.3 Port Snettisham

The 5-7 km-wide Speel River pluton (Drinkwater et al., 1989; fig. 3.57) extends from just S of Taku Inlet to beyond Endicott Arm. It is composed of sphene-bearing to sphene-rich hornblende-biotite tonalite, which contains PFC and CPS/solid state fabrics. In agreement with Drinkwater et al. (1989), this study recorded a variation in fabric type across the pluton, the strongest (CPS) fabrics locating near the intrusive margins and PFC fabrics in central parts of the pluton. All the fabrics from the pluton and adjacent country rocks are associated with steep foliations parallel to the regional trend. Lineations pitch close to 90° and are defined by aligned euhedral laths of amphibole and plagioclase in the PFC foliation planes and by a mineral stretching lineation in the CPS foliations. Strain, measured from mafic enclaves, varies from x/z =

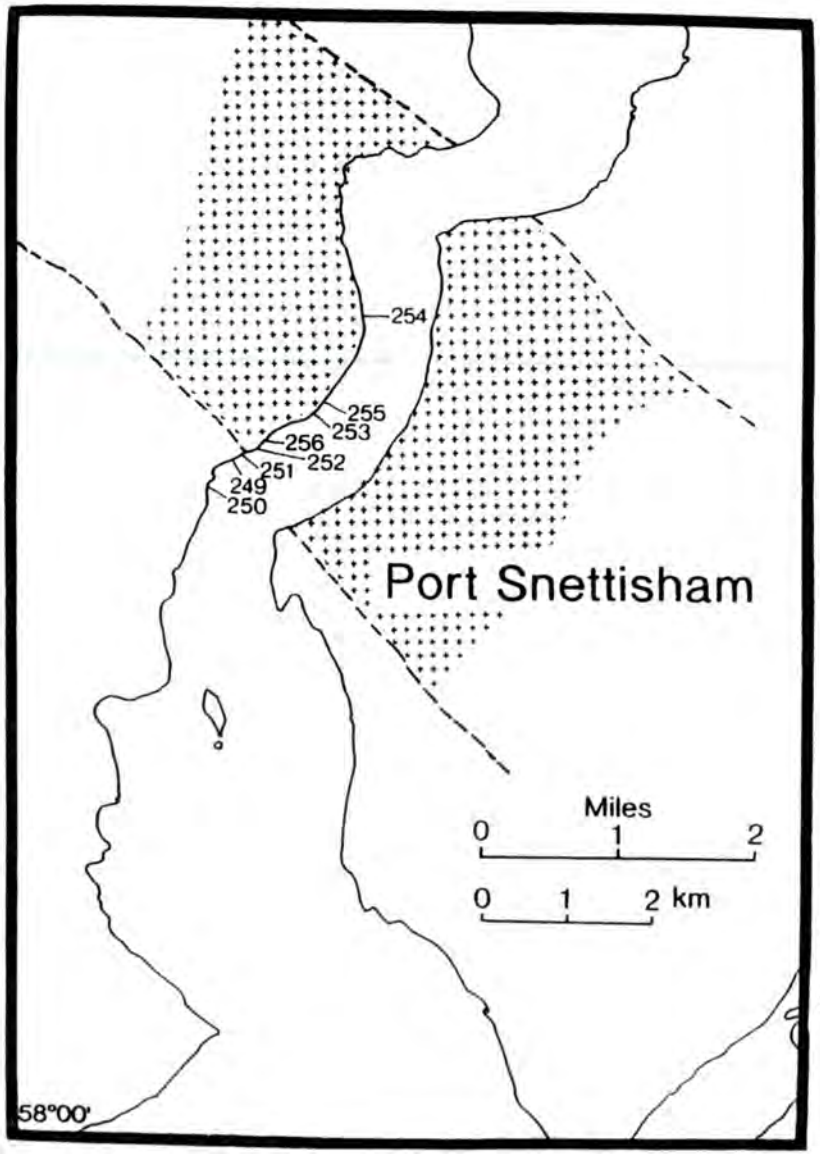

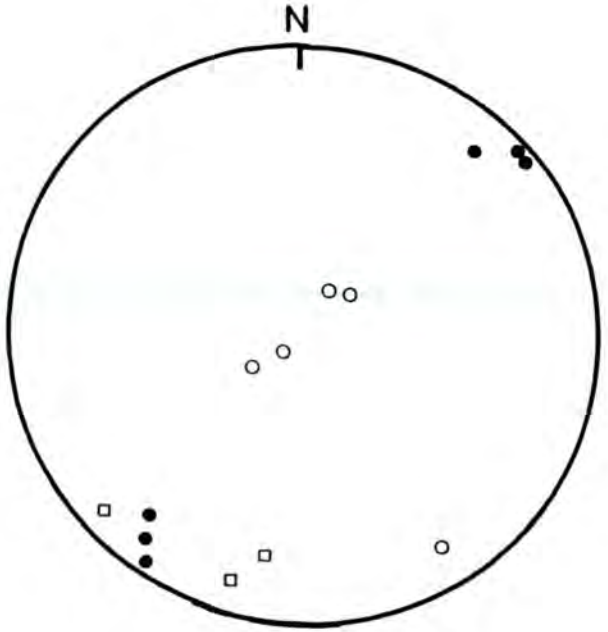

Figure 3.57

Lithology and location map of Port Snettisham. Shading = intrusives. Structural data on Lambert equal area stereonet: open square = PFC fabric; solid circle = CPS fabric; open circle = CPS lineation. n = 129)

4 in the central PFC fabric-dominated region, to x/z = 43 near the SW contact with greenschist and amphibolite grade metasediments, which include psammites, pelites and minor calc-silicate. K-values are between 0.02 and 0.20. The high strain zone extends about 1km NE from the contact and contains top-to-the-SW shear sense indicators (fig. 3.58). Some boudins show an apparent top-down-to-SW shear sense, but this is attributed to oversteepening of the foliation in certain sections, tilting them back towards the NE (fig. 3.59). This zone can be correlated with the shear zone seen in other parts of the belt, at the southwest edge of the Great Tonalite Sill.

3.4 Tracy Arm

The tonalite body in Tracy Arm (fig 3.60) is composed of garnet-bearing hornblende-biotite tonalite and contains PFC and CPS fabrics, which are parallel to those in the country rocks to the SW. Gehrels et al. (1991) have dated the pluton as approximately 61Ma and Hollister et al. (1987) indicated that it was emplaced at a pressure of approximately 5 kb. The metasediments to the SW are dominantly garnet to sillimanite grade psammites and semi-pelites, but highly deformed appinites are also present near the relatively sharp intrusive contact. Deformed amphiboles in the appinite have asymmetric pressure shadow "tails", which indicate top-to-the-SW shear (fig. 3.61). The presence of dextral and sinistral ductile shears, sinistrally verging folds and SE-plunging fold hinges, imply that there is no consistent lateral shear sense. The foliations in the wall rocks are steep and the average lineation pitch within the foliation plane is almost 90°.

In the SW, the tonalite is heterogenous and contains many elongate mafic enclaves of dioritic composition (fig. 3.62), from which maximum x/z strains of 11 are indicated. K-values were not obtained due to the lack of 3-D exposure, however it is assumed that they are again less than 1. Locally, magmatic disruption of syn-plutonic dykes has produced dark banding parallel to the regional foliation. Ductile/CPS deformation is low except close to or at the tonalite/country rock contact where it

Figure 3.58 Foliation parallel shear sense is indicated by a sheared vein. Transport is top-to-the-SW (left).

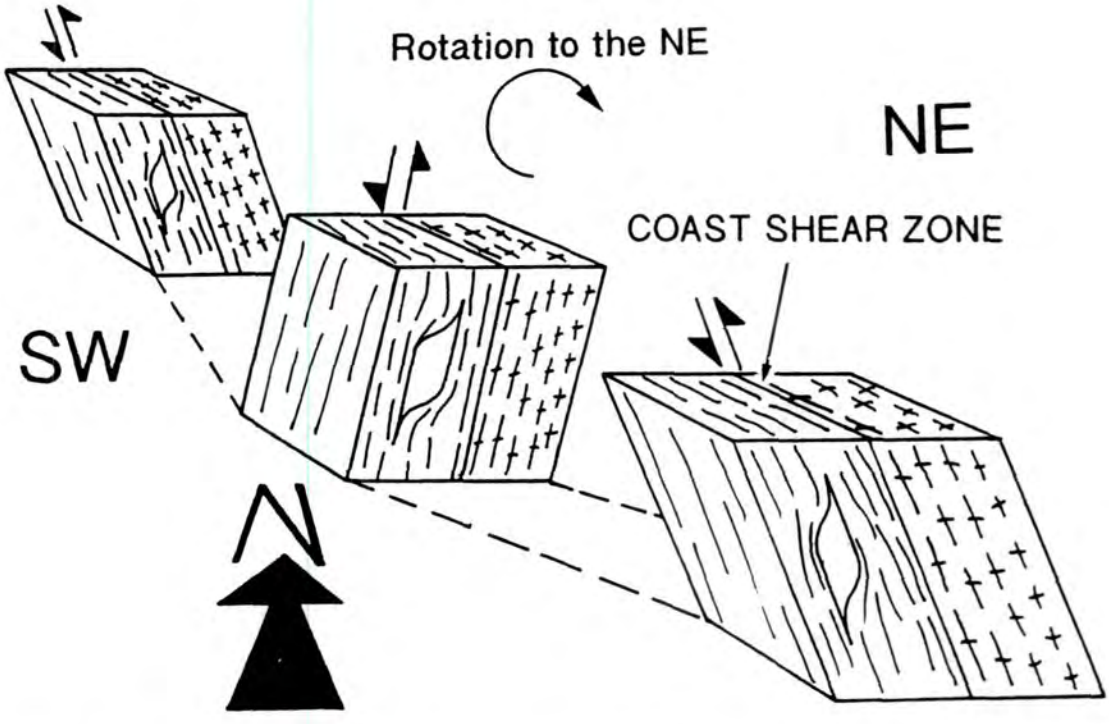

Figure 3.59 Block diagram illustrating the effect of back-rotation on top-to-the-SW shear sense indicators in the Great Tonalite Sill shear zone. The middle block has been rotated towards the NE.

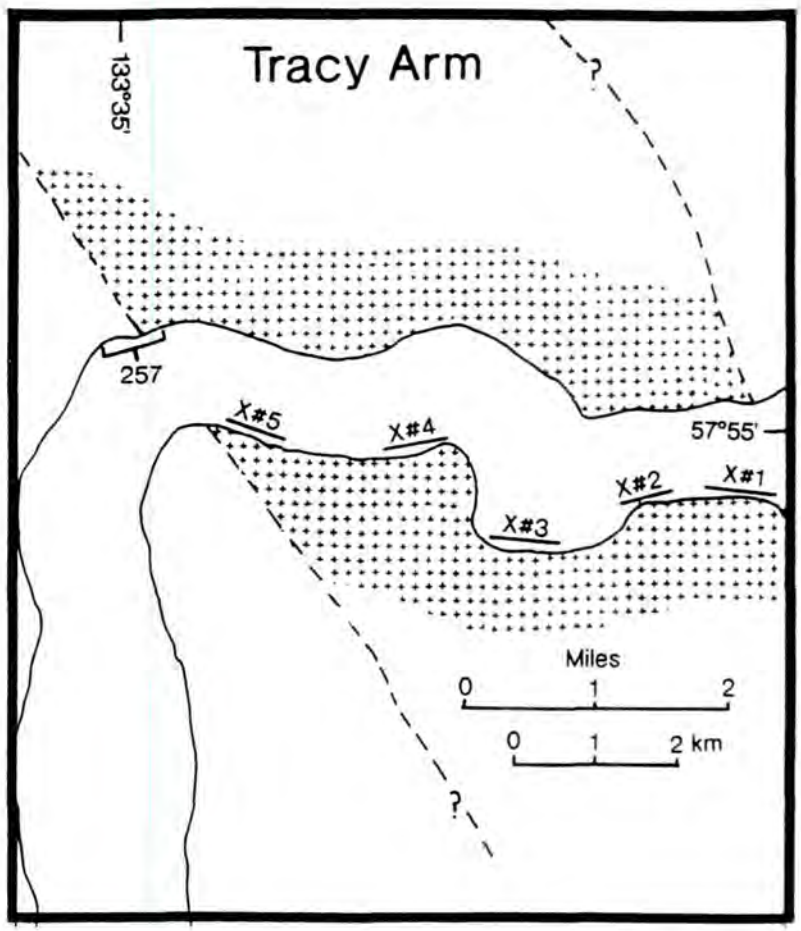

Figure 3.60 Lithology and location map of Tracy Arm. Shading = intrusives. Localites with an "#" indicate enclave strain data points.

Figure 3.61 Asymmetric pressure shadow tails on amphibole foliation fish indicate top-to-the-SW (right side up) shear sense in appinite. Pencil for scale.

Figure 3.62 XZ profile of elongate mafic enclaves within the tonalite in the SW part of the tonalite body at Tracy arm (location 257). X/Z strain values here approach 11.

masks original intrusive features and suggests that the Great Tonalite Sill shear zone at this point is relatively thin. Shear sense in the tonalite is similar to that in the country rocks and is apparent in both PFC and CPS states. However, PFC and later CPS shears show both top-to-the-NE and top-to-the-SE senses of motion, suggesting that a large pure shear strain was important during the crystallization interval.

3.5 Ford's Terror

Ford's Terror Inlet branches N from Endicott Arm and tonalite is exposed along most of its shorelines (fig. 3.63). From a sample taken at a location nearby in Endicott Arm, Stowell (1989) determined a depth of emplacement estimate for the pluton of about 5 kb. The rock is a sphene-bearing hornblende-biotite tonalite and it contains a dominant PFC fabric, which has been overprinted to varying degrees by solid state/CPS fabrics. This is most marked in the SW part, where it culminates in a zone of mylonite, which extends into the footwall country rocks to the SW. Shear sense is extremely variable and indicators include discrete ductile shears, asymmetric country rock boudins, fold vergence and sigma-porphyroclasts. Discrete, reverse top-to-the-NE or -SW, extensional top-to-the-SW, dextral and sinistral CPS shear sense indicators were all identified in this section and, taken together, these can most easily be interpreted as quadrimodal sets indicative of NE-SW directed subhorizontal contraction and pure shear. However, CPS deformation at the grain scale indicates a dominant shear sense of top-to-the-SW. CPS foliations dip steeply to the N and S or are vertical and lineations may plunge down dip with high pitch angles or may pitch to the SE, implying a sinistral component of movement (fig. 3.63).

Strains recorded in the PFC regime, by mafic enclaves (fig. 3.64), are generally highest towards the margins of the pluton and lowest in the centre. However, the very highest recorded strains do not coincide exactly with the margins, but are located

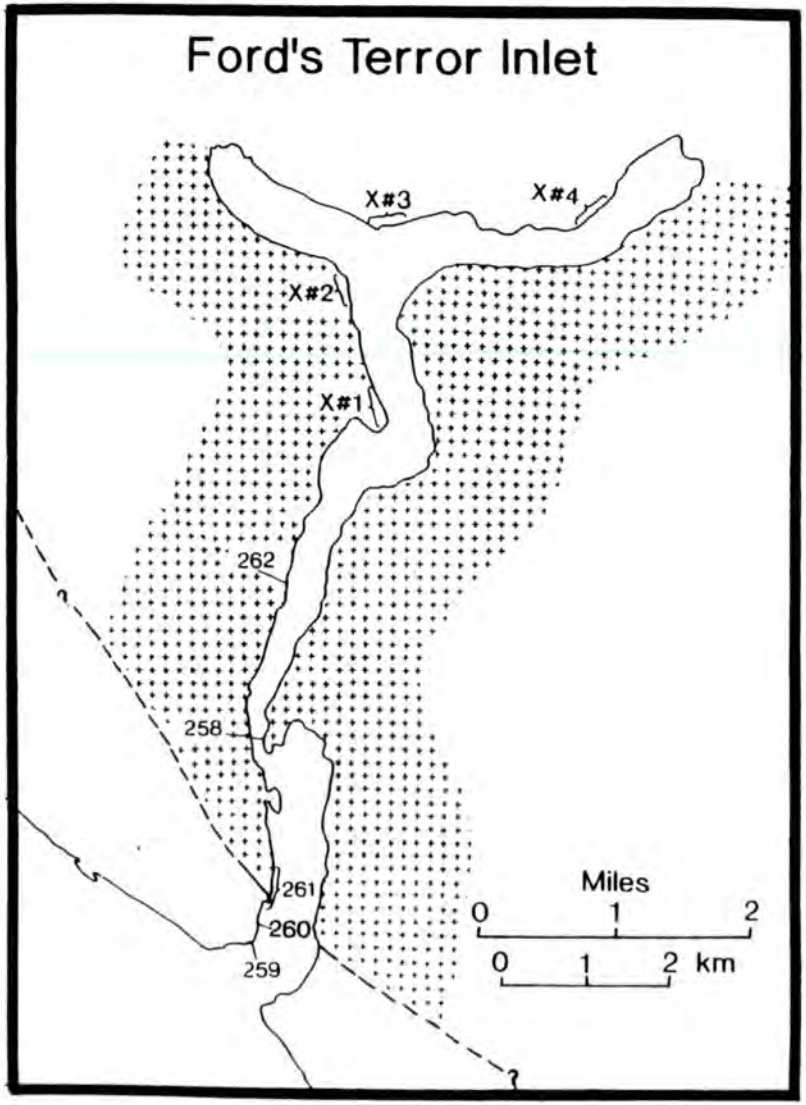

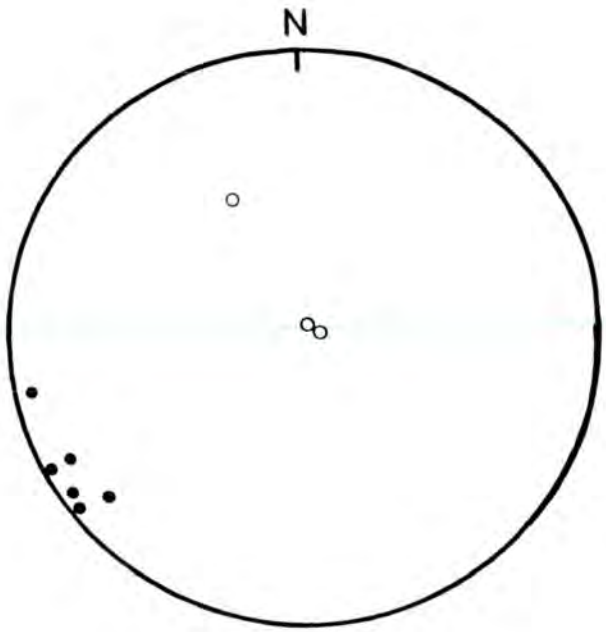

Figure 3.63

Lithology and location map of Ford's Terror Inlet, SE of Tracy Arm. Shading = intrusives. Lacalities with a "#" indicate enclave strain data points. Structural data: solid circle = foliation; open circle = lineation (Lambert equal area stereonet, n = 9).

Figure 3.64 XZ profile of deformed mafic enclaves in the tonalite body at Ford's Terror Inlet. Location 262.

around 2km inside them and the reasons for this, although unclear, are probably related to the existence of unmapped internal boundaries within the pluton. At the SW country rock contacts, there is a zone containing veins and xenoliths, plus a sheet-like, 70-80m-thick, highly deformed appinite body. Strong CPS/solid state deformation at the pluton margin has destroyed much of the original intrusive contact relationships, but away from the high strain zone, at the Narrows, a shallow sedimentary-type channel structure was recorded in the tonalite, which indicates that CPS/solid state deformation is not pervasive throughout the pluton and that the elongate nature of the Great Tonalite Sill plutons may reflect their original intrusive geometries. The latest stage of intrusion is represented by flat-lying to moderately-dipping granite pegmatite sheets, whose constituent minerals are aligned parallel to the fabric in their host rocks, indicating that the principal axes of deformation did not change their orientations significantly during crystallization of the pluton.

3.6 Thomas Bay

A 3km orthogonal transect into a 64Ma (McClelland, 1990) sphene- and garnet-bearing hornblende-biotite tonalite body is exposed at the northern end of Thomas Bay (fig. 3.65). Palaeobarometry indicates that the pluton was emplaced at pressures of 6 - 7 kb (McClelland et al. 1991a). A zone of intense CPS deformation occurs within the pluton measuring 1.7 km wide from the southwestern country rock contact. It is the most intense zone of ductile, solid state deformation recorded in the Great Tonalite Sill. At the SW edge of the pluton there is a zone of quartz-ribbon mylonite, which contains top-to-the-SW-directed SC fabrics, complex folds and top-to-the-SW shears. Fabrics ranging from weak CPS overprints on PFC fabrics to mylonites were recorded in this zone and it passes SW into sillimanite-grade, mylonitic psammites, in which a similar sense of shear dominates. Shear sense is variable, but shearing associated with the emplacement of the tonalite is generally consistent and has

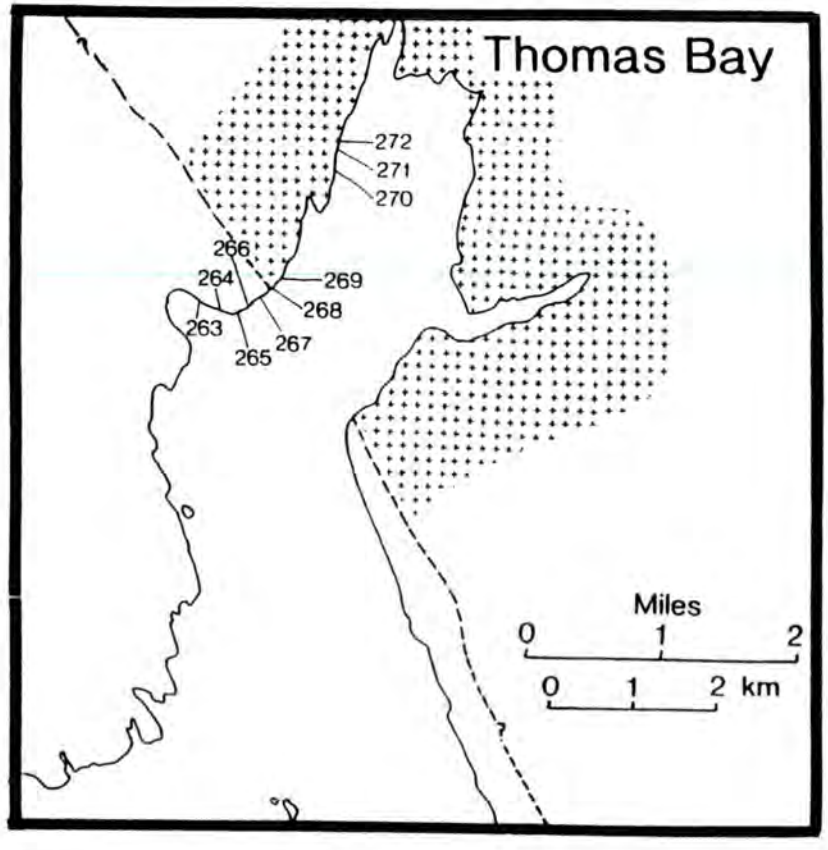

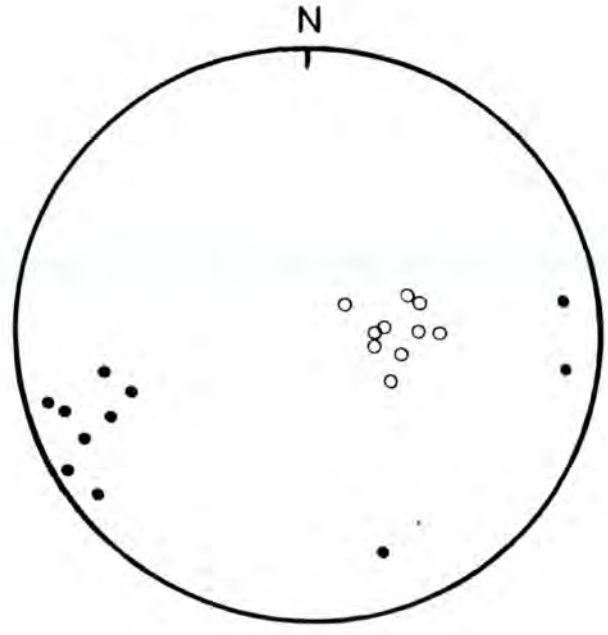

Figure 3.65

Lithology and Location map of Thomas Bay (Shading = intrusives). Structural data: solid circle = foliation, open circle = lineation (Lambert equal area stereonet, n = 21).

a reverse sense of top-to-the-SW. Many shallow- to moderately-dipping, discrete shears are consistent with this sense and commonly carry granitic melt (fig. 3.66). Foliations dip steeply NE and are associated with down-dip or SE-pitching lineations. Later, down-temperature brittle-ductile overprints record a phase of NE-SW extension or collapse, which is illustrated by extensional-down-to-the-NE shear bands. The contact between the tonalite and country rocks is sharp. However, irregular migmatitic veins of granitic composition lie subparallel to the gneissic foliation close to the contact and shallow-dipping veins emplaced into the dilational flats of small top-to-the-SW, discrete, ductile shears were recorded (fig. 3.67). The latter emplacement mechanism is similar to that recorded on a larger scale at Mount Juneau (figs. 3.53 & 3.54). Foliations in the country rocks and in the pluton dip steeply to the NE and contain down-dip stretching lineations, which indicate orthogonal shortening and reverse shear sense of top-to-the-SW.

3.7 LeConte Bay

At the time of the investigation (July 1991), LeConte Bay (Fig. 3.68) was icebound and access only to the the extreme SW edge of the Tonalite Sill was available. A good section however was recorded through the footwall (fig. 3.69), where, within about 3 km of the 60 Ma (McClelland 1990) main biotite-tonalite body, numerous steeply NE inclined tonalitic sheets occur in the metasediments. As the main pluton is approached from the SW, these change in thickness from less than a meter to several tens of meters and increase in density. Pervasive deformation associated with steeply NE inclined fabrics and downdip stretching lineations also increases to the NE. Sillimanite grade migmatite occurs closest to the contact and is cut by highly deformed concordant tonalite sheets and minor cross-cutting tonalitic to granitic veins, which are affected by a variety of structures active during emplacement. Shear sense indicators include asymmetric boudins, SC fabrics, pressure shadow tails on feldspar

Figure 3.66 Shallow, melt filled, top-to-the-SW (left) CPS shears, cutting the main NE dipping foliation. Thomas Bay.

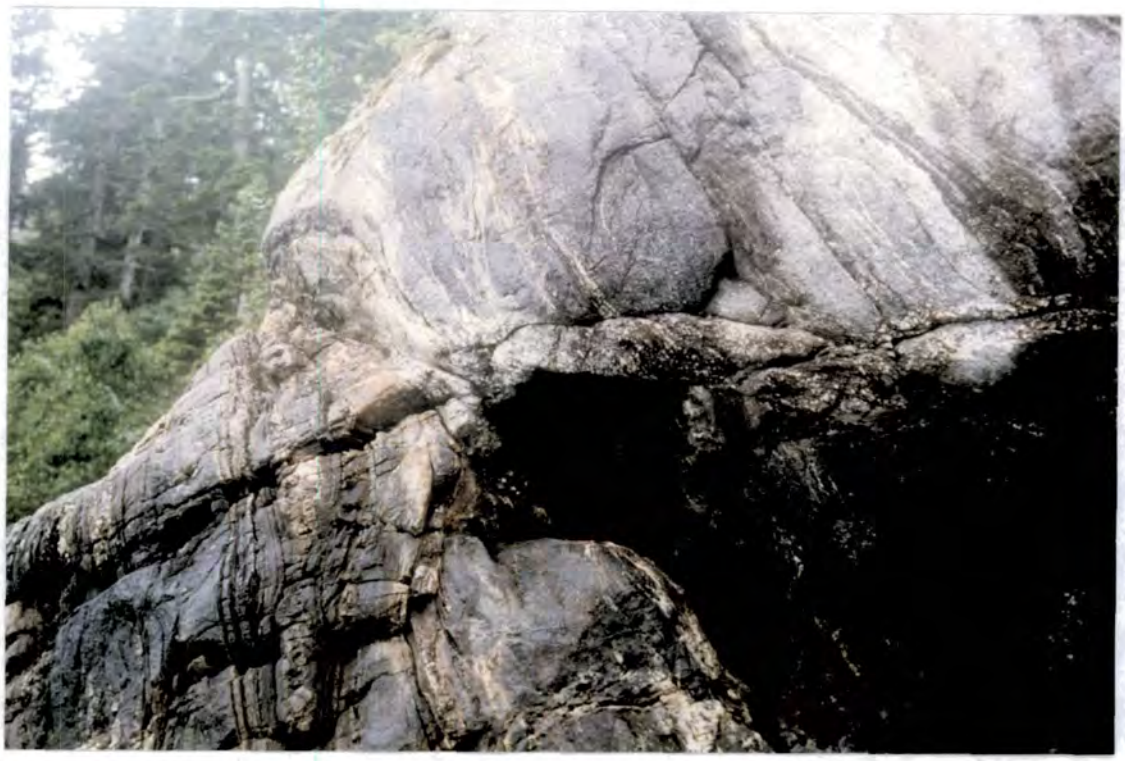

Figure 3.67 Foliation parallel tonalite sheets and metasedimentary gneiss screens, cut by a discrete ductile shear. The dilational flat has been exploited by late granitic melts.

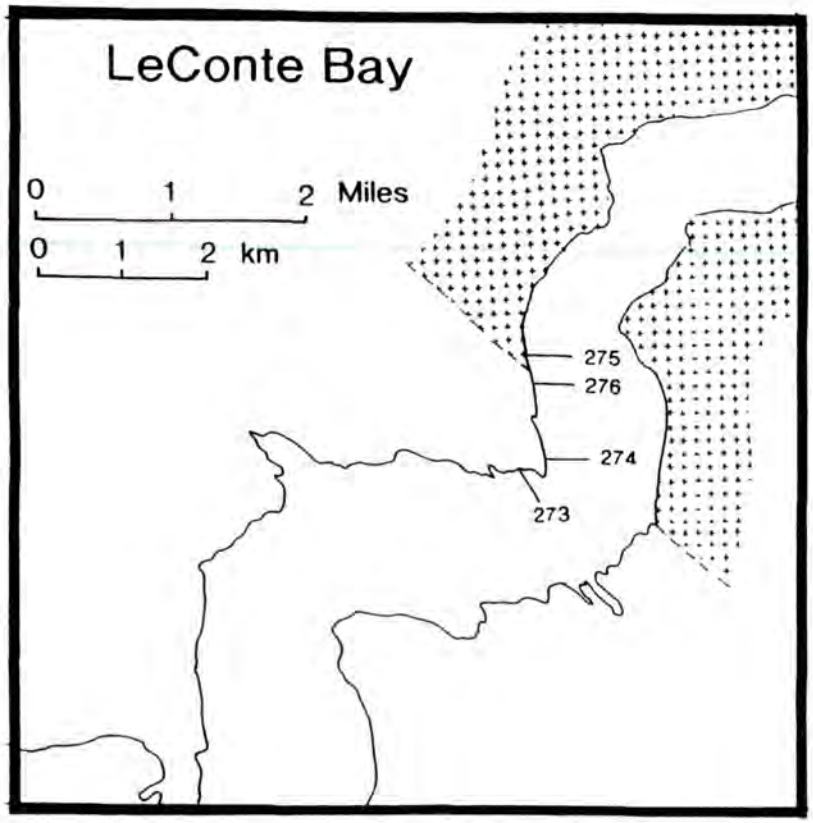

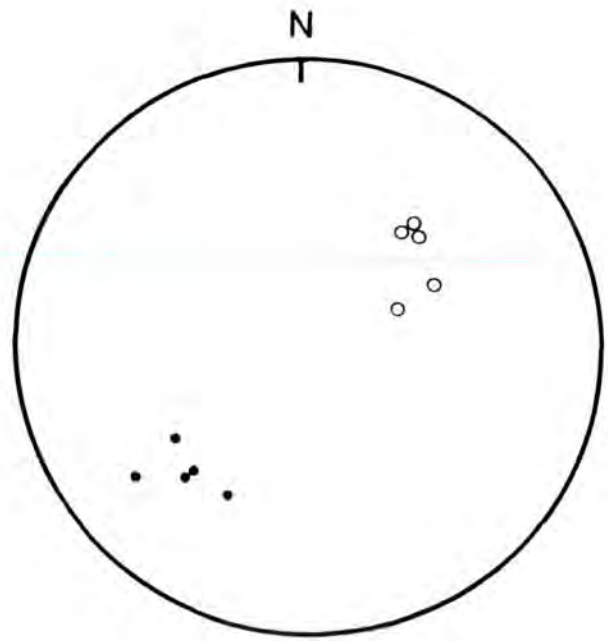

Figure 3.68

Lithology and locality map of LeConte Bay (Shading = intrusives). Structural data: solid circle = foliation; open circle = lineation (Lambert equal area stereonet, n = 10).

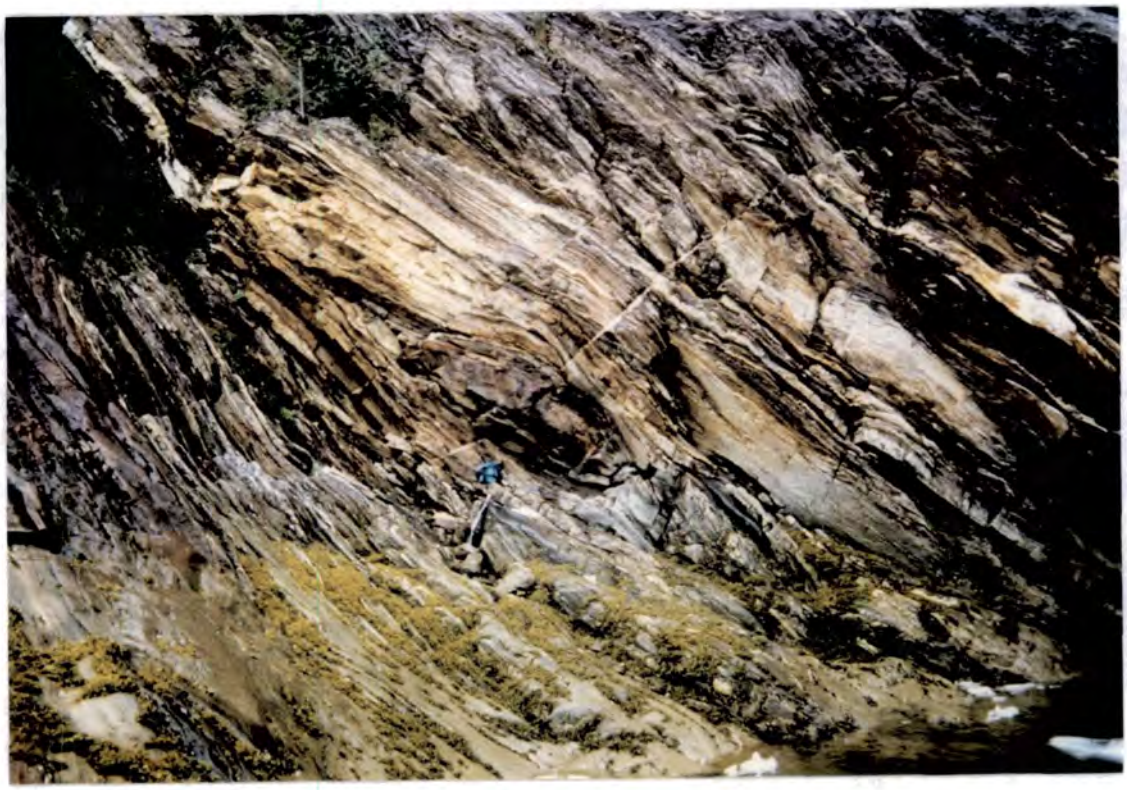

Figure 3.69 NE dipping country rock psammites, to the SW of the Great Tonalite Sill in LeConte Bay. Rucsac for scale.

porphyroclasts, and discrete shears. These indicate dominant top-to-the-SW movement. Chocolate tablet boudins, in which tonalite related granitic melts occur in the necks, indicate that a $K \equiv 0$ flattening strain component was associated with the synmagmatic deformation in the shear zone. Extensional-down-to-the-NE shears and some NE verging contractional folds are here interpreted to represent a late extension or collapse phase, in response to waning NE-SW directed shortening. The lineation plunge in these rocks varies between 69° and 79° SE, indicating, as with the Lake Dorothy ridge sections, a component of sinistral shear associated with the high angle reverse nature of the shear zone (fig. 3.68).

3.8 Bradfield Canal

85km SW along strike from LeConte Bay, a section through the Great Tonalite Sill is exposed at Bradfield Canal (fig. 3.70). The composite pluton is 2.6 km wide and is composed mainly of garnet-bearing, biotite-hornblende tonalite sheets. The country rocks to the NE are high grade gneisses containing the assemblages: quartz-biotite-sillimanite-amphibole-garnet and quartz-muscovite-biotite ± sillimanite. These gneisses have a moderately-dipping foliation and a down-dip stretching lineation, which is parallel to the hinges of tight, sideways-closing folds. Veins of granitic composition have intruded the gneiss and lie subparallel to or cut obliquely across the foliation. To the SW of the Great Tonalite Sill, the garnet-biotite-hornblende-epidote gneiss country rock contains a strong, NE-dipping foliation with NW-pitching to down-dip stretching lineations (fig. 3.71).

Shear sense is exhibited by discrete and often melt filled reverse and extensional top-to-the-SW shears, plus top-to-the-NE reverse shears: granitic melt has exploited their dilational pull-aparts in addition to the shear planes themselves. Overall shear sense is not clear, although a significant proportion of the discrete shears are conjugates indicating NE-SW directed shortening, but at a small scale, shear sense is

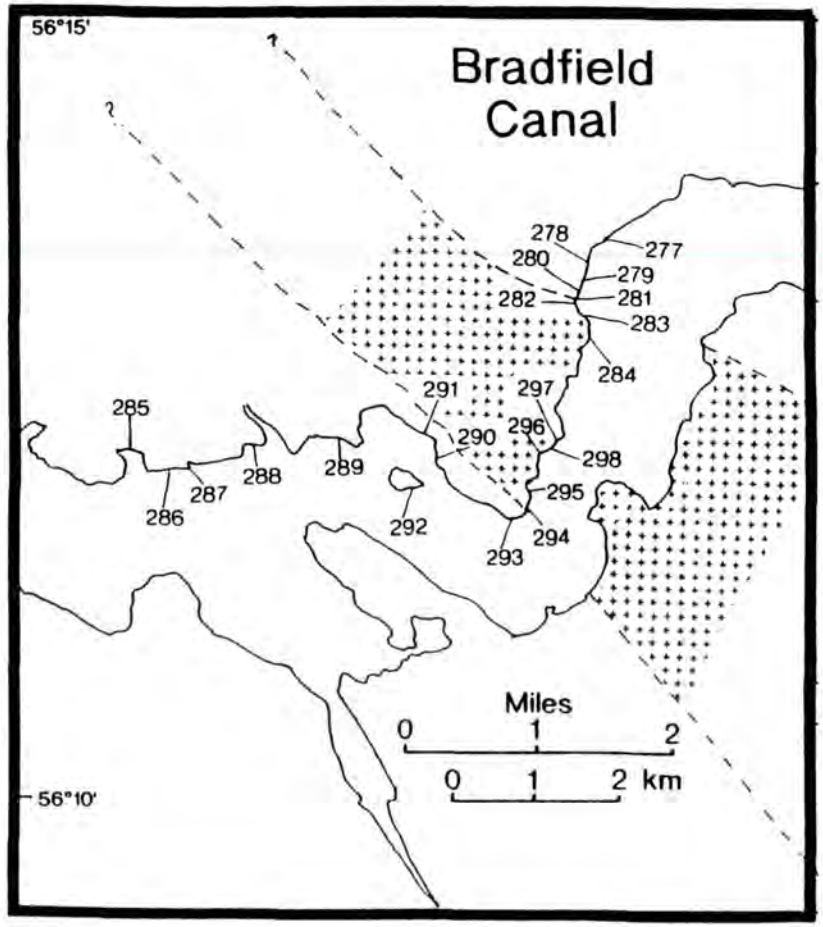

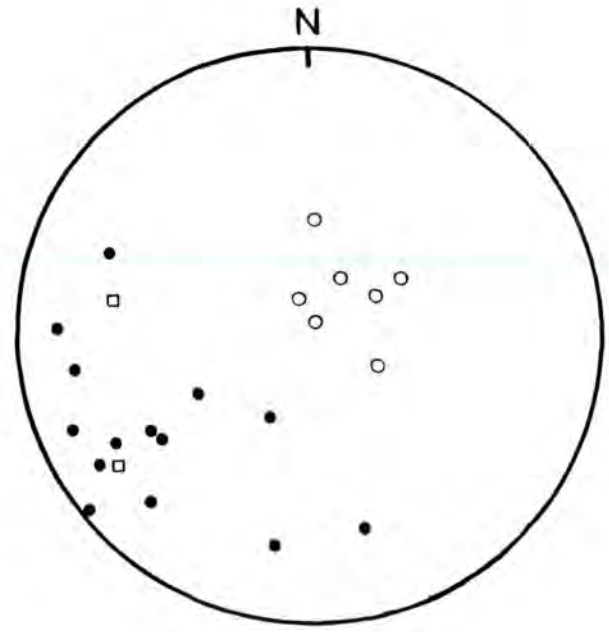

Figure 3.70

Lithology and locality map of Bradfield canal (shading = intrusives). Structural data: solid circle = CPS fabric; open circle = CPS lineation; open square = PFC fabric. n = 23).

consistently top-to-the-SW (fig. 3.72). Near the southwestern contact, granitic veins lie subparallel to the gneissose foliation (fig. 3.73) and other, conjugate, reverse and transcurrent shears appear to be fed by and root from small concentrations of melt. Close to the SW edge of the main pluton, tonalite sheets lie parallel to the gneissose foliation, but unlike other sections the strain does not increase significantly towards this contact. Syntectonic emplacement structures such as PFC fabrics and lock-up shears are preserved in close proximity to the contact indicating that the zone of ductile shear, commonly associated with this SW area, is not strongly in evidence. In fact, the crystal plastic strain component becomes much stronger towards the NE margin and is reflected by intense gneissose fabrics. Overall, this pluton is made up from numerous tonalite sheets, heterogenously deformed by crystal plastic processes, separated by screens of migmatitic country rock. Late features include shallow shears (commonly melt filled, fig. 3.74), which are dominantly top-to-the-SW reverse types, but are post-dated by granite pegmatite in flat-lying sills.

Bradfield Canal represents an unusual section through the Sill, in two ways. Firstly, the normal type of intense strain is absent, implying that the main locus of the shear zone is elsewhere - possibly to the NE, where stronger CPS foliations occur. Secondly, it may represent a higher crustal level through the sill than is commonly seen. This is suggested by the heavily veined and more obviously sheeted nature of the pluton, the latter in contrast to the more normal coalesced sheet situation.

3.9 Burroughs Bay

In the Burroughs Bay fjord section, a thin, possibly Palaeocene, hornblende-biotite tonalite pluton has been emplaced into sillimanite-grade gneisses and psammites, in the southwest, and a 336±34 Ma granodiorite (tentative date, Gehrels at al., 1991), in the northeast (fig. 3.75). The intrusion dips steeply northeast and measures 2 km wide at the N shore, but at the S shore its SW portion has been cut off

Figure 3.71 Steep down dip stretching lineation on a foliation surface in the country rock gneiss to the SW of the Great Tonalite Sill, Bradfield Canal. The foliation surface dips away from the veiwer in this picture and the lineation implies a component of sinistral movement.

Figure 3.72 Shear sense indicators in deformed granite veins suggesting top-to-the-SW (-left) shear.

Figure 3.73 XZ profile of some thin granitoid veins cutting metasediment gneiss near the SW contact with the main tonalitic mass to the NE.

Figure 3.74 Late, shallow, top-to-the-SW (-left) melt filled shears cut the main foliation in the main tonalite body at Bradfield Canal (see top of outcrop).

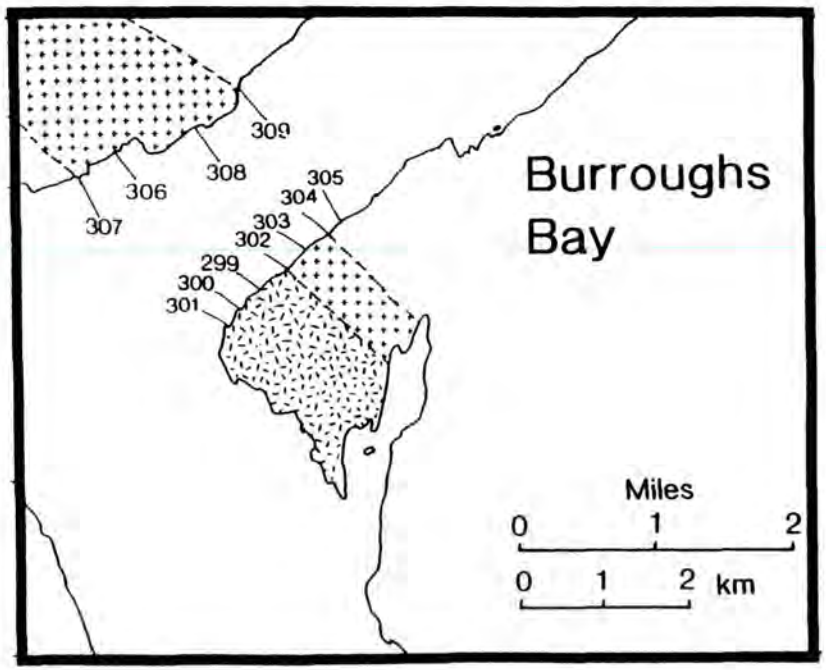

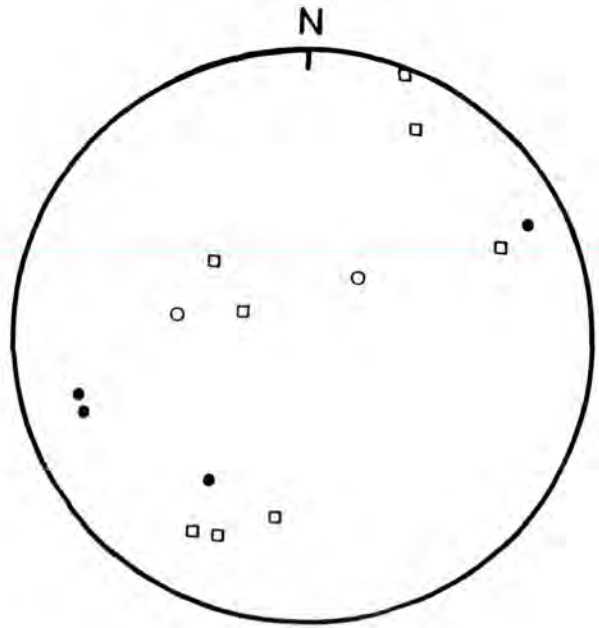

Figure 3.75

Lithology and locality map of Burroughs Bay. Crosses = Palaeocene Great Tonalite Sill; random shading = Eocene granodiorite pluton. Structural data: open square = PFC fabric; solid circle = CPS fabric; open circle = CPS lineation (Lambert equal area stereonet. n = 14).

by an undeformed Eocene(?) felsic granodiorite so that an outcrop width of only 0.65 km is preserved. The tonalite has well-developed PFC fabrics and PFC lock-up shears, but CPS deformational features are noticeably weak or absent, especially within the main body of the pluton. On the N shore, the SW contact has not been affected by the younger granodiorite and in this area the tonalite exhibits stronger CPS fabrics, indicating that as with other plutons in the belt, CPS deformation culminates at the SW margin. However, the zone of overprinting CPS deformation only extends to 40m north of this contact, implying that in contrast to more deformed plutons in the belt, this pluton may have been emplaced during the waning stages of shear zone movement. The most important feature of this pluton is theabundance of PFC lock-up shears, which are very well developed (figs. 3.76 & 3.77). These occur in conjugate sets, with both top-to-NW and top-to-the-SW senses of shear. After full crystallization, conjugate sets of both reverse and strike-slip solid state shears developed, as well as upright folds. These data, along with the PFC fabrics and lock-up shears, indicate that NE-SW-directed pure shear affected the tonalite body during the crystallization interval. Overall shear sense in the Burroughs Bay tonalite body is ambiguous, but top-to-the-SW shear is dominant on the S shore.

Tonalite emplacement took place mainly along veins and sheets, which lie parallel or subparallel to the gneissic foliation, but in addition, some high temperature CPS/solid state shearsoccur with granitic melts intruded along their medial planes. These melts are often of minimum granitic melt composition (plagioclase and quartz) and may represent anatectic country rock at the contact, which was then drawn into the active shears. This type of shear occurs in both the tonalite and the country rocks. Other, less important emplacement features include anastamosing vein networks, leading to small-scale stoping and isolation of blocks.

3.10 Walker Cove

Figure 3.76 PFC lock-up shears as they are seen in the field at location 302, Burroughs Bay. The arrows indicate the movement directions.

Figure 3.77 Close up of 3.76, showing the PFC lock-up shears in more detail, at location 302.

At least two types of tonalite, representing two phases of emplacement, occur on the S shores of Walker Cove, in an approximately 7 km wide zone (fig. 3.78). An older gneissic tonalite, which has been intruded by the younger, less deformed sphene-bearing hornblende-biotite tonalite, is composed of screens of tonalitic to granodioritic gneiss and migmatite. This occurs especially in the southwest and the screens may vary in thickness from tens of centimetres to tens of metres in width. At the contacts between younger tonalite sheets and older gneiss screens occur many veins, shears and shears with melt along them. These serve to break up the gneiss into xenoliths, which are in various stages of assimilation. However, mafic enclaves are not abundant. The younger tonalite (fig. 3.79) has a dominant PFC fabric of aligned plagioclase and amphibole laths, and is overprinted by a weak to moderately strong CPS fabric. It occurs as sheets trending NW-SE, which dip steeply to the southwest (commonly) or to the northeast. PFC lock-up shears can be discerned in the least deformed areas, which testify to its syntectonic intrusive history. Shear sense is neutral overall, as top-to-the-SW, top-to-the-NE, dextral and sinistral shears are all present, and this is consistent with a tectonic regime dominated by NE-SW directed shortening and pure shear. Strain in the younger tonalite is low ($y/z = 4$) in comparison with other plutons in the belt, which supports the idea that it was emplaced at a late stage in the deformation history of the zone.

3.11 Haines, Berners Bay and Boca de Quadra to the Skeena River

The following sections are taken from fieldwork carried out by D.H.W. Hutton between 1985 and 1991 and are summarised in Ingram & Hutton (*in prep*). These sections are included in order to extend the study from 420 km to ~800 km strike length of the Great Tonalite Sill belt, from Haines, Alaska, in the north, to the Skeena River, British Columbia, in the south. The descriptions are brief and as follows:

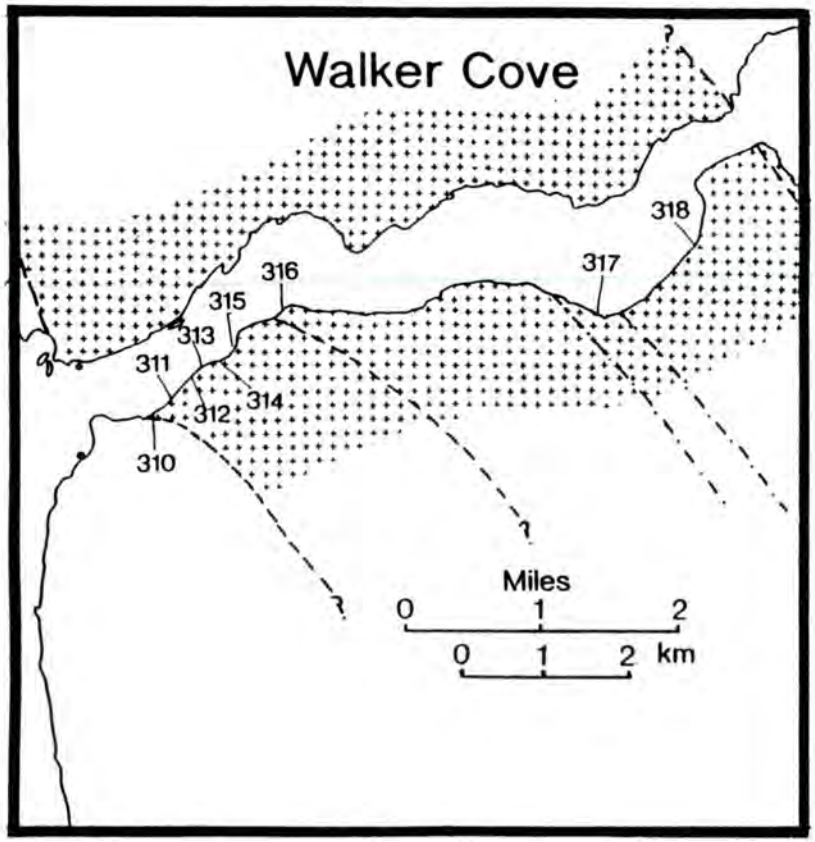

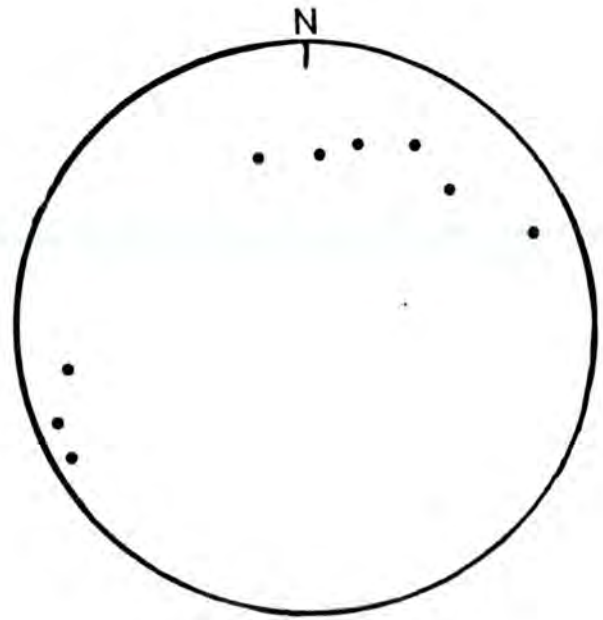

Figure 3.78

Lithology and locality map of Walker Cove. Shading = intrusives. Dashed lines = internal contacts. Structural data: solid circle = foliation. n = 9).

Figure 3.79 Outcrop view of the younger tonalite in Walker Cove.

3.11.1 *Haines*

The Tonalite Sill N and E of Haines (the Ferebee pluton of Redman et al., 1984), has been dated at 68Ma (Barker et al. 1986) and 83 Ma (Gehrels et al. 1991). This contains strong CPS fabrics at the NE and SW margins, with coplanar PFC fabrics preserved in the central region. Lineation pitches are close to 90° (fig. 3.80) and shear sense is top-to-the-SW, except near the NE contact, where the obliquity indicates a sinistral shear component. These are cut by discrete top-to-the-S shears, often filled by late, but probably cogenetic, melt, implying penecontemporaneity of magmatism and deformation.

3.11.2 *Berners Bay*

The hornblende-biotite tonalite at this locality is 7 - 8 km wide and belongs to the Mendenhall Glacier pluton (fig. 3.81, Brew & Ford 1986). Deformation in the SW part of this unit is dominated by strong NW-SE trending, steeply inclined, cataclastic fabrics, in which the tonalite has been reduced to a fine grained, unrecrystallized groundmass of angular grains, supporting larger, porphyroclastic fragments of feldspar. Secondary shear planes associated with the cataclasis are prolific and have a basic quadrimodal pattern with an implied K-value less than 1. This late defomation may be related to movement of the nearby Coast Range Megalineament (Brew 1978, e.g. fig. 3.1). In the NE, the original rock is locally preserved and this shows steep PFC fabrics with steep lineations and overprinting CPS strains with top-to-the-SW shear.

3.11.3 *Boca de Quadra*

The Great Tonalite Sill pluton here (fig. 3.4) is rather thin (1-2 km), highly deformed and compositionally heterogeneous, with, as well as tonalite, melagabbro

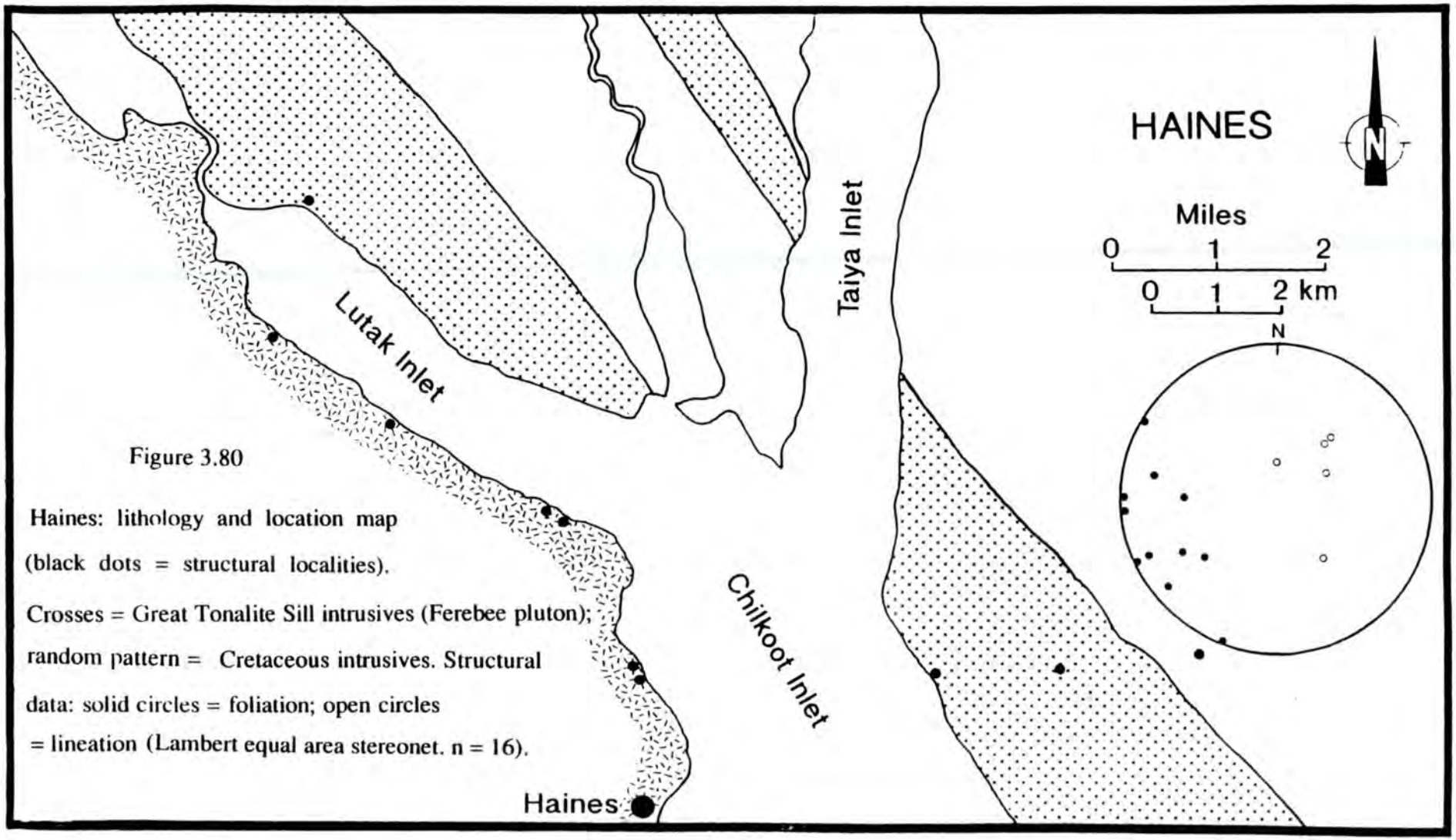

Figure 3.80

Haines: lithology and location map (black dots = structural localities). Crosses = Great Tonalite Sill intrusives (Ferebee pluton); random pattern = Cretaceous intrusives. Structural data: solid circles = foliation; open circles = lineation (Lambert equal area stereonet. n = 16).

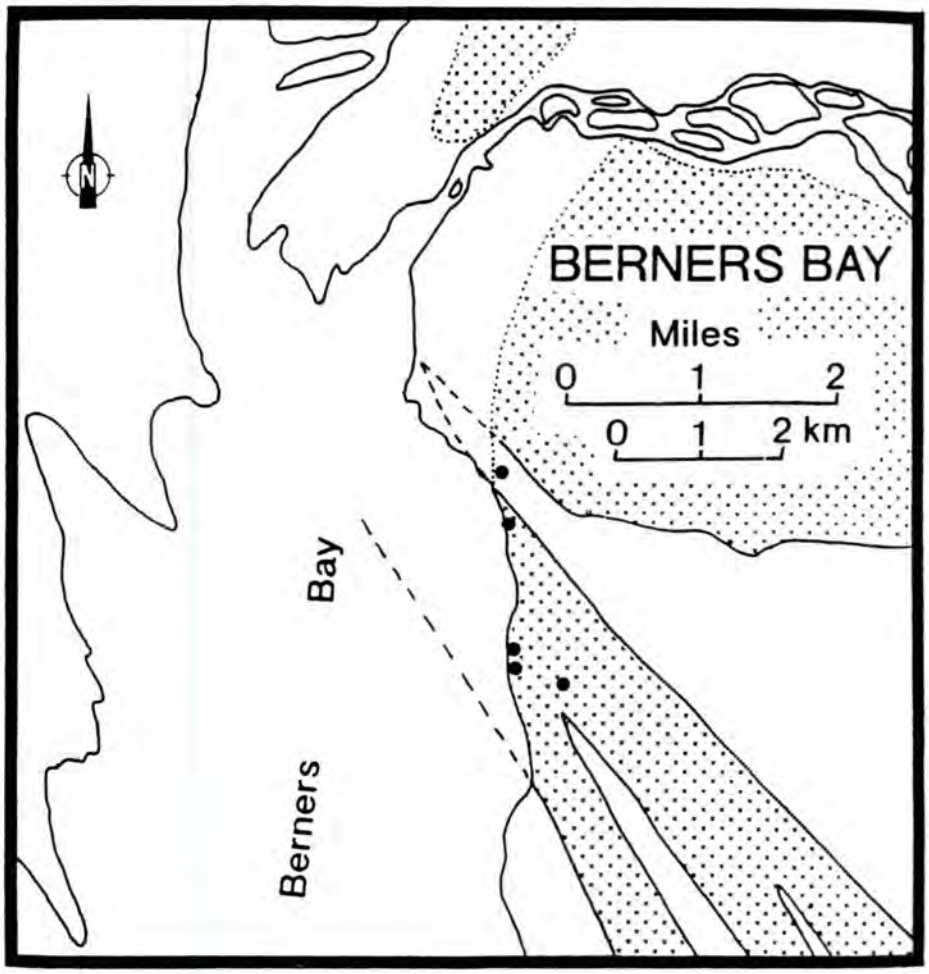

Figure 3.81 Berners Bay: lithology and location map (black dots = structural localities). Crosses = Great Tonalite Sill intrusives.

(appinite), granodiorite, trondjemite together with metasediment screens. Pervasive CPS fabrics dip moderately to steeply NE and E and overprint originally similarly inclined PFC fabrics. Solid state shear sense, particularly at the grain scale, is top-to-the-SW. Low temperature deformation is related to grain reducing, flat lying, discrete mylonite zones, which are often associated with gentle to moderately NW plunging lineations and oblique dextral/top-to-the-SW shear sense. On the southern margins of the Sill trondjemitic pegmatite sheets and bodies (55 Ma, Crawford & Crawford 1991) are cut by solid state steep fabrics with down dip lineations and top-to-the-E shear sense. This deformation, which is younger than the Great Tonalite Sill deformation may relate to the "Coast Shear Zone" of Crawford & Crawford (1991) (W. Crawford pers. comm.), which is generally outboard of the Great Tonalite Sill.

3.11.4 *Pearse Canal*

The Quottoon pluton (60 Ma, Crawford et al. 1987) occurs in several major sheeted units exposed on either side of the international border at the SW end of Pearse Canal (fig. 3.82A). Strong CPS fabrics dominate these rocks and foliation dips are moderately N to NE, with downdip stretching lineations. Near the hanging wall contact, deformation is heterogeneous and outcrop scale discrete shear zones are common. These show variable shear sense, but a set of gently inclined to flat-lying structures show consistent top-to-the-S movement, as in e.g. Bradfield Canal and Burroughs Bay. Smaller (grain and phenocryst) scale kinematics appear more consistently top-to-the-S or SW. At the SW contact strong solid state strains are associated with good top-to-the-SW shear indicators (especially asymmetric pressure shadows around feldspars). Aligned euhedral feldspars and hornblendes are also seen indicating that an original PFC fabric was generated in these rocks. The footwall schists in this section show abundant sillimanite and sillimanite after kyanite (L.S. Hollister pers. comm.), with crystals aligned parallel to the down dip stretching,

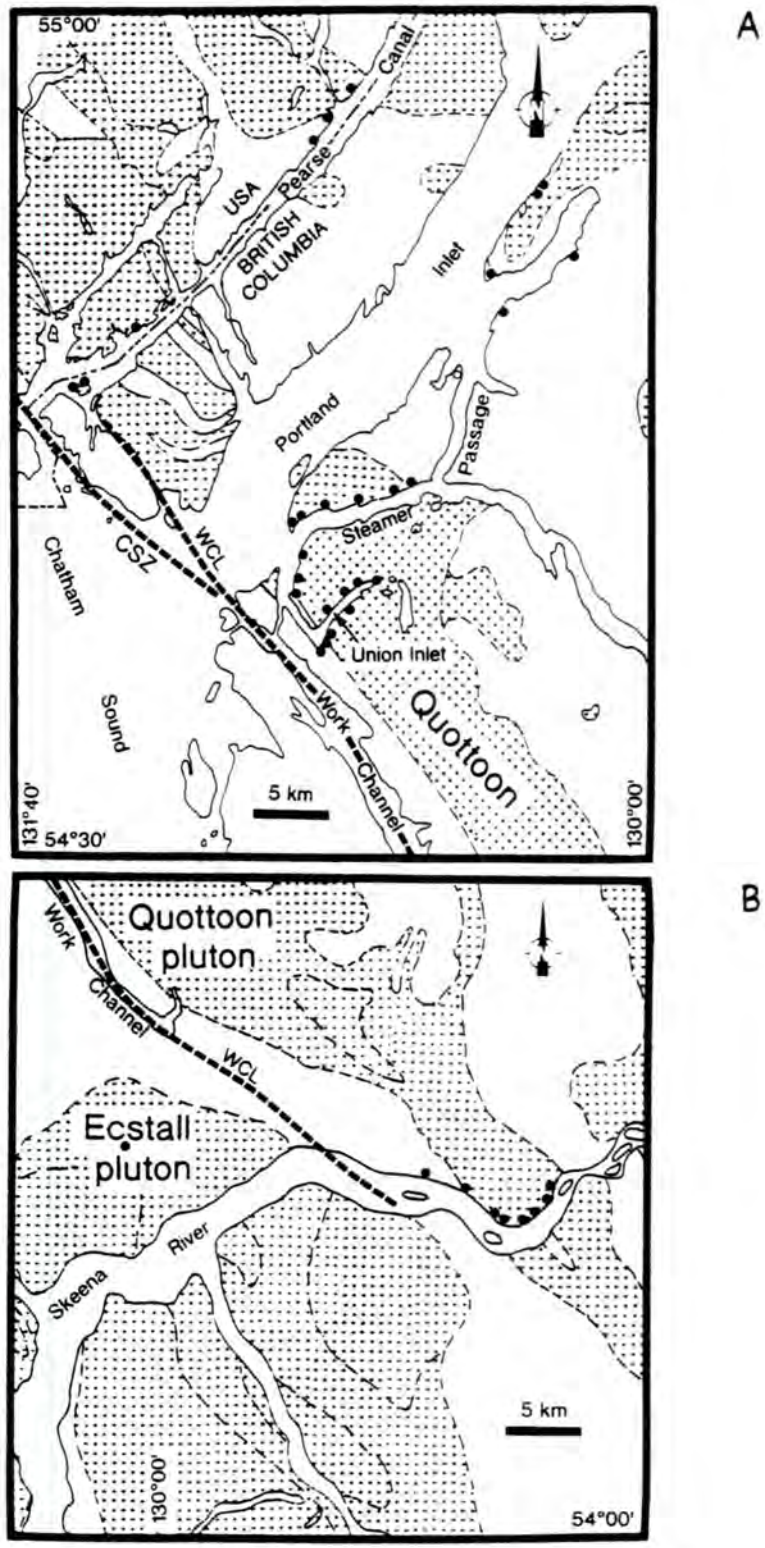

Figure 3.82 A. Pearse Canal, Steamer Passage and Union Inlet: Traverses and structural localities across the Quottoon pluton, British Columbia. B. The Skeena River traverse through the Quottoon pluton. Black dots = localities; shading = granitoids.

showing, as with other such sections, the contemporaneity of Tonalite Sill metamorphism with shear zone deformation.

3.11.5 *Steamer Passage and Union Inlet (B.C.)*

Two closely spaced traverses are combined here for ease of description. One is a complete section across the Tonalite Sill (Quottoon pluton) in Steamer Passage, at the SW end of Portland inlet. The other is a section from the centre of the Sill southwards into its footwall rocks in Union Inlet, 7km SE (fig 3.82A).

Fabrics and external contacts dip moderately to steeply NE, but in the central parts of the pluton strains are low (x/z approximately 3.5). PFC fabrics defined by hornblendes and plagioclase are well preserved in this central area and PFC down dip lineations are discernible in most outcrops. PFC lock up shears are well developed and although conjugate sets, implying a major component of pure shear associated with NE-SW contraction, are well represented, shears with a top-to-the-SW sense appear to be more common. Elsewhere, PFC tiling structures attest to this shear sense. PFC fabrics are intense at the NE contact of the pluton (Somerville Island), although CPS/solid state overprinting is strong and heterogeneously developed here. An increase in the degree of CPS overprinting can be traced southwards and in many situations, especially at the grain scale, top-to-the-SW shear is predominant. In the footwall schists within 300 meters of the pluton, vertical to steeply inclined intense fabrics deform zones of trondjemitic pegmatite in moderate temperature conditions (quartz is ductiley deformed, feldspar is semiductiley deformed). These pegmatites are correlated with those in Boca de Quadra (M.L. Crawford pers. comm. to D.H.W. Hutton) and dated at 55 Ma (Crawford & Crawford 1991). The deformation, which is younger than this and certainly younger than the Great Tonalite Sill/Quottoon pluton, has a steep down dip lineation and top-to-the-NE sense of motion. This is correlated with the younger Coast Shear Zone of Crawford & Crawford (1991) in the Prince Rupert - Boca de Quadra area. Deformation of this type also locally affects the

Quottoon tonalites, and complex outcrops containing intense CPS/mylonitic fabrics, with both top-to-the-SW and top-to-the-NE shear sense are seen close to the footwall schists.

3.11.6 *Skeena River*

The most southerly section through the Great Tonalite Sill is taken from the road and rail cuts through the Quottoon pluton, in excellent exposures on the north side of the Skeena River (fig. 3.82B). The main fabrics in the pluton dip steeply NE, are vertical and contain a well developed down dip lineation. A 200 metre wide zone of CPS/solid state mylonites is developed in the middle of the section, and in this a top-to-the-SW shear sense is dominant. On either side of this, PFC fabrics with numerous top-to-the-SW lock up shears are found. Towards the SW edge of the pluton CPS strains increase and solid state, top-to-the-NE shears become more common, although top-to-the-SW structures still predominate. The SW edge of the pluton is sheeted and has screens of metasediments containing SW-verging folds and top-to-the-SW extensional crenulation cleavages. Shallow, melt-filled shears, similar to those seen in the N (e.g. Thomas Bay) are common and also have a top-to-the-SW sense. Conjugate shears containing melt occur frequently and these were actively deformed synchronously with the melt emplacement. On the opposite (NE) flank of the Quottoon pluton, the cordierite-andalusite-garnet-sillimanite metasedimentary gneisses contain shear sense indicators, such as garnet pressure shadows and SC fabrics, with a similar reverse top-to-the-SW sense of shear.

3.12 Conclusions and structural summary of the Great Tonalite Sill

It is clear that observations in these additional sections through the Great Tonalite Sill expand and consolidate the major conclusions derived from the more

detailed studies in the Juneau area. Local variations apart, a remarkable consistency in structural architecture and history exists along nearly 800 km strike length. In the following sections the salient deformational features of the Great Tonalite Sill belt are discussed.

3.12.1 *The main (D_2) foliation*

Throughout the Great Tonalite Sill the main fabrics are remarkably consistent in attitude. These initiated when the rocks were not fully crystallized (PFC fabrics) and continued to be formed, during cooling and further crystallization, into the solid state (CPS fabrics). Figure 3.83 illustrates the combined PFC and CPS data, which define the main foliation and lineation from Haines, in the north, to the Skeena River, in the south. The mean D_2 foliation dips steeply northeast (strike/dip: 140°/74°NE) and contains within it a down-dip, nearly 90° pitching, lineation (plunge-azimuth: 64°-047°). These data indicate that the early formed PFC and late CPS fabrics are coplanar, reflecting a regime in which the principal strain axes remained fixed during and after the crystallization interval. The inferred orientation of the maximum principal stress axis, throughout the deformation interval, is thus NE-SW with a subhorizontal attitude. Shear sense parallel with the main foliation is consistently reverse top-to-the-SW and this has been observed in both PFC and CPS states.

3.12.2 *The discrete shears*

Two main types of shears occur in the rocks of the Great Tonalite Sill: (1) primary, PFC lock-up shears, and (2) later CPS shears.

PFC Lock-up shears. The PFC lock-up shears, which formed as the magma reached the rheological critical melt percentage (see section 1.3.2), are compiled on figure 3.84. The distribution of dominant reverse and more minor sinistral and dextral

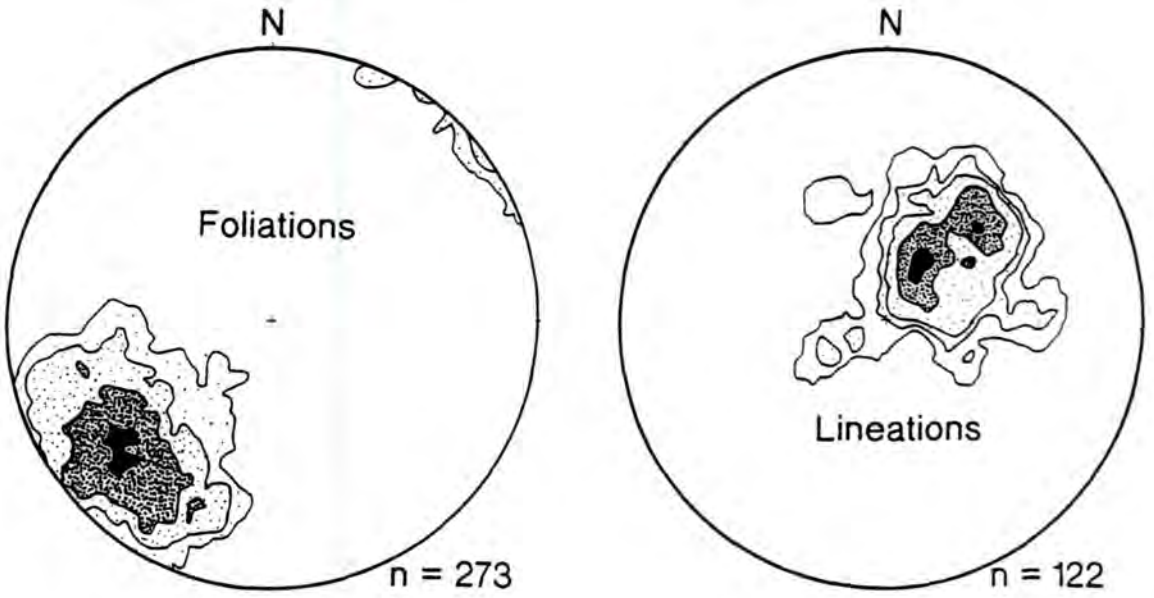

Figure 3.83 Lambert equal area stereonets of combined foliation and transport lineation from Haines, SE Alaska to the Skeena River, British Columbia. Contour intervals are: 1.5, 3, 5, 9.5, 14 percent.

shears, indicates the presence of four conjugate sets in a quadrimodal distribution: NW-SE striking, reverse top-to-the-SW and -NE, NNW striking dextral and ESE striking sinistral shears. Together they imply NE-SW horizontal contraction, with a degree of vertical extension, associated with these early (syn-magmatic) deformation increments.

CPS shears. Figure 3.85 illustrates the discrete CPS shear data coverage for the whole belt. They too define four similar conjugate sets in which the reverse shears dominate. Together, these form a quadrimodal set, with implied subhorizontal, NE-SW orientated ($0 < K < 1$) pure shear. Many of the CPS shears are filled with melt, which is considered cogenetic with the main intrusives, and this constrains the timing of these structures to within the mmagmatic history of the Great Tonalite Sill. Later shears, without melt, and down-temperature mylonitic shears retain a similar system of conjugates.

Although exceptions to the above generalisations occur in places, such as the presence of extensional PFC lock-up shears (usually dipping NE or SW), the implied deformation regime here, taken as a whole from early PFC structures to late melt- and dyke-filled shears, thus records consistent NE-SW contraction and vertical extension. Associated with this is a top-to-the-SW shear sense. Thus the general structural sequence is one of PFC fabrics closely followed by PFC lock-up shears, followed by coplanar overprinted CPS/solid state fabrics and the subsequent development of various types of discrete ductile shears. The constancy of their geometry through time suggests that all of these structures initiated in response to similarly orientated external stresses.

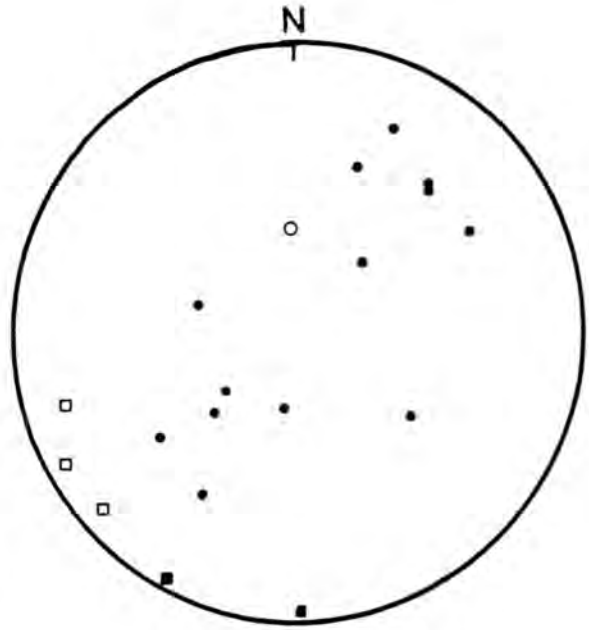

Figure 3.84 Representative sample of PFC lock-up shear data for the Great Tonalite Sill belt, showing a basic quadrimodal pattern (Lambert equal area stereonet: solid circle = reverse shear; open circle = extensional shear; open square = dextral shear; solid square = sinistral shear. n = 19).

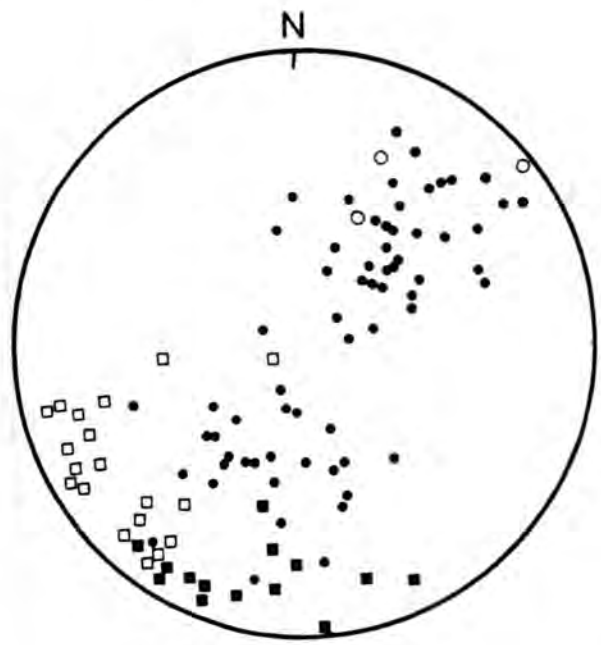

Figure 3.85 Total CPS shear data for the Great Tonalite Sill belt between Juneau and Walker Cove, showing quadrimodal pattern (Lambert equal area stereonet: solid circles = reverse shears; open circles = extensional shear; open squares = dextral shears; solid squares = sinistral shears. n = 106).

3.12.3 *The Great Tonalite Sill shear zone*

The most intense foliation and lineation development took place in a zone, approximately 10 km wide, centred on the southwest edge of the Great Tonalite Sill, called here the Great Tonalite Sill shear zone.

The strain profile of this shear zone shear zone is bell-shaped (see section 3.1.2): a rapid increase in strain is observed moving northeast from the footwall country rocks into the SW part of the Sill; a more gradual decrease in strain and relative fabric intensity is observed moving northeast through the remainder of the Sill. These features create the asymmetric profile. However, although strains are high in certain sections through this shear zone, calculations based on this profile from Taku Inlet indicate that the Great Tonalite Sill plutons were not more than five times their present (deformed) width.

The foliation-parallel shear sense is dominantly reverse top-to-the-SW, or northeast side up, and is indicated most convincingly at the grain scale. Taking into account the distribution of K-values across the Great Tonalite Sill, this simple shear component is interpreted to lie at, and close to, its southwestern edge. K-values are close to 1 at this point, but decrease towards 0 northeastwards, reflecting the increasing importance of flattening strains. Locally, extensional, top-to-the-SW structures were observed, but these were attributed to back-rotation of the previous reverse structures and the presence of extensional reidel shears (fig. 3.59).

Shear zone nomenclature. In this thesis the name "Great Tonalite Sill shear zone" is used to identify the high temperature shear zone, centred on the SW edge of the Great Tonalite Sill, which developed solely during the emplacement, cooling and subsequent solidification of the magmas that constitute this remarkable batholith. The PFC and high temperature CPS fabrics and structures within this zone together indicate that the shear zone was contractional and had a reverse shear sense of northeast over southwest: indeed, such kinematics are consistent along the entire

800km length of the sill described here. In places the Great Tonalite Sill shear zone is also spatially coincident with other previously documented shear zones, such as the Coast Shear Zone (Crawford & Crawford 1991, McClelland et al 1992) and may also lie close to or be coincident with the Work Channel Lineament (Crawford & Hollister 1982). However, these authors indicated that the latter shear zones locally contain significant west-side-up kinematic indicators. Thus the names of the above shear zones are not interchangeable with the Great Tonalite Sill shear zone. Their kinematic and structural differences probably reflect temporal changes in the deformational regimes within a spatially coincident zone.

3.12.4 *Pluton structure*

Observations from all the traverses in this study, indicate that the Great Tonalite Sill batholith is composed of many individual elongate tonalitic plutons, which are themselves composed of many foliation-parallel tonalitic sheets. Previous mapping (compiled most recently by Wheeler & McFeely 1991) and mapping from this study indicates that the width of the Sill, as a whole, varies from around 2 km, up to around 25 km, but is commonly around 10 km. Observations of the component plutons indicate that their contacts are concordant to the regional foliation, which dips steeply northeast, and have deformed widths ranging from 300 metres to 8 km or more. Direct measurements indicate that the sheets making up these plutons have widths ranging from <1 metre to around 100 metres, but widths greater than this are envisaged from field relationships and strain studies. The sheets are most easily recognised at the margins of plutons, where they have coalesced to the least degree and are separated by thick metasediment screens. However, in the interior parts, the sheets are less easily recognised and here the plutons maintain a more monotonous appearance. However, the plutons are by no means homogeneous. They are broken by the following foliation-parallel features: screens, or septa, of metasediment and synplutonic mafic material; zones of high strain; crystal plastic, or mylonitic, shear zones of varying extent; internal

contacts marked by e.g. differences in fabric intensity; zones abundant in mafic enclaves and xenoliths; and variations in petrography. In one particularly well exposed pluton (Mount Juneau pluton), detailed work revealed an internal structure of planar sheets, with chilled contacts on one side only, analogous to the pattern of dykes commonly observed in ophiolite complexes. Apart form the ubiquitous foliation-parallel sheets seen in all of the plutons, tonalitic intrusive material was also recorded within the medial planes of shears and in areas of net dilation, such as thrust flats and other pull-apart structures, in the overall implied contractional regime.

Figure 3.86 illustrates a simplified section through the Great Tonalite Sill, which is generally applicable to it along at least 700 km of strike length. It must be borne in mind that this pattern is more clearly developed in some sections than in others. In Bradfield Canal and Burroughs Bay, in particular, the apparent width of the Great Tonalite Sill shear zone is greatly reduced, reflecting that either: (1) the structural level at these locations is higher than in the rest of the belt and as such exposes a less well developed, pervasive, ductile shear zone, or (2) the Great Tonalite Sill intrusives in these sections were emplaced during the waning stages of shear zone deformation and thus do not record high defomational strains, or (3) both.

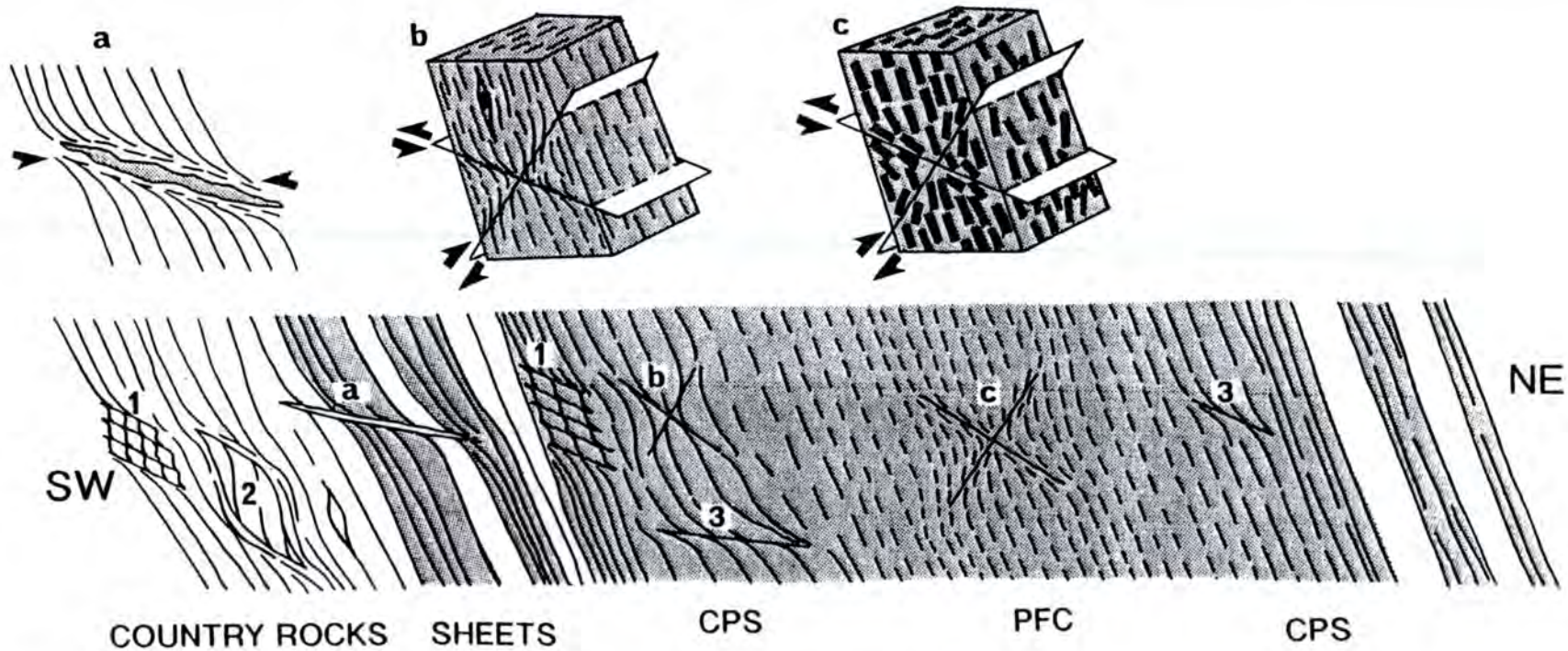

Figure 3.86 Generalised cross section through a single pluton of the Great Tonalite Sill belt, illustrating the salient features: (a) late stage, top-to-the-SW ductile shears, intruded by cogenetic melt; (b) secondary CPS foliations, with down dip lineations, cut by conjugate ductile shears, and sigma porphyroblasts; (c) primary PFC fabrics, with down dip lineations, cut by conjugate PFC lock-up shears. Top-to-the-SW shear sense criteria: (1) extensional crenulation cleavages; (2) asymmmetric boudins; (3) low-angle, late, top-to-the-SW shears.

CHAPTER 4
MICROSTRUCTURAL EVOLUTION

4.1 Introduction

This chapter is designed to illustrate the range of fabrics and microstructures that dominate the plutons of the Great Tonalite Sill. It incorporates the detailed analysis and description of fabrics and structures in the field, in hand specimens and in thin sections. It is not the purpose of this chapter to discuss in depth the deformation mechanisms and textures seen in the rocks. The underlying purpose is to chart the evolution of fabric types, from the initial magma, through the crystallization interval and into the solid state regime, in order to gain a feel for the overall sequence of events during prolonged, progressive deformation of a crystallizing and cooling batholith. Interpretations deduced from these studies strive to reveal the main controlling factors prevalent during progressive deformation. Physical factors include (i) the percentage of melt present, (ii) the mineralogy of the rock, and environmental factors include (iii) temperature, (iv) pressure and (v) shear stress. Strain rate is another factor which may have a bearing on the deformation. However, this is difficult to quantify and therefore it is assumed constant for the Great Tonalite Sill shear zone as a whole, although local outcrop scale variations probably occurred.

Of particular interest are the deformational fabrics and structures that define the transitions, between different physical and rheological states, experienced by granitoid rocks during their crystallization interval and subsequent cooling. The two main transition intervals exhibited by the rocks of the Great Tonalite Sill are:

(1) ***Pre-full crystallization (PFC) - crystal plastic strain (CPS) transition.*** This occurs in the vicinity of the rheological critical melt percentage of magmas (Arzi 1978) and is typified by structures associated with "lock-up" i.e. the point at which the crystals in the magma interact, thus forcing the effective viscosity to rise dramatically.

(2) ***Brittle - ductile transition.*** According to Gapais (1989), this occurs at around 500-550°C and marks a sharp increase in bulk strength in cooling granitoids. Essentially it marks the transition between homogenous foliations at high temperatures (>500-550°C) and the field of discrete macroscale deformation zones at low temperatures (<500-550°C).

In a crystallizing and cooling (i.e. retrograde) system, both of these transitions mark a change from homogenous distribution of strain, in the form of pervasive foliations, to heterogenous strain distributions, typically in mesoscale and macroscale shear zones. Both transitions mark fundamental and considerable increases in bulk strength of magma and solid, which are inextricably linked to the relative proportions of strong and weak fractions present in the rock or magma. Gapais (1989) stated that solid state deformational structures in granites provide much information concerning the thermal and mechanical states during deformation. Similar information is also provided by the pre-full crystallization (PFC) lock-up structures and PFC fabrics. The microstructures and their implications will now be explored.

4.2 Microstructural characteristics of the Pre-full crystallization fabrics

Pre-full crystallization (PFC, Hutton 1988a) fabrics and lineations, by implication, represent deformation which occurred before all of the mineral phases had crystallized fully. The deformation mechanism involves the rotation and alignment of early formed crystal laths, commonly feldspar and amphibole, which are suspended in

an uncrystallized matrix. The resultant fabric is composed of aligned, internally undeformed phenocrysts, with an interstial matrix of late crystals such as quartz.

The granitoids of the Great Tonalite Sill often display well developed PFC fabrics and, within these, strong although not intense lineations, which are coplanar and colinear with the regional shear zone deformation. These fabrics are commonly located in the less deformed central parts of individual plutons, away from the petrological and rheological boundaries which occur at country rock contacts, where the ductile, solid state deformation, if present, is dominantly partitioned.

Figure 4.1A illustrates the microstructure of a well developed PFC fabric within the late synkinematic (55 - 60 Ma, Brew et al 1989) Taku Cabin tonalite (Drinkwater et al 1990) (Turner Lake pluton), in Taku Inlet. Figures 4.1B & 4.1C show hand specimens of well developed PFC fabrics as they may be seen in the field. In thin section, the subhedral to euhedral, twinned, zoned plagioclase and euhedral, twinned amphibole laths are aligned defining the PFC fabric. Both these main phases, which are internally undeformed, are associated with interstitial quartz biotite and sphene. Solid state deformation is sparse and manifests itself in the form of poorly developed myrmeckite and in quartz some undulose extinction, and isolated large subgrains. This fabric indicates that the deformation was synmagmatic and that it did not affect the tonalite once its melt content had passed below the rheological critical melt percentage (RCMP, Arzi 1978) (see chapter 1).

Similarly, figure 4.2 shows a PFC fabric, expressed dominantly as an alignment of plagioclase laths. However, in this case the margins of the laths are more irregular and there are more abundant, smaller subgrains of quartz at grain boundaries than in 4.1. In addition, rare internal deformation of plagioclase, in the form of slightly bent composition planes, and microclining occurs. These factors indicate that deformation continued for a short time after full crystallization, enough to slightly modify the PFC fabric with crystal plastic strain (CPS, Hutton 1988a) deformation. However, the presence of magmatic features such as zoning, a good alignment of dominantly non-

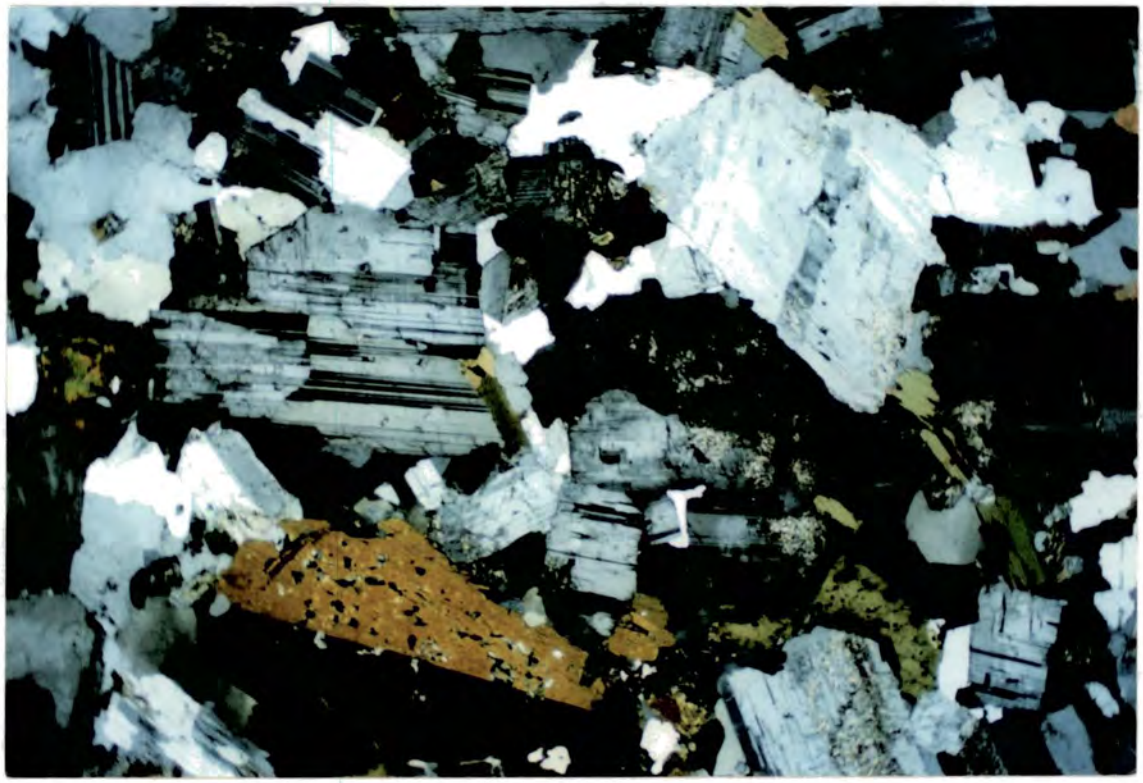

Figure 4.1A Well developed PFC fabric in thin section. Location 161, Taku Inlet. Field = 18 mm.

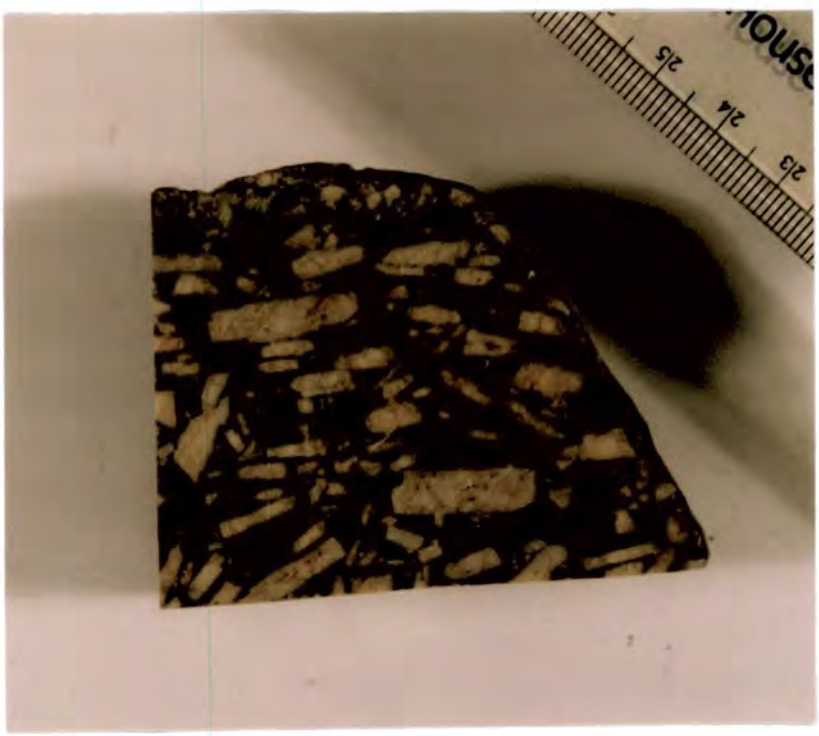

Figure 4.1B Hand specimen of a well developed PFC fabric from a minor mid Cretaceous tonalitic intrusion on Juneau Island, Douglas.

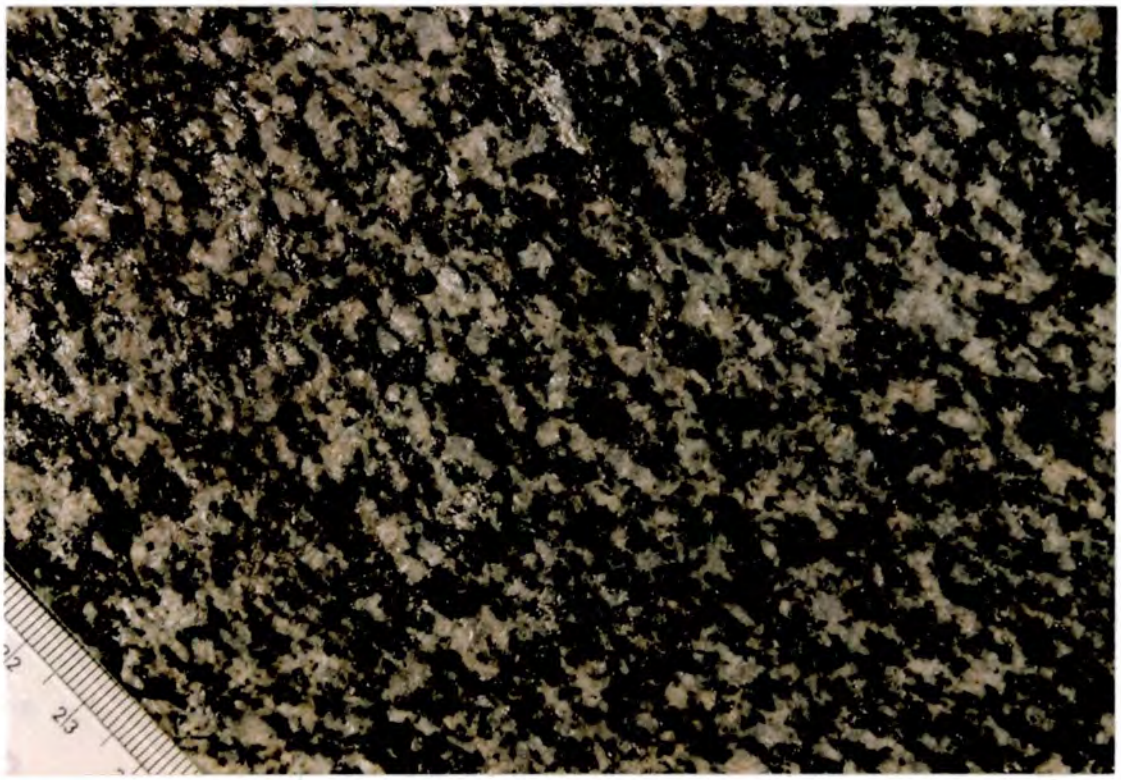

Figure 4.1C Hand specimen of a well developed PFC fabric in tonalite from location 302, Burroughs Bay (XZ plane).

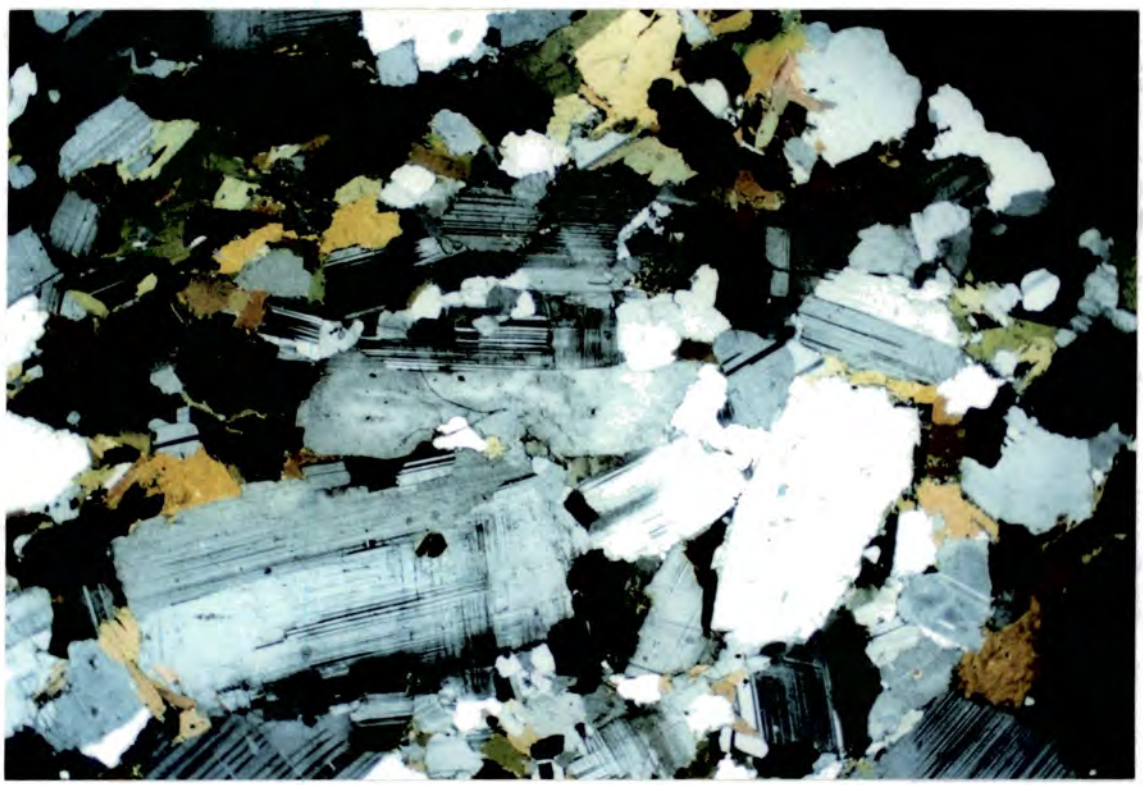

Figure 4.2 PFC fabric in the Burroughs Bay tonalite. Location 304. Field = 18 mm.

internally deformed plagioclase laths and interstitial quartz, indicates that the fabric is only very weakly overprinted by CPS deformation.

In summary, the features in 4.1 and 4.2 are the result of the rigid body rotation and aligment of non-internally deformed, non-equidimensional, early crystallized phases, suspended in a melt which subsequently crystallized to form the interstitial phases. Such deformation is therefore regarded as the first deformation recorded in the Great Tonalite Sill plutons. It has been shown in chapter 3 that the PFC fabrics throughout the Great Tonalite Sill are parallel to the regional shear zone trend, and it is evidence such as this which leads the author to conclude, in agreement with Brew & Ford (1981), that its component plutons were emplaced syntectonically.

4.3 Microstructure of the Pre-full crystallization lock-up shears

Shear sense in the magmatic state is provided by discrete shears, defined by euhedral laths of plagioclase and amphibole (commonly), which swing into parallelism with the shear plane. These are termed PFC lock-up shears (Hutton & Ingram 1992, Ingram & Hutton 1992).

During progressive deformation of a crystallizing magma, the PFC fabric development intensifies, until the melt content drops to the RCMP (Arzi 1978). At this point the bulk strength increases rapidly due to interaction between the crystal laths, and it is here that the discrete, planar, PFC lock-up shears develop. In essence they represent a sudden switch from pervasive homogenous deformation and the formation of PFC fabrics, to heterogenous deformation and the formation of discrete zones of shear, in the final stages of the magmatic state. The following descriptions will highlight the evidence for this interpretation and provide a detailed account of their microstructure in general.

Figures 4.3A and 4.4 show examples of PFC lock-up shears in thin section, with the planes of section cut perpendicular to the shear planes and parallel to the shear

transport directions. The shear in figure 4.3A trends shallowly from bottom left to top right and cuts the steeper foliation with a top-to-the-right sense. The line drawing on figure 4.3B clearly illustrates this relationship. Figure 4.4, which is finer grained, shows this relationship much more clearly, without the need for a line drawing. Obvious features seen in thin section include euhedral crystal shapes of plagioclase and amphibole, the presence of distinct oscillatory zoning in plagioclase and the interstitial nature of quartz and biotite. These features are typical of PFC deformation incurred in the magmatic state, dominantly by free rotation and alignment of crystals. The rock in 4.3A does not contain a large component of CPS deformation. However, in order for the PFC lock-up shears to form, a significant degree of interaction of the crystals must have taken place in order to transmit the strain from the locked areas into the discrete zones. It is this interaction which has been responsible for the minor amounts of subgrains seen at grain boundaries, and the strained extinction seen in quartz. These features are typical of CPS deformation, but represent a minor component in this example.

Taken together, the deformational features in this example indicate that a transition exists in deforming magmas, controlled dominantly by the relative proportions of melt and crystals i.e. the relative proportions of weak and strong components. The transition period essetially marks the hiatus between fully magmatic state deformation and fully solid state deformation, although it appears to have components of both. Perhaps the most important implication from this is the information it provides about the timing of deformation with respect to crystallization state. The presence of PFC lock-up shears in a rock indicates that (1) it was emplaced syntectonically and (2) the deformation continued at least until the RCMP was reached, at which point the lock-up shears developed.

The line drawing in figure 4.5 illustrates the lock-up shears as they are seen in the field, in coarse grained tonalite. Figures 3.76 & 3.77 (chapter three) show PFC lockup shears in the tonalite pluton in Burroughs Bay from which figure 4.5 was derived. Typically they are between 10 cm and 1 m long and have a zone of deflection

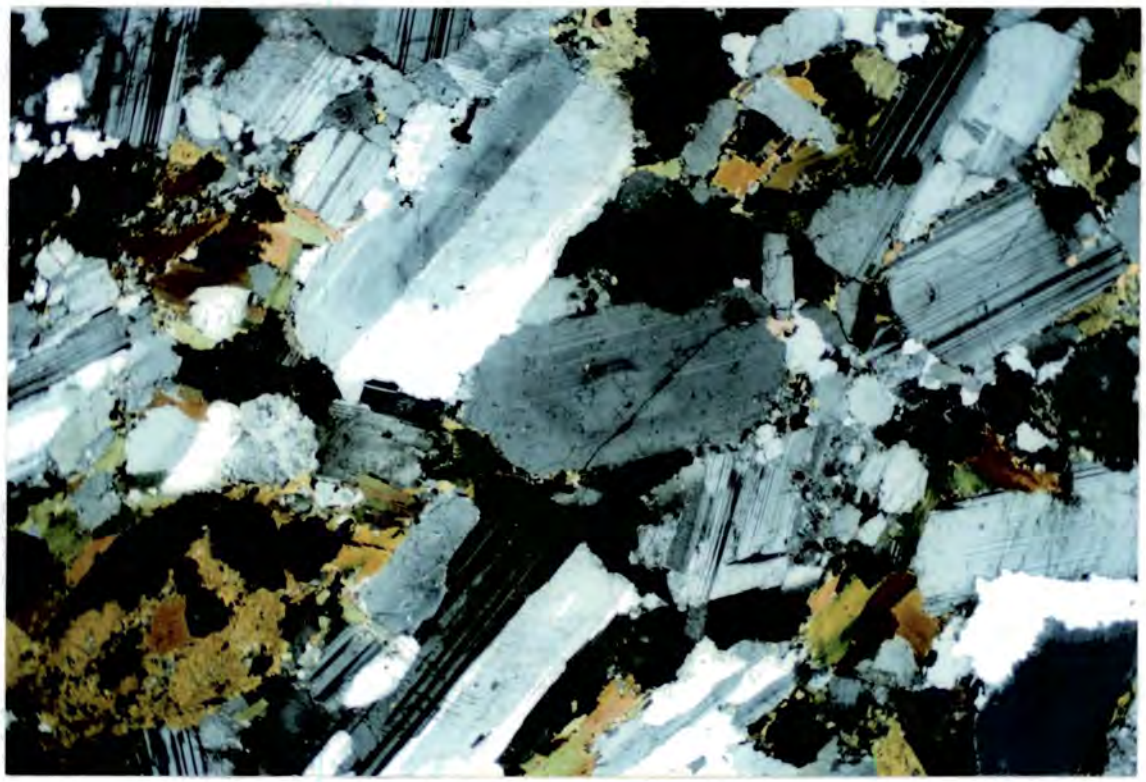

Figure 4.3A Thin section, cut at right angles to the PFC lock up shear plane, from location 302, Burroughs Bay. Field = 18 mm.

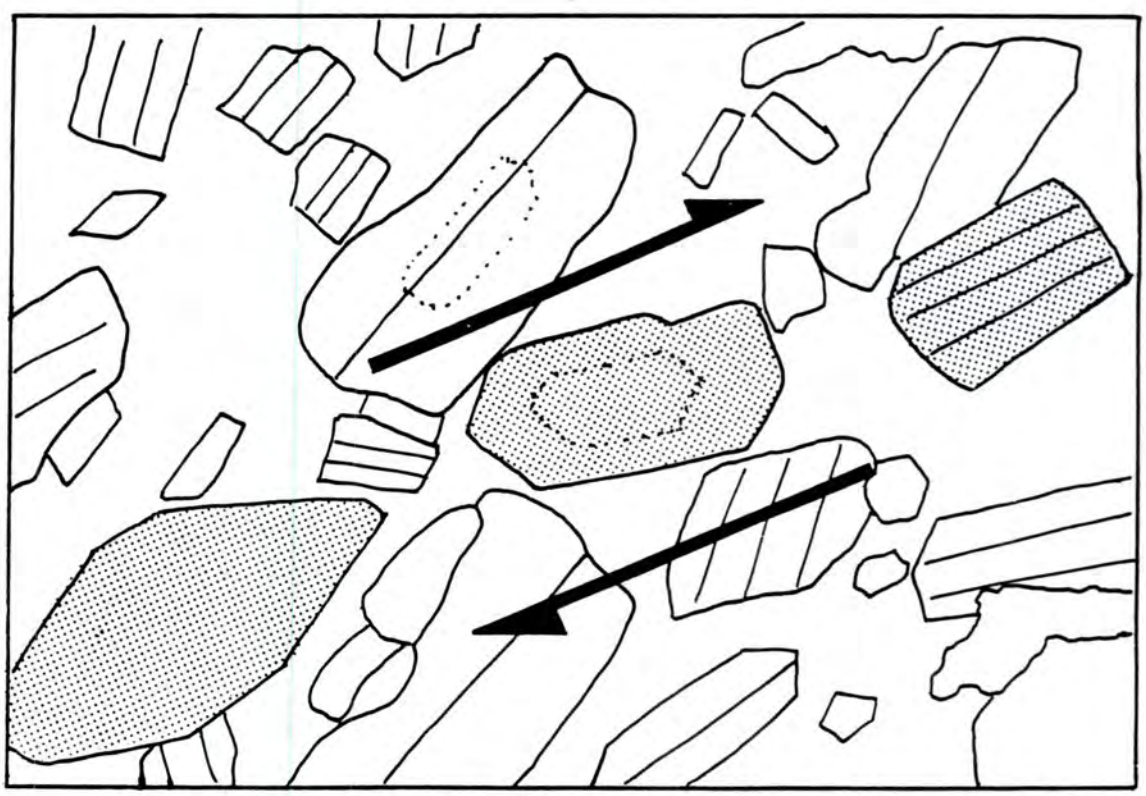

Figure 4.3B Line drawing illustrating figure 4.3A. The shaded crystals lie along the PFC lockup shear plane.

Figure 4.4 PFC lockup shears from a minor late Cretaceous tonalitic pluton, Juneau Island, Douglas. Note the higher axial ratio and finer grain size of the feldspars, and closer spacing of the shears, with respect to figure 4.3A. Plane polarized light, field = 18 mm.

Figure 4.5 Line drawing of PFC lockup shears as they are seen in the field. Rectangular crystals = feldspars, black crystals = hornblende/biotite. From location 302, Burroughs Bay.

measuring 2-3 cm wide. The spacing of individual shears may typically vary from 2-3 cm to > 10 cm, for coarse grained tonalites. However, figure 4.4 shows that the dimensions and grain size of the crystals have an important control, as the shear spacing in this case has dropped to < 1 cm. The implications of this will now be discussed.

The author suggests that the smaller spacing of the shears, as illustrated in figure 4.4, was caused mainly by the higher axial ratio and the smaller grain size of the plagioclase laths, which enabled them to rotate in response to transmitted stress more easily (i.e. a shorter period of rotation) and prevented larger domains within the crystallizing magma from locking up. Differential strain rates may also have had an effect, but it is not possible to investigate the degree of control exerted by this here. Three important implications may be drawn from these examples.

(1) Grain size has an effect upon the spacing of PFC lock-up shears. Smaller crystals may allow a closer spacing.

(2) The dimensions of crystals have an effect upon shear spacing. Longer thinner crystals may allow a closer spacing.

(3) The grain size and dimensions of crystals may have a fundamental effect on the bulk strength and therefore the yield point of granitoid magmas.

Thus it may be implied that magmas containing predominantly large stubby crystals have a higher bulk strength, at a given apparent melt percentage, than those with small elongate crystals. However, data contained herein is not sufficient to allow a fuller examination of this possibility, and therefore it must be left for further study.

4.4 Early microstructural evolution of crystal plastic strain fabrics

Once a magma has crystallized fully and there is little or no melt left, continued deformation at elevated temperatures will induce the formation of solid state, or crystal plastic strain (CPS) fabrics, involving plastic deformation of the mineral phases and their further alignment. All the phases will have some degree of internal plastic deformation. The type of fabrics produced are very similar to gneissose metamorphic fabrics, although it must be understood that the heat during deformation is provided by the cooling pluton itself, rather than an external source (Hutton 1988a).

Figure 4.6A shows a thin section of a tonalite PFC fabric, which has been modified by CPS deformation. The mineral phases are characterised as follows: (1) *Plagioclase*. The main phenocryst phase, plagioclase, still retains a PFC alignment, but the crystal shapes now vary from anhedral to euhedral and some are internally deformed, showing curved composition planes, and in places strain induced lamellae have formed. Large crystals retain the original oscillatory zoning, but smaller plagioclases have no zoning and certain crystals in addition do not retain twinning, due to dissolution. Twinning is also erased in areas where myrmeckitic intergrowths with quartz are well developed. Figure 4.6B shows a close-up of myrmeckite, from the same sample, and the loss of twin planes in close proximity to this texture. (2) *Hornblende*. Hornblende crystals are generally subhedral and not internally deformed, implying that they represent a resistant fraction. (3) *Biotite*. Biotite micas have been bent and fractured - they bend around the phenocrysts and porphyroclasts of plagioclase and define the main CPS fabric orientation. (4) *Quartz*. Quartz is the most deformed phase and is present as elongate, polycrystalline lenses. Much of the quartz has intense strained extinction and forms elongate lenses of subgrains. These lenses also define the orientation of the CPS fabric.

Figure 4.7 shows another example of the onset of CPS deformation, but this time in a tonalite with a smaller grain size. Obvious CPS deformation again includes:

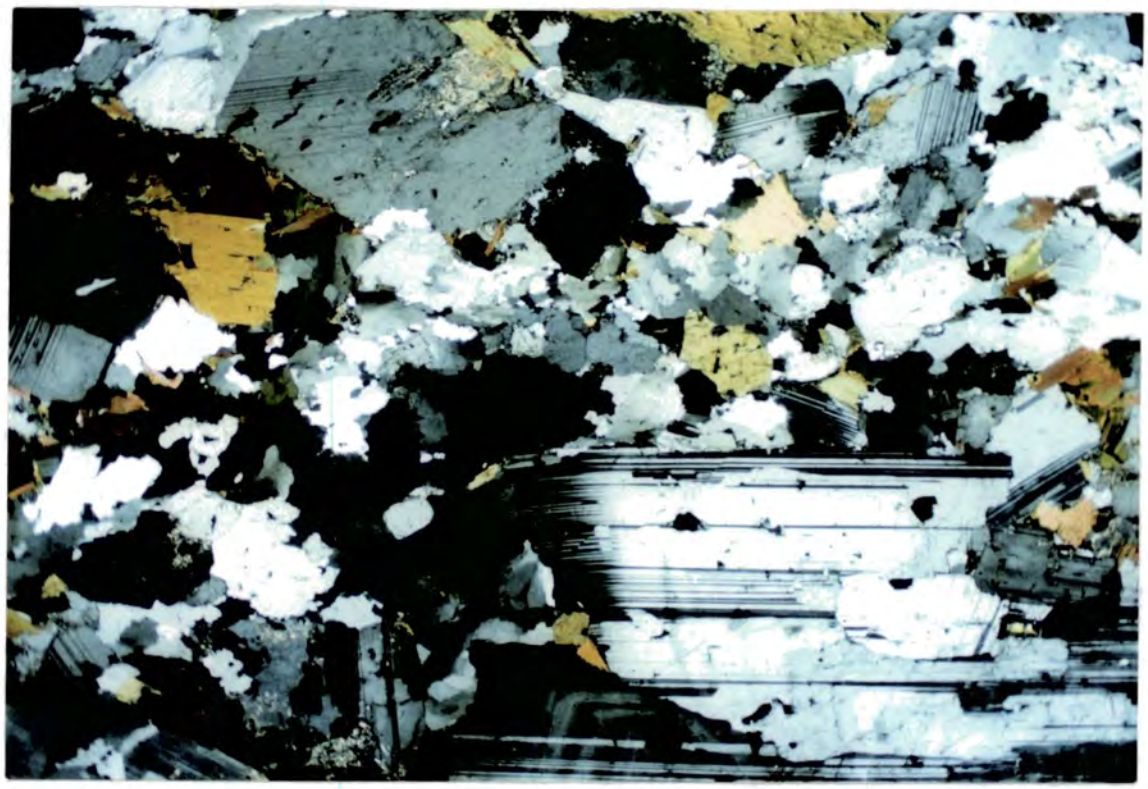

Figure 4.6A PFC fabric with CPS modification, from location 255, Port Snettisham. Field = 18 mm.

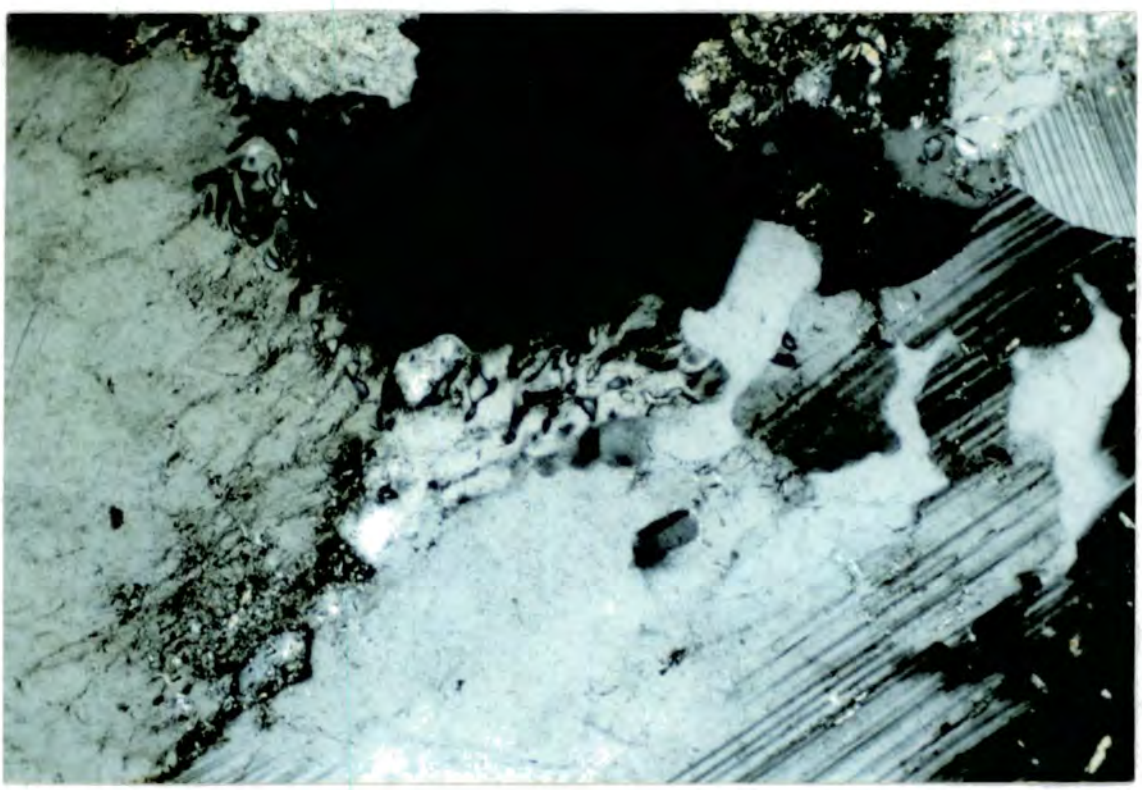

Figure 4.6B Myrmeckite texture in tonalite from location 255, Port Snettisham. Field = 2mm.

(1) bent plagioclase laths, (2) bent and aligned swathes of biotite, (3) elongate lenses of quartz subgrains, and (4) the development of myrmeckite at quartz/plagioclase boundaries.

The deformation textures seen in these examples indicate that deformation occurred for a short time after full crystallization of the original magmas, but long enough to leave significant evidence of PFC fabrics and the onset of CPS fabrics. In addition, the CPS fabric orientations are coplanar with the original PFC fabrics, indicating that the principal strain axes remained fixed during the crystallization intervals. Essentially, the CPS overprint has emphasised the pre-existing PFC/magmatic state deformation fabrics.

4.5 Microstructural characteristics of the CPS/solid state fabrics

The following examples of deformed tonalitic rocks, from the Great Tonalite Sill plutons, show the deformational features of progressively stronger CPS fabrics, which have overprinted the original PFC fabrics. Such fabrics are usually located close to rheological boundaries, such as pluton contacts, in zones of varying width. The following progression is typical of that which is encountered on approaching a contact from a more central, less deformed parts of a typical pluton. Most of the fabrics in this section are interpreted to have formed at elevated temperatures (> 500°, Simpson 1985, Gapais 1989) and therefore they represent high temperature plastic deformation. The reasons for this interpretation will be discussed.

4.5.1 *Weak - moderate CPS fabric development*

Figure 4.8 shows a PFC fabric with a moderately well developed CPS overprint: (1) *Plagioclase.* The main phase, plagioclase phenocrysts show distinct rounding due to deformation, which has resulted in anhedral to subhedral crystal

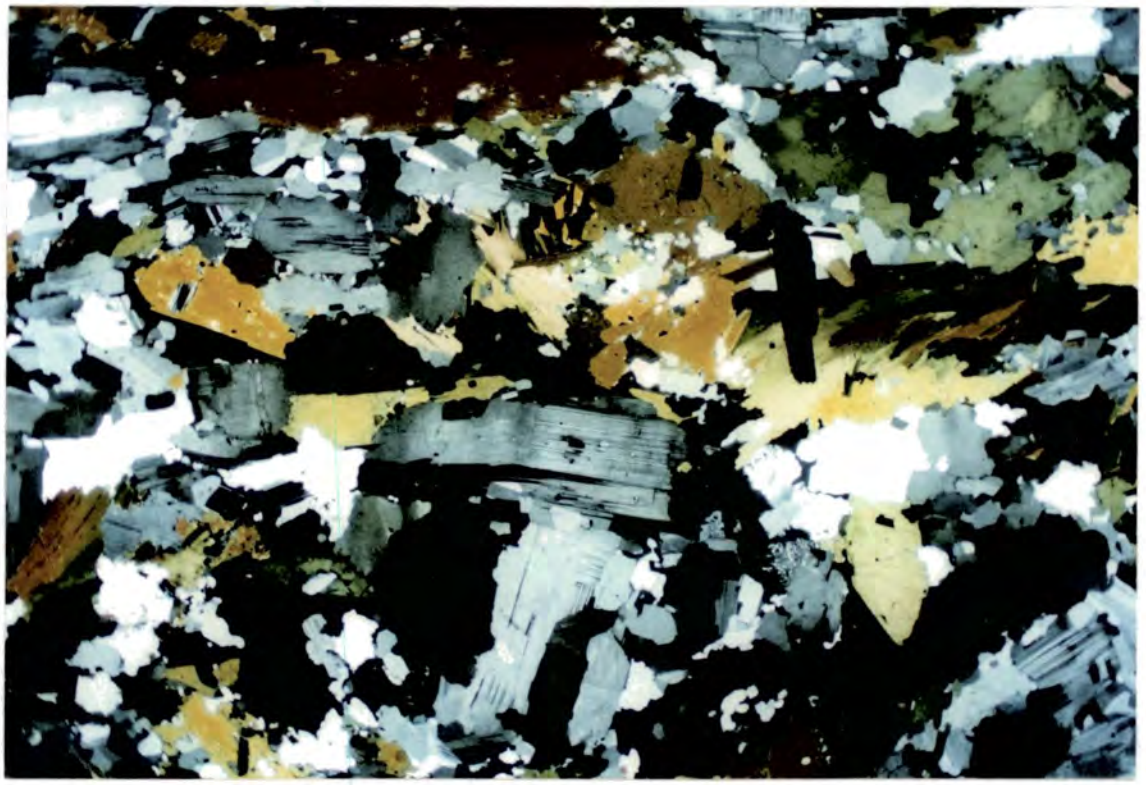

Figure 4.7 PFC fabric modified by crystal plastic deformation. Location 258, Ford's Terror Inlet. Field = 18 mm.

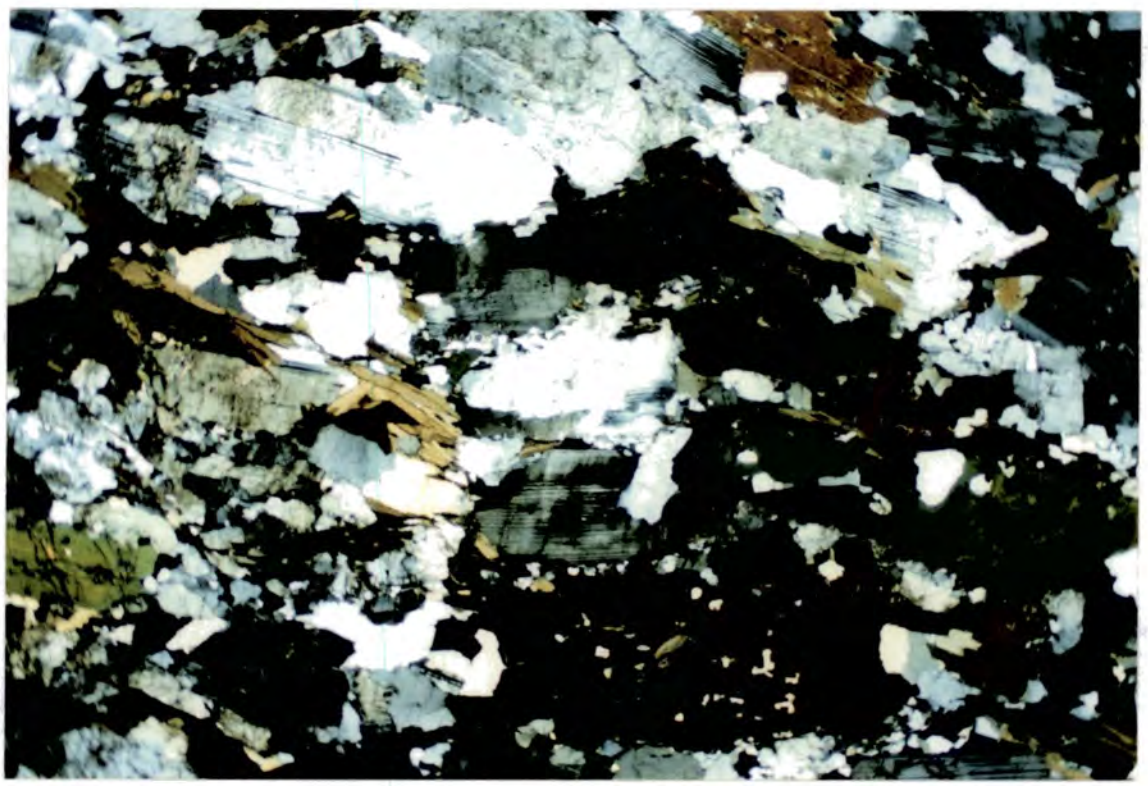

Figure 4.8 CPS fabric overprinting a PFC fabric. Location 367, Herbert Glacier (Mendenhall Glacier pluton). Field = 18 mm.

shapes. At plagioclase/plagioclase grain contacts, crystal plastic strains have been incurred in response to dynamic recrystallization associated with the high normal stresses during progressive deformation, and areas of fine subgrains have thus developed (e.g. Spry 1969, Tullis & Yund 1985). However, there is also evidence for fracturing of plagioclase grains, indicating that brittle deformation mechanisms took place. Some porphyroclasts also retain original zoning features, which indicates that plastic strains were not high, or did not act over a long enough interval to destroy the zoning by recrystallization. (2) *Quartz*. Quartz has also been transferred into and recrystallized within pressure shadows, at the ends of the elongate plagioclase porphyroclasts, due to implied diffusive mass transfer. In general, quartz forms elongate lenses or short ribbons, which wrap around the porphyroclasts and are separated form other quartz ribbons by biotite stringers. Each lens, or ribbon, is composed of many subgrains and in places they are linked up in groups with plagioclase subgrains. (3) *Biotite*. Biotite laths are deformed and wrap around composite quartz - plagioclase augen, forming good shear sense indicators. In general, the alignment of biotite swathes defines the trend of the CPS fabric. Additionally, biotite is bent and sometimes fractured in places. (4) *Hornblende*. The other mafic phase, hornblende, is present as subhedral to anhedral laths, but is in general not internally deformed. (5) *Sphene*. Sphene, which is an accessory phase, is commonly euhedral, but is also fractured in places.

4.5.2 *Moderate - strong CPS fabric development*

Figure 4.9A shows more advanced CPS fabric development. The main changes from 4.8 are as follows: (1) *Plagioclase*. This phase forms totally anhedral, rounded to elongate porphyroclasts, surrounded by thin zones of fine subgrains, which have an annealed texture in areas of particularly high subgrain density. Rarely, crystals retain faint zoning, but generally this is absent due to recrystallization effects (Tullis & Yund 1985). Original twinning is, to a large extent, retained, but strain induced lamellae, or

twins, have developed in addition to these. Grain size is, in general, smaller than in figure 4.8. (2) *Quartz*. This appears highly strained in some of the abundant ribbons, but in others it appears unstrained due to complete recrystallization. The ribbons define the main CPS fabric trend. (3) *Hornblende*. The crystals are elongate, anhedral and lens-like, parallel to the fabric trend. (4) *Biotite*. The intensity of the biotite deformation has increased and the stringers of laths are longer and thinner, and surround more elongate augen of other phases. Figure 4.9B shows a hand specimen of tonalite with deformation characteristics similar to those mentioned above.

4.5.3 *Strong CPS fabric development*

The thin section in figure 4.10A shows a strongly developed CPS fabric in tonalite and figure 4.10B shows a hand specimen of a tonalite with a similarly well developed CPS fabric. The most striking difference between this example and figure 4.9 is the overall reduction in grain size, but other specific developments are listed below.

(1) *Plagioclase*. All the porphyroclasts are reduced in grain size and have long axes parallel to the main fabric, and there are many more fine subgrains at their boundaries. Zoning is completely absent. (2) *Quartz*. The quartz occurs as highly elongate lenses, which are for the most part internally undeformed, indicating recrystallization.

(3) *Amphibole*. This phase is not preserved here. (4) *Biotite*. The elongate laths form trains or stringers parallel to the main CPS fabric, and the beginnings of SC fabric development is evident from their disposition.

Very strong crystal plastic deformation at elevated temperatures can result in the formation of protomylonites: rocks containing >50% of relict crystals within a syntectonically grain size reduced matrix (Wise et al. 1984). An example of such a mylonite is shown in figure 4.11. Strain data, on the basis of deformed mafic enclaves, indicates that in this sample the x/z ratio is 29. This high strain has resulted in the vast reduction in overall grain size, with respect to the other previous samples, although

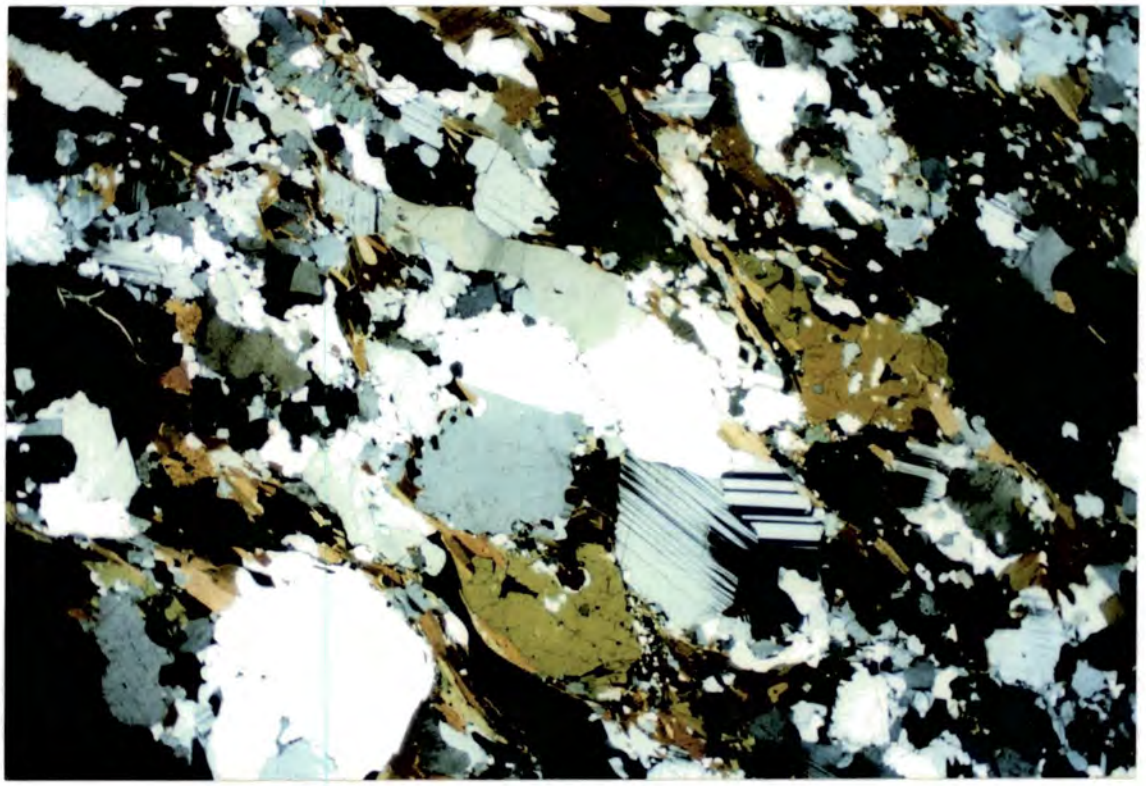

Figure 4.9A Thin section of a well developed CPS fabric. Location 390, Lemon Creek Glacier pluton. Field = 18 mm.

Figure 4.9B Hand specimen of tonalite with a well developed CPS fabric. Location 400 Lemon Creek Glacier pluton.

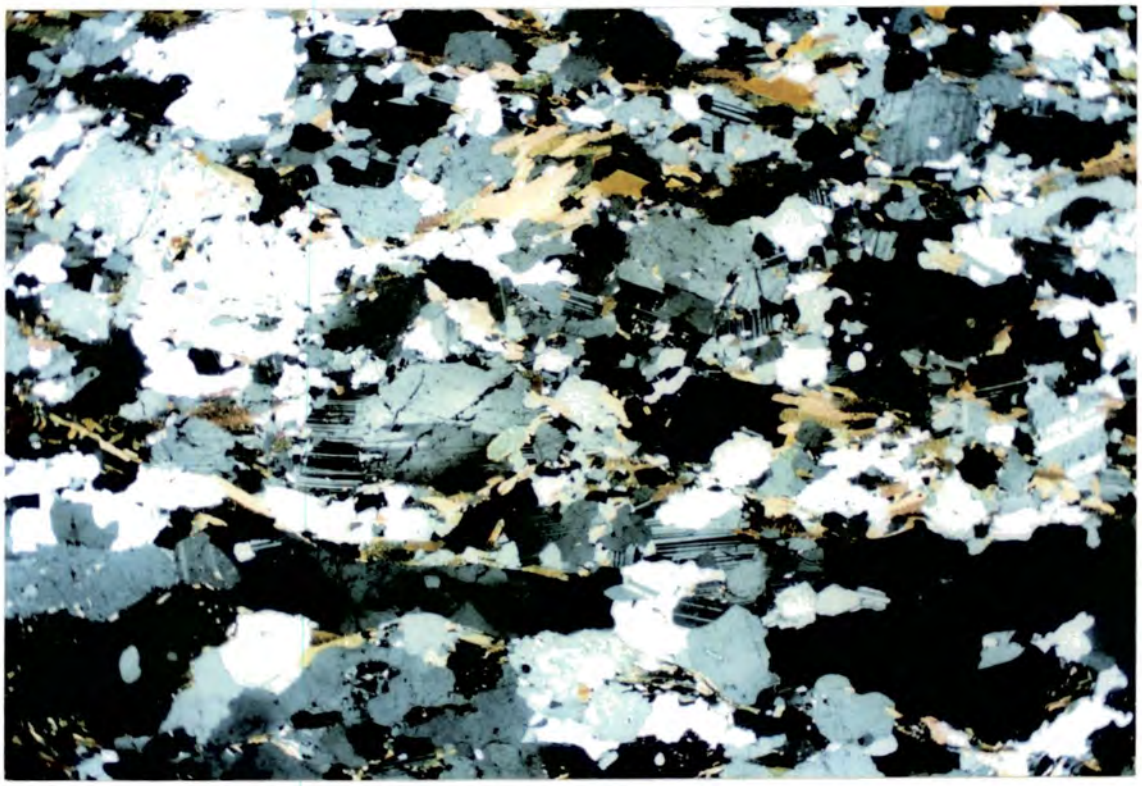

Figure 4.10A Strong CPS fabric in tonalite from the Mount Juneau pluton at location 114, Taku Inlet. Field = 18 mm.

Figure 4.10B Hand specimen of tonalite with strong CPS fabric development at location 400, Lemon Creek Glacier pluton.

scattered, large porphyroclasts of plagioclase remain. Elongate quartz ribbons and stringers of biotite anastomose around the porphyroclastic augen and define the CPS fabric. However, the presence of fractured plagioclase porphyroclasts indicates that a late component of the deformation was probably incurred in the down-temperature regime, around the 500-550°C brittle-ductile transition for feldspars.

Overall, the progression from 4.8 to 4.11 shows the effects of progressive deformation during the cooling interval of a typical Great Tonalite Sill pluton, from the tonalite solidus to the brittle-ductile transition for granitoids in general.

4.6 Microstructure of the mylonitic fabrics and shear zones

The following examples of mylonitic tonalite all come from locations close to the highly strained SW contacts of plutons in the Great Tonalite Sill belt. It has been previously mentioned in this thesis that high crystal plastic strains occur in these areas, whereas lower strains are located in the central parts of the individual plutons. In places these strains are high enough to develop the mylonitic fabrics described below. The high strain zones, in general, coincide with the axis of the regional shear zone associated with the Great Tonalite Sill and its immediate footwall rocks to the SW. In general, mylonites represent syntectonic grain size reduction associated with ductile strain or crystal plastic processes (Wise et al. 1984). Two main categories of mylonite are present in these rocks: (1) High temperature mylonites, containing plastic, annealed textures, and (2) lower temperature mylonites, typified by brittle-ductile textures.

4.6.1 *Brittle-ductile mylonite*

The thin section in figure 4.12 shows a fine to medium grained orthomylonite. Orthomylonites are essentially represented by a moderately recovered matrix produced by crystal plastic processes, with some annealing (Wise et al. 1984). The three main

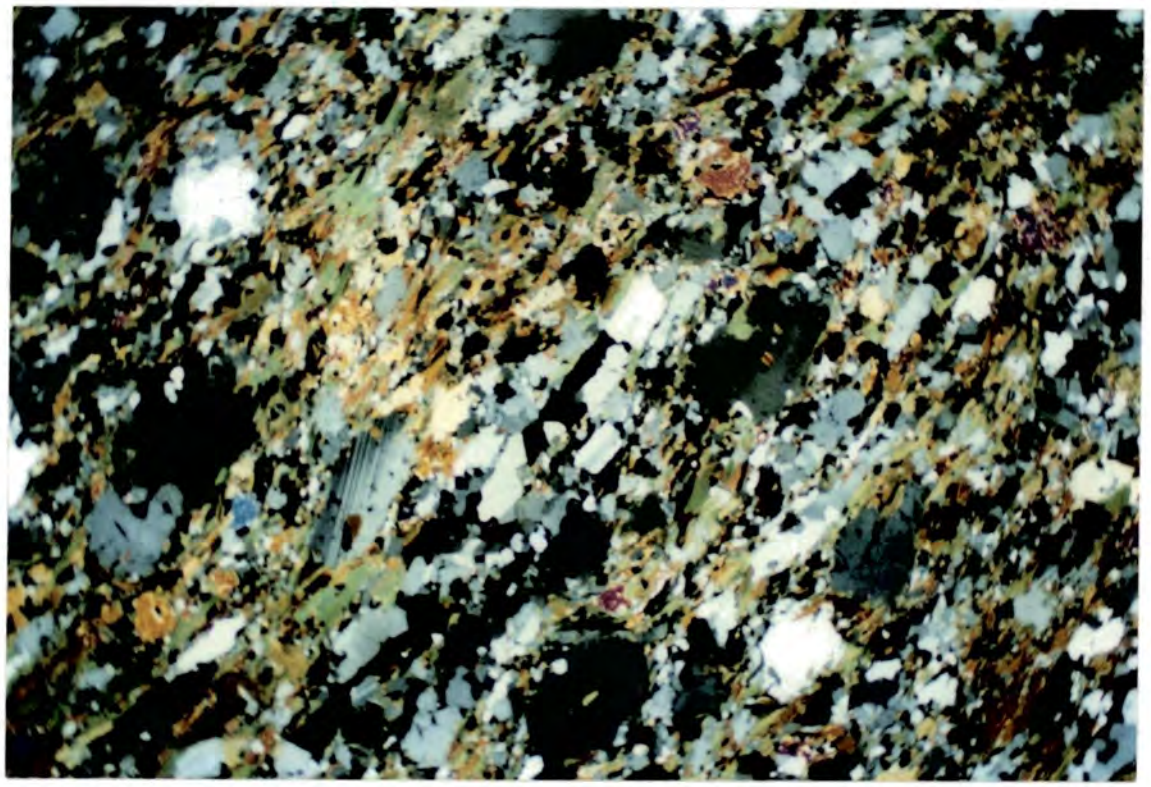

Figure 4.11 Tonalite protomylonite from location 18, Mendenhall Glacier pluton. Field = 18 mm.

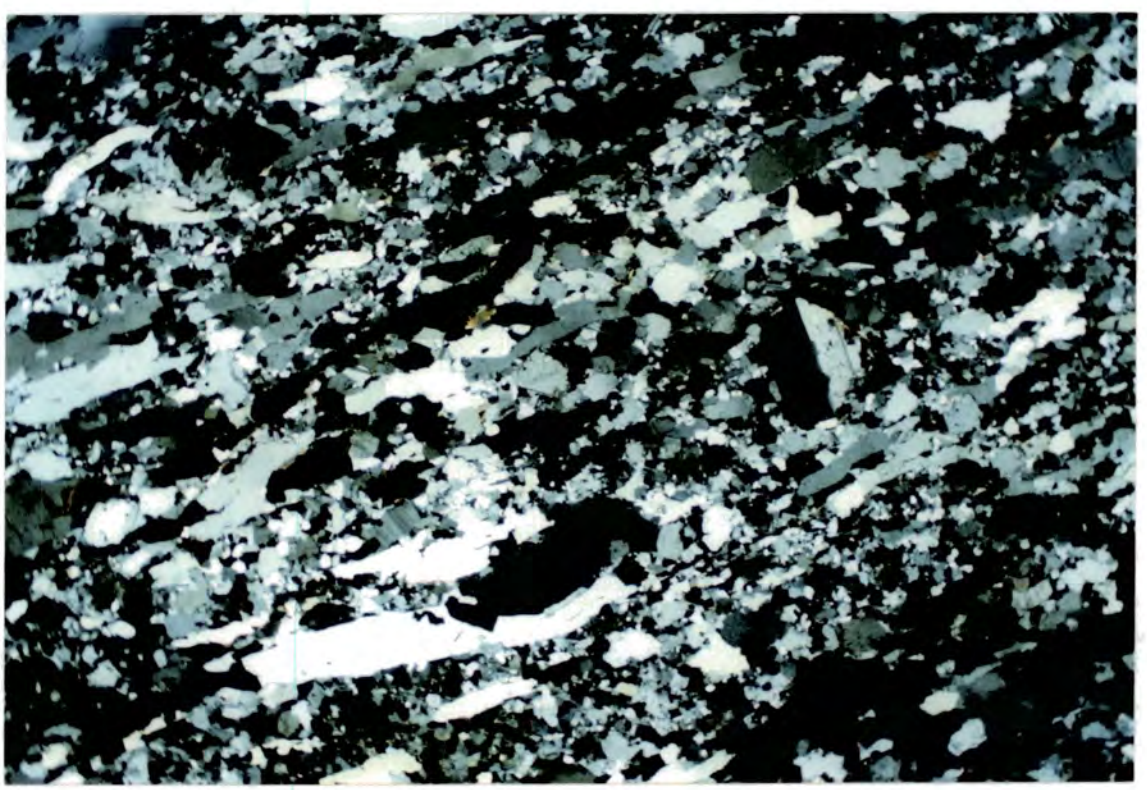

Figure 4.12 Tonalitic, porphyroclastic quartz ribbon mylonite at location 269, Thomas Bay. Field = 18 mm.

phases present exhibit the following characteristics: (1) *Feldspar*. Feldspar appears as fine subgrains and also as medium grained porphyroclasts. This phase does not retain original zoning and shows evidence for widespread recrystallization at high temperatures. However, the feldspars also exhibit brittle deformation features such as fracturing. (2) *Quartz*. The behaviour of quartz during deformation was purely ductile and very elongate ribbons of optically continuous quartz are present. Only weak straining of quartz is seen in places, which isolates large subgrains in the ribbons. The ribbons are pervasive and define the main CPS fabric trend. Myrmeckite is commonly developed between the subgrains of quartz and plagioclase. (3) *Biotite*. Biotite is present in small amounts and has a much reduced grain size, with respect to the previous examples of CPS tonalite.

Although this rock is highly strained, it still retains relict plagioclase as porphyroclasts, many of which are equidimensional. This implies that, although quartz has been ductilely deformed, the deformation as a whole did not take place at a suitable temperature to initiate wholly ductile behaviour in plagioclase. Thus this mylonite is considered to have formed in the brittle-ductile regime for granitoids.

4.6.2 *High temperature ductile mylonite*

The following examples illustrate two stages in the development of high temperature (probably >550°C) orthomylonites, in the Great Tonalite Sill. The first example, in figure 4.13, shows a fine grained quartz ribbon mylonite. The dominant feature is the presence of elongate, strained, polycrystalline quartz ribbons parallel to the main CPS/solid state foliation plane. More importantly, the fine grained groundmass of quartz and plagioclase subgrains has a good annealed texture. In contrast to figure 4.12, the grain size of the groundmass is unimodal and does not contain porphyroclasts or brittle features. In addition, there is no myrmeckite development in this example, which indicates a predominance of high temperature

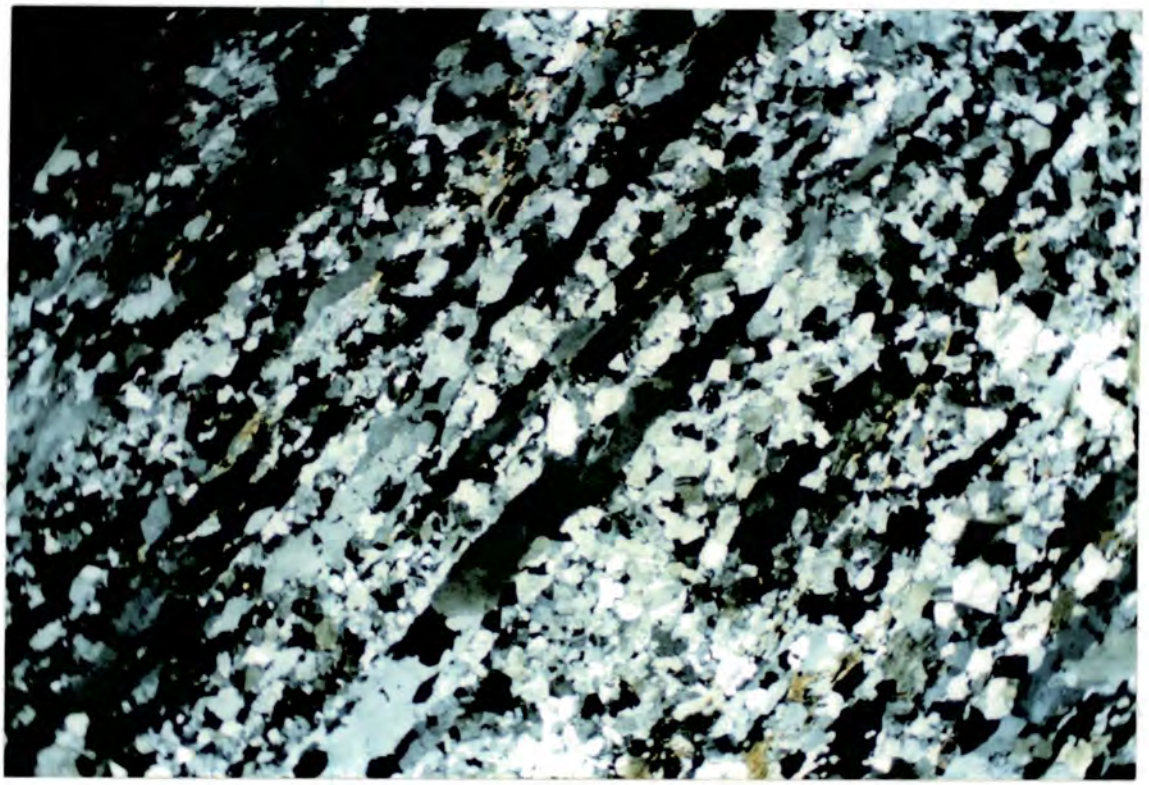

Figure 4.13 Fine grained, tonalitic, quartz ribbon mylonite from location 261, Ford's Terror Inlet. Field = 18 mm.

deformation. Biotite appears as fine grained trains or wisps, parallel to the foliation plane, especially at the flanks of quartz ribbons.

The ultramylonite (extensively annealed mylonite; Wise et al. 1984) thin section in figure 4.14A represents the approximate equivalent of the rock in figure 4.13, but at a stage further in the deformation sequence. For the purpose of comparison between the two deformational textures, the difference in grain size between these two examples will be overlooked. The most obvious difference between the two is the lack of well developed, elongate quartz ribbons in figure 4.14A. The quartz ribbons present in this case are shorter and contain more abundant, smaller subgrains, and other strain induced features. This implies that early developed, more elongate, strain free ribbons have been broken down and the subgrains distributed through the rock. The annealed texture seen in the groundmass in figure 4.13 is more evenly developed in this later example, implying that dissolution of plagioclase has been important during the strain history. Another important feature, which represents the final recorded deformation, is the presence of microscale shear bands. These shear bands are interpreted here as the forerunners of full SC fabric development and are best exhibited by the thin biotite trains, seen trending from bottom left to top right in figure 4.14A and 4.14B. These indicate top-to-the-SW shear sense and they are pervasive throughout this rock.

In summary, these mylonitic rocks, containing high temperature (probably greater than 550°C) CPS/solid state fabrics, represent some of the most highly strained tonalites seen in the whole of the Great Tonalite Sill belt.

4.7 Microstructural features of the discrete CPS shears

There are many discrete shears which occur in the Great Tonalite Sill plutons. In chapter three, the abundant discrete, ductile shears were analysed with regard to their geometric distribution and implied strain component, and their relationship to regional deformation. This section deals with the microstructure of two common types

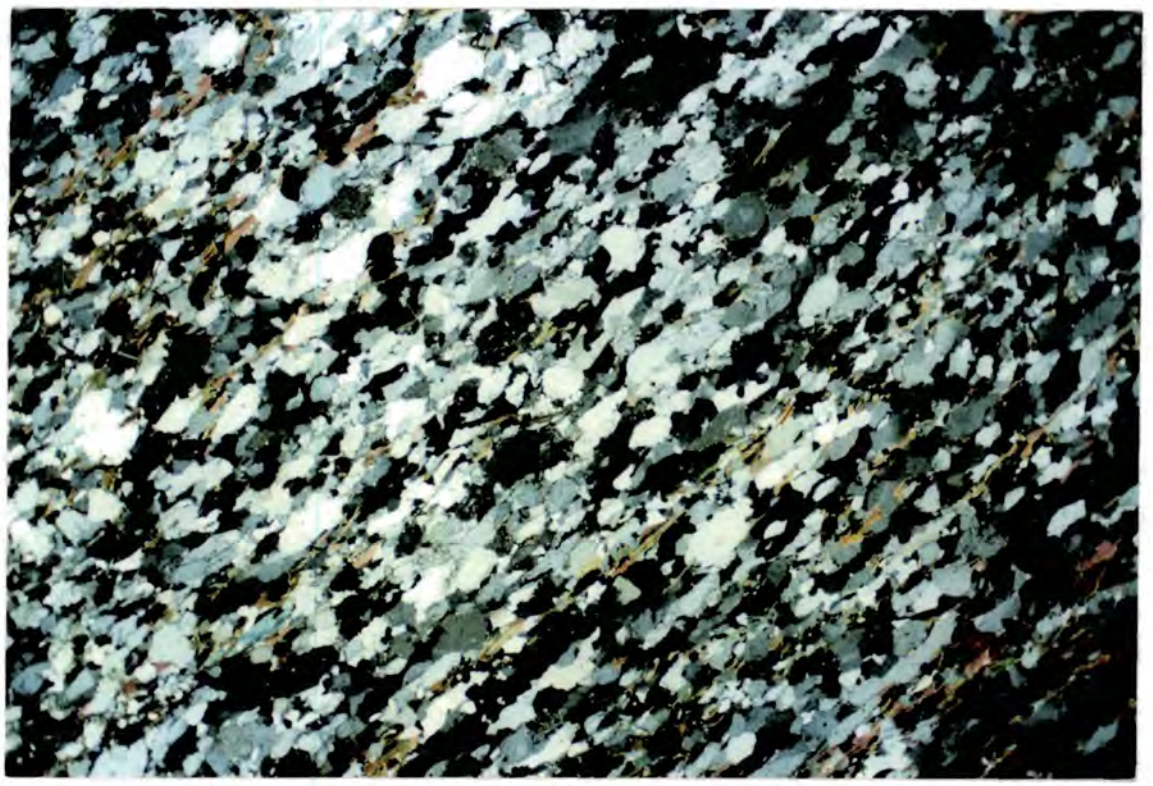

Figure 4.14A High temperature tonalite mylonite, with incipient top-to-the-right (SW) shear bands marked by deflected biotite trains. Location 261, Fords Terror Inlet. Field = 18 mm.

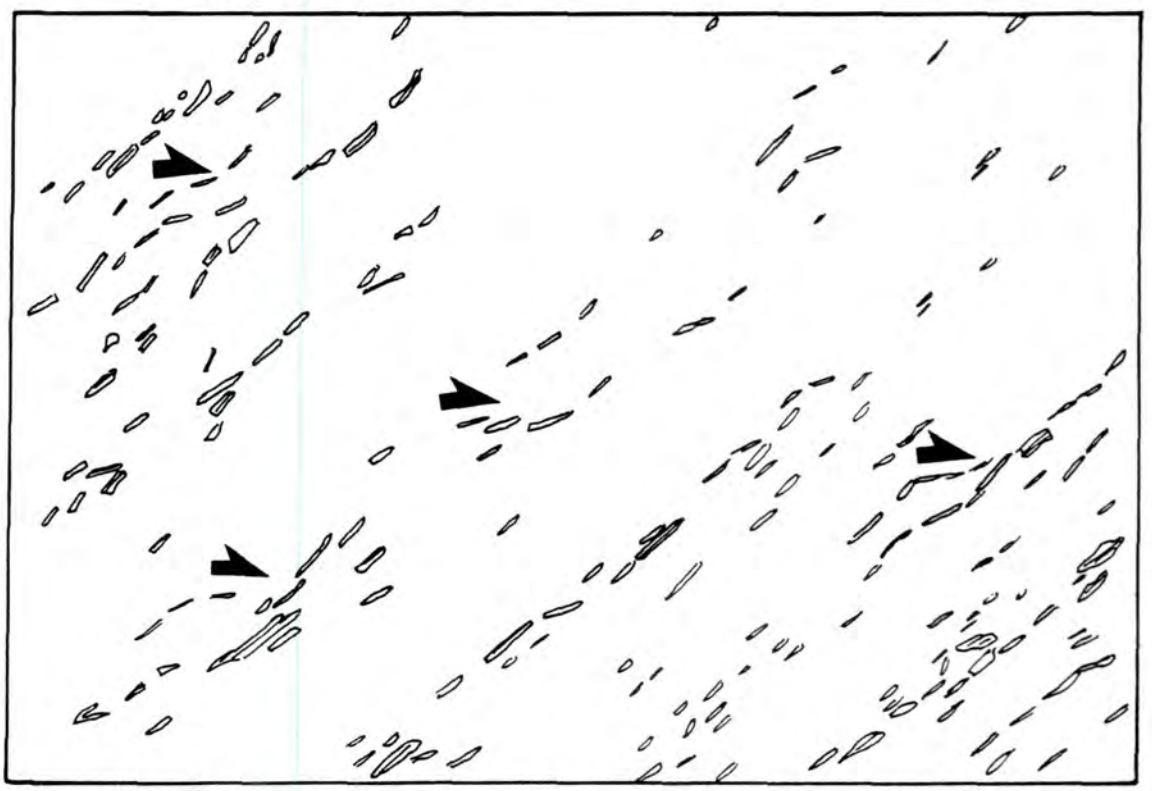

Figure 4.14B Line drawing of figure 4.14A illustrating the top-to-the-right (SW) shears. Field = 18 mm.

of shear: (1) *high temperature, ductile shears*, and (2) *lower temperature brittle-ductile shears*. Both types of shear are associated with overall NE-SW directed shortening and concomittant pure shear, during retrograde deformation of the tonalite/granodiorite plutons, and occur in sequence from (1) to (2). Very late, down-temperature, cataclastic shears and faults are also present in the plutons, but these will not be described here.

4.7.1 *The high temperature discrete shears*

In brief, these shears have a microstructure typified by strong annealing textures. Figure 4.15 shows this annealing in a granodiorite from Taku Inlet. The rock in thin section at first glance does not appear to be highly deformed: (1) *Plagioclase*. The plagioclase and alkali feldspars occur as equant crystals, often possessing 120° triple point contacts with other feldspars and quartz. Zoning is absent which suggests, along with the annealed textures, that recrystallization of feldspar was widespread. (2) *Quartz*. Quartz generally appears as crystals in optical continuity, which may be equant or lensoid, although some crystals exhibit strained extinction and minor marginal subgrains, probably related to later down temperature deformation. However, in hand specimen (fig. 4.16) the shear is quite clearly defined, mainly by mafic trains (biotite) swinging into the shear plane. Thus, although the main textural characteristics point to a high temperature origin, the fact that the shears represent heterogenous and not steady state deformation implies that such shears occurred at or above the upper limit of the 500-550°C brittle-ductile temperature bracket in granitoids (Gapais 1989).

4.7.2 *The brittle-ductile discrete shears*

The brittle-ductile discrete shears postdate the high temperature discrete shears, but they retain similar overall orientations to the latter, and indicate continued progressive deformation, with similar orientations of the principal strain axes, into the

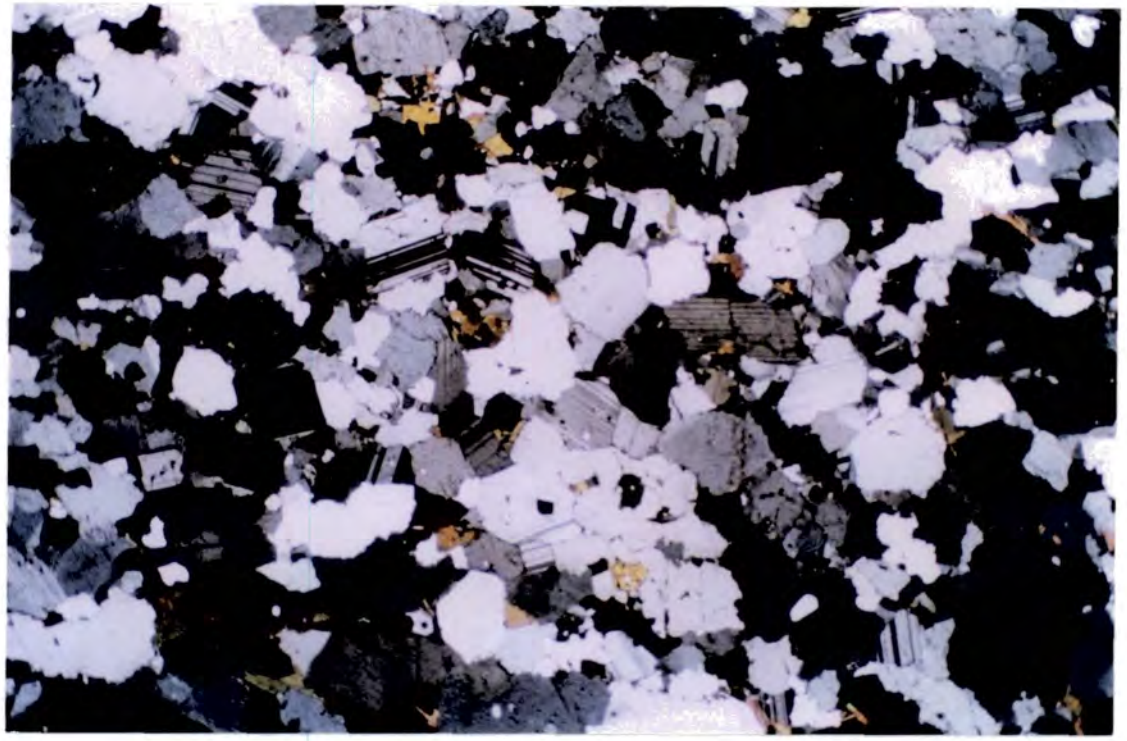

Figure 4.15 Thin section of the medial plane of a high temperature CPS shear in granodiorite. Location 150, Taku Inlet. Field = 18 mm.

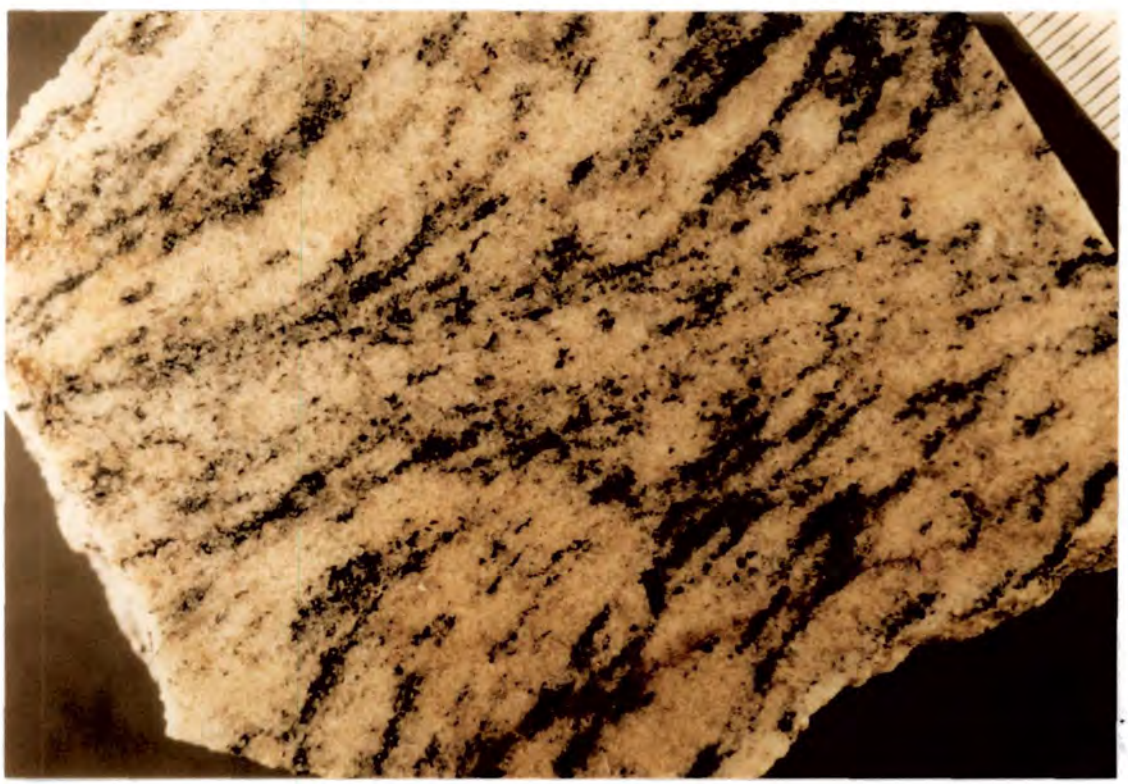

Figure 4.16 Hand specimen illustrating the shear from which figure 4.15 was taken. Scale in mm.

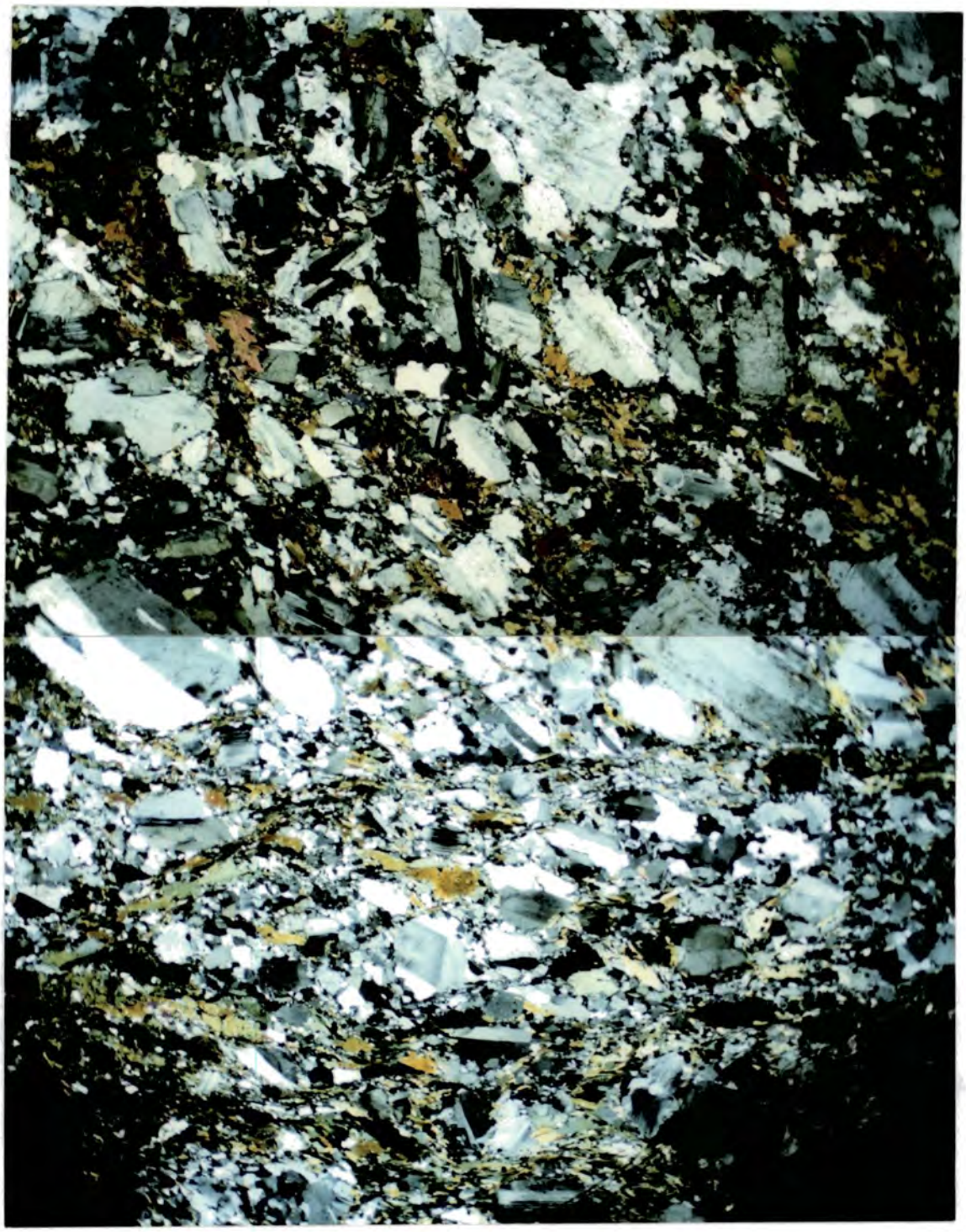

Figure 4.17 Thin section of a brittle-ductile shear: weakly deformed shear zone wall (top) grades into the highly deformed medial plane (bottom) of the shear. Location 323, Herbert glacier. Field = 18mm.

down temperature regime. Figure 4.17 shows an 18mm x 16mm thin section of one of these brittle-ductile shears. On initial inspection, the most striking feature is the change in deformation state moving from the top of the section to the bottom. The upper portion of the section shows subhedral to euhadral laths of plagioclase, which define a good PFC fabric, with an alignment running from the top of the picture to the bottom. The lower portion of the section shows anhedral to subhedral porphyroclasts of plagioclase, with much reduced grain size. Abundant subgrains of the same phase are associated with closely spaced, microscale shear bands in this lower region. The shear bands have an SC relationship, which indicates a top-to-the-left sense of shear. Another obvious feature, which agrees with this shear sense, is the pronounced swing in orientation of the plagioclase crystals' composition planes, and hence, by implication, their original long axes. Their alignment changes form an upright orientation, at the top, through intermediate orientations, to an approximately left-right orientation parallel to the medial plane of the shear, at the bottom. A map of the plagioclase laths and porphyroclasts, plus the microscale shear bands, illustrates the above interpretation in figure 4.18. From the pattern of microscale shear bands it is possible to interpret a simple chronology for their initiation and propagation. The first shear bands to initiate (S_1) are those which trend from top left to bottom right. At a critical stage during the development of these, the shallower, left-right trending shear bands (S_2) cut through them, parallel to the shears zone walls. Subsequently, or contemparaneously, the shear bands trending from top right to bottom left (S_3) cut the early sets in an SC type relationship.

More detailed analysis of the thin section reveals that dynamic formation of quartz and feldspar subgrains were dominant deformation mechanisms. Fracturing of feldspar grains is also common, but additionally there is much evidence for plagioclase dissolution. Feldspar dissolution, however, is not pervasive, as original compositional zoning is preserved, even in the medial plane of the shear (fig 4.17, bottom right). Figure 4.19 shows a close-up of plagioclase, which has been dissolved and subsequently recrystallized in the pressure shadow of its parent plagioclase lath.

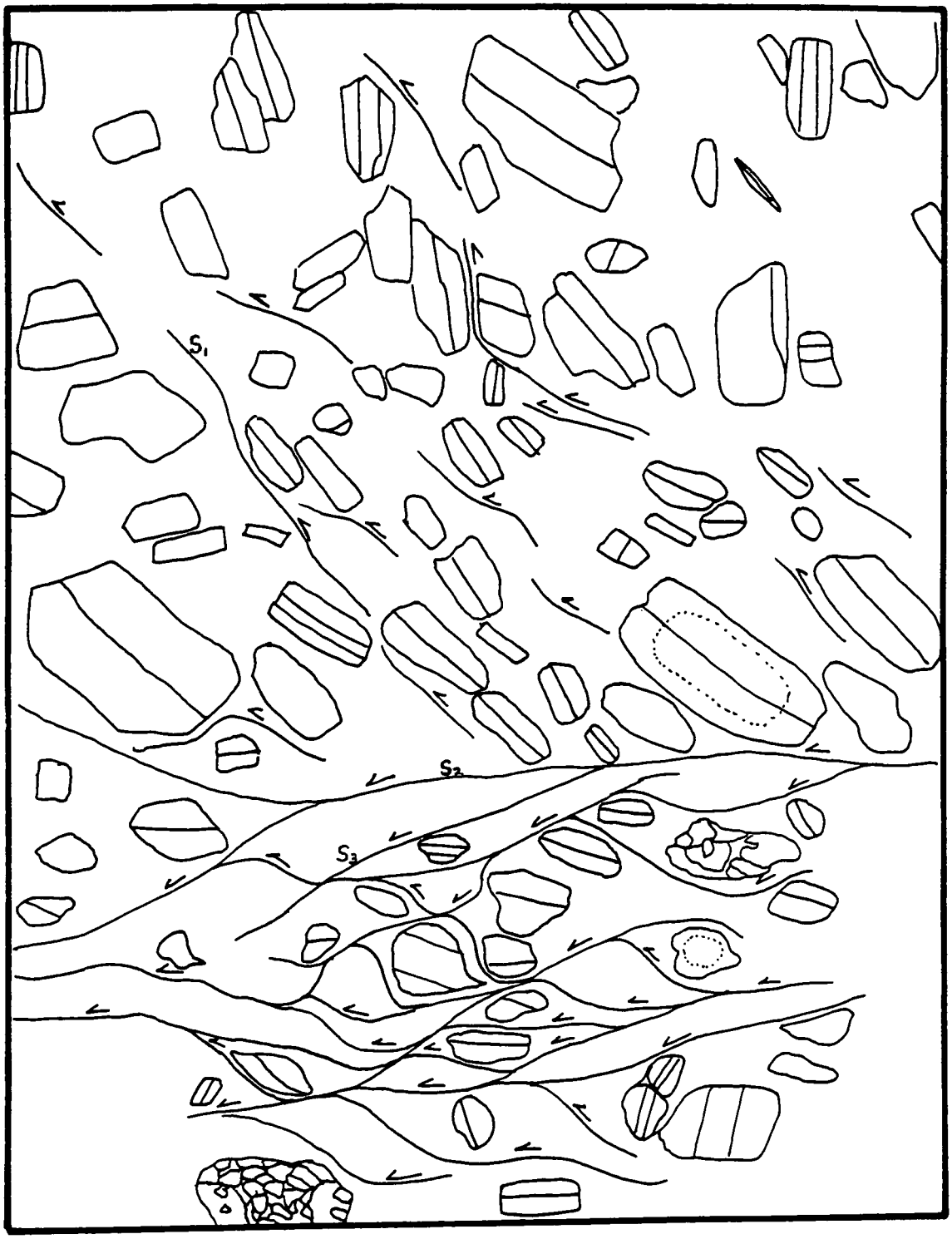

Figure 4.18 Line drawing of figure 4.17 showing plagioclase crystals and microshear planes with their implied slip directions. Field = 18 mm.

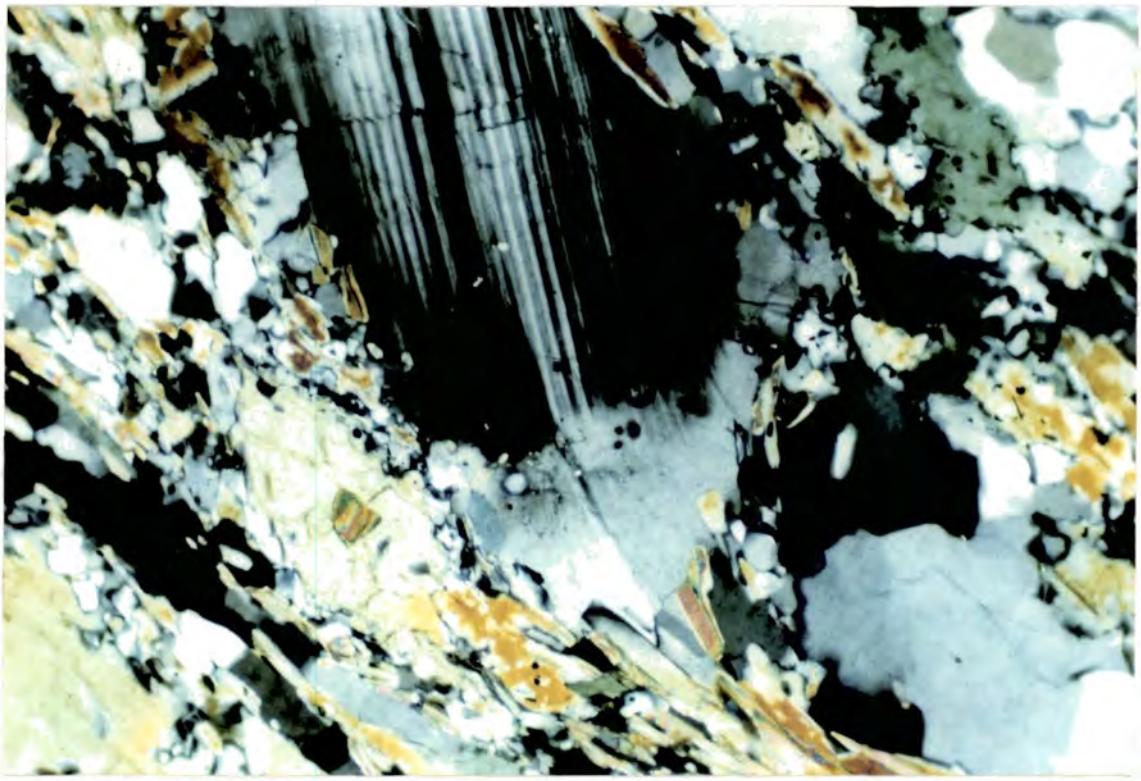

Figure 4.19 Deformed plagioclase lath showing the occurrence of both brittle fractures and recrystallized plagioclase within a pressure shadow, from the same shear shown in figs. 4.17 & 4.18. Field = 2 mm.

However, the same lath also shows evidence of fracturing. Both brittle and ductile processes have obviously taken place during the deformation interval of this shear zone, and hence it has been termed here a brittle-ductile shear.

Other phases present include biotite and amphibole. These are commonly located along the microscale shear zones (especially biotite) and thus the author interprets that the biotite stringers/ribbons, and to a lesser extent the deformed elongate amphibole crystals, facilitated deformation more easily than the other phases, at the implied temperature conditions: below the 500 - 550°C brittle-ductile transition for the initiation of heterogenous deformation in granitoid rocks (e.g. Gapais 1989).

Coplanar brittle/cataclastic deformation is not recorded in the Great Tonalite Sill plutons, but anastomosing, discordant, zones of such deformation and more discrete faults do occur. However, these structures are not regarded here as having a great significance with respect to the Great Tonalite Sill shear zone and its dominant magmatic, ductile and brittle-ductile fabrics and structures.

4.8 Summary

The descriptions above indicate that the Great Tonalite Sill rocks, in general, underwent progressive deformation during their complete crystallization and subsequent cooling interval. Magmatic/PFC fabrics represent the initial deformation at high temperatures and the latest deformation is in the from of lower grade, coplanar, brittle-ductile fabrics. It has been possible to view an almost complete range in fabric types between these two end-members in the Sill rocks.

The most intense CPS fabrics are commonly located at pluton contacts, and are best developed in the oldest intrusives as these have been exposed to deformation for the longest periods, or alternatively they have experienced higher strain rates, but the latter is hard to identify. Later rocks, emplaced during the waning stages of shear zone

movement, preserved PFC deformational structures to a much greater degree. Thus, rocks emplaced during the intervening period will record varying degrees of overprinting and development of CPS fabrics at the expense of early PFC fabrics.

At two points during this retrograde deformation sequence, two major rheological transitions took place, which have been recorded and characterised by certain fabrics and structures. In basic terms, these represent the rheological transitions from magma to high temperature solid, and high temperature solid to low temperature solid: the (1) PFC/CPS and the (2) brittle-ductile transitions respectively. The following points summarise what the author believes is a typical chronological sequence of fabrics, structures, textures and implied deformation mechanisms, for the Great Tonalite Sill as a whole:

(1) ***Pre-full crystallization (PFC) fabrics.*** PFC fabrics develop in the crystallizing magma and involve the rotation and alignment of early formed, non-equidimensional, crystal laths, which are suspended in an uncrystallized matrix, in response to external stresses. These fabrics continue to develop during deformation, if the melt content remains above the Rheological Critical Melt Percentage (RCMP, 30-35% melt).

(2) ***PFC lock-up - the PFC/CPS transition.*** When the melt percentage drops to the RCMP during crystallization, the bulk strength of the magma increases dramatically (see chapter 1) and induces the partitioning of strain into discrete "lock-up shears". In basic terms these shears mark the transition between homogenous PFC/magmatic state deformation and heterogenous PFC deformation. In effect, they represent the precursor to high temperature CPS/solid state textures and structures, which develop after most of the remaining melt has crystallized. It is also implied here that the development of these structures is additionally controlled by crystal grain size, dimensions of the crystal laths and that, taken together, these factors may affect the bulk strength of granitoid magmas. Strain rate may also have an effect upon development of the shears.

(3) ***High temperature crystal plastic strain (CPS) fabrics.*** These develop after the melt content has dropped significantly below the RCMP. However, only after full crystallization of all the remaining melt do *all* the phases record CPS deformation. Early fabrics involve weak modification and further emphasis of PFC fabrics at high temperatures. Later fabrics involve (chiefly): dynamic recrystallization and dissolution of feldspar (Spry 1969, Tullis & Yund 1985), formation of quartz ribbons, bending and kinking in biotite, elongation of amphibole and overall grain size reduction. In extreme cases, intense CPS deformation results in the formation of high temperature mylonites which have strong annealed textures. These types of fabrics develop at temperatures geater than 500-550°C (e.g. Gapais 1989).

(4) ***The brittle-ductile transition.*** Brittle-ductile fabrics occur at or below 500-550°C and involve brittle behaviour in plagioclase, bending/kinking of biotite and ductile behaviour in quartz (Simpson 1985). In the Great Tonalite Sill these features are developed most convincingly in late, brittle-ductile discrete shears, and the late brittle-ductile mylonites located closest to the SW edge of the Sill.

CHAPTER 5
ORIGIN, ASCENT AND EMPLACEMENT OF THE GREAT TONALITE SILL

5.1 What does the Great Tonalite Sill represent?

5.1.1 *The tectonic regime*

From the previous discussion, it is clear that the Great Tonalite Sill is very long, thin and highly focused. It retains similar structures and kinematics along its entire length, implying that the same large-scale process, leading to its genesis and deformation, took place over a very long distance (>900 km). It is obvious that this process has plate tectonic dimensions and that the Great Tonalite Sill belt now exposed contains information which has a fundamental bearing on the evolution of the western Cordillera of North America.

The plutons of the Great Tonalite Sill belt are localised along a linear structural discontinuity, within a contractional regime (Brew 1988) in which a large pure shear (K = 0) and a lesser, reverse, top-to-the-SW simple shear (K = 1) component were concentrated (Hutton & Ingram 1992). Dating of the syntectonic component plutons indicates that this regime and the resultant shear zone persisted from at least 81 Ma (Wooden, J.L., written comm. to Brew, D.A., 1990) to 55 Ma (Brew 1988, Gehrels et al. 1991). The cause of the contraction, and concomitant reverse shear, was the movement of the outboard Insular superterrane northeastward against the western margin of the Intermontane superterrane (Monger et al. 1982). The remarkable linearity of the Great Tonalite Sill initially led Brew & Ford (1977, 1978) to imply that

it had been emplaced along a hypothetical plate boundary. More recently, Wood et al (1991) stated that the spatial variation in $^{40}Ar/^{39}Ar$ mineral ages for the Great Tonalite Sill, near Holkam Bay, southeast Alaska, suggested that it was emplaced near the boundary between hot, high grade metamorphic rocks to the east and cooler, medium grade metamorphic rocks to the west. This again implies that it was emplaced at the boundary between two different crustal entities, or terranes.

A further discussion of arguments for and against the Great Tonalite Sill as a terrane boundary, is contained in section 6.5.

5.1.2 *The origin of the intrusives*

Introduction. The rocks of the Great Tonalite Sill belt are consistently calc-alkaline and dominantly metaluminous and fall into the tonalite - granodiorite - quartz monzodiorite - quartz diorite fields of Streckeisen (1973). Sill rocks with Palaeocene (c.60 Ma) ages have higher silica contents than the older sill rocks and are mostly granodiorite, but are included in the Great Tonalite Sill grouping, due to closely similar ages and locations (Brew 1988). The consistent composition of the magmas strongly indicates that the source was deep and homogeneous. The chemical and isotopic compositions of the rocks indicate that they were sourced from a combination of subduction related magmas (Arth et al. 1988), such as those derived from the melting of underplated mantle-derived basalts (Chappell & Stephens 1988, Fyfe 1988, Silver & Chappell 1988) and a lesser component of partially melted ancient crustal rocks (Samson et al 1991). The data supporting this conclusion are detailed below.

Petrographical implications. The tonalites and granodiorites of the Great Tonalite Sill consistently contain small but significant volumes of mafic and ultramafic rocks. These consist of older appinitic, precursors to the main intrusives and coeval synplutonic dykes and cogenetic mafic enclaves. The appinitic suites of early intrusives are coarse grained hornblende- and biotite-bearing rocks of ultramafic to intermediate

composition. Rocks such as these have been interpreted as cumulates from volatile K-rich basaltic or andesitic magma (French 1966, Hall 1967) and are commonly regarded as relatives of the deeply sourced (i.e. mantle-derived) lamprophyric group (Hunter & Rock 1987). Further evidence of a mantle component is the common occurrence of mafic or dioritic, cogenetic enclaves. These enclaves occur in similar granitoid rocks worldwide and commonly have ellipsoidal to spherical shapes, crenellate margins, fine grained chilled margins, and are often associated with synplutonic dyking. Barbarin & Didier (1992) indicated that the enclaves represent only 1-2% of the volume of calc-alkaline granite plutons in general and it is widely accepted (see Ebertz & Nicholls 1988, Frost & Mahood 1987) that they represent uncrystallised mafic magma within an uncrystallised granitoid host. Nd isotope studies from the British Caledonian plutons (Holden et al. 1987) indicated higher εNd values (typically two units higher) in the enclaves with respect to their host, which implied the synplutonic injection of mafic magma into a granitoid magma. In conclusion, Hyndman & Foster (1987), Hutton & Reavy (1992) and others suggest that the mafic material present in the granitoid plutons represents the end product of high temperature mantle-derived magma injected into the lower crust. This process caused partial melting and the formation of granitoid melts which encorporated, by mixing and mingling to varying degrees, the mantle component. For the above reasons, the author invokes a model for the Great Tonalite Sill batholith, in which a mantle component plays a significant role in the petrogenesis.

Isotopic implications. Previous models for possible sources of the Coast Plutonic Complex envisaged that there were two contributing end members: (1) crust with a large mantle component and (2) crust of the adjacent accreted terranes (e.g. Barker et al. 1986). According to Arth et al. (1988) the initial $^{86}Sr/^{87}Sr$ ratios for the Coast Plutonic Complex as a whole, taken from samples in the Ketchikan area (0.7041-0.7064), are similar to the overall range found in magmatic arcs at convergent plate margins. Higher initial ratios than the Coast Plutonic Complex intrusives (>0.710) have been found in some magmatic arc batholiths underlain by Precambrian

crust e.g. Pioneer batholith of Montana (Arth et al. 1986), and on this basis Arth et al. (1988) implied that the Ketchikan area magmas were derived from Palaeozoic or younger crust, not from Precambrian crust. Initial strontium ratios for the Great Tonalite Sill alone (0.70636-0.7064) indicate that these intrusives lie just outside the field of magmatic arc plutons (fig. 5.1). The similarity in initial ratios between the central orthogneisses of the Coast Plutonic Complex and the plutons of the Great Tonalite Sill further allows the possibility that the former contributed partial melts to the latter.

Neodymium isotope studies on the Sill rocks indicate that the plutons posses εNd values of less than -4, reflecting that a component of older, more silicic crustal rocks was involved. Combining these Nd data with Sr data confirms that the Great Tonalite Sill rocks indeed lie outside the island arc field. The data overall, indicate that the sources for these plutons were dominantly mafic and contained components of subduction-related magma and relatively immature crust (Arth et al. 1988).

More recent work (Samson et al. 1991a) indicated that the Great Tonalite Sill rocks have higher $^{87}Sr/^{86}Sr$ ratios and lower εNd values compared with the surrounding terranes and MORB (fig. 5.2). This suggested, in contrast to the implications of Arth et al. (1988), that older, Precambrian, continental crust with a more negative εNd and higher $^{87}Sr/^{86}Sr$ initial ratio must have been involved in the magma production. Zircon inheritance data indicates that this older component has an average Early Proterozoic age, and is attributable to the Yukon Tanana terrane (Gehrels et al. 1990). This implied that the Great Tonalite Sill plutons were produced from the melting of these ancient crustal rocks and a younger component from the mantle or the surrounding, juvenile terranes. Taking into account the implications of the appinite suites, the abundance of cogenetic mafic enclaves and synplutonic dyke material present in the Sill rocks, it is most likely that the juvenile component was derived directly from the mantle.

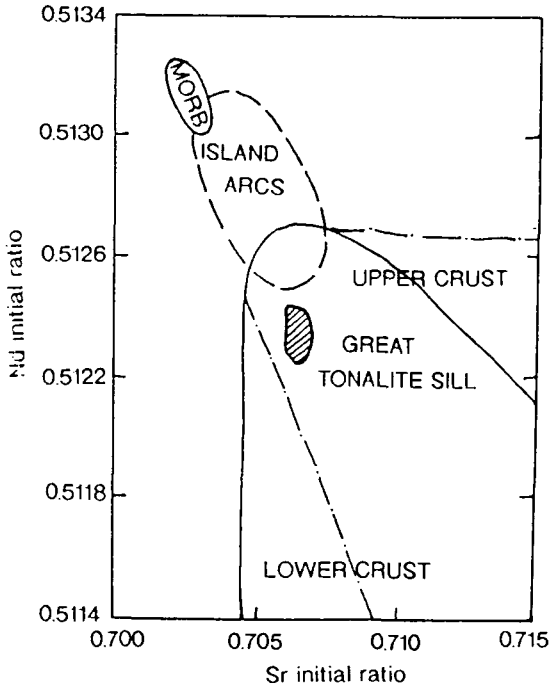

Figure 5.1 Plot of initial $^{87}Sr/^{86}Sr$ ratio versus initial $^{143}Nd/^{144}Nd$ for plutons of the Great Tonalite Sill in the Ketchikan area (Arth et al. 1988), showing fields for possible magma sources (Zartman 1984).

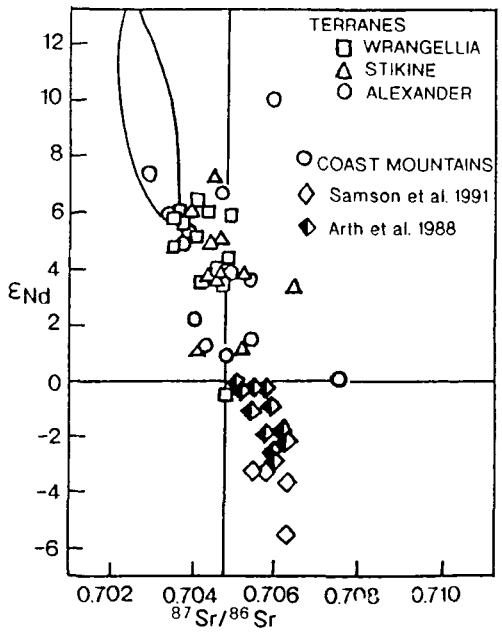

Figure 5.2 Initial εNd versus initial $^{87}Sr/^{86}Sr$ for samples of the: Great Tonalite Sill (Coast Mountains Batholith, Samson et al. 1991a); the Alexander and Stikine terranes (Samson et al. 1989); the Wrangellia terrane (Samson et al. 1990).

Summary. In summary, the Great Tonalite Sill rocks:

(1) are calc-alkaline in composition,

(2) do not strictly represent the roots of an island arc,

(3) were produced essentially from a combination of mantle-derived magmas and partially melted Precambrian lower crustal rocks, and

(4) were emplaced into a long, tenuous, orogen-parallel contractional shear zone of plate tectonic dimensions.

5.2 The tectonic model for granitoid petrogenesis

5.2.1 *Shear zones and crustal thickening*

In chapter 1, the temporal and spatial coincidence of zones of granitoid magmatism and crustal shear zones was briefly discussed. In this section, the relationship between deep crustal shear zones and granitoid petrogenesis will be discussed in more detail, especially with regard to their role in causing the genesis of the granitoid magmas in the first instance. In addition, aspects of shear zone control over magma ascent and emplacement will be approached.

Transcurrent shear zones. As reviewed by Hutton and Reavy (1992), zones of major transcurrent shear are related to granitoid magmatism both spatially and temporally. Examples include the Hercynian shear zones of Iberia (Castro 1985, 1986, Reavy 1989) and Brittany (Nicolas et al. 1977, Strong & Hanmer 1981), the Caledonian of the British Isles (Hutton 1982, 1988a, 1988b, McCaffrey 1989, 1992), Newfoundland (Hanmer 1981), Saudi Arabia (Davies 1982) and the Lachlan Fold Belt of Australia (Morand 1988). These granitoids are syntectonic with the shear zones into which they were emplaced. In general, the main features which demonstrate synchroneity of magmatism and shear zone activity include: (1) elongate plutons whose

long axes coincide with shear zones, (2) Coplanar CPS and PFC fabrics which are parallel to, and continuous with, the fabrics in the shear zone, (3) PFC lock-up shears in the plutons, (4) the synkinematic growth of metamorphic minerals in the thermal aureole, and others (see section1.6.3).

The above shear zones, associated with syntectonic magmatism, are consistenly transpressional, which means that coeval simple shear and shortening occurred across the zones ($0<K<1$ strains). In simple terms this means that their walls were squeezed together during transcurrent shear and the material in the shear zones was both shortened horizontally and extruded vertically (Sanderson & Marchini 1984) (fig. 5.3). Hutton & Reavy explored further the possibility of granitoid petrogenesis within this framework and produced models for: (1) plutons with a mantle component, and (2) those without a mantle component. The former model has applications to the Great Tonalite Sill rocks, which have an important mantle component, and will be discussed in more detail. For reasons similar to those in section 5.1.2, the Caledonian Granites of the British Isles were considered to have a mantle component involved in their petrogenesis. Mantle-derived mafic material initiated partial melting of the lower continental crust to produce these particular granitoids in NW Ireland and Scotland.

Transcurrent shear zone granitoids with a mantle component. The model of Houseman et al. (1981), concerning the thermal evolution of continental convergent belts, has particular relevance to the shear zones in which large amounts of shear zone induced crustal thickening has occurred in conjunction with mantle-signature granitoid magmatism. In essence, when crust thickens during crustal shortening, the underlying mantle lithosphere also thickens. When this happens, a cold, dense lithospheric root is forced into the surrounding asthenosphere (fig. 5.4). At a critical point, the thickened layer, or root, that forms the transition from the strong lithosphere to the convecting asthenosphere, becomes gravitationally unstable and is convectively removed, being replaced by hotter asthenospheric material (fig. 5.5). This exposes the overlying crust and remaining lithospheric mantle to asthenospheric temperatures, leading to

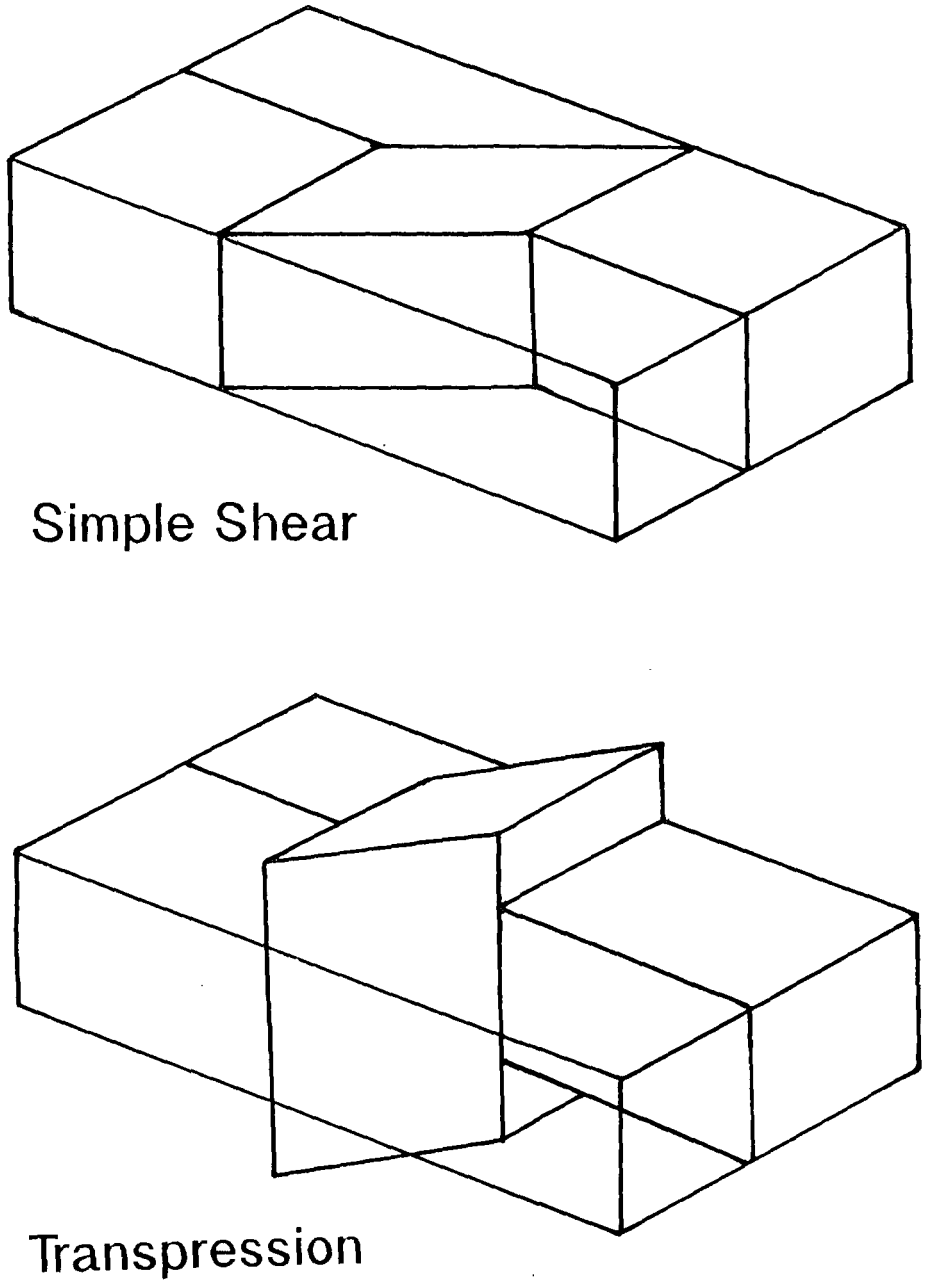

Figure 5.3 Transpression model of Sanderson & Marchini (1984): transcurrent shear and coeval shear zone normal contraction.

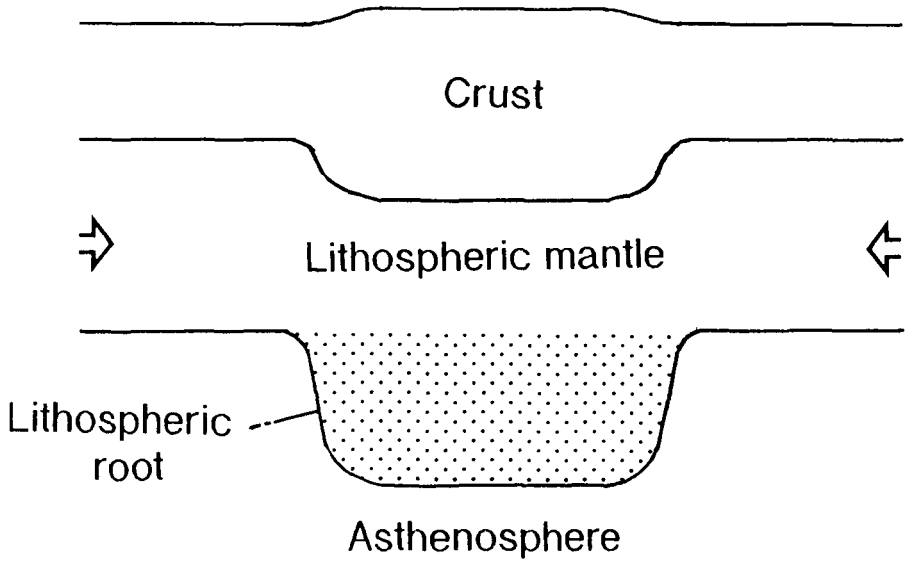

Figure 5.4 Simple cartoon cross section of a convergent orogen, showing depression of the lithosphere/asthenosphere boundary and formation of a mantle lithospheric root (Houseman et al. 1981).

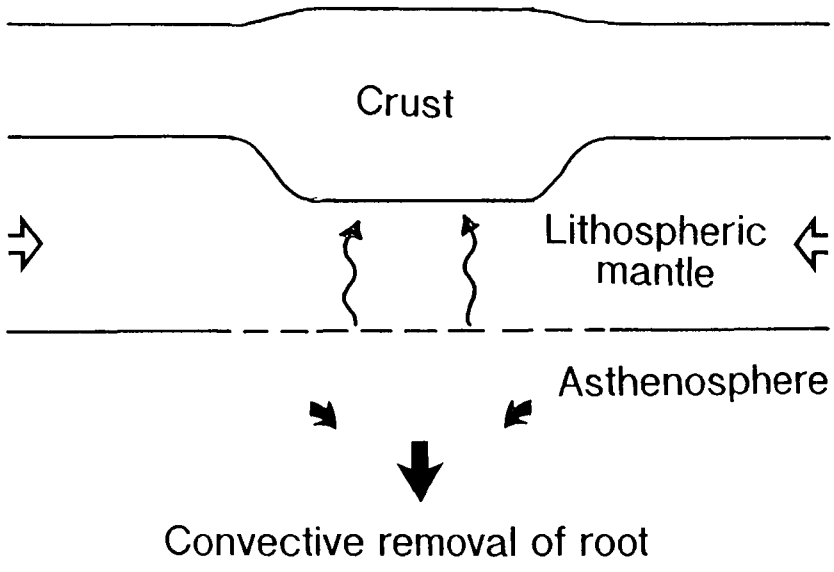

Figure 5.5 Convective removal of the unstable, thickened, lithospheric root exposes the base of the crust to asthenospheric temperatures (Houseman et al. 1981).

metamorphism, rapid uplift of the crust and the generation of magmas with a significant mantle component.

Hutton & Reavy (1992) applied this model to the British Caledonian Granites and stressed that thickening of the lithosphere was synchronous with the granite emplacement and sinistral shear in this province. In addition to overall thickening of the lithosphere, the thickening of the continental crust is accentuated in the vicinity of the principal terrane-bounding faults, causing the formation of downward protuberances, or corrugations, at the base of the crust. Convective removal of the lithospheric mantle keel will generate mantle melts, which will rise and selectively melt the corrugations at the base of the crust. The melts produced from these protuberances will hybridise and/or mingle with the mantle melts and ascend along the adjacent shear zones. The final emplacement mechanisms of these granitoid melts will be controlled by shear zone kinematics.

Contractional, reverse shear zones. In their model, the above authors conclude that it is the crustal thickening that causes the magmatism, not the existence of the shear zones directly. This therefore implies that granitic magmatism will be initiated in zones of crustal thickening, regardless of the kinematics of the attendant shear zones. Reverse shear zones, in which there is a large component of pure ($K<1$) shear, may also cause thickening of the lithosphere. This means that during reverse, simple shear, the walls of the shear zone are squeezed together, causing coeval contraction across the shear zone and vertical extension (fig. 5.6). This is equivalent to the transpression model of Sanderson & Marchini (1984) translated into the reverse shear scenario.

5.2.2 *Crustal thickening in the northwestern Cordillera.*

Previous work has documented the existence of an extensive orogenic and magmatic belt in the northwestern Cordillera (the Coast Mountains orogen), which is

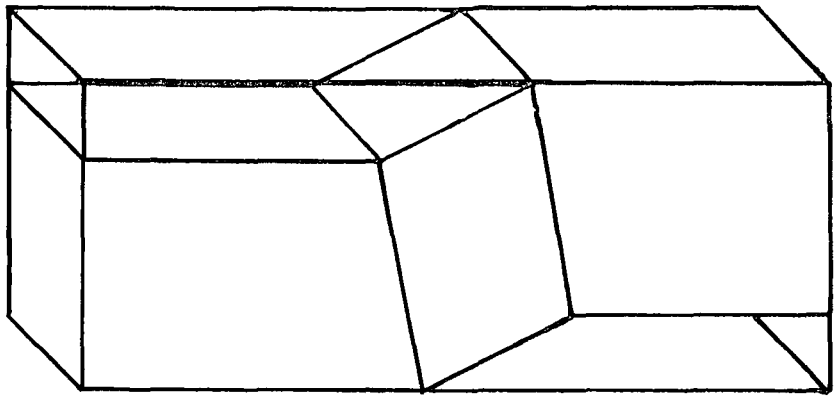

Reverse Simple Shear

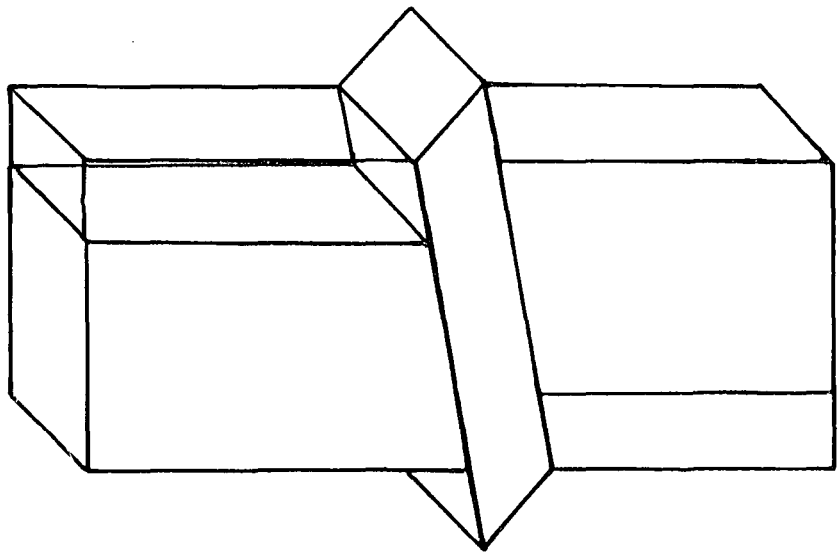

Reverse Sense Transpression

Figure 5.6 Reverse "transpression": reverse simple shear with a component of pure shear, causing orthogonal contraction and vertical extension.

related to a major crustal thickening event. This event occurred during the collision interval of the Intermontane and Insular superterranes, from mid Cretaceous to early tertiary time. The Great Tonalite Sill was emplaced into the thickened crustal pile along an extensive shear zone, some 10 to 15 Myr after the initial thickening began, and represents some of the oldest plutons of the Coast Plutonic Complex (Crawford et al. 1987, Brew et al. 1989, Gehrels et al. 1991a).

The Intermontane/Insular superterrane boundary represents a fundamental crustal boundary separating the two largest allochthonous fragments in the North American Cordillera. Structural, stratigraphic and geochronological relations along this boundary indicate that substantial west-vergent compression and concomitant crustal thickening occurred there in mid-Cretaceous time. The zone of orogeny associated with this period of deformation extends for more than 1200 km along strike in southeast Alaska, British Columbia and northern Washington (Rubin et al. 1990) (fig. 5.7). Previous structural field studies (Misch 1966, Crawford et al. 1987, Rubin et al. 1990, McClelland et al. 1992) indicated that a mid Cretaceous fold and thrust belt was localised along the eastern margin of the Alexander terrane (Insular supeterrane). This belt now consists of an imbricate series of thrust sheets with a total thickness of over 20 km, which have remarkable similarities in timing and kinematics along the extensive 1200 km strike length. One of these thrusts, the Sumdum-Fanshaw fault, has been traced from Juneau to the Ketchikan-Prince Rupert area and, according to McClelland et al. (1992), is believed to represent the major superterrane-bounding fault (fig. 5.8). Structural studies carried out by the author confirm the occurrence of brittle, west-vergent thrusts in the schists, slates and fine grained volcaniclastics of the Taku terrane and Gravina belt rocks immediately to the west of the Great Tonalite Sill in the Juneau area (fig. 5.9). It seems unlikely that this type of deformation was restricted to only one side of the terrane boundary and it is therefore probable that thrusting also occurred in terranes belonging to the Intermontane superterrane.

Timing of these thrust belts in southeast Alaska is constrained by plutons, in the Alexander terrane and the Gravina belt, whose compositions range from ultramafic,

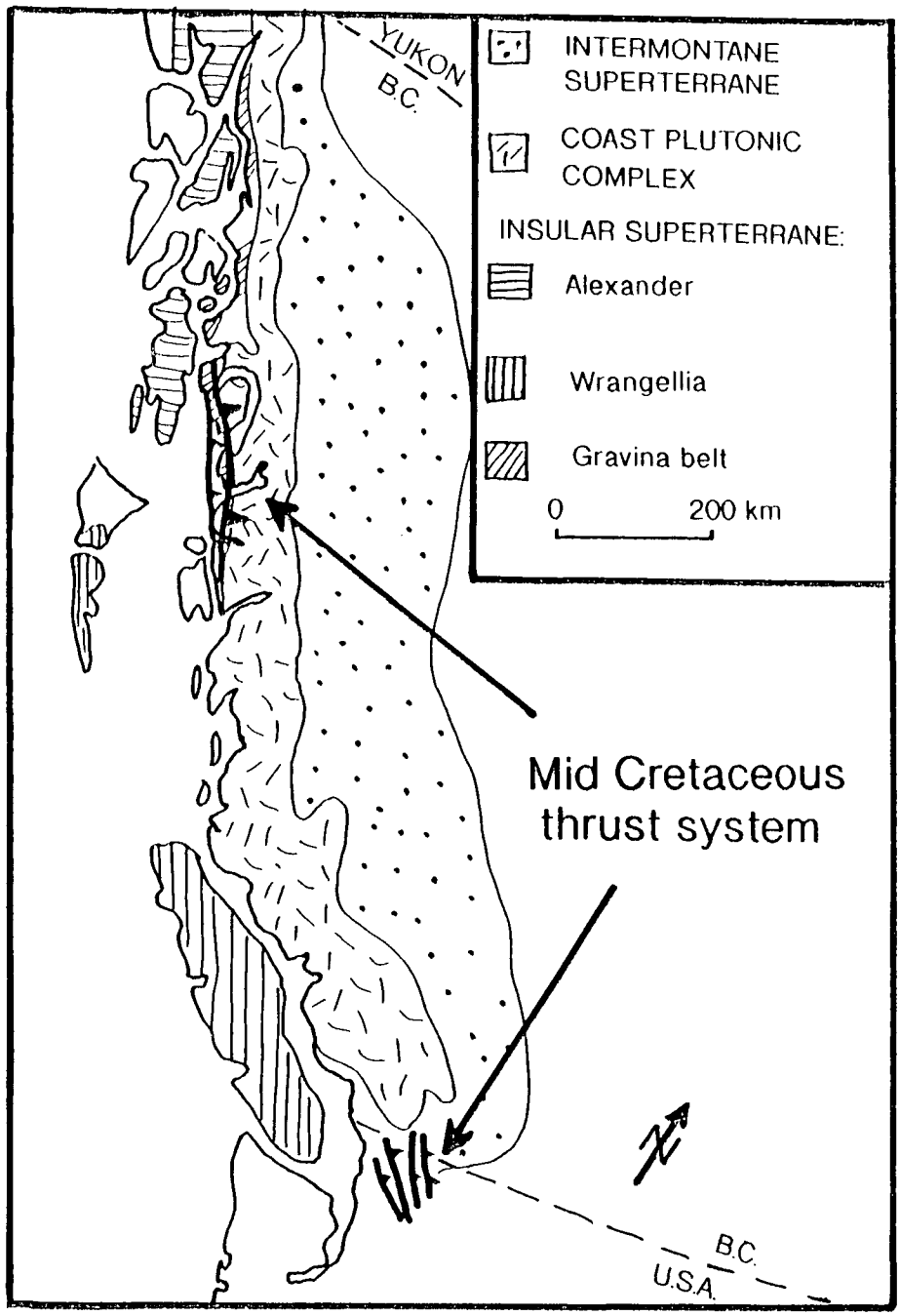

Figure 5.7 Distribution of mid-Cretaceous thrusting in the northwestern Cordillera (from Rubin et al. 1990).

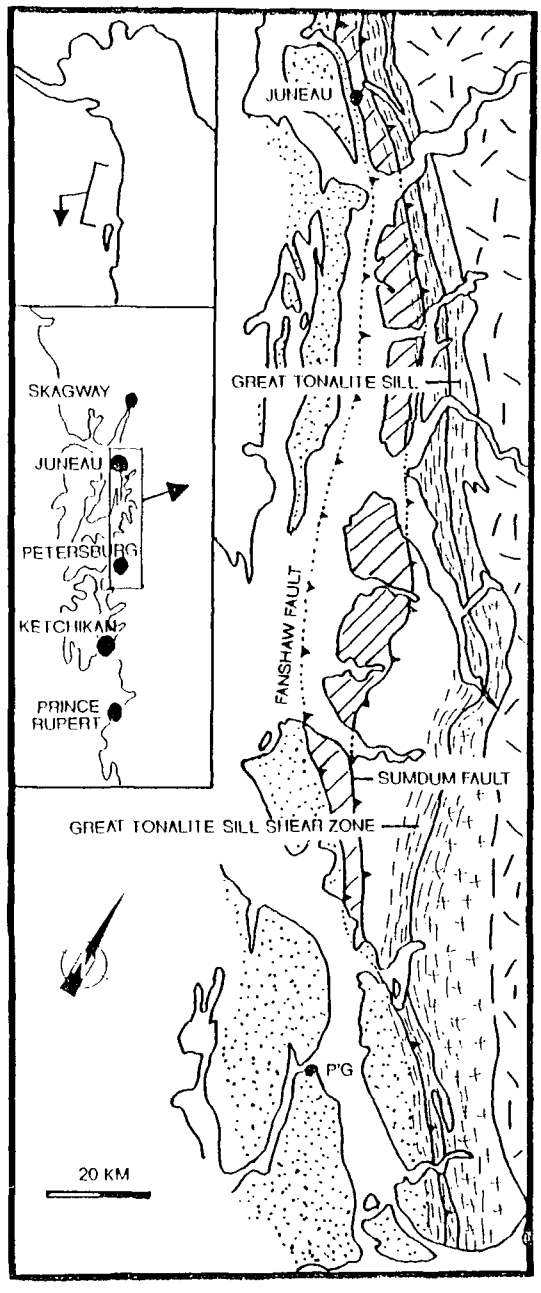

Figure 5.8 Sketch map (modified from Gehrels et al. 1990 and McClelland et al. 1991a) of a 250 km section of the Sumdum-Fanshaw fault system to the west of the Great Tonalite Sill and the Great Tonalite Sill shear zone, between Juneau and just south of Petersburg. First order terranes and intrusives: stipple = Gravina belt, diagonal shading = Taku terrane, unshaded = Yukon Tanana terrane (Gehrels et al. 1990), Random shading = Coast Plutonic Complex.

Figure 5.9 West vergent brittle thrusts within the Gravina belt bedded tuffs and volcaniclastics, north of Auke Bay, Juneau district. Baseball cap for scale.

through tonalite, to granodiorite. The 95-101 Ma plutons are cut by the west-vergent thrusts, indicating a lower age limit of 95 Ma, but the 90 Ma plutons cut the thrusts (Rubin et al. 1990, McClelland et al. 1992a), thus providing a mid Cretaceous upper limit for the thrusting. Thrusting and folding also occurred at the same time in a parallel, east vergent, belt to the east of the Cordilleran orogen (e.g. Rusmore & Woodsworth 1988), thus indicating symmetry of vergence across the orogen, the axis lying within the Coast Plutonic Complex. Fabrics and structures, associated with the Great Tonalite Sill and its associated shear zone, truncate the west-vergent thrusts (e.g. McClelland et al. 1992), and indicate a Late Cretaceous to early Tertiary interval in which deformation and plutonism were concentrated at the southwest edge of the Coast Plutonic Complex.

Overall, the deformational structures indicate a regime of widespread compression and a protracted history of contractional deformation, associated with coeval calcalkaline arc plutonism. Rubin et al. (1990) suggested two models to explain the origin of the mid Cretaceous thrust belt: (1) The first model implies that a subduction zone and a marginal basin existed between the Insular and Intermontane superterranes, prior to mid Cretaceous, and that thrusting was associated with their initial collision (fig. 5.10). The synchroneity of the deformation, along 1200 km of strike length, indicates that the two superterranes were approximately parallel, with nearly linear edges; (2) The second model implies that the mid Cretaceous contraction occurred in an intra-arc setting, and that thrusting was caused by collapse of a series of marginal basins and a magmatic arc (fig. 5.10). A subduction zone between the Insular and Intermontane superterranes did not exist prior to thrusting and the thrust system overprinted a pre-exisiting tectonic boundary. Contractional deformation was contemporaneous with arc magmatism reflecting an intra-arc tectonic scenario.

McClelland et al. (1992b) state that there is extensive mid Cretaceous and younger tectonic overprinting and disruption, which masks pre-mid Cretaceous structures. On the basis of proposed similarities between arc-related, late Jurassic to early Cretaceous basinal strata, which lie in an extensive belt between the Intermontane

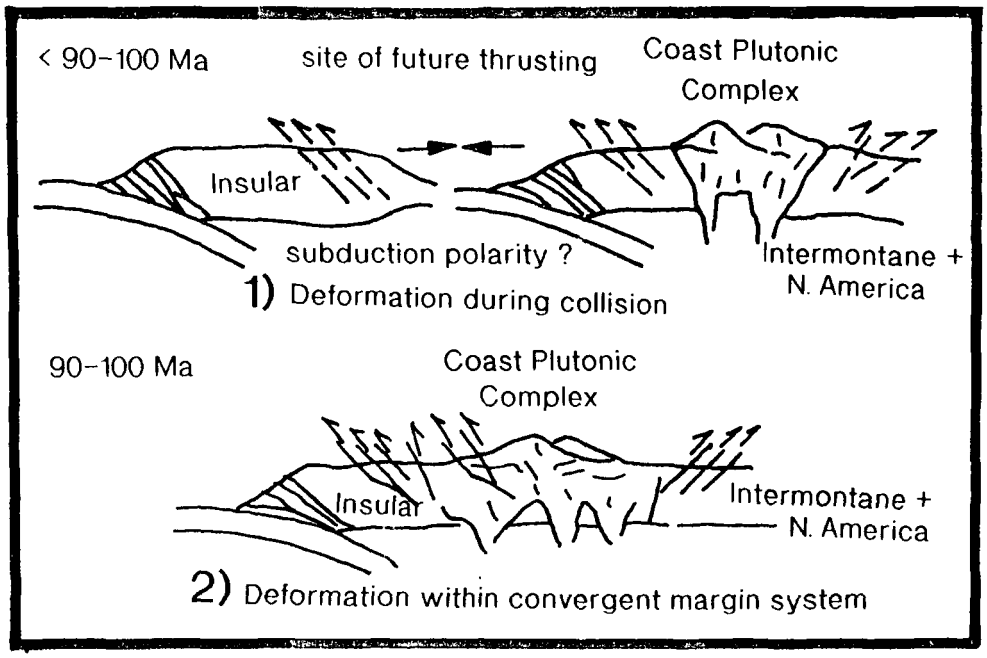

Figure 5.10 Tectonic model for the origin of mid Cretaceous deformation within the Coast Plutonic Complex (Rubin et al. 1990). Model 1) adapted from Goodwin (1975) and Monger et al. (1982). Model 2) adapted from Berg et al. (1972), Monger et al. (1972), Armstrong (1988) and Van der Heyden & Woodsworth (1988).

and Insular superterranes, they suggested that the initial collision occurred in mid Jurassic time. In their model, the mid Cretaceous thrusting event was associated with contractional deformation brought about by changes in subduction zone parameters. This is in general agreement with (2) above. In both (1) and (2), after the mid Cretaceous deformation, magmatism was concentrated at the boundary of the two superterranes, resulting in the formation of the Coast Plutonic Complex.

Crawford et al. (1987) indicated that the Coast Plutonic Complex between Prince Rupert and Terrace, British Columbia, developed in two stages between mid Cretaceous and mid Eocene. The initial stage involved crustal thickening during contractional deformation, attributed to the collision of the Insular and Intermontane supeterranes, between 100 Ma and 70 Ma i.e. mid Cretaceous collision. Continued uplift of the orogen during this period, in response to east-dipping subduction, is evidenced by syn- to post-orogenic marine and non marine, upper Cretaceous, foredeep sequences (Rubin et al. 1990). The earliest recognised events associated with crustal thickening in the core of the orogen, involve pervasive ductile deformation associated with the emplacement of tonalitic sills, from about 85 Ma to 50 Ma. During orogeny, supracrustal rocks were buried to depths of 25-30 km (also McClelland et al. 1991a) and the total crustal thickening associated with the initial event may have exceeded 60 km (Crawford et al. 1987). The second stage in the development of the Coast Plutonic Complex involved uplift between 60 Ma and 48 Ma, associated with coeval voluminous tonalitic magmatism, anatexis, and the development of ductile shear zones, which raised the deeply buried rocks to shallow crustal levels. It is this second stage of deformation and tonalitic magmatism which produced the Great Tonalite Sill rocks in British Columbia.

5.2.3 *The Great Tonalite Sill and tectonics.*

Considering the main points contained in the preceeding sections, a tectonic model for the petrogenesis of the Great Tonalite Sill rocks must take into account some important points. The Great Tonalite Sill plutons: (1) are calcalkaline, (2) do not strictly represent the roots of an island arc, (3) contain a large mantle component, (4) contain a lesser Precambrian lower crustal component and (5) are associated with a long, thin, contractional ($0<K<1$), reverse, crustal scale shear zone (the Coast Shear Zone), situated in an extensive zone of contractional and crustal thickening, into which they (6) were emplaced syntectonically, and (7) at depths greater than 20 km.

The Great Tonalite Sill shear zone. The Great Tonalite Sill shear zone and its correlatives e.g. Coast Shear Zone, Work Channel Lineament, is a dominant structural feature of the Coast Mountains of southeast Alaska and British Columbia. The Work Channel Lineament, for example, marks a metamorphic discontinuity of 3-5 kbar in the Prince Rupert area, between the Intermontane and Insular supeterranes and it therefore represents a major crustal break (Crawford & Hollister, 1982), which most probably reached the base of the crust during active deformation. Excepting minor local variations, the Great Tonalite Sill shear zone exhibits consistent kinematics along its entire length. The rocks so deformed indicate the presence of: (1) a pure shear ($K\cong0$), orogen-normal, component of strain, and (2) a simple shear ($K\cong1$) component of strain, which was associated with transport of the rocks to the northeast over rocks to the southwest (see section 3.1.2). Together, these components describe a reverse, "transpressional" shear zone (fig. 5.6). Within the Coast Mountains orogen, this represents a zone of exceptionally high shear strains and crustal thickening, which is likely to have had an added topographic effect at the base of the crust.

The genesis of the Great Tonalite Sill. Considering the petrogenetic model of Hutton & Reavy (1992), the extra crustal thickening associated with the Great

Tonalite Sill shear zone produced a narrow downward projecting feature at the base of the crust, superimposed upon an already overthickened lithosphere. After convective removal of the unstable lithospheric root, this corrugation was exposed to mantle melts at asthenospheric temperatures and was preferentially melted. The subsequent melts hybridised and mingled with the mantle melts and were channelled by the Great Tonalite Sill shear zone, before final emplacement higher in the crust. The sequence of events leading to the genesis of the Great Tonalite Sill magmas is modelled as follows (see fig. 5.11):

(1) Crustal thickening and orogeny associated with the collision of the Insular and Intermontane superterranes, plus the initial development of the Great Tonalite Sill shear zone.

(2) Further development of the Great Tonalite Sill shear zone at the Insular/Intermontane superterrane boundary, to produce an important corrugation at the base of the crust and correspondin g downward deflection of the mantle lithosphere.

(3) Removal of the overthickened lithospheric root into the mantle and its replacement by asthenospheric material.

(4) Exposure of the base of the crust and the Great Tonalite Sill shear zone corrugation to asthenospheric material and temperatures.

(5) Production of granitoid rocks with mantle and lower crustal components.

(6) Ascent and emplacement of the tonalitic rocks along the Great Tonalite Sill shear zone.

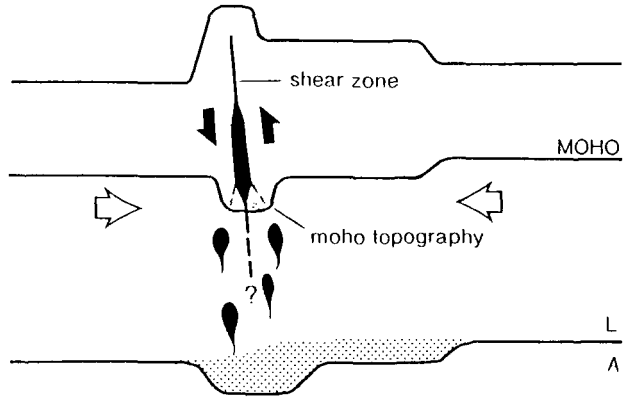

Figure 5.11 Petrogenetic model for the Great Tonalite Sill. L is lithospheric mantle; A is asthenosphere. The lithospheric mantle keel (shaded) is destroyed by convecting asthenosphere and mantle diapirs rise up to melt off the Moho topography created by focused crustal thickening at the base of the Great Tonalite Sill shear zone. The tonalites thus formed rise up the shear zones as dykes to emplacement levels higher in the crust.

5.3 Ascent of the Great Tonalite Sill magmas

A mechanism for the ascent of the Great Tonalite Sill plutons must be able to transport mafic magmas, and granitoid magmas with a high mafic component, from the base of the thickened crustal pile, high into the mid to upper crustal levels. The petrological, chemical and isotopic compositions of the Sill rocks, indicate that they have large mantle and lesser ancient lower crustal components. This indicates that there was limited contamination of the magmas with other crustal rocks during ascent and that, with respect to true granites, they may have had relatively low viscosities. In turn, this implies that ascent of the magmas was relatively rapid. The ascent mechanism should therefore be able to accommodate rapid transport of the magmas through the crust, and allow only limited interaction with the host rocks.

5.3.1 *Diapiric ascent*

According to Marsh (1982), diapirism as an ascent mechanism through the lithosphere, is a slow process and works best in unusually hot, viscous wall rock, such as that encountered in the lower crust and upper mantle. The main restriction on upward movement is drag exerted on the diapir, which is controlled by the value of the viscosity at the contact. To allow an acceptable ascent velocity, the roof rock must be heated to at least its solidus temperature, which permits a certain degree of mixing between the wall rock and the ascending magma. It has been concluded that unless bodies of magma have radii >10 km, they cannot penetrate singly through the lithosphere and will reach equilibrium, and death, deep in the crust. Repeated ascent along the same path is needed for a successful traverse of the lithosphere. In addition, Marsh (1982) concluded that for diapiric ascent through the lithosphere, the viscosity of the wall rock in contact with the magma must be in the order of 10^{15} to 10^{16} Pas,

which gives rise to an ascent velocity for the inital diapir of 5×10^{-9} ms^{-1}. Later diapirs, ascending along the same path, will have ascent velocities in the order of 1×10^{-7} ms^{-1}.

As a result of calculations such as these, the applicability of diapirs for the ascent of large volumes of magma through the lithosphere has been questioned (Bateman 1984, Brun et al. 1990, Hutton 1992). In the example of the Flamanville pluton of NW France, Brun et al (1990) indicated that formation of the pluton, within soft sediments of the shallow upper crust, probably resulted from in situ expansion of a granitic body, fed by magma injected through the brittle crust (e.g. by dykes), rather than from ballooning related to diaprirism. Bateman (1984) implied that the lack of descriptions of structures formed during the passage of granitoid magmas, suggests that they ascend in a manner which leaves a minimal trace e.g. dykes. He added that ascent often occurs while the magma is acting, in rheological terms, as a fluid and stressed that there is a paucity of real evidence for the diapiric ascent of such fluids.

It seems that the main factor in determining whether ascent occurs as dykes or diapirs, is the viscosity of the ascending magmas. In essence, highly viscous magma will ascend as diapirs and magma with low viscosity will ascend as dykes. Bateman (1984) therefore concluded that only bodies with a high crystal content and enough heat, to create a partially molten carapace of country rocks, could ascend as diapirs. This implies that the magma has already crystallised to a high degree (>50% crystals) when its forms a diapir and therefore has a very limited lifespan, before its death at the RCMP (75% crystals), the point at which ascent is arrested.

Although recent work has shown that granitic diapirs do exist (e.g. England 1992), much work implies that they do not represent an effective mechanism by which large volumes of magma may ascend through the lithosphere.

5.3.2 *Ascent by dyking*

In contrast to diapirism and other transport mechanisms, such as porous flow through a partially molten matrix (Sleep 1974, McKenzie 1984), rapid transport of

magma through the lithosphere occurs via a dyking or sheeting process. Work concerning dykes and their propogation has generally been concentrated on those with mafic compositions, as these are observed in abundance both in oceanic and continental crust and in many different tectonic settings. The widespread occurrence of dykes suggests that magma driven fracture, or sheeting, is the dominant mechanism for magma transport through the crust and lithosphere. This process is capable of rapidly transporting magma through cold and brittle rock without extensive solidification (Lister & Kerr 1991).

In previous papers e.g. Spence & Sharp (1985) and Spence & Turcotte (1985), workers have derived theoretical solutions for the propogation of magma driven fractures in which it has been assumed that buoyancy forces of the rising magmas are negligible. Although these are relevant to sill formation higher in the crust, they do not address the formation of dykes fully, as density differences between melt and host rock are neglected. Later theoretical work on dyke propogation took into account three important factors: (1) elasticity, (2) fluid mechanics and (3) buoyancy (Spence et al. 1987, Lister 1990, Lister & Kerr 1991).

Lister & Kerr (1991) conclude that vertical transport in dykes is dominated by a balance between two main opposing forces: (1) the buoyancy head, caused by the density difference between the magma and host, which drives the magma upwards, (2) the viscous drag, or viscous pressure drop, caused by friction at the walls of the dyke, which resists the upward motion of the magma towards the dyke tip, caused by (1). If (1) is always greater than (2), then the dyke will continue to propogate upwards. These authors also concluded that: (3) flow may also be driven by gradients in the overpressure of the magma. However, provided the tectonic stress perpendicular to the plane of the dyke does not vary significantly with depth, internal overpressure will remain constant and will therefore the magma flow will not be affected, (4) the resistance of the host rock to fracture is only important during nucleation of a dyke and may be generally neglected, (5) elastic forces exerted by the host rocks are only significant near the dyke tip and have a very minor role, (6) cessation of dyke

propogation is only likely to be related to crystallisation of magma in the dyke tip, triggered by e.g. a drop in pressure caused by a drop in velocity of the upwelling magma, (7) the level of neutral buoyancy (LNB) is the point at which the magma has a greater density than its host and motion ceases, causing crystallisation of the magma. Some overshooting of the LNB may occur, depending on the width of the dyke and the supply rate of the magma from below. Another important conclusion states that (8) it is not possible to close an already filled dyke by squeezing together the wall rocks, since infinitely large elastic pressures would be required. In such a scenario the dyke will instead decrease in width until the contents fully crystallize.

Dykes, once established, are therefore difficult to arrest unless the upward force cause by the buoyancy head is exceeded by the frictional drag. Conclusions (4) and (5) above indicate that, overall, elastic forces exerted by the host rocks are not important. This has implications for magma transport and emplacement in compressional regimes, such as those in which plate tectonic stresses are present at convergent margins. Following on from the model of dyke propogation by overpressure induced wedging (Anderson 1951), Pollard & Johnson (1973) calculated that the country rock at the tip of a dyke, or sill, experiences extremely high localised extension, which allows rapid propogation of the dyke along a plane continuous with the length of the sill. Quantitative calculations indicate that the yield strength, of the host rock at the dyke tip, required to resist ductile failure is in the region of 1800 times the driving pressure of the magma (fig. 5.12). Conclusion (7) above implies that once the dyke has propogated in the manner just described, it will be impossible to close it again by exerting pressure normal to its walls.

Solitons. Experimental modelling by Whitehead & Helfrich (1990) indicated that solitary waves may be supported in pre-existing magma conduits and that they behave nearly like solitons (solitary waves that are conserved upon collision with any other waves). Theoretically, these waves have closed streamlines and will retain a constant surface area (i.e. there is no turbulence) and they are preferable to diapirs as

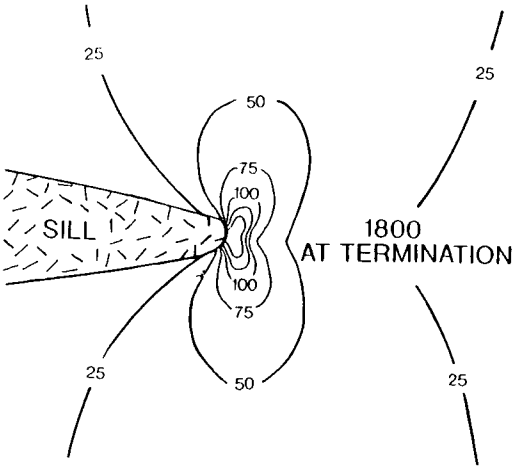

Figure 5.12 Contours of values of yield stress required to resist ductile failure at a sill termination, assuming the magma pressure=1 (after Pollard & Johnson 1973).

they represent a much more efficient mode of transport. Calculations suggest that a substance transported by solitons, from some deep mantle source, might be chemically or isotopically unaltered by the time it arrives at high levels in the crust. This has enormous implications for granitic magmas with mantle signatures and little crustal contamination.

The applicabilty of solitons to transport in dykes has not as yet been approached fully, as the above modelling concerns only one-dimensional conduits. Further work in two dimensions is required, in order to address the feasability of rapid vertical transport in dykes with minimal crustal contamination.

5.3.3 *Discussion*

Flow in magma. From Lister & Kerr (1991), a form of Poiseuilles equation in the laminar flow regime is as follows:

$$u = -(\omega^2/3\eta)\Delta p$$

where u = mean velocity, ω =dyke width, η = magma viscosity, Δp = pressure gradient.

Table 5.1 shows a variety of dyke widths, viscosities and pressure gradients for a number of hypothetical dykes. It can be seen from these examples that, for a given ascent velocity, magma travelling through a narrow dyke must have a lower viscosity compared to magma travelling in a wider dyke. However, as pointed out by Lister & Kerr (1991) and Hutton (1992), the ascent velocity must be sufficiently rapid to prevent the magma crystallising in the dyke, thus preventing further ascent.

Field data. From field data collected in southeast Alaska, it can be seen that the widths of the elongate, dyke- or sill-like, plutons of the Great Tonalite Sill may vary from a few hundred metres, to several kilometres. However, the plutons themselves cannot be regarded as self-contained dykes because they are made up from

Dyke width ω (metres)	Viscosity η (Pas)	Press. grad. Δp (Pa/m)	Velocity u (m/s)
0.5	10^2	1	8.33 × 10-4
		10	8.33 ×10-3
		100	8.33 × 10-2
	10^5	1	8.33 × 10-7
		10	8.33 × 10-6
		100	8.33 × 10-5
	10^7	1	8.33 × 10-9
		10	8.33 × 10-8
		100	8.33 × 10-7
100	10^7	1	3.33 × 10-4
		10	3.33 × 10-3
		100	3.33 × 10-2
	10^5	1	3.33 × 10-2
		10	3.33 × 10-1
		100	3.33
500	10^7	1	8.33 × 10-3
		10	8.33 × 10-2
		100	8.33 × 10-1
	10^5	1	8.33 × 10-1
		10	8.33
		100	83.33
1000	10^7	1	3.33 × 10-2
		10	3.33 × 10-1
		100	3.33
	10^5	1	3.33
		10	33.33
		100	333.33

Table 5.1

many smaller sheets. It is these sheets which may be regarded as individual dykes, as they constructed the plutons during repeated ascent along similar paths.

The present exposure level in southeast Alaska represents a slice through the crust at 20-30 km depth at the time of magma ascent. Essentially, this level records data concerning both the ascent and emplacement mechanisms and therefore implications for both these processes may be deduced, side by side. Field evidence indicates that component sheets in the plutons may vary in width from <1 m to in excess of 50 m. The sheets, or dykes, recorded at the lower end of the scale, indicate that granitoid magmas may easily propogate along narrow dykes, without causing premature crystallisation and arrest of propogation. It is these narrow granitoid dykes which cast some doubt on previous assumptions concerning the average values for the viscosities of granitoid magmas. It has been generally accepted that granitic magmas are several orders of magnitude higher in viscosity than basaltic magmas: the viscosity of basaltic magma (e.g. Lister & Kerr 1991) is commonly assumed to be 10^2 Pas and that of granitoid magma, 10^7 Pas (e.g. Pitcher 1979). Observations of internal sheeting within the Mount Juneau pluton, north of Juneau, indicate that sheets <1 m in width can develop during the transport and emplacement of tonalitic magma. As Table 5.1 shows, velocities calculated using a velocity of 10^7 Pas for dykes of <1 m are much too slow to allow propogation of a dyke, without crystallisation of the magma. In fact these rates are similar in magnitude to those calculated for the diapiric rise of large magma batches (15 cm/yr, Marsh 1982). Therefore the field data implies that the velocity must be greater and the effective viscosity must be lower (see also Hutton 1992).

Petrographic implications for viscosity. It is clear that the tonalitic magmas of the Great Tonalite Sill contain a large mafic component in addition to a lower crustal component. The magmas are not granite *sensuo stricto* but are at the more mafic end of the scale. Implications from field studies of these rocks suggest that tonalitic to

dioritic magmas have much lower viscosities than those envisaged by Bottinga & Weill (1977), Pitcher (1979) and Hall (1987) for granites in general.

5.4 Emplacement of the Great Tonalite Sill

As mentioned in section 5.3.3, the present exposure level in southeast Alaska permits observation of the ascent and emplacement mechanisms, for the Great Tonalite Sill plutons, at the same level. Field observations indicate that the magmas rose through the crust and were emplaced as steeply inclined dykes, or sheets. Plutons were essentially formed by the coalescence of many granitic sheets, implying that construction was a by product of the repeated ascent, crystallisation and arrest of such sheets. At certain levels, notably higher structural levels, the interaction of the propogating magma batches with pull-apart structures and other crustal anisotropies becomes more important. Perhaps most important of all, the elongate Great Tonalite Sill plutons are intimately associated with a transpressional (reverse sense) shear zone, which is believed to traverse much of the crust. Their spatial relationship is consistent along its entire length and implies a direct relationship between tectonics and granitoid emplacement in southeast Alaska.

5.4.1 *Emplacement into a contractional shear zone*

The Great Tonalite Sill was emplaced into an active, contractional shear zone (Great Tonalite Sill shear zone) with a simple shear component of NE over SW. The fact that granitic magma can intrude crust that is actively undergoing compression, leads to the conclusion that space does not need to be created to permit emplacement. There is no space problem and a relatively simple mechanism is invoked. Emplacement of granitoids into transcurrent and extensional shear zones has already been documented (e.g. Hanmer 1981, Castro 1985, Hutton 1988, Hutton et al. 1990,

McCaffrey 1989, McCaffrey 1992, Reavy 1989) and now the Great Tonalite Sill fills the the third category of emplacement into a contractional/ thrust regime, thus completing the trinity of syntectonic, shear zone-related, end-members.

As previously stated, the Great Tonalite Sill is composed of many coalesced, steeply-dipping, tonalitic plutons, which are themselves made up from many individual, steeply-dipping, sheets. Strain studies (section 3.1.6) indicate that the plutons, although highly deformed in particular areas, do not owe their present shape to excessive shear zone-related deformation, but were originally long, narrow and sheetlike. The pluton contacts, both W and E, are sheeted and individual sheets vary in thickness from <1 metre to in excess of 50 metres. As reviewed by Hutton (1992), granite emplacement mechanisms in transcurrent, extensional and contractional (thrust sense) shear zones may be dominated by multiple granitic sheeting parallel to the walls and the deformation fabrics. The Great Tonalite Sill plutons provide abundant evidence for such foliation-parallel sheeting processes, related to both ascent and emplacement mechanisms. The sheets and plutons were emplaced obliquely or at high angles to the principal stress directions and are not of the type invoked by Anderson (1951) (fig. 5.13). In the case of the Great Tonalite Sill, the maximum principal stress is orientated almost at right angles to the shear zone walls (fig. 5.14). This implies that the magmatic wedging stress of the propogating sheets must overcome the compressional stresses of the shear zone. Pollard and others (Pollard & Johnston 1973, Roberts 1970) indicated that excess pressure of the magma over the compressive wall-rock stresses creates very high localized tensile and shear stresses at a propogating dyke tip, which easily overcome the wall-rock strength and allow rapid propogation of the dyke tip (fig. 5.12) (see also Hutton 1992).

Structural and metamorphic observations confirm that foliation-parallel, reverse dip slip movement occurred during emplacement of the magma sheets. Stated simply, this means that the sheets propogated along shear planes. The sheets appear to have exploited active shear planes for the following reasons: (1) they represent structural anisotropies, and (2) the rock along their medial planes is constantly deforming and

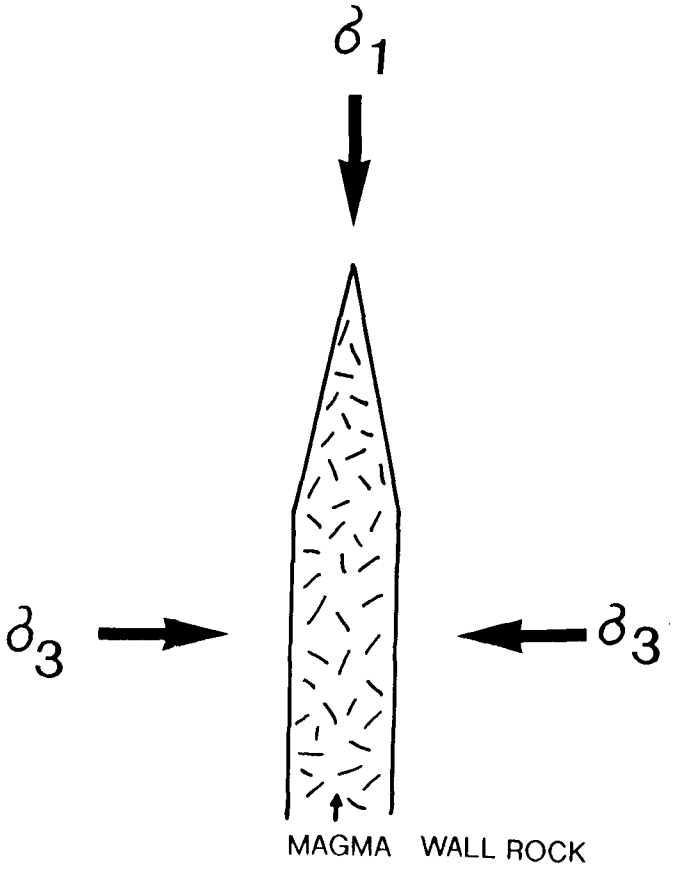

Figure 5.13 Classic Andersonian dyke and the orientation of its associated principal stresses.

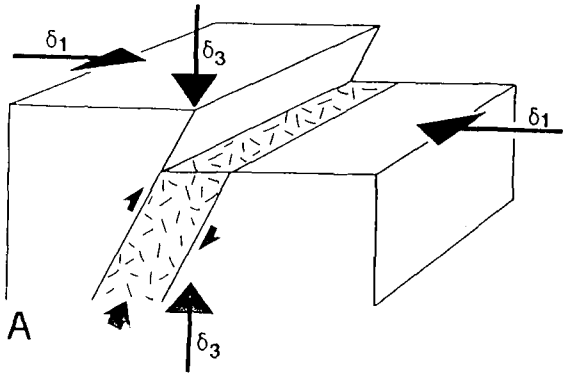

Figure 5.14 Emplacement into a contractional regime: Orientation of principal stress axes with respect to the intrusive sheet (after Hutton, 1992).

therefore weak (see also Hutton 1992). Shear planes are therefore long, narrow zones of weakness, and as such are energetically favourable to a propogating dyke or sheet tip. It is probable that the plutons of the tonalite sill belt were emplaced by such sheet wedging mechanisms.

At a higher level in the Mount Juneau Pluton (on Mount Juneau), occur moderately NE-dipping primary magmatic sheets with one-way chilled contacts, at least 30 m long and varying in thickness upwards from 0.3 m (see section 3.2.4 for details). The pattern of chilling, in addition to other intrusive relationships and geometries, invokes an emplacement mechanism in which dilatant releasing bends or thrust flats are exploited by intruding magma (fig. 5.15). This emplacement style has been observed on small outcrop to full pluton scale in southeast Alaska. A similar emplacement mechanism has previously been described by Rykkelid (1987), who indicated that the gabbro and granodiorite of the Sunnhordland Batholith, west Norway, had been emplaced into such a releasing bend (fig. 5.16). Two-way chilled contacts between the gabbro and granodiorite, plus the presence of load structures indicate that the magmas had passively filled the space. In contrast, the Mount Juneau pluton exposed at Mount Juneau represents a combination of both 'forceful' and 'permitted' emplacement: It is proposed that the invading melt actively helped to wedge open the thrust flat via repeated injections of granitic magma. It is probable that early sheets were split in two by subsequent sheets to form the pattern of one-way chilled contacts.

Small scale emplacement features. Additionally there is much outcrop data which indicates that melt is drawn into active shears, which deform either magmas close to their rheological critical melt percentage (RCMP), or anatectic, migmatitic, country rock. Many shallow, reverse, top-to-the-SW shears cut the sill rocks and the country rocks close to the pluton contacts and, often, these shears have incipient granitic melts emplaced along them. This implies that the shears may link up the interstitial pockets of melt, drawing them into concentrations along the shear planes.

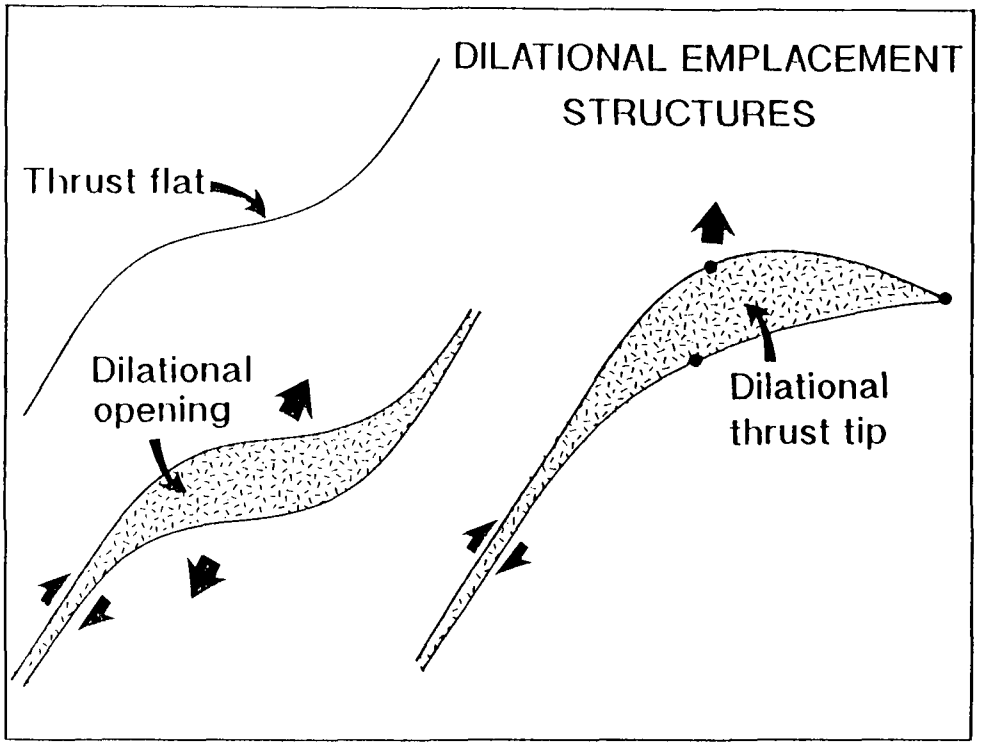

Figure 5.15 Dilational emplacement structures within an overall contractional regime.

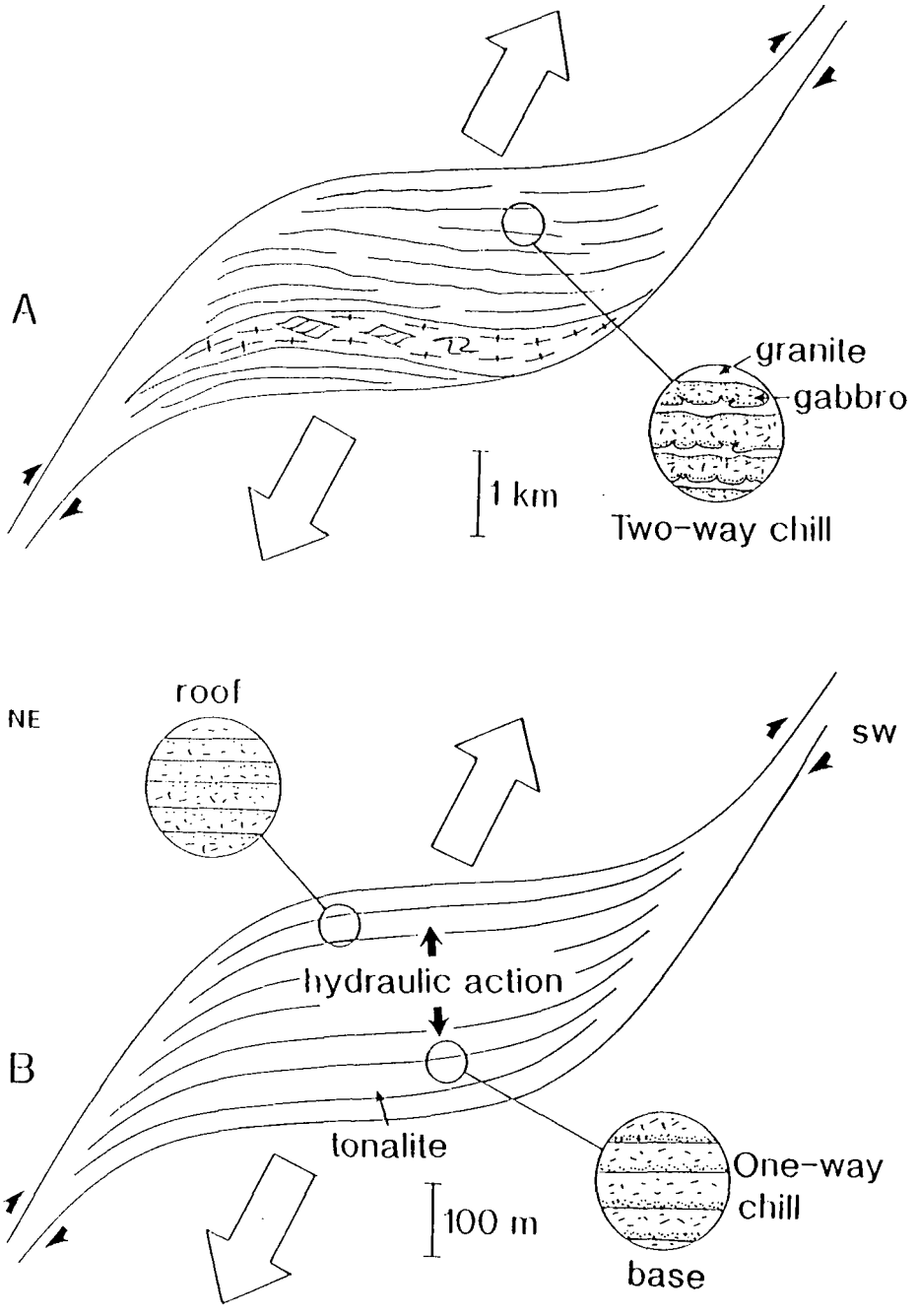

Figure 5.16 Models for granitoid emplacement into a thrust flat: (A) Stolmen gabbro, Greenland, passively emplaced into thrust releasing bend (modified from Rykkelid 1987) (B) Mount Juneau Pluton, emplaced by wedging and sheeting into a dilational thrust flat.

Other, more minor emplacement mechanisms include small-scale marginal stoping, veining and general veining features consistent with emplacement into fracture systems.

5.5 Conclusions

5.5.1 *The Intrusives*

The Great Tonalite Sill rocks are calc-alkaline (Brew 1988) and were sourced form rocks with a large mantle component and partially melted ancient crustal rocks (Arth et al. 1988, Samson 1991a). Evidence for these components comes from three main areas:

(1) Significant quantities of mafic and ultramafic rocks occur in the tonalitic plutons e.g. appinites, cogenetic mafic enclaves and synplutonic dykes, and these are likely to have mantle signatures. They also indicate the coexistence of mafic and granitoid magma: indeed, the cogenetic mafic enclaves/synplutonic dykes, in particular, imply the synplutonic injection of mafic magma into a granitoid magma.

(2) Negative εNd values indicate that the Great Tonalite Sill intrusives contain a component of older, more evolved silicic crustal rock, in addition to the mantle component (Samson et al. 1991a).

(3) In addition to (2), the Sill rocks have higher $^{87}Sr/^{86}Sr$ initial ratio values than their surrounding terranes and M.O.R.B., again indicating that older continental crust was involved (Arth et al. 1988, Samson et al 1991a).

Although the strontium initial ratios for the Coast Plutonic Complex as a whole indicate that the plutons represent the roots of a magmatic arc, the Great Tonalite Sill signature plots outside this field (Arth et al. 1988). This, along with the remarkable fucused linearity of the plutonic belt, indicates that the Great Tonalite Sill does not represent the roots of an island arc. Instead, it delineates a deformation zone.

5.5.2 *Petrogenesis*

(1) ***The general model.*** Transpressional shear zones cause crustal thickening, which in turn causes the formation of a mantle lithosphere topography (Hutton & Reavy 1992). When this thickened lithospheric root develops to a critical point, it may be convectively removed and replaced by hotter asthenospheric material, which exposes the base of the crust to elevated mantle temperatures (Houseman et al 1981). This induces the anatexis of lower crustal material which then mixes and mingles with mantle melts, producing granitoid magma with a substantial mantle component (Hutton & Reavy 1992).

(2) ***The specific model.*** Crustal thickening has occurred extensively in the NW Cordillera, associated with the mid Cretaceous to Palaeocene collision interval, and suggests strongly that formation of a lithospheric root in response to this was likely. The Great Tonalite Sill is associated with an intensely focused late Cretaceous to Palaeocene crustal scale shear zone, with a pure shear ($K \cong 0$) orogen normal component and a simple shear ($K \cong 1$) component of strain. This shear zone (the Great Tonalite Sill shear zone) probably reached the base of the crust and caused focused crustal thickening along 800 km or more. Thus a perturbation or corrugation was produced at the base of the crust, which was preferentially melted after removal of the lithospheric root, and the subsequent melts migrated along the adjacent shear zone, forming the Great Tonalite Sill.

5.5.3 *Ascent of the magmas*

The Great Tonalite Sill shear zone must have transported the mantle-derived melts rapidy through the crust, along the shear zone, in order ro prevent excessive solidification in the conduit and contamination with juvenile crust.

Diapirs. It has been concluded that diapiric ascent is a slow process (Marsh 1982), thus facilitating significant interaction of magma with continental crustal rocks and much solidification after relatively little movement. This is not a plausible ascent mechanism for the Sill magmas.

Dykes. Ascent by dyking is a rapid process and magmas may be transported through the crust and lithosphere without extensive solidification and contamination (Lister & Kerr 1991). Dykes propogate due to extremely high localised tensile stresses at their tips and are difficult to arrest unless the upward buoyancy force is exceeded by the frictional drag. They exploit inisotropies in rocks, such as zone weakened by shearing, and theoretical modelling indicates that, once formed, they are impossible to close again. The width of dykes and the velocity of transport are determined by the viscosity of the magma: low viscosity leads to rapid propogation rates and narrow dykes. The present outcrop represents both the ascent and emplacement level: the component sheets exposed within the plutons have widths (<1 to >50 metres) which imply that the effective viscosity of tonalitic magmas may be significantly lower than those previously published for true granites.

5.5.4 *Emplacement*

The Great Tonalite Sill magmas ascended and were emplaced dominantly as non-Andersonian dykes/sheets. Emplacement of the sheets took place along a compressional shear zone axis, implying that space does not need to be created to accomodate granitoids. At deep levels the sheets propogated along shear zone weaknesses and, perhaps more commonly at higher levels, in dilational pull aparts (dilational flats) within ramp-flat shear zone geometries. The higher level emplacement mechanisms may, in part, be related to closer interaction of the shear zones with the free surface.

CHAPTER 6
THE IMPLICATIONS FOR PLATE TECTONICS

6.1 Allochthonous terranes

During the opening of the Pacific Ocean, from latest Precambrian through the early Palaeozoic, the western edge of North America was a passive continental margin, across which grew, undisturbed, a miogeoclinal wedge, for at least 700 million years. Since Triassic to middle Jurassic time, the margins of the Pacific Ocean have been dominated by convergent or transform movements. Subduction related to these movements consumed all of the Palaeozoic Pacific ocean, leaving behind offscraped, accreted, allochthonous, Palaeozoic terranes. It follows that younger outboard terranes must also be regarded as allochthonous, unless proven otherwise (Coney et al. 1980).

On the basis of differences in faunal diversity between separate belts in the western Canadian Cordillera, Monger and Ross (1971) originally suggested that two different ecological belts had been broken and juxtaposed, by implied dextral movements parallel to the north American margin. Faunal and lithological studies (e.g. Monger & Ross 1971, Monger et al. 1972, Monger & Price 1979) indicated that upper Paleozoic stratigraphic sequences in the Insular and Intermontane superterranes (see section 2.1.2) may have belonged to the Tethyan faunal realm and are atypical of, and therefore allochthonous to, the continental interior of North America. Monger et al. (1982) suggested that tectonic accretion of the Intermontane superterrane to the North American craton, and the Insular superterrane to the Intermontane superterrane, caused the formation of two major regional tectonic welts in the Canadian Cordillera: the Omenica Crystalline belt and the Coast Plutonic Complex respectively (see chapter

2). Concentrated within these belts were intense deformation, regional metamorphism, granitoid magmatism, uplift and erosion. The Coast Plutonic Complex formed in response to this deformation mainly in Cretaceous to Tertiary time and, during the late Cretaceous to early Tertiary, emplacement of the Great Tonalite Sill took place along its southwestern edge. The Great Tonalite Sill therefore provides a valuable record of the kinematics and deformation prevalent during the accretion interval subsequent to initial collision of the Intermontane and Insular superterranes.

The following sections provide a brief review of extant data and models concerning plate and terrane motions and regional tectonics. Subsequently, these will be considered in the light of new geological data acquired during this study.

6.2 Existing plate trajectory modelling

The plate model of Engebretson et al. (1985) formed the basis of a computer program developed by Debiche et al. (1987), which was designed to simulate the position of terranes with time as they were driven by the oceanic plates. The terrane (plate) trajectories were calculated by back modelling and the main variables which define this are: 1) the stage poles describing the motion of oceanic plates with respect to the continent, 2) the sequence of plates carrying the terrane, 3) the time of docking of the terrane, 4) the coordinates of the point of docking. For docking times of 120Ma and 90Ma the most striking feature is the presence of a strong easterly component of plate motion with respect to Cordilleran North America. This is capable of transporting terranes with equatorial faunas to North America, especially Alaska, from the western Pacific. The plate trajectories are directed largely orthogonally (fig. 6.1), with a lesser component of dextral movement, relative to the North American margin. However, the model indicates that if terrane docking times of 60 Ma and 30 Ma are chosen, the northerly component of motion becomes dominant reflecting a regime in oblique dextral transpression.

Depending on the plate reconstruction model chosen, the dextral component of motion can be increased or reduced for particular terranes. In particular, around 85Ma, when the Kula plate is interpreted to have broken away from the Farallon plate (Woods & Davies 1982), there is uncertainty about the location of the ridge separating them. The southern ridge option of Engebretson et al. (1985) was chosen by Debiche et al. (1987) in part because this provides rapid northerly transport during the Late Cretaceous, as required by paleomagnetic results from terranes (fig. 6.2, see section 6.5). However, if the northern ridge option was chosen, a terrane located in the area between the two options would continue to move with the Farallon plate orthogonally towards the North American margin. This is an example of ambiguity inherent in such modelling techniques and suggests that, although the gross movement of plates and terranes may be deduced from these studies, details concerning the collision dispersion tectonics at the time of docking are lacking and cannot be accurately modelled using this method.

From the mapping of Palaeocene to middle Eocene magnetic anomalies over oceanic crust that accreted at the Kula-Pacific spreading centre, Lonsdale (1988) indicated that, prior to 57Ma, relative motions between the Kula plate and the North American margin were orthogonal, and that NE-directed underthrusting related to these motions took place along the Pacific Northwest Subduction Zone (fig 6.3). Oblique subduction did not occur until after 55Ma in his model, which assumes a slower rate of northward motion compared with Engebretson et al (1985). The 55 Ma switch in the plate movement vector coincided with the birth of the Aleutian subduction zone, which most likely changed the slab-pull stresses on the oceanic lithosphere. Strike slip faults developed as a result of this and caused the rapid, post 55 Ma, northward movement of allochthonous terranes. Recent data derived from large-scale fluid migration studies also supports the view that oblique subduction did not occur until after 55-56 Ma. This particular study identified a significant, rapid, dewatering event at this time, which Goldfarb et al. (1991) suggest was caused by

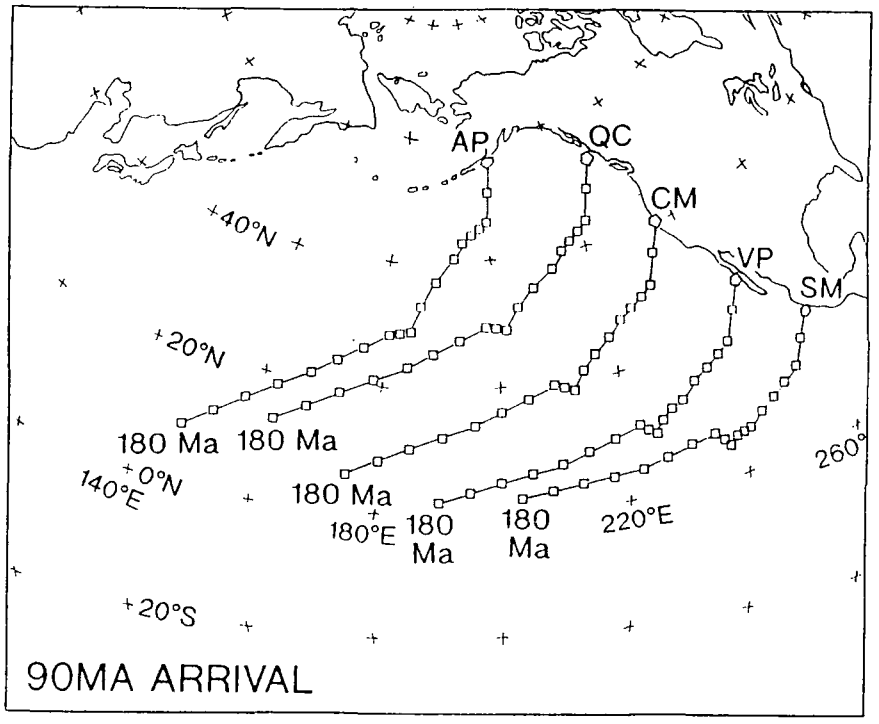

Figure 6.1 Trajectories of the Farallon plate in fixed North America coordinates, determined by backward modelling every 5Ma from the arrival time of 90Ma (From Debiche et al. 1987).

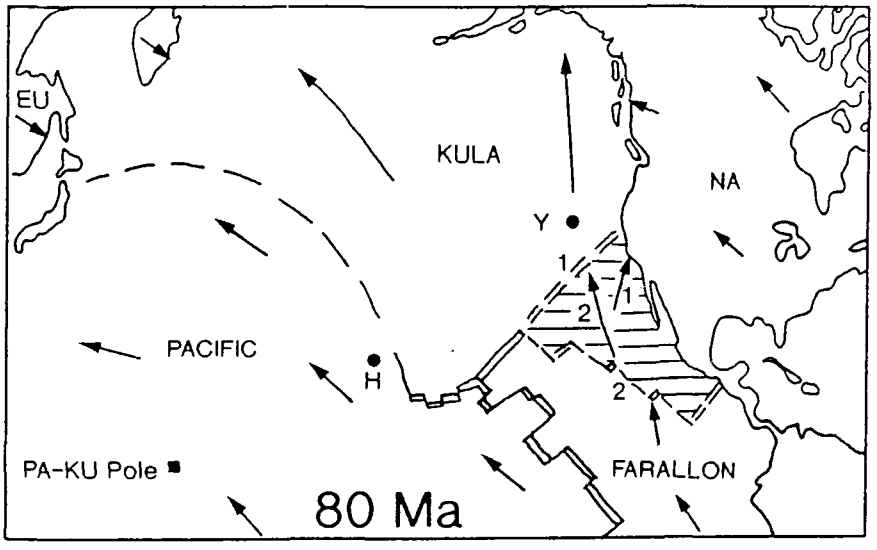

Figure 6.2 Reconstruction, in fixed hotspot reference frame, of plate motions at c.80Ma. Length of arrows is proportional to velocity. Shaded area = uncertainty: 1 = northern option for Kula-Farallon ridge, 2 = southern option (velocity arrows numbered accordingly). Solid circles: Hawaiian (H) and Yellowstone (Y) hotspots; solid square: Euler pole for relative motion of Pacific and Kula plates. Modified from Engebretson et al. (1985).

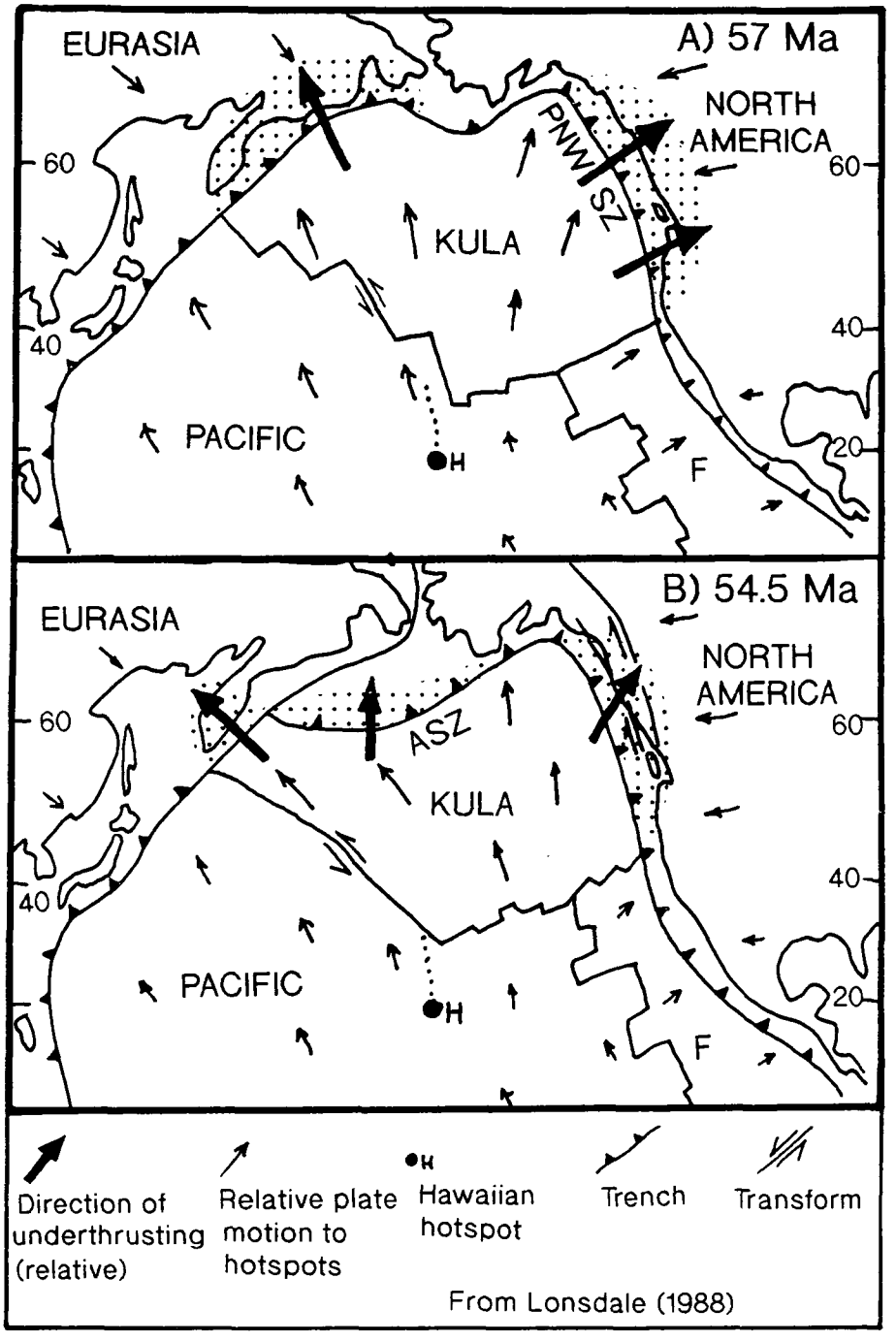

Figure 6.3 Hypothetical reconstructions and motions of the Kula plate, just before (A) and after (B) its early Eocene westward swerve: **A.** Construction from Lonsdale (1988) is similar to Engebretson (1985) but with a slower northward movement of Kula, causing more orthogonal subduction on the North American margin. **B.** After 55 Ma, oblique subduction caused development of strike slip faults and rapid northward transport of terranes (from Lonsdale 1988). Shading = subducted slab.

increased crustal permeabilities, related to a shift from convergent to partly transcurrent tectonics.

It is apparent, from the above examples, that the assumed northward velocity of the Kula plate has a great bearing on the implied tectonic regime at the Kula/North America boundary, and hence the relative motions of allochthonous terranes, with respect to the North American margin. Engebretson et al (1985) used a faster northward velocity than Lonsdale (1988) for the Kula plate and from this he implied that the convergence took place in a dextrally transpressive regime. Lonsdale (1988), using the slower Kula plate velocity, implied that the late Cretaceous to Palaeocene Kula-North America convergence was normal to the continental margin.

One of the main aims of this thesis is to use the geological field data from the Great Tonalite Sill to help to resolve uncertainties such as these. Modelling, using the techniques discussed above, can only be as accurate as the assumptions encorporated into them. This conclusion underlines the importance of testing models such as these with detailed field studies, focused at plate and terrane boundaries: the deformation zones containing structures from which relative terrane movements during, and subsequent to docking may be deduced.

6.3 The Great Tonalite Sill as a kinematic record

In chapters two and five, the value of the Great Tonalite Sill, as an accurate record of the kinematics prevalent during its emplacement, has been already stressed. From the conclusions of chapter three, it is clear that, together, the structures along this belt show a remarkable consistency, unparalleled in other parts of the Coast Mountains. The Sill has plate tectonic dimensions and, as such, the structures contained within it have more than local importance. Chapter five drew upon this conclusion and, within it, the origin, ascent and emplacement of the batholith was modelled in terms of large scale, contractional plate tectonics. This section seeks to

expand on these themes and make conclusions about the exact nature and timing of the contractional kinematics along the belt as a whole. From this it will be possible to make important inferences concerning the relative movements between the Insular and Intermontane superterranes and hence the relative movements of the Kula and Farallon plates with respect to the North American margin.

Firstly, the the overall structure and kinematics of the belt will be briefly reviewed.

6.3.1 *Structure and kinematics*

Essentially, the Great Tonalite Sill belt is a steeply NE-inclined ductile shear zone, separating the Intermontane and Insular superterranes. It was intruded by tonalitic magmas with mantle and lower crustal signatures, in late Cretaceous to early Tertiary times, during active deformation.

PFC deformation. The deformation which was incurred in the magmatic state (detailed in chapter three) is displayed in the Great Tonalite Sill as (1) PFC fabrics and lineations, (2) tiling fabrics, (3) PFC lock-up shears, and (4) strained mafic enclaves. The present orientations of these features indicate that a regime of dominant NE-SW directed contraction and concomittant $0<K<1$ pure shear, accompanied by lesser NE over SW directed reverse simple shear, was in effect during the crystallization interval of the deforming magma. No evidence for major strike slip movements was recorded.

CPS/solid state deformation. CPS/solid state deformational structures, and their implications for large scale kinematics, are similar to, and coplanar with, those detailed above, although these structures formed subsequent to full crystallization of the plutons.

These structures, incurred in both the magmatic and solid states, have been shown to occur along an extensive strike length, in excess of 750 kilometres. This

implies, in basic terms, that the movement of the Insular superterrane, during part of its accretion interval, was directed orthogonally with respect to the Intermontane superterrane (fig. 6.4). There is no evidence in support of either major sinistral or major dextral movements within this belt, either during or after emplacement. and full crystallization, of the Great Tonalite Sill magmas.

6.3.2 *Timing of kinematics*

Gehrels et al. (1991a) carried out an extensive U-Pb geochronological survey of the plutons of the Great Tonalite Sill in southeast Alaska, and their paper represents the latest and most accurate dating of these plutons. Additionally, their paper includes a review of other relevant geochronological work previously carried out on the Sill belt and table 6.1 summarises the combined data.

These U-Pb dates indicate that the deformation, which affected the plutons during their crystallization intervals, occurred from at least 83 Ma (82.6 ± 2.4) to around 55 or 57 Ma, i.e. late Cretaceous to Early Tertiary (Palaeocene). There is a certain degree of implied diachroneity of magma emplacement along the strike of the Great Tonalite Sill: older dates are found in the north and become younger southwards. This suggests that the edges of the two superterranes were probably originally slightly irregular, and that magma emplacement was first initiated in the north, perhaps linked to the earliest contractional event. However, all the plutons in the above table, regardless of their age, contain PFC fabrics, lineations and structures, which consistently indicate that contraction and reverse shear occurred in the magmatic state. Abundant evidence exists indicating that the older plutons were more pervasively affected by prolonged, progressive deformation into the down-temperature regime, in the form of coplanar and colinear CPS/solid state fabrics, than the younger plutons. Younger plutons often contain the well developed PFC fabrics, but later post-

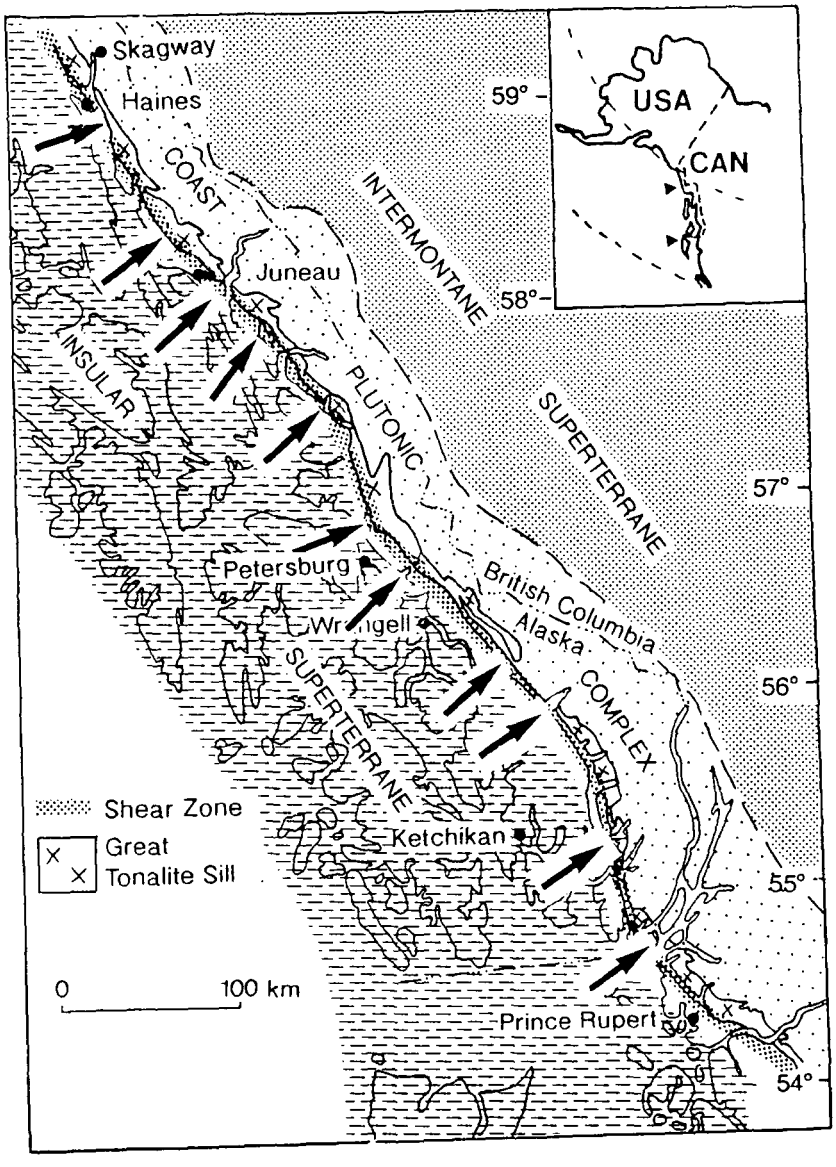

Figure 6.4 Movement of the Insular with respect to the Intermontane superterrane, inferred from foliation and transport lineation data, coupled with shear sense data, from individual traverses in SE Alaska and British Columbia (Haines and B.C. mapping by D.H.W. Hutton).

Pluton	U-Pb age (Ma)	Author
Ferebee (Haines)	68 (disc) and	Barker et al. (1986)
	82.6 ± 2.4 (disc)	Gehrels et al. (1991a)
Mendenhall (Berners B.)	61.5 ± 1.5 (disc)	Gehrels et al. (1991a)
Annex Lakes (Taku)	58.5 ± 2.5 (disc)	Gehrels et al. (1991a)
Carlson Creek E. (Taku)	66.4 ±0.8	Gehrels et al. (1991a)
Carlson Creek W. (Taku)	67.4 ± 0.8	Gehrels et al. (1991a)
Mount Juneau (Taku)	71.6 ± 1.2 (disc)	Gehrels et al. (1991a)
Mount Juneau	81 (disc)	Wooden (pers. comm. to Brew, 1990)
Tracy Arm	60.4 ± 1.3 (disc)	Gehrels et al. (1991a)
Endicott Arm	59.3 ± 0.8	Gehrels et al. (1991a)
Thomas Bay	63.5 ± 1	McClelland et al. (1990)
LeConte Bay	59.5 ± 1	McClelland et al. (1990)
Quottoon (B.C.)	58.6 ± 0.8	Gehrels et al. (1991a)
northern end	55	Arth et al. (1988)
northern end	57 ± 1	Saleeby & Rubin (1989)
	(disc = discordant)	

Table 6.1 U-Pb dating of the Great Tonalite Sill plutons.

crystallization CPS deformation is poorly developed, or absent. These data indicate that, although there is an implied diachroneity in the magma emplacement, and hence deformation, from north to south, there is no evidence for a diachronous change in the implied kinematics from north to south. Thus it is concluded here that a consistent regime in orthogonal contraction and concomittant NE over SW reverse shear was active, along the whole length of the Great Tonalite Sill belt, between 83 and 55 to 57 Ma (late Cretaceous to early Tertiary).

6.4 The Great Tonalite Sill - does it mark a major terrane boundary?

6.4.1 *Contrasts across the Great Tonalite Sill.*

The Great Tonalite Sill is the most extensive, continuous, composite granitoid batholith in the Coast Mountains and is associated with the most extensive known shear zone, the Great Tonalite Sill shear zone. Both features extend for at least 700km along strike, more probably greater than 1000km. The shear zone has been intruded by the Great Tonalite Sill plutons, whose petrological, chemical and isotopic compositions indicate that they were sourced from a combination of subduction related magmas (Arth et al. 1988), which were probably underplated beneath the crust (Chappell & Stephens 1988, Fyfe 1988, Silver & Chappell 1988), and a component of partially melted, ancient lower crustal rocks (Samson et al. 1991b). The known length of the combined Great Tonalite Sill and its shear zone, far outstrips the known length of any other feature lying between the Intermontane and Insular superterranes and therefore it is suggested here that, together, they represent the effective terrane boundary. In support, the work of Wood et al. (1991) on the spatial variation in $^{40}Ar/^{39}Ar$ mineral ages for the Great Tonalite Sill near Holkam Bay, SE Alaska, suggested that it was emplaced near the boundary between hot, high grade metamorphic rocks to the E and cooler, medium grade metamorphic rocks to the W. In the southern part of the belt the Work Channel Lineament and Quottoon pluton of British Columbia (Crawford & Crawford 1991), marks a similar discontinuity active during the early Tertiary, which shows uplift of rocks to the east of the Great Tonalite Sill (relative to the west) of about 15 km between 60 Ma and 50 Ma (Crawford & Hollister 1982). A probable northern extension of the Great Tonalite Sill, within the Maclaren Metamorphic Belt, south Central Alaska, was also emplaced within a deep-crustal shear zone (Valdez Creek shear zone). Systematic differences in metamorphic grade across this dyke-like pluton, indicate that it marks the boundary across which hot, upper amphibolite facies

rocks, previously accreted to North America, were emplaced over cooler, lower grade rocks, equivalent to the Insular superterrane (Davidson et al. 1992). Other metamorphic studies by Himmelberg et al. (1991) indicated the presence of an inverted sequence of Barrovian metamorphic isograds, west of the Great Tonalite Sill (Juneau area), which increases in grade eastwards, towards a maximum, located at the western margin of the Sill. Here the metamorphic data indicates a thermal peak of about 750°C, with pressures of about 9-11 kbar. The inverted gradient is attributed to contractional deformation and thermal metamorphism associated with the collision of the Insular and Intermontane superterranes, combined with the subsequent thermal metamorphism caused by the initial stages of tonalite emplacement in a NE dipping shear zone. Metamorphism caused by the final emplacement phase of the Great Tonalite Sill, during uplift, re-equilibrated the country rock geobarometers nearest to the contact at depths corresponding to 5-6 kbar (Himmelberg et al. 1991).

Collectively, these data indicate that there is indeed a significant, metamorphic, contrast across the Great Tonalite Sill. The Sill is fundamentally associated with a major shear zone, which essentially separates low grade rocks (to the west) from high grade (to the east), and marks a zone across which large vertical (east side up) movements have taken place. Other data show that the magmas, which coalesced to form the Great Tonalite Sill, were emplaced syntectonically and were derived partly form the lower crust and partly from the mantle. As such, these magmas must have traversed the crust and it is highly likely that their transport took place along a major crustal break, i.e. a terrane boundary.

6.4.2 *Links across the Great Tonalite Sill.*

Gehrels et al. (1990) and McClelland et al. (1990) placed the fundamental boundary between the Intermontane superterrane and the Insular superterrane west of the Great Tonalite Sill, along a thrust fault system (Sumdum-Fanshaw fault system) which they have traced from the Juneau area at least as far as the Ketchikan - Prince

Rupert Region. On the basis of general similarities between basinal sequences, small highly metamorphosed conodont faunules, U/Pb discordia from detrital zircons and Sm/Nd data indicative of Proterozoic derivation, they correlated rocks immediately west of the Sill with the Yukon-Tanana terrane, which underlies a large portion of Yukon and eastern Alaska (Samson et al. 1991b, McClelland et al. 1991a, McClelland et al. 1991b, Rubin & Saleeby 1991, Gehrels et al. 1992). This terrane is a product of episodic continental arc magmatism and the latest phase of this took place in late Triassic to early Jurassic time. The Yukon Tanana terrane thus belongs to the Intermontane superterrane. The work of Gehrels et al. (1990) and McClelland et al. (1990) therefore suggests that the Great Tonalite Sill does not separate different terranes. McClelland et al. (1991a) suggested that the rocks either side of the Sumdum-Fanshaw Fault system were juxtaposed at depths corresponding to 7.1-11.8 ± 1 kbar and temperatures of 465-890°C, during the collision of the Insular and Intermontane superterranes, in the middle Cretaceous. Following this, in the late Cretaceous to Paleocene, the fault system was truncated by the steeper Great Tonalite Sill and Great Tonalite Sill shear zone features, at depths corresponding to 7.5-7.7 ± 1 kbar. Their work therefore suggests that the Great Tonalite Sill is a minor feature, which does not represent the boundary separating the Insular and Intermontane superterranes.

6.4.3 *The Great Tonalite Sill: evidence for a major crustal break.*

Recent work by Wood et al. (1991) has documented a systematic decrease in $^{40}Ar/^{39}Ar$ mineral ages from west to east across the Great Tonalite Sill, which is consistent with its emplacement between higher grade rocks of the Coast Plutonic Complex and lower grade rocks of the western metamorphic belt, to the west. They suggested that, during uplift, the Coast Plutonic Complex would have been effectively decoupled from the western metamorphic belt, until the Great Tonalite Sill had fully crystallized. These data therefore indicate that the Great Tonalite Sill, which is

fundamentally linked to the only major, plate tectonic scale, ductile shear zone in the Coast Mountains (the Great Tonalite Sill shear zone - correlated with parts of the Coast Shear Zone), represents a major crustal break. This is corroborated by chemical and isotopic data from the Sill (Arth et al. 1988) and implications from the tectonic models for granitoid petrogenesis and ascent (sections 5.2 & 5.3). Together, these indicate that the magmas originated from deep levels (the upper mantle), implying that the shear zone which sourced them traversed the crust. It is possible that this steep shear zone represents the reactivation of a major crustal ramp which was connected to the flat represented by the Sumdum-Fanshaw fault of Gehrels et al. (1990) and McClelland et al. (1990) (see fig. 6.5). However, there is no direct evidence to support this. The known length of the Great Tonalite Sill combined with its associated shear zone is longer than any other feature lying between the Intermontane and Insular superterranes, and therefore it is concluded here that this probably represents the effective terrane boundary.

6.5 Palaeomagnetic data from the western Cordillera

6.5.1 *Anomalous palaeomagnetic inclinations - dextral strike slip?*

Paleomagnetic data recorded from the western Cordillera are consistent with large northward displacements of tectonostratigraphic terranes along the ancient North American coastline. A body of paleomagnetic data has been built up over the past decade (e.g. Monger & Irving 1980, Beck et al. 1981, Stone et al. 1982, Irving et al. 1985, Rees et al. 1985), which indicates that the Insular and Intermontane superterranes contain anomalously shallow paleomagnetic inclinations, with respect to the continental interior of North America. Simple interpretations of these data indicate that the terranes originated between 2000 and 3000 km south of their present locations, and that, during northerly transport, clockwise rotations also took place.

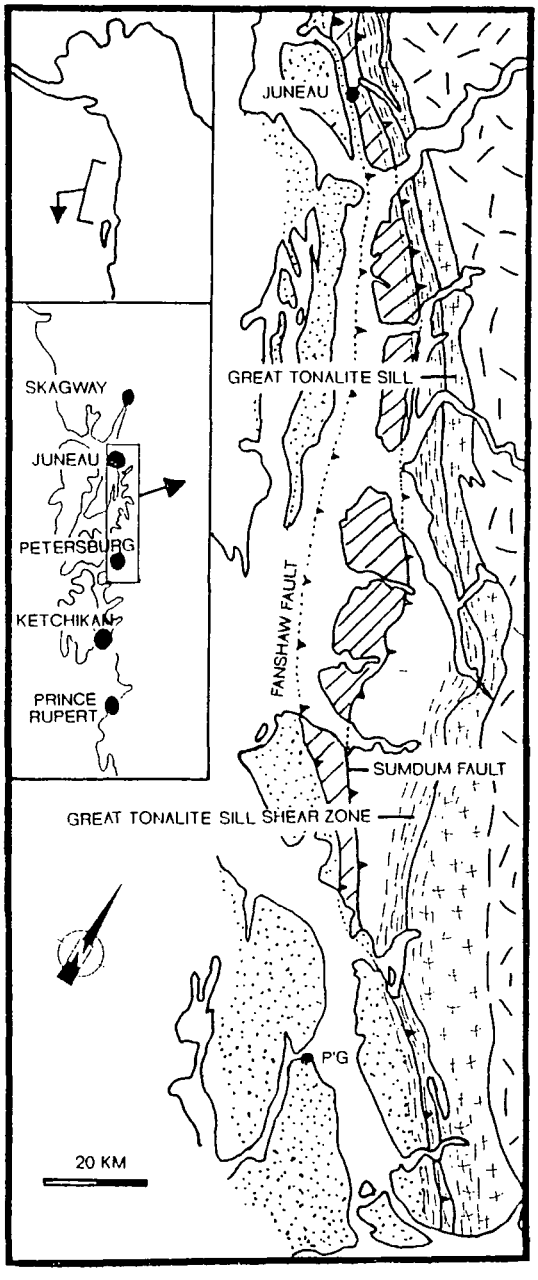

Figure 6.5 Sketch map (modified from Gehrels et al. 1990 and McClelland et al. 1991a) of a 250 km section of the Sumdum-Fanshaw fault system to the west of the Great Tonalite Sill and the Great Tonalite Sill shear zone, between Juneau and just south of Petersburg. First order terranes and intrusives: stipple = Gravina belt, diagonal shading = Taku terrane, unshaded = Yukon Tanana terrane (Gehrels et al. 1990), Random shading = Coast Plutonic Complex.

However, these interpretations are based on certain strict assumptions inherent in the paleomagnetic analytical techniques, which are discussed in section 1.8, and if these break down, then more complex movements than simple northward motion may also provide equally satisfactory explanations for the anomalous data.

Modelling (Umhoefer 1987, Umhoefer et al. 1989), using existing palaeomagnetic data bases, suggests that most of SE Alaska, SW Yukon, western British Columbia and NW Washington were originally located more than 2000km south, around the lattitude of Baja California, in the mid Cretaceous. Large dextral movements are inferred to have taken place between 90 and 55 Ma (e.g. Thrupp and Coe, 1986). Irving et al. (1985) recorded paleomagnetic data from mid Cretaceous plutons in British Columbia, which suggested that a composite block (named 'Baja British Columbia' by E. Irving), composed of Wrangellia, the Coast Plutonic Complex, the Cascade Terrane, Stikinia and perhaps Quesnellia, probably underwent northerly displacement of about 2400km and clockwise rotation of 40-70°, between the Late Cretaceous and Early Tertiary, with respect to North America. They also discovered that the present lattitudes of Cordilleran terranes are more dispersed than their apparent paleolattitudes and, on this basis, suggested that the composite 'Baja B.C.' block was fragmented and 'smeared out' during northward transport along the edge of cratonic N. America, during late Cretaceous-Early Tertiary times.

6.5.2 *Anomalous palaeomagnetic data - regional tilt?*

Stratigraphic, geochronological, metamorphic and structural data indicate post-Mid Cretaceous NE-over-SW tilting of extensive areas of the Coast Plutonic Complex and Northern Cascades. This can account for much of the discordance recorded in paleomagnetic poles from the western Cordillera, especially Cretaceous plutons within the Coast Plutonic Complex. It is important to stress that the majority of the data collected form the Coast Plutonic Complex are from plutonic rocks. It is generally held that plutons are the rock formations of last resort with regard to paleomagnetic

sampling (Cox & Hart 1986) because it is rarely possible to determine how much a pluton has been tilted subsequent to emplacement. Nevertheless, one of the assumptions made by paleomagnetic workers when sampling plutons is that present horizontal equals palaeohorizontal. Rarely, it is possible to calculate the palaeohorizontal from e.g. overlapping sediments, but usually it is not possible. Tabor et al. (1982) recorded SW-dipping Eocene sediments overlapping the Mt. Stuart batholith in the Cascades. When this Eocene tilt is restored to horizontal, the anomalous palaeopole returns to concordance with the Cretaceous reference pole. NE-increasing depths of metamorphism, NE-decreasing K-Ar ages and relative uplift of 15km to the NE of the Spuzzum pluton (Bartholemew, 1979), also indicates tilting to the SW. The NE-decreasing $^{40}Ar/^{39}Ar$ dates, which also decrease with higher altitude, in the Holkam Bay area of southeast Alaska (50km SE of Juneau, Wood et al. 1991) suggest that the entire Coast Plutonic Complex underwent rapid uplift and cooling during early Tertiary time. Crawford & Hollister (1982) recorded a metamorphic discontinuity of 3-5kb, at about 700C, across the Work Channel Lineament in British Columbia, which indicates rapid E-side-up movement of the Intermontane Superterrane with respect to the Insular Superterrane during the Eocene. Structural studies indicate the presence in SE Alaska and British Columbia of a long (>800km) and relatively narrow (<30km) high angle reverse shear zone (the Great Tonalite Sill shear zone), with a top-to-the-SW simple shear component, located at the SW edge of the Great Tonalite Sill (Hutton & Ingram 1992, Ingram & Hutton 1992 in prep), which was active from c.90Ma to c.60Ma. Considering the model of Irving et al. (1985), large amounts of dextral strike slip kinematic indicators would be expected within the Great Tonalite Sill belt, which is interpreted here to be a zone of major crustal weakness. However, although the Great Tonalite Sill was emplaced during the same period, it records no major strike slip kinematic indicators. In addition, no significant amounts of clockwise block rotation have been documented by geological field studies over a protracted strike length, to account for the rotation of the anomalous palaeopoles. Considering the assumptions made when acquiring palaeomagnetic

samples, the assumption that palaeohorizontal equals present horizontal (e.g. Cox & Hart 1986, Umhoefer 1987, Umhoefer et al. 1989) totally breaks down within the areas affected by the shear zone. This suggests that paleomagnetic studies of mid Cretaceous to Tertiary plutons, located near or within it, must take into account tilting on an axis parallel to it (striking 320 degrees).

Recently, Butler et al. (1989 & 1991) concluded that much of the anomalous paleomagnetic data recorded in the Coast Plutonic Complex and Northern Cascades (e.g. Irving et al., 1985) did not require large scale northward translation (as suggested by e.g. Beck et al. 1989, Irving et al. 1985, Umhoefer 1987 and Umhoefer et al. 1989), but are more reasonably explained by NE-side-up tilting of the sampled plutons. Considering figure 6.6 one can appreciate the discordance of a representative sample of the palaeopoles, from the 'Baja British Columbia' block, with respect to the Cretaceous reference palaeomagnetic pole. This diagram also illustrates the two end-member mechanisms which would account for this: (1) around 60° clockwise rotation and 18° flattening of the expected palaeopole, or (2) 29° northeast-side-up rotation of the expected palaeopole, about a horizontal axis parallel to the North American margin. Butler et al. (1991) highlight paleomagnetic data from Jurassic volcanic rocks of the Santa Lucia-Orocopia and Baja-Borderland allochthons of coastal California and Baja California, which, after revisions to the Mesozoic apparent polar wander path for North America are taken into account, indicate that their paleolattitudes are concordant. Studies by Ross (1985) and James & Mattinson (1988), which took into account post-25Ma strike-slip offsets, indicated that basement rocks of the coastal allochthons can be correlated with basement rocks directly across the San Andreas and related fault systems, and therefore the large dextral displacements suggested by other workers are unnecessary.

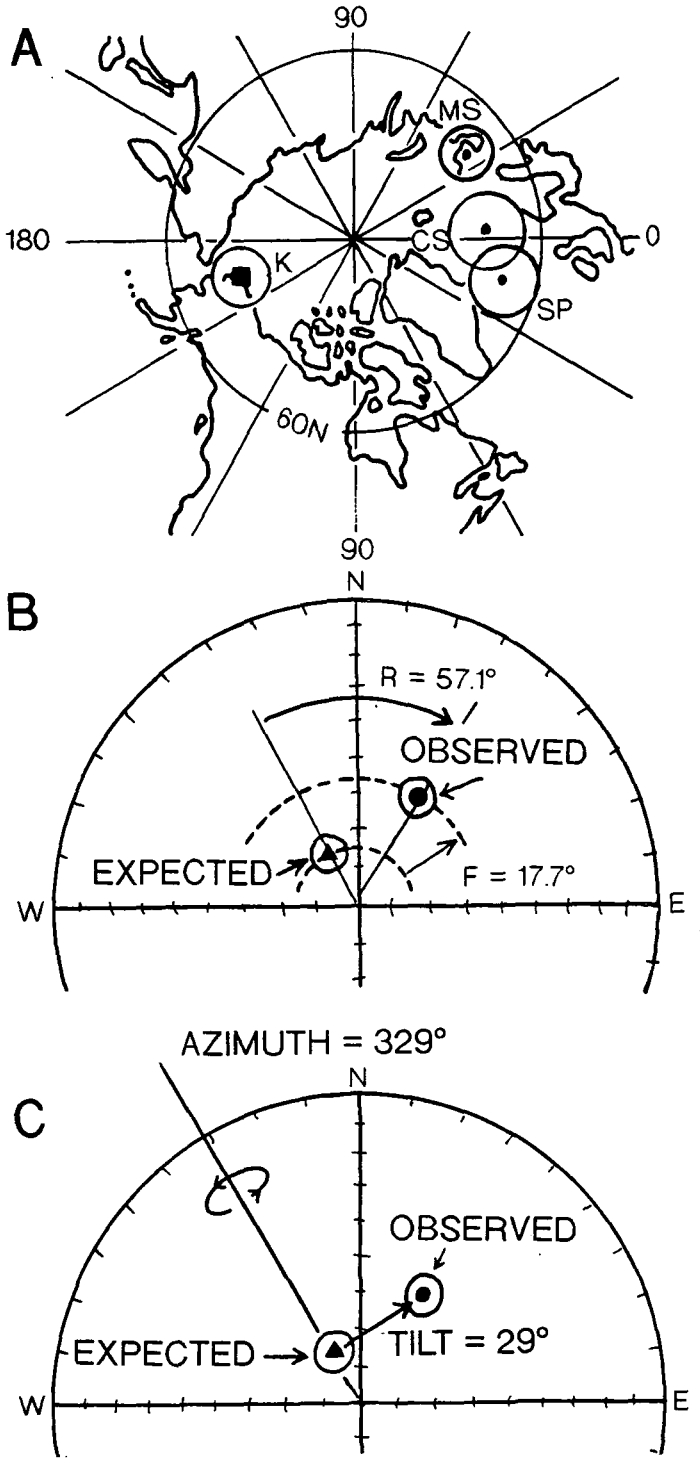

Figure 6.6 **A.** Cretaceous reference pole (K) and discordant poles from Spuzzum and Porteau plutons (SP), Captain Cove and Stephens Island plutons (CS), and Mount Stuart Batholith (MS). **B.** Equal area projection of expected direction of mid Cretaceous magnetic field shown by triangle with surrounding circle of 95% confidence. Observed palaeomagnetic direction from Suzzum and Porteau plutons shown by solid circle with circle of 95% confidence. Observed direction is diverted from expected direction by clockwise rotation (R) about a vertical axis by 57.1° and flattening of inclination (F) by 17.7°. **C.** Observed direction is diverted from expected direction by northeast side up rotation of 29° about horizontal axis with azimuth = 329° (from Butler et al. 1989).

6.5.3 *Palaeobarometric determinations of tilt*

Recently, it has been suggested by Ague & Brandon (1992) that new methods, based on hornblende barometry (Hammarstrom & Zen 1986), may be used to determine the palaeohorizontal in granite batholiths, and therefore to correct palaeomagnetic data for tilting effects. Their studies indicated that the mid Cretaceous plutonic rocks of the Peninsular Ranges Batholith of Coastal southern and Baja California, and the Mount Stuart Batholith of the Cascade Range in northern Washington, have palaeohorizontals that are not equal to present horizontal. However, the tilt corrections implemented by Ague & Brandon (1992) for these batholiths do not account for the anomalous palaeomagnetic inclinations, without significant additional northward migration of the host plutons.

Their results indicated that the Northern Peninsular Ranges batholith has indeed been tilted by significant amounts: 19 ± 5.4° to the west (western part) and 15 ± 3.3° to the west (eastern part) along axes striking 160 ± 5.5° and 161 ± 7.9° respectively (fig. 6.7). The Mount Stuart Batholith yielded results which suggested that it had been tilted by 8 ± 3° to the southwest along an axis striking 055 ± 38.1°. They conclude that the Peninsular Ranges Batholith and the Mount Stuart Batholith originated at the same latitude in mid Cretaceous and were transported northwards by 1000 ± 450 km and 2,900 ± 700 km to their present positions, respectively, with about 300 km of this movement being attributable to Neogene opening of the Gulf of California. Thus Ague and Brandon (1992) advocate both considerable northward migration coupled with significant northeast over southwest tilting, since the mid Cretaceous for both these batholiths.

However, the above results are based on the assumption that the trend of the calculated contours of palaeodepth are parallel to the actual trend of the tilt axis of the plutons. If this is not the case, then tilting may have occurred along an axis with a different strike orientation. Previous work has shown that tilting of the Peninsular Ranges Batholith by 21° along an axis with an azimuth of 320° (Butler et al. 1991), the

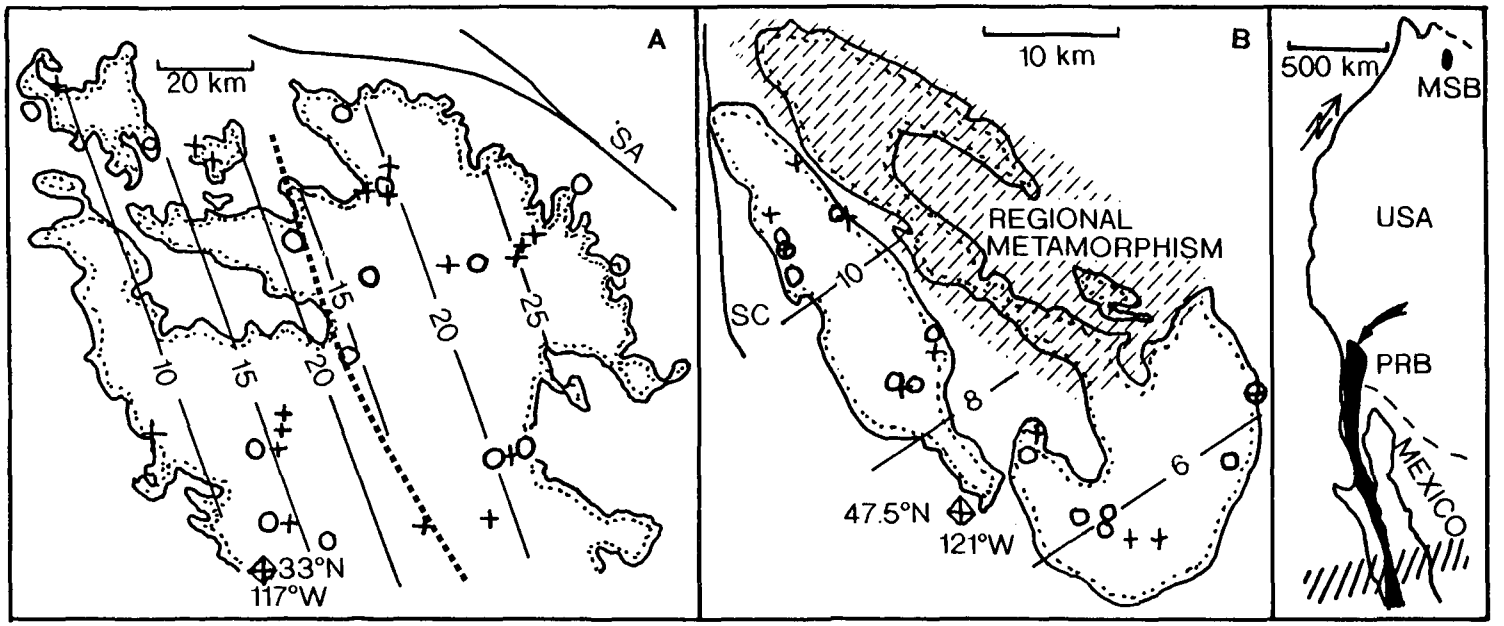

Figure 6.7 Contour maps of height from present sea level to best fit palaeosurface for the Peninsular Ranges and Mount Stuart batholiths (Ague & Brandon 1992). +, o: samples with residual errors (average 1.2 km, maximum 3.74 km) above and below the best fit surface, respectively. **A.** Northern Peninsular Ranges Batholith (PRB) California (see arrow on right). SA = San Andreas Fault System. Dashed line = major fault. **B.** Mount Stuart Batholith (MSB), Washington. SC = Straight Creek Fault. Regional metamorphism masks the NE part. Contoured as in A. Diagonal shading (far right) indicates approximate palaeolatitude for PRB and MSB.

palaeopole direction will rotate into coincidence with the expected mid Cretaceous palaeopole. Further support for the latter argument comes from the structural geology of the area: in the case of the Peninsular Ranges Batholith region, the mean structural trend is approximately 320° and thus it would seem reasonable to elect to choose a tilt axis which is parallel to this trend, in preference to one at an oblique angle (approximately 23° clockwise) to it, such as that provided by the palaeodepth contours. It is difficult to interpret the trend of the Mount Stuart Batholith palaeodepth contours, as the quoted error is so large (55 ± 38.1°).

In conclusion, the studies by Ague & Brandon (1992) do not resolve the tilt versus northward transport controversy, but they provide valuable evidence that east side up tilting of plutons in the Western Cordillera of America has taken place. Thus, the orientation of palaeohorizontal in the plutons of the Peninsular Ranges and Mount Stuart Batholiths cannot be assumed to coincide with present horizontal.

6.6 Field data - northward migration or regional tilt?

Following the above discussion of current models for the evolution of the Western Cordillera, based on results from palaeomagnetic studies, it is now appropriate to compare the models with the geology in the field. The following sections briefly compare and contrast conclusions drawn from present and extant field geological studies with the modelling.

Dextral strike slip. If the anomalous palaeomagnetic data, recorded in the Insular and Intermontane superterranes, do indicate that large dextral (> 2000 km) movements took place in the western Cordillera, then this should be amply reflected by major dextral faults and shear zones affecting rocks in the field. However, although much effort has been expended in search of major dextral shear zones, there has been limited success in this respect. There have been difficulties regarding the

accommodation of large northward displacements, inferred by the dextral strike slip models, along known faults in western North America. Field observations on major faults (e.g. Gabrielse 1984, Price & Carmichael 1986) have only recorded cumulative dextral offsets in excess of approximately 1000km, and this falls well short of the offsets required by the anomalous palaeomagnetic data. The Great Tonalite Sill is therefore of vital importance in this regard, as it was emplaced during the interval of implied rapid dextral terrane movements. The synmagmatic deformation of this body is of considerable interest, since strain was focused into this rheologically weak zone, thus forming structures which recorded the ambient, large scale tectonics. However, the data recorded during this study indicate that there is no significant dextral strike slip movement anywhere along the Great Tonalite Sill, or in its adjacent wall rocks. The author concludes, from this data set, that northward displacements of terranes during northward displacement on this shear zone and superterrane boundary did not occur during late Cretaceous and early Tertiary times. If this structure is in any way representative of the regional picture, severe doubts must exist as to the general concept of large northward movement and dextral shear.

Field evidence supports tilting. Conclusions, derived from voluminous field structural and kinematic data, indicate that the Great Tonalite Sill represents an influential zone, in which significant downbending of the rocks to its NE and upbending of rocks to its SW has occurred. This essentially created a wide area in which effective NE-side-up tilting and concomittant shallowing of the palaeopoles occurred (figure 6.8). It is evident, from the published maps of Umhoefer (1989) and Butler et al. (1989), that the plutons sampled for palaeomagnetic study are in close proximity to the Intermontane/Insular superterrane boundary and, although the area studied for this thesis has not been the subject of a major palaeomagnetic effort, the terranes in question are regarded by all concerned to continue into this area. It is equally likely that the Great Tonalite Sill shear zone continues southeastwards into the area in which most of the palaeomagnetic determinations have been made. Hence, by

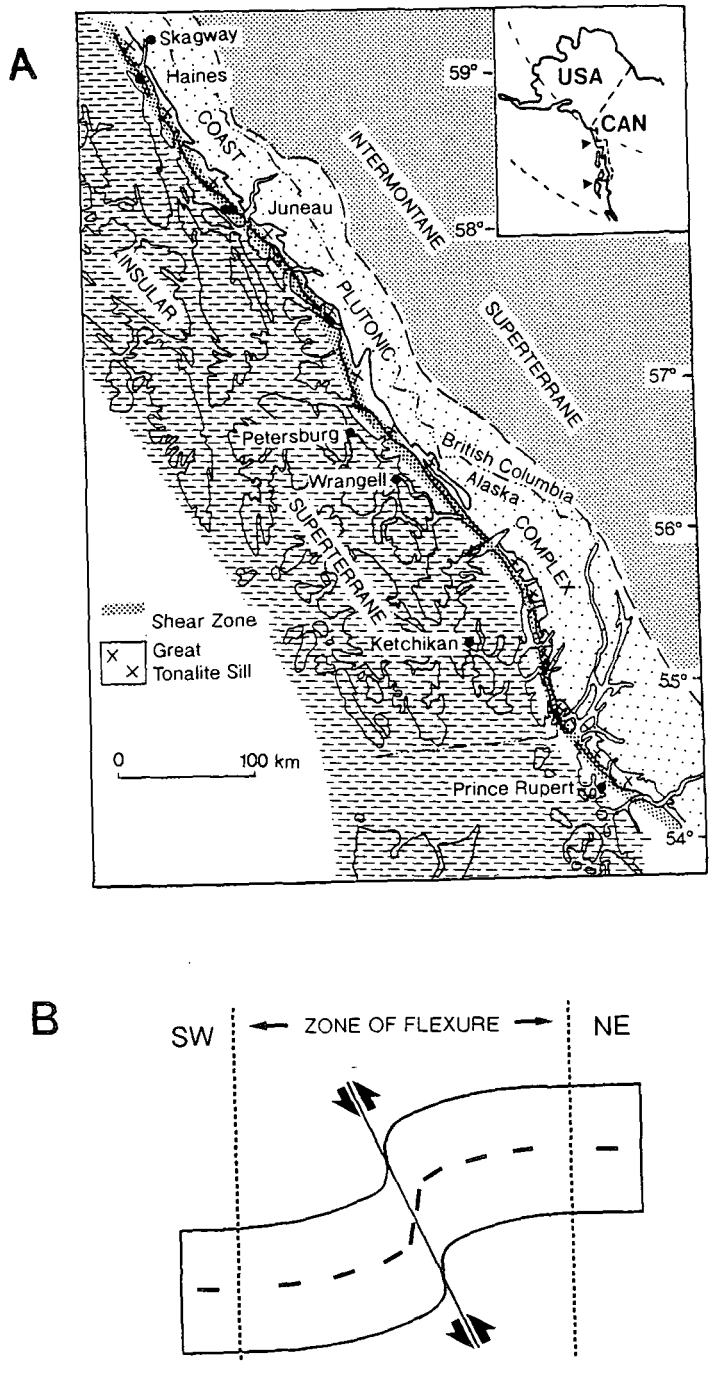

Figure 6.8 **A.** location map of the Great Tonalite Sill and its shear zone. **B.** Cross section running NE-SW across the Great Tonalite Sill shear zone, showing the implied zone of flexure. Thick dashes = palaeohorizontal. IM = Intermontane superterrane, INS = Insular superterrane.

implication, the area in which the palaeomagnetic determinations were made was influenced by the shear zone associated with the Great Tonalite Sill. If true, this immediately rules out the possibility that the palaeohorizontal in the sample localities was equal to the present horizontal: one of the major assuptions built into the palaeomagnetic analytical technique. This implication is strongly supported by evidence for significant westward tilting of the Peninsular Ranges Batholith (Ague & Brandon 1992).

In conclusion, the extant palaeomagnetic data cannot discriminate between large northward translation and westward tilting, without recourse to detailed field structural data. Further, there are additional palaeomagnetic data which independently suggest that westward tilting is a more likely explanation. It therefore seems likely here that NE-over-SW tilting was a more important factor in creating the anomalously shallow palaeopoles, rather than major northward translations.

6.7 Strain and kinematic partitioning

The above sections suggest that the Great Tonalite Sill carries a complete record of all the kinematic indicators associated with dispersion tectonics at the Insular/Intermontane superterrane boundary, for the period during and immedialtely after pluton emplacement. It is now necessary to entertain the possibility that a so far unidentified, kinematic component has been partitioned into another geographically separate zone. This hypothetical zone may lie on the eastern (continental) side, or the western (Pacific) side of the Sill. A short review of current thinking on kinematic and strain partitioning, and further appraisal of the Great Tonalite Sill, is set out below.

Kinematic and strain partitioning. In oblique convergent zones, kinematic partitioning may be temporal, in which case, for example, an early phase of strike slip

may be overprinted by a later phase of orogen-normal compression or partitioning may be spatial and arranged in order to allow simultaneous orogen-parallel and -normal motion, or it may be a combination of both (Holdsworth & Strachan 1991, Strachan et al. 1992). Alsop & Hutton (1992) suggest that although the concept of strain localisation and partitioning gathers support, original lithological variability may have an influence on the localisation of deformational processes and geometries in the mid crust.

The Great Tonalite Sill. In the case of southeast Alaska, the juxtaposition of two superterranes and the subsequent intrusion of large amounts of rheologically weak tonalitic melt, at or near their actively deforming boundary, has probably been responsible for the partitioning of high contractional strains into the Great Tonalite Sill and its associated shear zone. According to Engebretson et al. (1985), the boundary between the Kula and North American plates was dominated by highly oblique dextral transpression, during the emplacement and crystallization interval. According to foliation and transport lineation data from Haines to Prince Rupert (fig. 6.9) the Great Tonalite Sill, its shear zone and adjacent rocks to the E and W record only orogen-normal contraction. It is possible that a dextral component was taken up along another, spatially removed, zone, but such a zone has not yet been described or linked with the Great Tonalite Sill and the Great Tonalite Sill shear zone. Possibilities include the Tintina fault and Rocky Mountain Trench, which lies at least 350km to the E, but spatial partitioning of strike slip and orogen-normal contraction has not previously been documented over such a wide zone. In addition it is possible that strike slip movements have been accommodated along faults outboard of the present North American margin, but again, serious possibilities in this area have not been thoroughly documented, although the USGS has carried out reconnaissance scale field studies within this area for at least fifteen years (D.A. Brew, pers comm.). It is concluded here that, although there is a distinct possibility for partitioning strike slip movement into

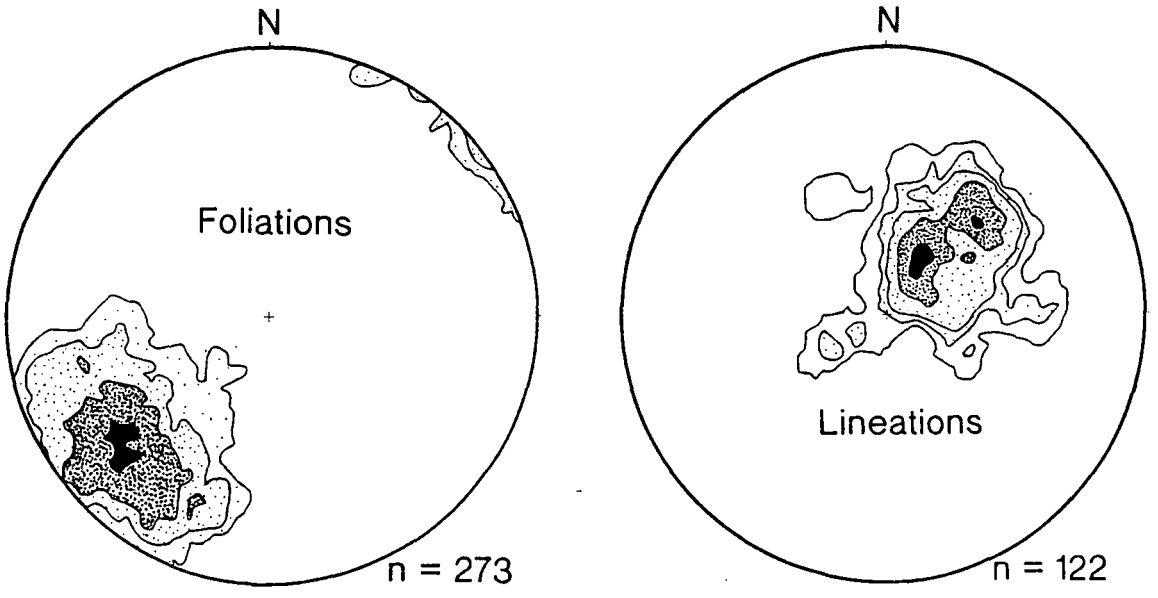

Figure 6.9 Total foliation and lineation data from Haines (Alaska) to the Skeena River (B.C.). Contour intervals = 1.5, 3, 5, 9.5, 14 percent.

other areas, it is unlikely that this would take place while an uncrystallized, rheologically weak, Great Tonalite Sill was in existence.

6.8 Summary

This chapter illustrates the importance of applying the results of field geological observations to extant and generally accepted models, for large scale tectonics and plate movements based largely on remote sensing techniques and laboratory work. Obviously, if a tectonic model is good, the rock structures seen in the field will amply reflect this. In the case in point, field data are in opposition to plate tectonic models based on apparently facile interpretations of anomalous palaeomagnetic data advocating large scale northward transport. They tend to support a more "fixist" mechanism, invoking orthogonal collisions/tectonics and coeval tilting of the palaeohorizontal downwards towards the west, which equally accounts for the anomalous palaeomagnetic patterns.

The following points reiterate the salient conclusions and implications from previous work and the work of the author:

(1) ***Plate modelling.*** Cretaceous plate modelling, based on stage poles of rotation, invokes dextral oblique subduction of the Kula plate under the North American plate. However, Palaeocene to mid Eocene magnetic anomaly interpretations invoke orthogonal subduction, until 55 Ma.

(2) ***Great Tonalite Sill - kinematic record.*** It records NE-SW directed pure (flattening) shear with coeval NE over SW reverse simple shear, at the Insular/Intermontane superterrane boundary, from 83 to 55 Ma.

(3) ***Great Tonalite Sill - terrane boundary.*** It is likely to be associated with a crustal scale shear zone and lies between the Insular and Intermontane superterranes. It is the dominant feature at this boundary and therefore *represents* the boundary.

(4) ***Palaeomagnetic data.*** Anomalous palaeomagnetic data indicates either: in excess of 2000 km northward movement of terranes with clockwise rotations, or NE over SW tilt of the sampled plutons over a wide area. Field geology supports the tilt hypothesis.

(5) ***The Great Tonalite Sill - Kinematic/strain partitioning.*** In the absence of any other detailed information, the Great Tonalite Sill appears to record the actual relative movements between the Intermontane and Insular supeterranes, and hence the Kula/North America relative movements, during late Cretaceous and early Tertiary. There is no data to support the idea of kinematic partitioning during this period.

CHAPTER 7
CONCLUSIONS

The Great Tonalite Sill of southeast Alaska and British Columbia is a syntectonic batholith (Brew & Ford, 1981) and detailed structural studies indicate that it was emplaced into an active compressional shear zone, during prograde regional metamorphism (Hutton & Ingram, 1992). The plutons making up the Great Tonalite Sill were emplaced at depths corresponding to pressures of about 5 to 7 kb (Hollister 1982, Crawford & Hollister 1982, Hollister et al. 1987, Stowell 1989, McClelland et al. 1991, Wood et al. 1991, Davidson et al 1992) dominantly by sheeting and diking mechanisms. Available U-Pb geochronology of the Great Tonalite Sill and western Coast Plutonic Complex suggests that the plutons were emplaced between around 81 Ma to around 57 Ma (Wooden, J.L., written comm. to Brew 1990, Gehrels et al. 1991). The intruding magma sheets overcame the compressional plate tectonic stresses by wedging apart their wall rocks whilst propogating along rheologically weak shear zones. In addition, emplacement took place in zones of net dilation, such as thrust flats or releasing bends. The plutons inherit a composite structure due to the periodic sheeting process, and therefore a range of crystallization dates should be expected within a single composite pluton.

The Great Tonalite Sill and its associated shear zone represent a lineament along which high contractional strains, associated with the collision of the Intermontane and Insular superterranes, were partitioned. The shear zone is dominated by NE-SW-directed pure shear, but there is also a component of NE-side-up reverse shear. The Great Tonalite Sill did not record any significant strike-slip kinematic indicators during its emplacement into the orogen-parallel shear zone and magmatic-state structures (e.g. PFC fabrics, lineations and lock-up shears; tiling fabrics) indicate

that the maximum compressive stress acting upon it was directed orthogonally. The present horizontal is not equivalent to palaeohorizontal within the areas affected by the Great Tonalite Sill shear zone, as it essentially represents a zone of flexure which tilted palaeohorizontal downwards towards the SW, affecting both the hangingwall and footwall rocks. The paleomagnetic inclinations would be shallowed by such a zone and biased towards apparently low paleolattitudes.

It is highly likely that the Great Tonalite Sill represents a terrane boundary: a major crustal discontinuity which decoupled at a basic level the Intermontane superterrane from the Insular superterrane. It is concluded, from the deformation and geochronological data, that its emplacement was associated with a major orthogonally-convergent event, during late Cretaceous to early Tertiary times. This kinematic model is in opposition to those based on paleomagnetic data, which envisage large (up to 2400km) dextral movements taking place between c.90 Ma and c.57 Ma (e.g. Irving et al. 1985, Umhoefer 1987, Umhoefer et al. 1989 and Thrupp & Coe 1986). It corroborates the model of Lonsdale (1988), which indicates that the Kula plate, between its birth (initiation) at 85 Ma and death (subduction) at 55 Ma, was subducted orthogonally beneath the North American plate.

The following sections will now expand on this general summary, detailing specific conclusions from relevant chapters, and finally detailing a genetic model for the Great Tonalite Sill:

7.1 Main conclusions from chapter 3

7.1.1 *The Shear Zone*

The Great Tonalite Sill plutons are concordant to a steeply NE-inclined regional shear zone, here called the Great Tonalite Shear zone. This shear zone has magmatic and high temperature ductile deformation associated with it and was active

during emplacement of the Sill. Its length is in excess of 750 km and its width is, at most, 20 km.

The shear zone fabrics, both magmatic/PFC and solid state/CPS, define a remarkably consistent, NE dipping regional D_2 fabric, associated with an equally consistent down dip (nearly 90° pitch) stretching lineation. Whilst variations in lineation plunge do occur in some sections, which may show SE or NW pitches and implied sinistral or dextral components, these appear to have no overall tectonic significance, as no correlation exists between such areas and large scale, low angle deflections in the trace of the Sill. Shear sense associated with the magmatic and high temperature ductile deformation is consistently top-to-the-SW.

In terms of overall strain, both magmatic/PFC and and solid state/CPS fabrics are dominantly flattening ($0<K<1$). This essentially suggests a pure shear flattening with *Z* orientated subhorizontally NE-SW. However, a component of simple shear dominates at the SW edge of the Sill, with *X* plunging steeply NE, associated with NE over SW movement. Northeast of this, the flattening strain component dominates and its magnitude gradually decreases northeastwards.

Quantitative strain studies in Taku Inlet indicate that if strain is removed from the deformed plutons, they would not extend to more than five times their present widths.

7.1.2 *Shear sense.*

Shear sense associated with the homogenous magmatic and high temperature deformation in the Great Tonalite Sill shear zone, which was incurred during the emplacement and crystallization of the Sill magmas, is consistently top-to-the-SW. Other workers (Gehrels & McClelland 1988, Crawford et al. 1989, McClelland et al. 1992) have recorded east-side-down indicators in areas correlated with this shear zone, such as the Coast Shear Zone, and hence it is concluded here that these indicators do not strictly belong to the Great Tonalite Sill shear zone as descibed by the author. It is

likely that these latter shear sense indicators were related to later, down-temperature overprinting events, after full crystallization of the Great Tonalite Sill.

Shear sense is also exhibited by discrete shears and these often form conjugate arrays. The early PFC lock-up shears define a basic conjugate pattern, which amply demonstrate that NE-SW directed shortening and pure shear strains were incurred before the Great Tonalite Sill was fully crystallized. Ductile discrete shear arrays follow the basic PFC pattern and define quadrimodal sets, which indicate NE-SW directed pure shear (flattening) strains. These shears developed throughout the crystallization interval and form a progression, from early melt-filled shears, through to later ductile or brittle-ductile types. The latter are most prominently developed as flat or gently NE inclined shears, with consistent top-to-the-SW shear sense.

7.1.3 *The plutons*

Petrography. The plutons have heterogenous compositions, but a medium to coarse grained hornblende-bioitie tonalite is dominant, with garnet and sphene commonly occurring as accessory phases. Granodiorites, medium grained diorites, plentiful synplutonic dykes and microdioritic enclaves are also found. Early, coarse grained appinitic rocks, found near pluton contacts, are though to represent the precursors of the main tonalitic intrusions. Small amounts of dense, dark green, retrogressed ultramafic rocks also occur as xenoliths, and these are interpreted here as mantle derived material, brought up by the tonalites during emplacement.

Pluton structure. The Great Tonalite Sill batholith is composed of many individual elongate tonalitic plutons, whose contacts are concordant to the steeply NE dipping regional foliation. Individual plutons have deformed widths which vary from 300 m to 8 km or more, and the width of the Sill as a whole varies from around 2 km to around 20-25 km. Sheets making up the plutons have widths ranging from <1 metre to >100 metres and are most easily recognised at pluton contacts, separated by country

rock screens. Internally, the plutons are heterogenous: screens of country rock, zones of high strain, internal contacts, zone abundant in mafic enclaves and petrographic variations are dominant features. Spectacularly well developed sheeting was observed in one well exposed pluton, which indicates that sheet wedging mechanisms, similar to those implied in sheeted dyke complexes, may have been important in pluton construction. Overall, there is abundant evidence in all the plutons and their country rocks which supports a strong genetic relationship between active shears and the concentration of magma. This relationship is evident from centimetre scale to plate tectonic scale in the Great Tonalite Sill belt.

The author concludes that the c.450 km long section of the 2-20 km wide Great Tonalite Sill, between Juneau and Walker cove near Ketchikan, was intruded along the axis of a ductile shear zone (Great Tonalite Sill shear zone) of similar dimensions. The shear zone is dominated by flattening strains, with Z orientated subhorizontally NE-SW and X plunging steely NE. There is also a simple shear component concentrated at the SW edge of the Sill which indicates NE over SW movement. Contemporaneity of Great Tonalite Sill emplacement and deformation indicates that this regime was active between 83 and 55 Ma (Late Cretaceous to early Tertiary, Gehrels et al. 1991a).

7.2 Main conclusions from chapter 4

The Great Tonalite Sill rocks experienced progressive retrograde deformation during their complete crystallization and subsequent cooling interval. Magmatic/PFC fabrics represent the initial deformation at high temperatures (above the tonalite solidus), and the latest deformation is in the form of lower grade, coplanar, brittle-

ductile fabrics. The range in fabric types between these two end-members have been viewed in the Sill rocks during this study.

Strain intensity. The most intense CPS fabrics are commonly located at pluton contacts, and are best developed in the oldest intrusives, as these have been exposed to deformation for the longest periods. Later rocks, emplaced during the waning stages of shear zone movement, preserved PFC deformational structures to a much greater degree. Thus, rocks emplaced during the intervening period will record varying degrees of overprinting and development of CPS fabrics at the expense of early PFC fabrics.

Rheological Transitions. At two points during this deformation sequence, two major rheological transitions took place, which have been recorded and characterised by certain fabrics and structures. In basic terms, these represent the rheological transitions from magma to high temperature solid (the granitoid solidus), and high temperature solid to low temperature solid: the (1) PFC/CPS and the (2) brittle-ductile transitions respectively. The following points summarise a typical retrograde sequence of fabrics, structures, textures and implied deformation mechanisms, for the Great Tonalite Sill as a whole:

(1) ***Pre-full crystallization (PFC) fabrics.*** PFC fabrics develop in the crystallizing magma and involve the rotation and alignment of early formed, non-equidimensional, crystal laths, which are suspended in an uncrystallized matrix, in response to external stresses. These fabrics continue to develop during deformation, if the melt content remains above the Rheological Critical Melt Percentage (RCMP, 30-35% melt).

(2) ***PFC lock-up: the PFC/CPS transition.*** When the melt percentage drops to the RCMP during crystallization, the bulk strength of the magma increases dramatically (see chapter 1) and induces the partitioning of strain into discrete "lock-up shears",

which mark the transition between homogenous PFC/magmatic state deformation and heterogenous PFC deformation. They represent the precursor to high temperature CPS/solid state textures and structures, which develop after most of the remaining melt has crystallized. The grain size and dimensions of the crystals may also have an important effect upon bulk strength..

(3) ***High temperature crystal plastic strain (CPS) fabrics.*** These develop after the melt content has dropped significantly below the RCMP. However, only after full crystallization of all the remaining melt do *all* the phases record CPS deformation. Early fabrics involve weak modification of PFC fabrics at high temperatures, but later fabrics involve (chiefly): dynamic recrystallization and dissolution of feldspar (Tullis & Yund 1985), formation of quartz ribbons, bending and kinking in biotite, elongation of amphibole and overall grain size reduction. In extreme cases, intense CPS deformation results in the formation of high temperature (> 500-550°C) mylonites.

(4) ***The brittle-ductile transition.*** Brittle-ductile fabrics occur at or below 500-550°C and involve brittle behaviour in plagioclase, bending/kinking of biotite and ductile behaviour in quartz (Simpson 1985). In the Great Tonalite Sill these features are developed most convincingly in late, brittle-ductile discrete shears seen throughout the Sill, and the late brittle-ductile orthomylonites (wise et al. 1984), which are coplanar to the regional foliation, located closest to the SW edge of the Sill.

7.3 Main conclusions from chapter 5

7.3.1 *The Intrusives*

The Great Tonalite Sill rocks are calc-alkaline (Brew 1988) and were sourced form mantle-derived rocks and partially melted ancient crustal rocks (Arth et al. 1988, Samson 1991a). Evidence for these components comes from three main areas:

(1) Significant quantities of mafic and ultramafic rocks occur in the tonalitic plutons e.g. appinites, cogenetic mafic enclaves and synplutonic dykes, and these are likely to have mantle signatures. They also indicate the coexistence of mafic and granitoid magma: indeed, the cogenetic mafic enclaves/synplutonic dykes, in particular, imply the synplutonic injection of mafic magma into a granitoid magma.

(2) Negative ε_{Nd} values indicate that the Great Tonalite Sill intrusives contain a component of older, more evolved silicic crustal rock, in addition to the mantle component (Samson et al. 1991a).

(3) In addition to (2), the Sill rocks have higher $^{87}Sr/^{86}Sr$ initial ratio (SIR) values than their surrounding terranes and M.O.R.B., again indicating that older continental crust was involved (Arth et al. 1988, Samson et al 1991a).

Although the SIRs for the Coast Plutonic Complex as a whole indicate that the plutons represent the roots of a magmatic arc, the Great Tonalite Sill signature plots outside this field (Arth et al. 1988). This, along with the remarkable focused linearity of the plutonic belt, indicates that the Great Tonalite Sill does not represent the roots of an island arc. Instead, it delineates a deformation zone.

7.3.2 *Petrogenesis*

(1) ***The general model.*** Transpressional shear zones cause crustal thickening, which in turn causes the formation of a mantle lithosphere topography (Hutton & Reavy 1992). When this thickened lithospheric root develops to a critical point, it may be convectively removed and replaced by hotter asthenospheric material, which exposes the base of the crust to elevated mantle temperatures (Houseman et al. 1981). This induces the anatexis of lower crustal material which then mixes and mingles with mantle melts, producing granitoid magma with a substantial mantle component (Hutton & Reavy 1992).

(2) ***The specific model.*** Crustal thickening has occurred extensively in the NW Cordillera, associated with the mid Cretaceous to Palaeocene collision interval, and suggests strongly that formation of a lithospheric root in response to this was likely. The Great Tonalite Sill is associated with an intensely focused late Cretaceous to Palaeocene crustal scale shear zone, with a pure shear ($K \cong 0$) orogen normal component and a simple shear ($K \cong 1$) component of strain. This shear zone (the Great Tonalite Sill shear zone) probably reached the base of the crust and caused focused crustal thickening along 800 km or more. Thus a perturbation or corrugation was produced at the base of the crust, which was preferentially melted after removal of the lithospheric root, and the subsequent melts migrated along the adjacent shear zone, forming the Great Tonalite Sill.

7.3.3 *Ascent of the magmas*

The Great Tonalite Sill shear zone must have transported the mantle-derived melts rapidy through the crust, along the shear zone, in order ro prevent excessive solidification in the conduit and contamination with juvenile crust.

Diapirs. It has been concluded that diapiric ascent is a slow process (Marsh 1982), thus facilitating significant interaction of magma with continental crustal rocks and much solidification after relatively little movement. This is not a plausible ascent mechanism for the Sill magmas.

Dykes. Ascent by dyking is a rapid process and magmas may be transported through the crust and lithosphere without extensive solidification and contamination (Lister & Kerr 1991). Dykes propagate due to extremely high localised tensile stresses at their tips and are difficult to arrest unless the upward buoyancy force is exceeded by the frictional drag. They exploit anisotropies in rocks, such as zones weakened by shearing, and theoretical modelling indicates that, once formed, they are impossible to close again. The width of dykes and the velocity of transport are determined by the viscosity of the magma: low viscosity = rapid propagation and narrow dykes. The present outcrop represents both the ascent and emplacement level. Component sheets exposed within the plutons have widths (<1 to >50 metres) which imply that the effective viscosity of tonalitic magmas must be significantly lower than those previously published for true granites.

7.3.4 *Emplacement*

The Great Tonalite Sill magmas ascended and were emplaced dominantly as non-Andersonian dykes/sheets. Emplacement of the sheets took place along a compressional shear zone axis, implying that space does not need to be created to accomodate granitoids. At deep levels the sheets propagated along shear zone weaknesses and, at higher levels, in dilational pull aparts (dilational flats) within ramp-flat shear zone geometries. The higher level emplacement mechanisms may, in part, be related to closer interaction of the shear zones with the free surface.

7.4 Main conclusions from chapter 6

7.4.1 *Plate modelling*

Mid Cretaceous (120-90 Ma) plate modelling, based on stage poles of rotation, indicates that plates were directed largely orthogonally with respect to the North American margin, although dextral oblique subduction of the Farallon plate is proposed around 90 Ma (Debiche et al. 1987, Engebretson et al. 1985), and hence northward transport of terranes. Another model, this time based on the mapping of magnetic anomalies, invokes dominantly orthogonal relative motion of the Kula plate relative to the North American plate, from around 85 Ma (birth of Kula) to around 55 Ma, after which increasingly oblique convergence of the Kula and North American plates took place. Thus Lonsdale (1988) indicated that the northward transport of terranes took place post-55 Ma.

7.4.2 *The Great Tonalite Sill as a kinematic record*

The Great Tonalite Sill is a crustal scale shear zone with plate tectonic dimensions (800 × 20 km), and it provides us with a record of the relative motions between the Insular and Intermontane superterranes. Thus, it provides information about the relative motions which took place between the Kula and North American plates.

The PFC structures and coplanar overprinting CPS structures exhibited by the plutons, indicate that a regime of NE-SW directed pure shear was active during the late Cretaceous to early Tertiary (83 to 55 Ma) crystallization interval. No transcurrent shear was recorded during the same period. Thus the Great Tonalite Sill data supports the model of Lonsdale (1988), which advocates orthogonal subduction of the Kula plate under the North American plate margin.

7.4.3 *The Great Tonalite Sill - a terrane boundary*

The Great Tonalite Sill is associated with the only plate tectonic scale, magmatic and ductile shear zone in the Coast Mountains. It lies between the Intermontane and Insular superterranes and marks a major, NE-dipping, metamorphic discontinuity across which high grade rocks, to the NE, were uplifted relative to lower grade rocks, to the SW. This shear zone sources mantle melts, implying that it must have traversed the entire crust in order to do so. Although another shear zone (Sumdum-Fanshaw fault sysytem) exists a short distance outboard of the Great Tonalite Sill, it is concluded here that the Great Tonalite Sill shear zone is dominant and represents the superterrane boundary.

7.4.4 *Palaeomagnetic data*

Anomalously shallow Cretaceous palaeomagnetic inclinations from SE Alaska, British Columbia and Washington may be explained by either: (1) northward movements of terranes in excess of 2000 km, with clockwise rotations, or (2) systematic NE over SW tilting of the sampled plutons.

The extant palaeomagnetic data cannot distinguish between these models due to uncertainties concerning the attitude of palaeohorizontal in the sample localities. Field geological data have not revealed the existence of major zones of dextral shear invoked by (1) above. On the contrary, kinematic data from the Great Tonalite Sill show consisitent orogen normal, NE over SW reverse shear, which caused more widespread flexure of the palaeohorizontal down towards the SW, both in its hangingwall, to the NE and it footwall, to the SW. Thus field evidence supports the tilt hypothesis. In support, recent barometric determinations (Ague & Brandon 1992) indicate that tilting of the Peninsular Ranges and Mount Stuart batholiths *has* occurred and thus their palaeohorizontals do not coincide with the present horizontal.

7.4.5 *Kinematic/strain partitioning*

It is possible that a strike slip kinematic component, linked to the Great Tonalite Sill shear zone, exists and has not been identified. However, it is unlikely that such zones would have been initiated whilst an uncrystallized Great Tonalite Sill was in existence. Thus the PFC structures and kinematic indicators in the plutons reflect the actual relative plate movement which took place between 83 and 55 Ma (late Cretaceous to early Tertiary). In opposition to extant oblique subduction models, these structures invoke orthogonal subduction of Kula under the North American plate.

7.4.6 *The Great Tonalite Sill - the plate tectonic model*

The Great Tonalite Sill contributes data which the author believes (also Ingram & Hutton 1992, in prep.) brings together existing work into a single, elegant model which explains salient features of this orogenic belt, between the late Cretaceous and early Tertiary. This model contains the following points:

(1) The Great Tonalite Sill marks the Insular/Intermontane superterrane boundary and, as such, its structures record the actual movement along this boundary, hence reflecting the Kula/NorthAmerica motion.

(2) Between 85 and 55 Ma, the relative motion of the subducting Kula plate to the North American plate was orthogonal (Lonsdale 1988). This is substantiated by the deformed Great Tonalite Sill plutons, whose emplacement initiated around 83 Ma and ceased between 57 and 55 Ma. These dates for the Sill tie in closely with the birth (initiation) and death (subduction) of the Kula plate. Therefore there is a genetic relationship between changes in plate movement and episodes of magmatism (Engebretson et al. 1984, Lonsdale 1988).

(3) The anomalous Cretaceous palaeomagnetic data seen in the Intermontane and Insular superterranes, has been caused by systematic flexure of the crust either side of

the Great Tonalite Sill shear zone, which tilted palaeohorizontal downwards towards the SW. Dextral strike slip models were based on misinterpretations of data from the period in question.

(4) Dextral strike slip began at 55 Ma, after the final phase of Great Tonalite Sill emplacement, and coincides with the birth of the Aleutian trench (Engebretson et al. 1984). At this time, movement on brittle dextral faults was initiated, causing dispersion of terranes in the region of 1000 km. Movement was accomodated along faults such as the Northern Rocky Mountain Trench, the Denali Fault and the Coast Range Megalineament (Gabrielse 1985, Goldfarb 1991).

REFERENCES

Ague, J.J. & Brandon, M.T., (1992) Tilt and northward offset of Cordilleran batholiths resolved using igneous barometry: Nature, v. 360, p. 146-149.

Alsop, G.I. & Hutton, D.H.W., 1992, Major southeast-directed Caledonian thrusting and folding in the Dalradian rocks of mid-Ulster: implications for Caledonian tectonics and mid-crustal shear zones. Geological Magazine (in press).

Anderson, E.M., (1951) *The dynamics of faulting*. Edinburgh: Oliver & Boyd.

Arth, J.G., Zen, E-an, Sellers, G. & Hammarstrom, J., (1986) High initial Sr isotopic ratios and evidence for magma mixing in the Pioneer batholith of southwest Montana. Journal of Geology, v. 94, p. 419-430.

Arth, J.G., Barker, F. & Stern, T.W., (1988) Coast batholith and Taku plutons near Ketchikan Alaska: petrography, geochronology, geochemistry, and isotopic character. American Journal of Science, v. 288-A, p. 461-489.

Arzi, A.A., (1978) Critical phenomena in the rheology of partially melted rocks. Tectonophysics, v. 44, p. 173-184.

Balk, R., (1937) Structural behaviour of igneous rocks: Memoir of the Geological Society of America 3, 177 pp.

Barbarin, B. & Didier, J., (1992) Genesis and evolution of mafic microgranular enclaves through various types of interaction between coexisting felsic and mafic magmas, *in* Proceedings, Second Hutton Symposium on the Origin of Granites and Related Rocks, September 1991: Transactions of the Royal Society of Edinburgh: Earth Sciences, V 83, p. 145-153.

Barker, F. & Arth, J.G., (1984) Preliminary results, Central Gneiss Complex of the Coast Range batholith, southeastern Alaska: the roots of a high-K, calc-alkaline arc?: Physics of the Earth and Planetary Interiors, v. 35, p. 191-198.

Barker, F., Arth, J.G. & Stern, T.W., (1986) Evolution of the Coast batholith along the Skagway traverse, Alaska and British Columbia: American Mineralogist, v71, p632-643.

Bartholemew, P.R., (1979) Geology and metamorphism of the Yale Creek area, B. C. [M.S. thesis]: Vancouver, University of British Columbia, 105p.

Bateman, R., (1984) On the role of diapirism in the segragation, ascent and final emplacement of granitoids: Teconophysics, v. 110, p. 210-31.

Beck, M.E., (1991) Case for northward transport of Baja and coastal southern California: Paleomagnetic data, analysis, and alternatives: Geology, v. 19, p. 506-509.

Beck, M.E. Jr., Burmeister, R,F. & Schoonover, R., (1981) Palaeomagnetism and tectonics of the Cretaceous Mt. Stuart batholith of Washington: translation or tilt? Earth and Planetary Science Letters, v56 p. 336-342.

Behrmann, J.H. & Platt, J.P., (1982) Sense of nappe emplacement from quartz C-axis fabrics: an example from the Betic Cordilleras (Spain): Earth and Planetary Science Letters, v. 59, p. 208-215.

Berg, H.C., Jones, D.L. & Richter, D.H., (1972) Gravina-Nutzotin belt - Tectonic significance of an upper Mesozoic sedimentary and volcanic sequence in southern and southeastern Alaska: U.S. Geological Survey Professional Paper 800-D, p. 1-24.

Berger, A.R. & Pitcher, W.S., (1970) Structures in Granitic Rocks: A commentary and critique on granite tectonics: Proceedings of the Geological Association, v81, p.441-461.

Berthé, D., Choukroune, P. & Jegouzo, P., (1979) Orthogneiss, mylonite and non-coaxial deformation of granites: the example of the South Armorican Shear Zone: Journal of Structural Geology, v. 1, p. 31-42.

Blumenfeld, P. & Bouchez, J.L., (1988) Shear criteria in granite and migmatite deformed in the magmatic and solid states: Journal of Structural Geology, v. 1, p. 31-42.

Bohlen, S.R. & Liotta, J.J., (1986) A barometer for garnet amphibolites and garnet granulites: Journal of Petrology, v. 27, p. 1025-1056.

Bohlen, S.R., Wall, V.J. & Boettcher, A.L., (1983) Experimental investigations and geological applicationsof equilibria in the system FeO-TiO_2-Al_2O_3-SiO_2-H_2O: American Mineralogist, v. 86, p. 1049-1058.

Bottinga, Y. & Weill, D.F., (1972) The viscosity of magmatic silicate liquids: a model for calculation: American Journal of Science, v272, p.438-475.

Brew, D.A., (1988) Late Mesozoic and Cenozoic igneous rocks of southeastern Alaska - A synopsis: U.S. Geological Survey Open File Report, 88-405, 29 pp.

Brew, D.A. & Ford, A.B., (1977), Preliminary geologic and metamorphic-isograd map of the Juneau B-1 quadrangle, Alaska: U.S. Geological Survey Miscellaneous Field Studies Map MF-846, scale 1:25,000, 1 sheet.

Brew, D.A. & Ford, A.B., (1978) Megalineament in southeastern Alaska marks southwest edge of Coast Range batholithic complex: Canadian Journal of Earth Sciences, v15, no.11, p1763-1772.

Brew, D.A. & Ford, A.B., (1981) The Coast plutonic complex sill, southeastern Alaska. In: *The U.S. Geological Survey in Alaska: Accomplishments During 1980* (eds: Albert, N.R.D. & Hudson, T.L.), U.S. Geological Survey Circular 823-B, p. 96-99.

Brew, D.A. & Ford, A.B., (1983) Comment on 'Tectonic accretion and the origin of the two major metamorphic and plutonic welts in the Canadian Cordillera': Geology, v11, p. 427-428.

Brew, D.A. & Ford, A.B., (1984) Tectonostratigraphic terranes in the Coast plutonic-metamorphic complex, southeastern Alaska. In: *The United States Geological Survey in Alaska: Accomplishments during 1982* (eds: Reed, K.M. & Bartsch-Winkler, Susan): U.S. Geological Survey Circular, 939, p. 90-93.

Brew, D.A. & Morrell, R.P., (1980) Intrusive rocks and plutonic belts of southeastern Alaska, U.S.A.: U.S. Geological Survey Open-File Report 80-78.

Brew, D.A. & Morrell, R.P., (1983) Intrusive rocks and plutonic belts of southeastern Alaska, U.S.A.: In: Roddick, J.A. (ed.) Circum-Pacific plutonic terranes. Geological Society of America, Memoir 159, p. 171-193.

Brew, D.A., Ford, A.B. & Himmelberg, G.R., (1989) Evolution of the western part of the Coast plutonic-metamorphic complex, south-eastern Alaska, USA: A summary: In: Evolution of Metamorphic Belts (eds: Daly, J.S., Cliff, R.A. & Yardley, B.W.D., 1989) Geological Society Special Publication No. 43, pp. 447-452.

Brew, D.A., Himmelberg, G.R., Loney, R.A. & Ford, A.B. (1992) Distribution and characteristics of metamorphic belts in the south-eastern Alaska part of the North American Cordillera: Journal of Metamorphic Geology, v. 10, p. 465-482.

Brun, J.P., Gapais, D., Cogne, J.P., Ledru, P. & Vigneresse, J.L., (1990) The Flamanville Granite (Northwest France): an unequivocal example of a syntectonically expanding pluton. Geological Journal, v. 25, p. 271-286.

Buddington, A.F., (1959) Granite emplacement with special reference to North America: Geological Society of America, Bulletin, v70, p.671-747.

Butler, R.F., Gehrels, G.E., McClelland, W.C., May, S.R. & Klepacki, D. (1989) Discordant paleomagnetic poles from the Canadian Coast Plutonic Complex: Regional tilt rather than large-scale displacement?: Geology v17, p. 691-694.

Butler, R.F., Dickinson, W.R. & Gehrels, G.E., (1991) Palaeomagnetism of coastal California and Baja California: alternatives to large-scale northward transport: Tectonics, v10, no.3, p.561-576.

Cas, R.A.F. & Wright, J.V., (1987) Volcanic successions modern and ancient: a geological approach to processes products and successions: Allen & Unwin, London, 528pp.

Castro, A., (1985) The Central Extremadura Batholith: Geotectonic implications (European Hercynian Belt) - An outline: Tectonophysics, v. 120, p. 57-68.

Castro, A., (1986) Structural patterns and ascent model in the Central Extremadura Batholith, Hercynian Belt, Spain: Journal of Structural Geology, v. 8, p. 633-645.

Chappell, B.W. & White, A.J.R., (1974) Two contrasting granite types: Pacific Geology, v. 8, p. 71-86.

Chappell, B.W. & White, A.J.R., (1984) I- and S- type granites in the Lachlan Fold Belt, southeastern Australia. *In,* Xu Keqin & Tu Guangchi (eds.) Geology of granites and their metallogenic relations, p. 87-101, Beijing, Science Press.

Chappell, B.W. & Stephens, W.E., (1988) Origin of infracrustal (I-type) granite magmas. Transactions of the Royal Society of Edinburgh: Earth Sciences, v79, p.71-86.

Clough, C.T., Maufe, H.B. & Bailey, E.B., (1909) The cauldron subsidence of Glen Coe and associated igneous phenomena: Quarterly Journal of the Geological Society of London, v. 65, p. 611-676.

Coney, P.J.; Jones, D.L. & Monger, J.W.H. (1980) Cordilleran suspect terranes: Nature, v288, p. 329-333.

Courrioux, G., (1987) Oblique diapirism: the Criffel granodiorite/granite zoned pluton (southwest Scotland): Journal of Structural Geology, v9, p313-330.

Cox, A. & Hart, R.B., (1986) Plate Tectonics: How it works. Blackwell Scientific Publications, Inc, Oxford.

Crawford, M.L. & Hollister, L.S., (1982) Contrast of Metamorphic and Structural histories across the Work Channel Lineament, Coast Plutonic Complex, British Columbia: Journal of Geophysical Research, v87, p. 3849-3860.

Crawford, M.L., Hollister, L.S. & Woodsworth, G.J., (1987) Crustal deformation and regional metamorphism across a terrane boundary, Coast Plutonic Complex, British Columbia: Tectonics, v6, no.3, p. 343-361.

Crawford, M.L., Crawford, W.A. & Cook, R.D. (1989) Magmatism and tectonism, central Coastal orogen, Alaska and British Columbia: EOS, Transactions of the American Geophysical Union, v70, p. 1299.

Crawford, M.L. & Crawford, W.A. (1991) Magma emplacement in a convergent tectonic orogen, southern Revillagigedo Island, southeastern Alaska: Canadian Journal of Earth Sciences, v28, p. 929-938.

Cruden, A.R., (1988) Deformation around a rising diapir modelled by creeping flow past a sphere: Tectonics, v. 7, p. 1091-1101.

Daly, R.A., (1933) Igneous rocks and the depths of the Earth: McGraw-Hill, New York, USA.

Davies, F.B., (1982) Pan-African granite intrusion in response to tectonic volume changes in a ductile shear zone from northern Saudi Arabia: Journal of Geology, v. 90, p. 467-483.

Debiche, M.G., Cox, A. & Engebretson, D. (1987) The Motion of Allochthonous Terranes Across the North Pacific Basin: Geological Society of America Special Paper 207 pp. 49

Drinkwater, J.L.; Brew, D.A. & Ford, A.B. (1989) Petrographic and Chemical Description of the Variably Deformed Speel River Pluton, South of Juneau, Southeastern Alaska. In: Geologic Studies in Alaska by the U.S. Geological Survey, 1988 (eds: Dover, James H. & Galloway, John P.) U.S. Geological Survey Bulletin 1903.

Drinkwater, J.L.; Brew, D.A. & Ford, A.B. (1990) Petrographic and Chemical Data for the Large Mesozoic and Cenozoic Plutonic Sills East of Juneau, Southeastern Alaska: U.S Geological Survey Bulletin 1918.

Ebertz, G.W. & Nicholls, I.A., (1988) Microgranitoid enclaves from the Swifts Creek Pluton, SE Australia: textural and physical constraints on the nature of magma mingling processes in the plutonic environment: Geologische Rundschau, v. 77, p. 713-736.

Engebretson, D.C., Cox, A. & Gordon, R.G., (1984) Relative motions between oceanic plates of the Pacific basin: Journal of Geophysical Research, v. 89, p. 10291-10310.

Engebretson, D.C., Cox, A. & Gordon, R.G., (1985) Relative motions between oceanic and continental plates in the Pacific basin: Geological Society of America Special Paper, 206, 59pp.

England, R.W., (1990) The identification of granitic diapirs: Journal of the Geological Society, London, v147, pp931-933.

England, R.W., (1992) The genesis, ascent and emplacement of the Northern Arran Granite, Scotland: Implications for granitic diapirism: Geological Society of America Bulletin, v. 104, p. 606-614.

Etchecopar, A., (1977) A plane kinematic model of progressive deformation in a polycrystalline aggregate: Tectonophysics, v. 39, p. 121-139.

Faure, G., (1986) Principles of isotope geology (second edition). John Wiley & Sons, Chichester, p. 66-92.

Ferry, J.M. & Spear, F.S., (1978) Experimental calibration of the partitioning of Fe and Mg between biotite and garnet: Contributions to Mineralogy and Petrology, v. 66, p. 113-117.

Flinn, D., (1965) On the symmetry principle and the deformation ellipsoid: Geological Magazine, v. 102, p. 36-45.

France-Lanord, C. & Le Fort, P., (1988) Crustal melting and granite genesis during the Himalayan collision orogenesis: Transactions of the Royal Society of Edinburgh: Earth Sciences, v79, p.183-195.

French, W.J., (1966) Appinitic intrusions clustered around the Ardara pluton, County Donegal: Proceedings of the Royal Irish Academy, section B, v. 64, p. 303-322.

Frost, T.M. & Mahood, G.A., (1987) Field, chemical and physical constraints on mafic-felsic magma interaction in the Lamark Granodiorite, Sierra Nevada, California: Geological Society of America Bulletin, v. 99, p. 272-291.

Fyfe, W.S., (1988) Granites and a wet convecting ultramafic planet. Transactions of the Royal Society of Edinburgh: Earth Sciences, v79, p.339-346.

Gabrielse, H., (1985) Major dextral transcurrent displacements along the Northern Rocky Mountain Trench and related lineaments in north-central British Columbia: Geological Society of America Bulletin, v. 96, p. 1-14.

Ganguly, J. & Saxena, S.K., (1984) Mixing properties of aluminosilicate garnets: constrains from natural and experimental data, and applications to geothermo-barometry: American Mineralogist, v. 69, p. 88-97.

Gapais, D., (1989) Shear structures in deformed granites: Mechanical and thermal indicators: Geology, v17, p.1144-1147.

Gay, N.C., (1968) The motion of rigid particles in a viscous fluid during pure shear deformation of the fluid: Tectonophysics, v. 5, p. 81-88.

Gehrels, G.E., (1990) Late Proterozoic-Cambrian metamorphic basement of the Alexander terrane on Long and Dall Islands, southeast Alaska: Geological Society of America Bulletin, v. 102, p. 760-767.

Gehrels, G.E., Brew, D.A. & Saleeby, J.B. (1984) Progress report on U/Pb (zircon) geocnronologic studies in the Coast plutonic-metamorphic complex east of Juneau, southeastern Alaska. In: The United States Geological Survey in Alaska: Accomplishments during 1982 (eds: Reed, K.M. & Bartsch-Winkler, Susan) U.S. Geological Survey Circular 939, p. 100-102.

Gehrels, G.E. & McClelland, W.C., (1988) Early Tertiary uplift of the Coast Range barholith along west-side-up extensional shear zones: Geological Society of America, Abstracts with Programs, 21, A111.

Gehrels, G.E., McClelland, W.C., Samson, S.D., Patchett, P.J. & Jackson, J.L., (1990), Ancient continental assemblage in the northern Coast Mountains, southeast Alaska and northwest Canada: Geology, v. 18, p. 208-211.

Gehrels, G.E., McClelland, W.C., Samson, S.D. and Patchett, P.J. (1991a) U-Pb geochronology of Late Cretaceous and early Tertiary plutons in the northern Coast Mountains batholith: Canadian Journal of Earth Sciences v28, p. 899-911.

Gehrels, G.E., McClelland, W.C., Samson, S.D. & Patchett, P.J., (1991b) U-Pb geochronology of two pre-Tertiary plutons in the Coast Mountains batholith near Ketchikan, southeastern Alaska: Canadian Journal of Earth Sciences v28, p.894-898.

Gehrels, G.E., McClelland, W.C., Samson, S.D., Patchett, P.J. & Orchard, M.J. (1992) Geology of the western flank of the Coast Mountains between Cape Fanshaw and Taku Inlet, Southeastern Alaska: in press.

Ghent, E.D. & Stout, M.Z., (1981) Geobarometry and geothermometry of plagioclase-biotite-garnet-muscovite assemblages: Contributions to Mineralogy and Petrology, v. 76, p. 92-97.

Goldfarb, R.J., Snee, L.W., Miller, L.D. & Newberry. R.J., (1991) Rapid dewatering of the crust deduced from ages of mesothermal gold deposits: Nature, v. 354, p. 296-298.

Hall, A., (1967) The chemistry of appinitic rocks associated with the Ardara pluton, Donegal, Ireland: Contributions to Mineralogy and Petrology, v. 16, p. 156-171.

Hammarstrom, J.M., & Zen, E., (1986) Aluminium in hornblende: An empirical igneous barometer. American Mineralogist, v. 71, p. 1297-1313.

Hancock, P.L., (1985) Brittle microtectonics: principles and practice: Journal of Structural Geology, v. 7, p. 437-457.

Hanmer, S., (1981) Tectonic significance of the northeastern Gander Zone, Newfoundland: an Acadian ductile shear zone: Canadian Journal of Earth Sciences, v. 18, p. 121-135.

Harrison, T.M., (1981) Diffusion of argon in hornblende: Contributions to Mineralogy and Petrology, v. 78, p. 324-331.

Harry, W.T. & Emeleus, C.H., (1960) Mineral layering in some granite intrusions of S.W. Greenland: *From,* The Granite-Gneiss problem: Report of the International Geological Congress, XXI Session, Norden, 1960, part XIV, p. 172-181.

Himmelberg, G.R.; Brew, D.A. & Ford, A.B. (1991) Development of inverted metamorphic isograds in the western metamorphic belt, Juneau, Alaska: Journal of Metamorphic Geol.,v.9, p. 165-180.

Hodges, K.V. & Spear, J.S., (1982) Geothermometry, geobarometry and the Al_2SiO_5 triple point at Mt. Moosilauke, New Hampshire: American Mineralogist, v. 67, p. 1118-1134.

Holden, P., Halliday, A.N., and Stephens, W.E., (1987) Neodymium and strontium isotope content of microdiorite enclaves points to mantle input to granitoid production: Nature, v. 330, p.53-56.

Holder, M.T., (1979) An emplacement mechanism for post-tectonic granites and its implications for their geochemical features, *In:* (eds: Atherton, M.P. & Tarney, J.) Origin of granite bathliths, geochemical evidence. Shiva Publishing, Kent, England., p. 116-128.

Holdsworth, R.E. & Strachan, R.A., (1991) Interlinked system of ductile strike slip and thrusting formed by Caledonian sinistral transpression in northeast Greenland: Geology, v. 19, p. 51-513.

Hollister, L.S., (1982) Metamorphic evidence for rapid (2 mm/yr) uplift of a portion of the central gneiss complex, Coast Mountains, B.C.: Canadian Mineralogist, v20, p. 319-332.

Hollister, L.S. & Crawford,M.L., (1986) Melt-enhanced deformation: a major tectonic process. Geology, v. 14, p. 558-561.

Hollister, L.S., Grissom, G.C., Peters, E.K., Stowell, H.H. & Sisson, V.B., (1987) Confirmation of the empirical correlation of Al in hornblende with pressure of solidification of calc-alkaline plutons: American Mineralogist, v72, p. 231-239.

Houseman, G.A., McKenzie, D.P. & Molnar, P., (1981) Convective instability of a thickened boundary layer and its relevance for the thermal evolution of continental convergent belts: Journal of Geophysical Research, v. 86, p. 6115-6132.

Hunter, R.H. & Rock, N.M.S., (1987) Late Caledonian dyke swarms of northern Britain: spatial and temporal intimacy between lamprophyric and granitic magmatism around the Ross of Mull pluton, Inner Hebrides: Geologische Rundschau, v. 176, p. 805-826.

Hutton, D.H.W., (1977) A structural cross-section from the aureole of the Main Donegal Granite: Geological Journal, v. 12, p. 99-112.

Hutton, D.H.W., (1982) A tectonic model for the emplacement of the Main Donegal Granite, NW Ireland: Journal of the Geological Society, London, v 139, pp. 615-631.

Hutton, D.H.W., (1988a) Granite emplacement mechanisms and tectonic controls: inferences from deformation studies: Transactions of the Royal Society of Edinburgh: Earth Sciences: V 79, p. 245-255.

Hutton, D.H.W., (1988b) Igneous emplacement in a shear-zone termination: The biotite granite at Strontian, Scotland: Geological Society of America Bulletin, V100, p. 1392-1399.

Hutton, D.H.W., (1992) Granite sheeted complexes: evidence for the dyking ascent mechanism, *in*Proceedings, Second Hutton Symposium on the Origin of Granites and Related Rocks, September 1991: Transactions of the Royal Society of Edinburgh: Earth Sciences, V 83, p. 377-382.

Hutton, D.H.W., Dempster, T.J., Brown, P.E. & Becker, S.D., (1990) A new mechanism of granite emplacement: intrusion in active extensional shear zones: Nature, v 343, p.452-455.

Hutton, D.H.W. & Ingram, G.M., (1992) The Great Tonalite Sill of Alaska and British Columbia: emplacement into an active contractional high angle reverse shear zone (extended abstract), *in:* Proceedings, Second Hutton Symposium on the Origin of Granites and Related Rocks, September 1991: Transactions of the Royal Society of Edinburgh: Earth Sciences, V 83, p. 383-386.

Hutton, D.H.W. & Reavy, R.J., (1992) Strike-slip tectonics and granite petrogenesis: Tectonics, v. 11, p. 960-967.

Hyndman, D.W. & Foster, D.A., (1987) The role of tonalites and mafic dykes in the generation of the Idaho batholith: Journal of Geology, v. 96, p. 31-46.

Ingram, G.M. & Hutton, D.H.W., (1992) The Great Tonalite Sill: implications for late Cretaceous to early Tertiary collision tectonics in southeastern Alaska and British Columbia: submitted to Geological Society of America Bulletin, November 1992.

Irving, E.; Woodsworth, G.J.; Wynne, P.J. & Morrison, A. (1985) Palaeomagnetic evidence for displacement from the south of the Coast Plutonic Complex, British Columbia: Canadian Journal of Earth Sciences, v22, p. 584-598.

James, E.W. & Mattinson, J.M., (1988) Metamorphic history of the Salinian block: An isotopic reconnaissance. In: *Metamorphism and Crustal Evolution of the Western United States, Rubey v7,* edited by Ernst, W.G. pp. 938-952, Prentice-Hall, Englewood cliffs, N.J.

Karlstrom, K.E., (1989) Towards a syntectonic paradigm for granitoids: EOS, August 8, 1989.

Kligfield, R., Carmignani, L. & Owens, W.H., (1981) Strain analysis of a Northern Appenine shear zone using deformed marble breccias: Journal of Structural Geology, v. 3, p. 421-436.

Krogh, T.E., (1973) A low-contamination method for hydrothermal decomposition of zircon and extraction of U and Pb for isotopic age determinations: Geochima et Cosmochima Acta, v. 37, p. 485-494.

Leake, B.E., (1978) Granite emplacement: the granites of Ireland and their origin. In: *Crustal evolution in northwestern Britain and adjacent regions* (eds: Bowes, D.R. & Leake, B.E.) Geological Journal Special Publication, v. 10, p. 221-248.

Lisle, R.J., (1977) Estimation of the tectonic strain ratio from the mean shape of deformed elliptical markers: Geologie en Mijnbouw, v. 56 (2), p. 140-144.

Lister, G.S. & Hobbs, B.E., (1979) The simulation of fabric development during plastic deformation and its application to quartzite: the influence of deformation history: Journal of Structural Geology, v. 1, p. 283-297.

Lister, G.S. & Snoke, A.W., (1984) S-C Mylonites: Journal of Structural Geology, v. 6, p. 617-638.

Lister, J.R., (1990) Buoyancy-driven fluid fracture: the effect of material toughness and of low viscosity precursors: Journal of Fluid Mechanics, v. 210, p. 263-280.

Lister, J.R. & Kerr, R.C., (1991) Fluid-Mechanical Models of Crack Propagation and Their Application to Magma Transport in Dykes: Journal of Geophysical Research, v. 96, p. 10,049-10,077.

Lonsdale, P. (1988) Paleogene history of the Kula plate:- Offshore evidence and onshore implications: Geological Society of America Bulletin v. 100, p. 733-754.

McCaffrey, K.J.W., (1989) The emplacement and deformation of granitic rocks in a transpressional shear zone: the Ox Mountains Igneous Complex: Unpublished Ph.D., University of Durham.

McCaffrey, K.J.W., (1992) Igneous emplacement in a transpressive shear zone: Ox Mountains igneous complex: Journal of the Geological Society, London. v. 149, p. 221-235.

McClelland, W.C., (1990) The accretionary history of the Alexander terrane and structural evolution of the Coast Mountains batholith: evidence from geologic, geochronologic, and thermobarometric studies in the Petersburg region, central southeastern Alaska: Ph.D. dissertation, University of Arizona, Tucson, AZ.

McClelland, W.C., Anovitz, L.M. & Gehrels, G.E. (1991a) Thermobarometric constraints on the structural evolution of the Coast Mountains batholith, central southestern Alaska: Canadian Journal of Earth Sciences, v. 28, p. 912-928.

McClelland, W.C., Gehrels, G.E., Samson, S.D. & Patchett, P.J., (1991b) Protolith Relations of the Gravina Belt and Yukon-Tanana Terrane in Central Southeastern Alaska: Journal of Geology, v. 100, p.107-123.

McClelland, W.C., Gehrels, G.E.; Samson, S.D. & Patchett, P.J. (1992) Structural and geochronologic relations along the western flank of the Coast Mountains batholith: Stikine River to Cape Fanshaw, central southeastern Alaska. Journal of Structural Geology, v. 14, p. 475-489.

McKenzie, D.P., (1984) The generation and compaction of partially molten rock: Journal of Petrology, v. 25, p. 713-765.

Mahon, K.I., Harrison, T.M. & Drew, D.A., (1988) Ascent of a granitoid diapir in a temperature varying medium: Journal of Geophysical Research, v. 93, p. 1174-1188.

Marsh, B.D., (1982) On the mechanics of igneous diapirism, stoping, and zone melting: American Journal of Science, v. 282, p. 808-855.

Marre, J., (1986) The structural analysis of granitic rocks: North Oxford Academic, Oxford.

Merrihue, C.M. & Turner, G., (1966) Potassium - argon dating by activation with fast neutrons: Journal of Geophysical Research, v. 71, p. 2852-2857.

Misch, P., (1966) Tectonic evolution of the northern Cascades of Washington, *in* A symposium on the tectonic history and mineral deposits of the western Cordillera in British Columbia and neighbouring parts of the United States: Canadian Institute of Mining and Metallurgy Special Volume 8, p. 101-148.

Monger, J.W.H. & Ross, C.A. (1971) Distribution of Fusulinaceans in the western Canadian Cordillera: Canadian Journal of Earth Sciences, v. 8, p. 259-278.

Monger, J.W.H., Souther, J.G. & Gabrielse, H. (1972) Evolution of the Canadian Cordillera: a plate tectonic model: American Journal of Science v. 272, p. 577-602.

Monger, J.W.H. & Price, R.A. (1979) Geodynamic evolution of the Canadian Cordillera - progress and problems: Canadian Journal of Earth Sciences, v. 16, p. 770-791.

Monger, J.W.H. & Irving, E. (1980) Northward displacement of north-central British Columbia: Nature, v. 285, p. 289-293.

Monger, J.W.H., Price, R.A. & Templeman-Kluit, D. (1982). Tectonic accretion and the origin of the two major metamorphic and plutonic welts in the Canadian Cordillera: Geology, v. 10. p.70-75.

Monger, J.W.H. & Berg, H. (1987) Lithotectonic terrane map of western Canada and southeastern Alaska: U.S. Geological Survey Miscellaneous Field Studies Map MF 1874B, scale 1:2,500,000.

Morand, V.J., (1988) Emplacement and deformation of the Wyangela Batholith, New South Wales: Australian Journal of Earth Sciences, v. 35, p. 339-353.

Mortensen, J.K., (1992) Pre-mid-Mesozoic tectonic evolution of the Yukon-Tanana terrnae, Yukon and Alaska: Tectonics, v. 11, p. 836-853.

Murase, T. & McBirney, A.R., (1973) Properties of some common igneous rocks and their melts at high temperatures: Geological Society of America, Bulletin, v84, p.3563-3592.

Newton, R.C. & Haselton, H.T., (1981) Thermodynamics of the garnet-plagioclase-Al_2SiO_5-quartz geobarometer: In: Newton, R.C., Navarotsky, A. & Wood, B.J. (eds.) Thermodynamics of minerals and melts. Springer-Verlag, New York, U.S.A.

Nicolas, A., Bouchez, J.L., Blaise, J. & Poirier, J.P., (1977) Geological aspects of deformation in shear zones: Tectonophysics, v. 42, p. 55-73.

Öertel, G., (1955) Der pluton von Loch Doon in sudSchottland: Geotektonische Forschungen, v11, p.1-83.

Patterson, S.R., (1989) Are syntectonic granites truly syntectonic?: EOS, August 8.

Passchier, C.W. & Simpson, C., (1986) Porphyroclast systems as kinematic indicators: Journal of Structural Geology, v. 8, p. 831-843.

Pitcher, W.S. & Read, H.H., (1960) The aureole of the Main Donegal Granite: Quarterly Journal of the Geological Society of London, v. 116, p. 1-34.

Pitcher, W.S. & Berger, A.R., (1972) The geology of Donegal: A study of Granite Emplacement and Unroofing: Wiley Interscience, London

Pitcher, W.S. & Russell, M.A., (1977) Structural control of batholith emplacement in Peru: a review: Journal of the Geological Society, London, v133, p249-256.

Pitcher, W.S., (1978) The anatomy of a batholith: Journal of the Geological Society of London, v. 135, p. 157-182.

Pitcher, W.S., (1979) The nature, ascent and emplacement of granitic magmas: Journal of the Geological Society of London, v. 136, p. 627-662.

Plafker, G., (1990) Regional geology and tectonic evolution of Alaska and adjacent parts of the northeast Pacific Ocean margin: Proceedings of the Pacific Rim Congress 90, Australasian Institute of Mining and Metallurgy, Queensland, Australia, p. 841-853.

Pollard, D.D. & Johnston, A.M., (1973) Mechanics of growth of some laccolithic intrusions in the Henry Mountains, Utah. Bending and failure of overburden layers and sill formation: Tectonophysics, v 18, p.311-345.

Powell, C. McA. & Vernon, R.H., (1979) Growth and rotation history of garnet porphyroblasts with inclusion spirals in a Karakoram schist: Tectonophysics, v. 54, p. 25-43.

Price, R.A. & Carmichael, D.M., (1986) Geometric test for Late Cretaceous to Palaeocene intracontinental transform faulting in the Canadian Cordillera: Geology, v. 14, p. 468-471.

Ramsay, J.G. & Graham, R.H., (1970) Strain variation in shear belts: Canadian Journal of Earth Sciences, v. 7, p. 786-813.

Ramsay, J.G. & Huber M.I., (1983) The techniques of modern structural geology, volume 1: Strain Analysis: Academc Press Inc., London.

Ramsay, J.G. & Huber, M.I., (1987) The techniques of modern structural geology, volume 2: Folds and Fractures: Academic press, London, p. 595-640.

Read, H.H., (1957) The Granite Controversy: Geological Addresses Illustrating the Evolution of a Desputant: Hertsford, Thomas Murphy.

Reavy, R.J., (1989) Structural controls on metamorphism and syn-tectonic magmatism: the Portuguese Hercynian collision belt: Journal of the Geological Society, London, v 146, pp.649-657.

Redman, E., Retherford, R.M. & Hickock, B.D., (1984) Geology and geochemistry of the Skagway B-2 quadrangle, southeastern Alaska: *Alaska Division of Geological and Geophysical surveys, Report of Investigations 84-31.*

Rees, C.J., Irving, E. & Brown, R.L. (1985) Secondary magnetization of Triassic-Jurassic volcaniclastic rocks of the Quesnel terrane, Quesnel Lake, B.C.: Geophysical Research Letters, v12, p. 498-501.

Roberts, J.L., (1970) The intrusion of magma into brittle rocks. *In:* Newall, G. & Rast, N. (eds) *Mechanisms of igneous intrusion:* Geological Journal Special Publication, 2, p. 287-338.

Roddick, J.A., (1974) Setting of the Coats Plutonic Complex, British Columbia: Pacific Geology, v8, p.90-108.

Roscoe, R., (1952) The viscosity of suspensions of rigid spheres: British Journal of Applied Physics, v3, p.267-269.

Ross,D.C., (1985) Basement rocks of the Salinian block and southernmost Sierra Nevada and possible correlations across the San Andreas, San Gregorio-Hosgri, and Rinconada-Relic-King City fault zones: *U.S. Geological Survey Professional Paper 1317*, pp37.

Rubin, C.M., Saleeby, J.B., Cowan, D.S., Brandon, M.T. & McGroder, M.F. (1990) Regionally extensive mid-Cretaceous west-vergent thrust system in the northwestern Cordillera: implications for continent-margin tectonism: Geology v18, p. 276-280.

Rusmore, M. & Woodsworth, G.W., (1988) A note on the Coast-Intermontane belt transition, Mount Waddington map area, British Columbia, *in:* Current Research, Part E. Geological Survey of Canada Paper 89-1E, p. 163-176.

Rykkelid, E., (1987) Geologisk utvikling i Møkster/Selbjørn området [Ph.D. thesis]: University of Bergen, Norway.

Sabine, P.A., (1963) The Strontian granite complex, Argyllshire: Geological Survey of Great Britain Bulletin. v. 20, p. 193-214.

Saleeby, J.B. & Rubin, C.M., (1989) The western margin of the Coast Plutonic Complex (CPC) in southernmost SE Alaska: Geological Society of America, Abstracts with programs, v. 21, p. 139.

Samson, S.A., (1990) Nd and Sr isotopic characterization of the Wrangellia, Alexander, Stikine, Taku and Yukon Crystalline terranes of of the Canadian Cordillera [Ph.D. thesis]: University of Arizona, Tucson, AZ, U.S.A.

Samson, S.A., Patchett, P.J., McClelland, W.C. & Gehrels, G.E., (1991a) Nd and Sr isotopic constraints on the petrogenesis of the west side of the northern Coast Mountains batholith, Alaskan and Canadian Cordillera: Canadian Journal of Earth Sciences, v. 28, p. 939-946.

Samson, S.D., Patchett, P.J., McClelland, W.C. & Gehrels, G.E., (1991b), Nd isotopic characterization of metamorphic rocks in the Coast Mountains, Alaskan

and Canadian Cordillera: ancient crust bounded by juvenile terranes: Tectonics, v. 10, p. 770-780.

Sanderson, D.J. & Marchini, W.R.D., (1984) Transpression: Journal of Structural Geology, v. 6, p. 449-458.

Shaw, H.R., (1965) Comments on viscosity, crystal settling and convection in granitic magmas: American Journal of Science v263, p.120-152.

Shaw, H.R., (1969) Rheology of basalt in the melting range: Journal of Petrology v10, p.510-535.

Shaw, H.R., Wright, T.L., Peck, D.L. & Okamura, R., (1968) The viscosity of basaltic magma: an analysis of field measurements in Makaopuhi lava lake, Hawaii: American Journal of Science, v266, p.225-264.

Silver, L.T. & Chappell, B.W., (1988) The Peninsular Ranges Batholith: an insight into the evolution of the Cordilleran batholiths of southwestern North America: Transactions of the Royal Society of Edinburgh: Earth Sciences, v79, p.105-121.

Simpson, C. & Schmid, S.M., (1983) An evaluation of criteria to deduce the sense of movement in sheared rocks: Geological Society of America Bulletin, v. 94, p. 1281-1288.

Simpson, C., (1985) Deformation of granitic rocks across the brittle-ductile transition: Journal of Structural Geology, v. 7, p. 503 511.

Sleep, N.H., (1974) Segregation of magma from a mostly crystalline mush: Geological Society of America Bulletin, v. 85, p. 1225-1232

Sparks, R.S.J., Pinkerton, H. & McDonald, R., (1977) The transport of xenoliths in magmas: Earth and Planetary Science Letters, v35, p.234-238

Spence, D.A., & Sharp, P.W., (1985) Self-similar solutions for elasto-hydrodynamic cavity flow: Proceedings of the Royal Society of London, Series A, v. 400, p. 289-313.

Spence, D.A. & Turcotte, D.L., (1985) Magma-driven propagation of cracks: Journal of Geophysical Research, v. 90, p. 575-580.

Spence, D.A., Sharp, P.W. & Turcotte, D.L., (1987) Buoyancy-driven crack propagation: A mechanism for magma migration: Journal Fluid Mechanics, v. 174, p. 135-153.

Spera, F.J., (1980) Aspects of magma transport. In: Hargraves, R.B. (ed), *Physics of magmatic processes:* Princeton University Press, Princeton, New Jersey.

Spry, A., (1969) Metamorphic textures: Pergamon, Oxford, 350pp.

Stone, D.B., Panuska, B.C. & Packer, D.R. (1982) Paleolattitudes versus time for southern Alaska: Journal of Geophysical Research, v87 p. 3697-3707, 1982.

Stowell, H.H., (1989) Silicate and sulphide thermobarometry of low- to medium-grade metamorphic rocks from Holkam Bay, southeast Alaska: Journal of Metamorphic Geology, v7, p. 343-358.

Stowell, H.H. & Hooper, R.J., (1990) Structural development of the western metamorphic belt adjacent to the Coast Plutonic Complex: evidence from Holkham Bay: Tectonics, v9, p. 391-407.

Strachan, R.A., Holdsworth, R.E., Friderichsen, J.D. & Jepsen, H.F., (1992) Regional Caledonian structure within an oblique convergence zone, Dronning Louise Land, NE Greenland: Journal of the Geological Society, London, v. 149, 9. 359-371.

Streckeisen, A.L., (1973) Plutonic rocks - Classification and nomenclature recommended by IUGS Subcommision on Systematics of Igneous Rocks: Geotimes, v. 18, p. 26-30.

Strong, D.F. & Hanmer, S.K., (1981) The leucogranites of southern Brittany: origin by faulting, frictional heating, fluid flux and fractional melting: Canadian Mineralogist, v. 19, p. 163-176.

Sylvester, A.G., (1988) Strike slip faults: Geological Society of America Bulletin, v. 100, p. 1666-1703.

Tabor, R.W., Frizzel, V.A., Booth, D.B., Whetten, J.T., Waitt, R.B. & Zartman, R.E., (1982) Preliminary geologic map of the Skycomish River 1:100,000 quadrangle, Washington: U.S. Geological Survey Open-File Map 82-747, 31pp.

Thrupp, G.A. & Coe, R.S. (1986) Early Tertiary paleomagnetic evidence and the displacement of southern Alaska: Geology, v14, p. 213-217.

Tullis, J. & Yund, R.A., (1985) Dynamic recrystallization of feldspars: a mechanism for ductile shear zone formation: Geology, v. 13, p. 238-241.

Umhoefer, P.J. (1987) Northward translation of "Baja British Columbia" along the late Cretaceous to Paleocene margin of western north America: Tectonics, v6, no.4, p. 377-394.

Umhoefer, P.J.; Dragovich, J.; Cary, J. & Engebretson,D.C. (1989) Refinements of the "Baja British Columbia" plate-tectonic model for northward translation along the margin of western north America: Geophysical Monograph of the American Geophysical Union (ed. Hillhouse, J.W.), v50, p. 101-111.

Underhill, J.R. & Woodcock, N.H., (1987) Faulting mechanisms in high-porosity sandstones; New Red Sandstone, Arran, Scotland, in Jones, M.E. & Preston, R.M.F., eds., Deformation of Sediments and Sedimentary rocks: Geological Society Special Publication 29, p. 91-105.

Van der Molen, I. & Paterson, M.S., (1979) Experimemtal Deformation of Partially-Melted Granite: Contributions to Mineralogy and Petrology, v70, p.299-318.

Vernon, R.H.,(1983) Restite, Xenoliths and Microgranitoid Enclaves In Granites: Journal nad Proceedings, Royal Society of New South Wales. v. 116, p. 77-103.

Wheeler, J.O., Brookfield, A.J., Gabrielse, H., Monger, J.W.H., Tipper, H.W. & Woodsworth. G.J. (compilers) (1991) Terrane map of the Canadian Cordillera: Geological Survey of Canada, Map 1713A, scale 1:2,000,000.

White, S.H., Bretan, P.G. & Rutter, E.H., (1986) Fault-zone reactivation: kinematics and mechanisms: Philosophical Transactions of the Royal Society of London, v. A317, p. 81-97.

White, A.J.R. & Chappell, B.W., (1988) Some supracrustal (S-type) granites of the Lachlan Fold Belt: Transactions of the Royal Society of Edinburgh: Earth Sciences, v79, p.169-181.

Whitehead, J.A. & Helfrich, K.R., (1990) Magma waves and diapiric dynamics. In: (ed. M.P. Ryan) *Magma Transport and Storage:* John Wiley & Sons, Chichester.

Wise, D.U., Dunn, D.E., Engelder, J.T., Geiser, P.A., Hatcher, R.D., Kish, S.A., Odom, A.L. & Schamel, S., (1984) Fault-related rocks: Suggestions for terminology: Geology, v. 12, p. 391-394.

Wood, D.J., Stowell, H.H., Onstott, T.C. & Hollister, L.S., (1991) $^{40}Ar/^{39}Ar$ constraints on the emplacement, uplift, and cooling of the Coast Plutonic Complex sill, southeastern Alaska: Geological Society of America Bulletin, v103. p849-860.

Woodcock, N.H. & Underhill, J.R., (1987) Emplacement-related fault patterns around the Northern Granite, Arran, Scotland: Geological Society of America Bulletin, v. 98, p. 515-527.

Woods, M.T. & Davies. G.F., (1982) Late Cretaceous genesis of the Kula plate: Earth and Planetary Science Letters, v. 58, p. 161-166.

APPENDIX

MAFIC ENCLAVE STRAIN DATA:
SHAPE RATIOS, HARMONIC MEANS AND K-VALUES

XENOLITH DATA COLLECTED IN 1990

LOCATION 17: MENDENHALL GLACIER

y	z	y/z	1/(y/z)	x	z	x/z	1/(x/z)
71.00	2.00	35.50	0.03	29.00	0.70	41.43	0.02
15.00	1.00	15.00	0.07	38.00	0.40	95.00	0.01
45.00	2.00	22.50	0.04	28.00	1.20	23.33	0.04
11.50	2.50	4.60	0.22	13.00	1.50	8.67	0.12
32.00	1.00	32.00	0.03	25.00	0.70	35.71	0.03
16.00	0.80	20.00	0.05	13.00	2.00	6.50	0.15
11.50	1.00	11.50	0.09	10.50	6.00	1.75	0.57
8.00	1.00	8.00	0.13	30.00	1.00	30.00	0.03
38.00	1.00	38.00	0.03	17.00	0.50	34.00	0.03
15.00	1.00	15.00	0.07	38.00	1.00	38.00	0.03
25.00	0.80	31.25	0.03	20.00	3.50	5.71	0.18
29.00	1.00	29.00	0.03	43.00	0.70	61.43	0.02
22.00	0.70	31.43	0.03	17.00	1.20	14.17	0.07
10.50	1.50	7.00	0.14	16.00	1.00	16.00	0.06
23.00	2.00	11.50	0.09	42.00	0.80	52.50	0.02
23.00	2.00	11.50	0.09	20.00	2.50	8.00	0.13
16.00	2.00	8.00	0.13	18.00	0.70	25.71	0.04
16.00	1.00	16.00	0.06	26.00	0.50	52.00	0.02
10.00	1.50	6.67	0.15	10.50	2.00	5.25	0.19
6.00	1.40	4.29	0.23	14.00	1.50	9.33	0.11
26.50	3.00	8.83	0.11	5.50	1.50	3.67	0.27
23.00	1.50	15.33	0.07	21.00	0.80	26.25	0.04
9.50	1.50	6.33	0.16	15.00	2.20	6.82	0.15
11.00	1.30	8.46	0.12	29.00	0.80	36.25	0.03
8.50	1.00	8.50	0.12	17.00	1.80	9.44	0.11
11.00	3.00	3.67	0.27	11.00	0.80	13.75	0.07
5.00	1.30	3.85	0.26				
10.50	2.50	4.20	0.24				
22.00	2.00	11.00	0.09				
18.00	0.70	25.71	0.04				
17.00	0.80	21.25	0.05				
29.00	3.00	9.67	0.10				

Average y/z	15.17	Average x/z	25.41
St Deviation y/z	10.17	St Deviation x/z	22.18
Average 1/(y/z)	0.10	Average 1/(x/z)	0.10
Harmonic mean y/z	9.55	Harmonic mean x/z	10.30

HARMONIC:	Calculated x/y value	1.08
	Calculated K-value	0.034

LOCATION 18: MENDENHALL GLACIER

y	z	y/z	1/(y/z)	x	z	x/z	1/(x/z)
27.00	1.00	27.00	0.04	120.00	1.50	80.00	0.01
11.00	0.50	22.00	0.05	180.00	1.70	105.88	0.01
42.00	1.50	28.00	0.04	31.00	3.00	10.33	0.10
8.50	0.40	21.25	0.05	45.00	0.60	75.00	0.01
15.00	1.70	8.82	0.11	26.00	1.00	26.00	0.04
12.00	1.20	10.00	0.10	100.00	1.00	100.00	0.01
17.00	3.00	5.67	0.18	14.00	1.70	8.24	0.12
12.00	2.00	6.00	0.17	30.00	1.50	20.00	0.05
28.00	3.00	9.33	0.11	13.00	0.70	18.57	0.05
31.00	1.50	20.67	0.05	30.00	3.00	10.00	0.10
33.00	2.00	16.50	0.06	45.00	0.40	112.50	0.01
31.00	0.50	62.00	0.02	60.00	0.60	100.00	0.01
29.00	2.00	14.50	0.07	29.00	0.60	48.33	0.02
20.00	0.50	40.00	0.03	65.00	0.50	130.00	0.01
7.50	1.00	7.50	0.13	31.00	0.60	51.67	0.02
33.00	1.50	22.00	0.05	60.00	1.00	60.00	0.02
13.00	1.50	8.67	0.12	30.00	0.70	42.86	0.02
38.00	2.00	19.00	0.05	22.00	0.50	44.00	0.02

60.00	2.00	30.00	0.03	57.00	1.00	57.00	0.02
19.00	1.00	19.00	0.05	37.00	0.80	46.25	0.02
15.00	1.20	12.50	0.08	40.00	0.90	44.44	0.02
26.00	1.00	26.00	0.04	18.00	1.20	15.00	0.07
12.00	0.80	15.00	0.07	12.00	0.50	24.00	0.04
11.50	0.80	14.38	0.07				
8.00	0.50	16.00	0.06				
8.00	0.70	11.43	0.09				
12.00	1.70	7.06	0.14				
70.00	3.00	23.33	0.04				
20.00	1.00	20.00	0.05				
20.50	0.70	29.29	0.03				

Average y/z	19.10	Average x/z	53.48
St Deviation y/z	11.65	St Deviation x/z	36.46
Average 1/(y/z)	0.07	Average 1/(x/z)	0.04
Harmonic mean	13.93	Harmonic mean	28.57

HARMONIC:	Calculated x/y value	2.05
	Calculated K-value	0.27

LOCATION 19: MENDENHALL GLACIER

x	z	x/z	1/(x/z)	y	z	y/z	1/(y/z)
37.00	1.00	37.00	0.03	14.50	1.10	13.18	0.08
19.00	0.50	38.00	0.03	28.00	2.00	14.00	0.07
25.00	0.40	62.50	0.02	11.00	1.60	6.88	0.15
18.00	0.80	22.50	0.04	28.00	1.40	20.00	0.05
32.00	0.70	45.71	0.02	18.00	1.80	10.00	0.10
23.00	1.20	19.17	0.05	13.00	0.80	16.25	0.06
30.00	0.30	100.00	0.01				
50.00	1.20	41.67	0.02				
68.00	1.70	40.00	0.03				
16.00	0.40	40.00	0.03				
53.00	1.50	35.33	0.03				
57.00	1.20	47.50	0.02				
94.00	1.30	72.31	0.01				
27.00	1.30	20.77	0.05				
38.00	4.40	8.64	0.12				
55.00	5.00	11.00	0.09				
24.00	1.30	18.46	0.05				
32.00	0.80	40.00	0.03				
145.00	2.50	58.00	0.02				
32.00	0.90	35.56	0.03				
24.00	1.70	14.12	0.07				
60.00	3.00	20.00	0.05				
36.00	1.00	36.00	0.03				

Average x/z	37.58	Average y/z	13.38
St Deviation x/z	21.29	St Deviation y/z	4.61
Average 1/(x/z)	0.04	Average 1/(y/z)	0.08
Harmonic mean x/z	26.65	Harmonic mean y/z	11.90

HARMONIC:	Calculated x/y value	2.24
	Calculated K-value	0.33

LOCATION 39: JUNEAU ISLAND

x	z	x/z	1/(x/z)	y	z	x/z	1/(y/z)
4.20	1.50	2.80	0.36	5.70	2.50	2.28	0.44
6.50	1.20	5.42	0.18	4.00	3.50	1.14	0.88
4.30	1.90	2.26	0.44	4.50	3.00	1.50	0.67
6.00	1.60	3.75	0.27	2.00	1.80	1.11	0.90
4.00	1.70	2.35	0.43	2.50	2.00	1.25	0.80
4.50	1.50	3.00	0.33	3.50	1.50	2.33	0.43
3.40	1.30	2.62	0.38	4.00	2.50	1.60	0.63

7.70	2.00	3.85	0.26	4.00	1.20	3.33	0.30
3.50	1.50	2.33	0.43	5.50	3.00	1.83	0.55
7.00	2.00	3.50	0.29	3.00	1.30	2.31	0.43
7.50	4.50	1.67	0.60	4.50	2.00	2.25	0.44
6.50	2.50	2.60	0.38	6.00	2.50	2.40	0.42
7.00	4.00	1.75	0.57	5.00	1.50	3.33	0.30
4.50	0.80	5.63	0.18				
6.00	1.00	6.00	0.17				
3.00	2.00	1.50	0.67				

Average x/z =	3.19	Average y/z =	2.05
St Deviation x/z =	1.42	St Deviation =	0.74
Average 1/(x/z) =	0.37	Average 1/(y/z) =	0.55
Harmonic mean =	2.70	Harmonic mean =	1.81

HARMONIC:	Calculated x/y value	1.49
	Calculated K-value	0.67

LOCATION 58: SUNNY POINT

ROCK SAMPLE 58 (MM)

x	z	x/z	1/(x/z)	y	z	y/z	1/(y/z)
11.00	1.20	9.17	0.11	11.00	2.00	5.50	0.18
20.00	1.10	18.18	0.06	16.00	3.00	5.33	0.19
15.00	1.00	15.00	0.07	22.00	4.00	5.50	0.18
22.00	1.50	14.67	0.07	23.00	4.50	5.11	0.20
12.00	2.50	4.80	0.21	7.00	1.50	4.67	0.21
9.00	1.00	9.00	0.11	13.00	2.00	6.50	0.15
19.00	2.00	9.50	0.11	7.00	1.50	4.67	0.21
17.00	2.00	8.50	0.12	11.50	1.50	7.67	0.13
22.00	4.00	5.50	0.18	8.00	3.00	2.67	0.38
34.00	3.50	9.71	0.10	9.00	2.00	4.50	0.22
15.00	1.20	12.50	0.08	9.00	2.50	3.60	0.28
15.00	1.70	8.82	0.11	12.00	2.00	6.00	0.17
18.00	1.60	11.25	0.09	7.00	1.50	4.67	0.21
23.00	2.50	9.20	0.11	7.00	1.00	7.00	0.14
33.00	3.00	11.00	0.09	5.00	2.00	2.50	0.40
9.00	1.20	7.50	0.13	6.00	2.00	3.00	0.33
15.00	1.30	11.54	0.09	11.00	2.00	5.50	0.18
18.00	3.00	6.00	0.17	12.00	2.00	6.00	0.17
12.00	1.10	10.91	0.09	23.00	5.00	4.60	0.22
14.00	2.00	7.00	0.14	14.00	3.00	4.67	0.21
20.00	1.60	12.50	0.08	7.00	1.50	4.67	0.21
21.00	0.70	30.00	0.03	9.00	2.00	4.50	0.22
31.00	8.00	3.88	0.26	11.00	2.50	4.40	0.23
10.50	2.80	3.75	0.27	10.00	1.60	6.25	0.16
15.00	1.50	10.00	0.10	13.00	2.00	6.50	0.15
14.00	1.40	10.00	0.10	9.00	2.00	4.50	0.22
8.00	1.00	8.00	0.13	8.50	1.00	8.50	0.12
20.00	1.20	16.67	0.06	8.00	1.50	5.33	0.19
11.00	1.20	9.17	0.11	12.00	2.00	6.00	0.17
10.00	1.20	8.33	0.12	6.50	0.50	13.00	0.08
39.00	2.50	15.60	0.06	22.00	4.00	5.50	0.18
10.00	1.00	10.00	0.10	6.00	1.00	6.00	0.17
21.00	1.20	17.50	0.06				
19.00	1.30	14.62	0.07				
11.00	0.90	12.22	0.08				

Average x/z =	10.91	Average y/z =	5.47
St Deviation x/z =	4.94	St Deviation y/z =	1.96
Average 1/(x/z) =	0.11	Average 1/(y/z) =	0.20
Harmonic mean =	9.08	Harmonic mean =	4.95

HARMONIC:	Calculated x/y value	1.84
	Calculated K-value	0.38

LOCATION 79: TAKU INLET

y	z	y/z	1/(y/z)	x	z	x/z	1/(x/z)
80.00	21.00	3.81	0.26	63.00	17.00	3.71	0.27
106.00	24.00	4.42	0.23	40.00	18.00	2.22	0.45
54.00	14.00	3.86	0.26	70.00	23.00	3.04	0.33
120.00	23.00	5.22	0.19	60.00	17.00	3.53	0.28
48.00	10.00	4.80	0.21	110.00	24.00	4.58	0.22
175.00	28.00	6.25	0.16	60.00	15.00	4.00	0.25
30.00	15.00	2.00	0.50	60.00	14.00	4.29	0.23
90.00	12.00	7.50	0.13	16.00	10.00	1.60	0.63
95.00	15.00	6.33	0.16	130.00	3.00	43.33	0.02
147.00	23.00	6.39	0.16	120.00	17.00	7.06	0.14
60.00	20.00	3.00	0.33	100.00	17.00	5.88	0.17
52.00	23.00	2.26	0.44	110.00	20.00	5.50	0.18
120.00	16.00	7.50	0.13	50.00	10.00	5.00	0.20
140.00	33.00	4.24	0.24	80.00	12.00	6.67	0.15
170.00	45.00	3.78	0.26	40.00	16.00	2.50	0.40
170.00	19.00	8.95	0.11	40.00	12.00	3.33	0.30
36.00	5.00	7.20	0.14	87.00	10.00	8.70	0.11
140.00	26.00	5.38	0.19	65.00	18.00	3.61	0.28
50.00	14.00	3.57	0.28	70.00	14.00	5.00	0.20
90.00	25.00	3.60	0.28	40.00	10.00	4.00	0.25
90.00	22.00	4.09	0.24	160.00	26.00	6.15	0.16
25.00	7.00	3.57	0.28				
135.00	18.00	7.50	0.13				
150.00	25.00	6.00	0.17				
140.00	26.00	5.38	0.19				

Average y/z =	5.06	Average x/z =	6.37
St Deviation y/z =	1.81	St Deviation x/z =	8.64
Average 1/(y/z) =	0.23	Average 1/(x/z) =	0.24900898
Harmonic mean =	4.41	Harmonic mean =	4.01591944
	Now = x/z		Now = y/z

HARMONIC:

Calculated x/y value	1.09800764
Calculated K-value	0.06725136

LOCATION 80: TAKU INLET

y	z	y/z	1/(y/z)	x	z	x/z	1/(x/z)
30.00	10.00	3	0.33	65.00	15.00	4.33	0.23
23.00	6.00	3.83	0.26	22.00	4.00	5.50	0.18
32.00	7.00	4.57	0.22	60.00	10.00	6.00	0.17
22.00	6.00	3.67	0.27	35.00	8.00	4.38	0.23
26.00	8.00	3.25	0.31	11.00	2.50	4.40	0.23
60.00	9.00	6.67	0.15	30.00	7.00	4.29	0.23
55.00	12.00	4.58	0.22	26.00	8.00	3.25	0.31
23.00	7.00	3.29	0.30	36.00	4.50	8.00	0.13
32.00	12.00	2.67	0.38	35.00	10.00	3.50	0.29
45.00	7.00	6.43	0.16	25.00	5.00	5.00	0.20
120.00	19.00	6.32	0.16	40.00	6.50	6.15	0.16
35.00	6.00	5.83	0.17	26.00	7.00	3.71	0.27
29.00	8.00	3.63	0.28	15.00	2.50	6.00	0.17
30.00	6.00	5.00	0.20	21.00	3.00	7.00	0.14
30.00	8.00	3.75	0.27	28.00	4.00	7.00	0.14
18.00	6.00	3.00	0.33	30.00	9.00	3.33	0.30
25.00	7.00	3.57	0.28	70.00	9.00	7.78	0.13
65.00	9.00	7.22	0.14	19.00	4.00	4.75	0.21
40.00	12.00	3.33	0.30	45.00	7.00	6.43	0.16
23.00	5.00	4.60	0.22	20.00	5.00	4.00	0.25
40.00	11.00	3.64	0.28	80.00	19.00	4.21	0.24
35.00	9.00	3.89	0.26	20.00	6.00	3.33	0.30
35.00	10.00	3.50	0.29	24.00	5.00	4.80	0.21
120.00	13.00	9.23	0.11	40.00	9.00	4.44	0.23
35.00	8.00	4.38	0.23	35.00	10.00	3.50	0.29
32.00	10.00	3.20	0.31	46.00	8.00	5.75	0.17
24.00	9.00	2.67	0.38	36.00	8.50	4.24	0.24

35.00	8.00	4.38	0.23	37.00	7.00	5.29	0.19
20.00	4.50	4.44	0.23	22.00	9.00	2.44	0.41
33.00	10.00	3.30	0.30	28.00	10.00	2.80	0.36

Average y/z =	4.36	Average x/z =	4.85
St Deviation y/z =	1.52	St Deviation x/z =	1.45
Average 1/(y/z) =	0.25	Average 1/(x/z) =	0.22
Harmonic mean =	3.98	Harmonic mean =	4.45

HARMONIC:	Calculated x/y value	1.12
	Calculated K-value	0.08

LOCATION 89: TAKU INLET

x	z	x/z	1/(x/z)	y	z	y/z	1/(y/z)
12.00	3.00	4.00	0.25	65.00	17.00	3.82	0.26
47.00	13.00	3.62	0.28	27.00	4.50	6.00	0.17
8.50	2.50	3.40	0.29	18.00	3.00	6.00	0.17
16.00	2.50	6.40	0.16	17.00	3.50	4.86	0.21
25.00	4.50	5.56	0.18	12.00	3.00	4.00	0.25
18.00	4.00	4.50	0.22	36.00	4.50	8.00	0.13
20.00	5.00	4.00	0.25	10.00	3.00	3.33	0.30
10.00	4.00	2.50	0.40	13.50	3.00	4.50	0.22
30.00	8.50	3.53	0.28	8.00	3.50	2.29	0.44
214.00	15.00	14.27	0.07	5.50	1.70	3.24	0.31
35.00	7.00	5.00	0.20	8.00	1.50	5.33	0.19
31.00	5.00	6.20	0.16	36.00	12.00	3.00	0.33
13.50	4.50	3.00	0.33	17.00	2.00	8.50	0.12
25.00	9.00	2.78	0.36	30.00	4.50	6.67	0.15
30.00	6.00	5.00	0.20	20.00	2.50	8.00	0.13
16.00	5.50	2.91	0.34	16.00	3.00	5.33	0.19
13.00	4.00	3.25	0.31	10.00	3.50	2.86	0.35
77.00	13.00	5.92	0.17	30.00	5.00	6.00	0.17
18.00	4.50	4.00	0.25	17.00	6.00	2.83	0.35
70.00	17.00	4.12	0.24	34.00	10.00	3.40	0.29
26.00	4.50	5.78	0.17	16.00	4.00	4.00	0.25
56.00	10.00	5.60	0.18	18.00	4.50	4.00	0.25
75.00	25.00	3.00	0.33	20.00	4.50	4.44	0.23
14.00	4.00	3.50	0.29	20.00	4.00	5.00	0.20
26.00	11.00	2.36	0.42	10.00	2.50	4.00	0.25
26.00	3.50	7.43	0.13	9.00	2.50	3.60	0.28
56.00	14.00	4.00	0.25	50.00	20.00	2.50	0.40
19.00	5.00	3.80	0.26	10.50	4.00	2.63	0.38
21.00	6.00	3.50	0.29	14.00	2.00	7.00	0.14
20.00	6.00	3.33	0.30	30.00	9.00	3.33	0.30
104.00	9.00	11.56	0.09	10.00	2.50	4.00	0.25
20.00	5.00	4.00	0.25	7.00	2.50	2.80	0.36

Average x/z =	4.74	Average y/z =	4.54
St Deviation x/z =	2.50	St Deviation y/z =	1.71
Average 1/(x/z) =	0.25	Average 1/(y/z) =	0.25
Harmonic mean =	4.04	Harmonic mean =	4.00

HARMONIC:	Calculated x/y value	1.01
	Calculated K-value	0.01

LOCATION 90: TAKU INLET

x	y	x/y	1/(x/y)
1.20	0.40	3.00	0.33
0.70	0.25	2.80	0.36
3.50	0.80	4.38	0.23
1.60	0.50	3.20	0.31
2.00	0.50	4.00	0.25
2.00	0.75	2.67	0.38
1.10	0.40	2.75	0.36
4.30	1.20	3.58	0.28
1.80	0.50	3.60	0.28
2.40	1.00	2.40	0.42

4.50	1.30	3.46	0.29
2.30	0.75	3.07	0.33
5.50	1.80	3.06	0.33
4.50	2.60	1.73	0.58
3.50	2.20	1.59	0.63
6.50	1.20	5.42	0.18
7.50	1.90	3.95	0.25
9.00	2.00	4.50	0.22

total x/y	59.14	
stdev x/y	0.96	
Average 1/(x/y) =		0.33
Harmonic mean =		3.00

LOCATION 106: TAKU INLET

x	z	x/z	1/(x/z)	x	y	x/y	1/(x/y)
14.00	3.50	4.00	0.25	160.00	10.00	16.00	0.0625
3.50	0.80	4.38	0.23	150.00	14.00	10.71	0.09333333
30.00	4.50	6.67	0.15				
10.00	1.00	10.00	0.10				
38.00	5.00	7.60	0.13				
33.00	7.50	4.40	0.23				
85.00	8.00	10.63	0.09				
30.00	3.00	10.00	0.10				
30.00	2.50	12.00	0.08				
57.00	5.00	11.40	0.09				
8.00	2.00	4.00	0.25				
29.00	2.50	11.60	0.09				
20.00	3.00	6.67	0.15				
50.00	3.00	16.67	0.06				
12.00	1.50	8.00	0.13				
34.00	3.00	11.33	0.09				
24.00	3.50	6.86	0.15				
100.00	5.00	20.00	0.05				
16.00	4.00	4.00	0.25				
50.00	3.50	14.29	0.07				
16.00	3.50	4.57	0.22				
35.00	3.00	11.67	0.09				
7.00	2.00	3.50	0.29				

Average x/z =	8.88	Average x/y =	13.3571429
St Deviation x/z =	4.43		
Average 1/(x/z) =	0.14	Average 1/(x/y) =	0.07791667
Harmonic mean =	6.93	Harmonic mean =	12.8342246

LOCATION 107: TAKU INLET

x	z	x/z	1/(x/z)	y	z	y/z	1/(y/z)
30.00	7.00	4.29	0.23	7.00	2.00	3.50	0.29
7.00	2.00	3.50	0.29	7.50	3.00	2.50	0.40
7.00	1.00	7.00	0.14	10.50	1.50	7.00	0.14
12.00	3.50	3.43	0.29	9.00	6.00	1.50	0.67
20.00	4.00	5.00	0.20	16.00	9.00	1.78	0.56
26.00	6.00	4.33	0.23	18.00	3.50	5.14	0.19
22.00	6.00	3.67	0.27	18.00	2.00	9.00	0.11
13.00	1.50	8.67	0.12				
9.00	1.50	6.00	0.17				
8.50	1.50	5.67	0.18				
33.00	9.00	3.67	0.27				
7.00	2.50	2.80	0.36				
15.50	5.50	2.82	0.35				
63.00	11.00	5.73	0.17				
12.50	4.00	3.13	0.32				
14.00	3.00	4.67	0.21				
15.00	3.00	5.00	0.20				
8.50	2.00	4.25	0.24				
24.00	3.00	8.00	0.13				
7.50	2.00	3.75	0.27				

Average x/z =	4.77	Average y/z =	4.35
St Deviation x/z =	1.65	St Deviation y/z =	2.83
Average 1/(x/z) =	0.23180742	Average 1/(y/z) =	0.33761338
Harmonic mean =	4.31392584	Harmonic mean =	2.96196793

HARMONIC: Calculated x/y value 1.45643908
Calculated K-value 0.34626617

LOCATION 109: TAKU INLET

x	z	x/z	1/(x/z)	y	z	y/z	1/(y/z)
25.00	4.00	6.25	0.16	13.00	2.00	6.50	0.15
11.00	0.70	15.71	0.06	12.00	0.80	15.00	0.07
33.00	1.40	23.57	0.04	10.00	1.50	6.67	0.15
14.00	1.50	9.33	0.11	12.00	0.60	20.00	0.05
16.00	1.30	12.31	0.08	9.00	1.00	9.00	0.11
36.00	1.00	36.00	0.03	18.00	3.50	5.14	0.19
23.00	1.50	15.33	0.07	4.50	1.00	4.50	0.22
28.00	1.60	17.50	0.06	15.50	3.00	5.17	0.19
27.00	0.80	33.75	0.03	12.50	2.50	5.00	0.20
16.00	1.20	13.33	0.08	7.00	2.50	2.80	0.36
24.00	2.50	9.60	0.10	21.00	2.50	8.40	0.12
22.00	1.50	14.67	0.07	10.00	0.70	14.29	0.07
20.00	1.50	13.33	0.08	8.50	1.50	5.67	0.18
60.00	7.00	8.57	0.12	30.00	2.50	12.00	0.08
34.00	1.60	21.25	0.05	7.00	1.00	7.00	0.14
30.00	1.50	20.00	0.05	12.00	3.00	4.00	0.25
23.00	1.60	14.38	0.07	38.00	7.00	5.43	0.18
22.00	1.50	14.67	0.07	22.00	4.00	5.50	0.18
31.00	0.70	44.29	0.02	9.00	1.50	6.00	0.17
16.00	0.50	32.00	0.03	24.00	5.00	4.80	0.21
45.00	3.50	12.86	0.08	23.00	2.00	11.50	0.09
14.00	1.00	14.00	0.07	16.50	0.80	20.63	0.05
16.00	1.20	13.33	0.08	6.00	1.50	4.00	0.25
24.00	0.50	48.00	0.02	31.00	2.50	12.40	0.08
17.00	2.50	6.80	0.15	12.00	1.50	8.00	0.13
51.00	1.30	39.23	0.03	7.00	1.30	5.38	0.19
30.00	2.50	12.00	0.08	19.00	4.50	4.22	0.24
29.00	1.00	29.00	0.03	13.00	3.00	4.33	0.23
20.00	2.50	8.00	0.13	15.00	7.00	2.14	0.47
34.00	1.00	34.00	0.03	14.00	2.00	7.00	0.14

Average x/z =	19.77	Average y/z =	7.75
St Deviation x/z =	11.69	St Deviation y/z =	4.71
Average 1/(x/z) =	0.07	Average 1/(y/z) =	0.17118851
Harmonic mean =	14.62	Harmonic mean =	5.84

Measured x/y value = 11.39

HARMONIC: Calculated x/y value 2.50
Calculated K-value 0.52

LOCATION 109: TAKU INLET (CONTINUED)

x	y	x/y	1/(x/y)
80.00	11.50	6.96	0.14
35.00	2.50	14.00	0.07
23.00	3.50	6.57	0.15
55.00	6.50	8.46	0.12
246.00	25.00	9.84	0.10
27.00	3.00	9.00	0.11
63.00	4.00	15.75	0.06
10.00	2.00	5.00	0.20
41.00	3.50	11.71	0.09
64.00	10.00	6.40	0.16
60.00	4.00	15.00	0.07
78.00	5.00	15.60	0.06
28.00	4.00	7.00	0.14

30.00	8.00	3.75	0.27
44.00	4.00	11.00	0.09
95.00	5.50	17.27	0.06
43.00	1.50	28.67	0.03
50.00	2.50	20.00	0.05
25.00	2.50	10.00	0.10
51.00	6.00	8.50	0.12
100.00	7.00	14.29	0.07
17.00	2.00	8.50	0.12
32.00	3.70	8.65	0.12

total x/y	261.92	
Average x/y =	11.39	
St Deviation x/y =	11.40	
total		26.07
Average 1/(x/y) =		0.11
Harmonic mean =		9.21

LOCATION 118: TAKU INLET

x	z	x/z	1/(x/z)	y	z	y/z	1/(y/z)
14.00	2.00	7.00	0.14	34.00	6.00	5.67	0.18
30.00	1.20	25.00	0.04	3.50	1.00	3.50	0.29
20.00	0.60	33.33	0.03	7.00	1.50	4.67	0.21
56.00	0.60	93.33	0.01	6.00	1.50	4.00	0.25
27.00	0.80	33.75	0.03	6.00	2.00	3.00	0.33
18.00	0.30	60.00	0.02	11.00	2.50	4.40	0.23
19.00	0.80	23.75	0.04	18.00	2.00	9.00	0.11
13.00	2.00	6.50	0.15	9.50	1.50	6.33	0.16
43.00	6.00	7.17	0.14	10.00	6.50	1.54	0.65
6.50	0.50	13.00	0.08	8.00	2.50	3.20	0.31
18.00	1.50	12.00	0.08	18.00	4.50	4.00	0.25
60.00	2.00	30.00	0.03	11.00	1.50	7.33	0.14
18.00	1.50	12.00	0.08	20.00	3.50	5.71	0.18
43.00	0.50	86.00	0.01	9.00	0.70	12.86	0.08
54.00	1.00	54.00	0.02	10.00	1.20	8.33	0.12
110.00	3.00	36.67	0.03	9.50	1.50	6.33	0.16
16.00	0.80	20.00	0.05	8.00	2.50	3.20	0.31
17.00	2.00	8.50	0.12	15.00	2.50	6.00	0.17
19.50	2.50	7.80	0.13	9.00	3.00	3.00	0.33
17.00	0.40	42.50	0.02	13.00	4.00	3.25	0.31
36.00	3.00	12.00	0.08	7.00	2.50	2.80	0.36
20.00	0.80	25.00	0.04	9.00	1.00	9.00	0.11
20.00	1.00	20.00	0.05	14.00	5.00	2.80	0.36
21.50	1.50	14.33	0.07	9.50	1.50	6.33	0.16
16.00	1.50	10.67	0.09	9.00	1.80	5.00	0.20
36.00	1.00	36.00	0.03	16.00	1.50	10.67	0.09
12.00	0.70	17.14	0.06	12.00	4.00	3.00	0.33
13.00	1.00	13.00	0.08	15.00	8.00	1.88	0.53
17.00	3.50	4.86	0.21	11.50	1.00	11.50	0.09
6.00	1.70	3.53	0.28				

Sum total x/z =	768.83		Sum total x/z =	158.30	
Average x/z =	25.63		Average y/z =	5.46	
St Deviation x/z =	22.61		St Deviation y/z =	2.95	
Average 1/(x/z) =		0.07	Average 1/(y/z) =		0.24
Harmonic mean =		13.34	Harmonic mean =		4.15

HARMONIC:	Calculated x/y value	3.21
	Calculated K-value	0.82

LOCATION 123: TAKU INLET

y	z	y/z	1/(y/z)	x	z	x/z	1/(x/z)
100.00	1.50	66.67	0.02	46.00	2.20	20.91	0.05
45.00	2.00	22.50	0.04	40.00	0.70	57.14	0.02
25.00	1.50	16.67	0.06	26.00	1.00	26.00	0.04
17.00	1.00	17.00	0.06	37.00	1.20	30.83	0.03
13.00	1.50	8.67	0.12	50.00	1.00	50.00	0.02
26.00	1.50	17.33	0.06	70.00	1.00	70.00	0.01
20.00	1.30	15.38	0.07	22.00	1.70	12.94	0.08
34.00	2.00	17.00	0.06	71.00	1.00	71.00	0.01
8.00	0.70	11.43	0.09	28.00	1.20	23.33	0.04
26.00	1.50	17.33	0.06	35.00	0.70	50.00	0.02
92.00	1.50	61.33	0.02	13.00	0.50	26.00	0.04
13.00	1.00	13.00	0.08	36.00	0.50	72.00	0.01
16.00	1.00	16.00	0.06	102.00	1.50	68.00	0.01
33.00	1.00	33.00	0.03	78.00	1.00	78.00	0.01
30.00	1.50	20.00	0.05	22.00	1.00	22.00	0.05
70.00	2.00	35.00	0.03	52.00	1.80	28.89	0.03
200.00	9.00	22.22	0.05	8.20	0.80	10.25	0.10
9.50	1.00	9.50	0.11	24.00	1.00	24.00	0.04
21.00	1.20	17.50	0.06	25.00	0.60	41.67	0.02
6.50	0.50	13.00	0.08	30.00	1.20	25.00	0.04
12.00	0.50	24.00	0.04	14.00	1.00	14.00	0.07
12.00	0.90	13.33	0.08	22.00	1.00	22.00	0.05
7.50	1.50	5.00	0.20	22.00	1.50	14.67	0.07
40.00	2.00	20.00	0.05	20.00	0.50	40.00	0.03
34.00	3.00	11.33	0.09	40.00	0.60	66.67	0.02
13.00	1.00	13.00	0.08	18.00	0.70	25.71	0.04
23.00	1.50	15.33	0.07	59.00	2.00	29.50	0.03
				7.50	0.60	12.50	0.08
				29.00	1.20	24.17	0.04
				12.00	0.80	15.00	0.07

Average y/z =	20.46	Average x/z =	35.74		
Average 1/(y/z) =	0.07	Average 1/(x/z) =	0.04		
Harmonic mean =	15.29	Harmonic mean =	25.56		

HARMONIC: Calculated x/y value 1.67
Calculated K-value 0.19

LOCATION 124: TAKU INLET

y	z	y/z	1/(y/z)	x	z	x/z	1/(x/z)
25.00	3.00	8.33	0.12	113.00	31.00	3.65	0.27433628
38.00	4.50	8.44	0.12	50.00	4.00	12.50	0.08
20.00	3.50	5.71	0.18	23.00	7.00	3.29	0.30
23.00	1.70	13.53	0.07	160.00	20.00	8.00	0.13
7.00	1.30	5.38	0.19	60.00	8.00	7.50	0.13
26.00	1.70	15.29	0.07	23.00	4.00	5.75	0.17
12.00	1.20	10.00	0.10	16.00	2.70	5.93	0.17
14.00	1.50	9.33	0.11	10.00	1.20	8.33	0.12
20.00	6.50	3.08	0.33	10.00	4.00	2.50	0.40
18.00	2.50	7.20	0.14	50.00	1.00	50.00	0.02
19.00	3.50	5.43	0.18	15.00	2.50	6.00	0.17
18.00	2.70	6.67	0.15	27.00	2.20	12.27	0.08
18.00	1.50	12.00	0.08	22.00	5.00	4.40	0.23
14.50	3.00	4.83	0.21	11.00	3.50	3.14	0.32
15.00	3.00	5.00	0.20	30.00	0.60	50.00	0.02
8.00	1.70	4.71	0.21	22.00	1.50	14.67	0.07
16.00	3.00	5.33	0.19	21.00	2.80	7.50	0.13
14.00	6.00	2.33	0.43	15.00	1.00	15.00	0.07
28.00	9.00	3.11	0.32	70.00	8.50	8.24	0.12
16.00	3.00	5.33	0.19	13.00	2.50	5.20	0.19
18.00	2.80	6.43	0.16	15.00	0.50	30.00	0.03
9.00	2.00	4.50	0.22	7.50	2.50	3.00	0.33
14.00	2.00	7.00	0.14	18.00	3.00	6.00	0.17
12.00	3.50	3.43	0.29	19.00	5.50	3.45	0.29

13.00	1.00	13.00	0.08	11.00	1.30	8.46	0.12
18.50	5.00	3.70	0.27	107.00	5.00	21.40	0.05
10.00	3.50	2.86	0.35	38.00	1.50	25.33	0.04
36.00	4.00	9.00	0.11	23.00	1.50	15.33	0.07
105.00	15.00	7.00	0.14				
9.50	2.00	4.75	0.21				

Average y/z =	6.76	Average x/z =	12.39
St Deviation y/z =	3.34	St Deviation x/z =	12.65
Average 1/(y/z) =	0.18	Average 1/(x/z) =	0.15
Harmonic mean =	5.41	Harmonic mean =	6.53

HARMONIC — Calculated x/y value 1.21
Calculated K-value 0.11

LOCATION 130: TAKU INLET

x	z	x/z	1/(x/z)	y	z	y/z	1/(y/z)
21.00	5.00	4.20	0.24	39.00	5.00	7.80	0.13
6.00	1.50	4.00	0.25	11.00	0.80	13.75	0.07
24.00	1.50	16.00	0.06	8.00	1.00	8.00	0.13
15.00	2.00	7.50	0.13	14.00	2.00	7.00	0.14
24.00	1.50	16.00	0.06	20.00	1.80	11.11	0.09
28.00	2.00	14.00	0.07	18.00	3.50	5.14	0.19
18.00	1.00	18.00	0.06	16.00	1.50	10.67	0.09
14.00	1.00	14.00	0.07	9.00	0.80	11.25	0.09
8.00	1.00	8.00	0.13	16.00	1.50	10.67	0.09
8.00	1.30	6.15	0.16	32.00	11.00	2.91	0.34
27.00	2.00	13.50	0.07	10.00	4.00	2.50	0.40
14.50	2.50	5.80	0.17	14.00	2.00	7.00	0.14
7.50	1.50	5.00	0.20	11.00	0.70	15.71	0.06
29.00	1.00	29.00	0.03	8.00	0.80	10.00	0.10
17.00	3.00	5.67	0.18	19.00	1.50	12.67	0.08
16.00	2.00	8.00	0.13	22.50	1.70	13.24	0.08
11.00	2.00	5.50	0.18	13.00	1.20	10.83	0.09
14.00	0.80	17.50	0.06	19.00	1.00	19.00	0.05
18.00	1.00	18.00	0.06	10.00	1.30	7.69	0.13
10.00	1.30	7.69	0.13	28.00	8.00	3.50	0.29
6.00	1.50	4.00	0.25	23.00	1.50	15.33	0.07
50.00	2.50	20.00	0.05	14.00	1.00	14.00	0.07
8.00	1.00	8.00	0.13	11.00	2.00	5.50	0.18
15.00	2.50	6.00	0.17	21.50	1.80	11.94	0.08
19.00	1.50	12.67	0.08	16.00	2.00	8.00	0.13
16.00	1.00	16.00	0.06	13.00	2.00	6.50	0.15
10.00	1.50	6.67	0.15	14.00	1.50	9.33	0.11
10.00	2.00	5.00	0.20	18.00	1.40	12.86	0.08
26.00	1.30	20.00	0.05	14.00	7.00	2.00	0.50
17.00	1.50	11.33	0.09	5.00	2.00	2.50	0.40

Average x/z =	11.11	Average y/z =	9.28
St Deviation x/z =	6.29	St Deviation y/z =	4.36
Average 1/(x/z) =	0.12	Average 1/(y/z) =	0.15
Harmonic mean =	8.20	Harmonic mean =	6.58

HARMONIC: Calculated x/y value 1.25
Calculated K-value 0.12

LOCATION 134: TAKU INLET

x	z	x/z	1/(x/z)	y	z	y/z	1/(y/z)
22.00	1.50	14.67	0.07	6.00	0.60	10.00	0.10
11.00	0.80	13.75	0.07	9.00	0.60	15.00	0.07
19.00	1.50	12.67	0.08	17.00	1.50	11.33	0.09
21.00	1.20	17.50	0.06	20.00	1.50	13.33	0.08
13.00	1.20	10.83	0.09	30.00	2.20	13.64	0.07
17.00	1.00	17.00	0.06	10.00	0.60	16.67	0.06
26.00	1.50	17.33	0.06	25.00	2.00	12.50	0.08
21.00	0.70	30.00	0.03	19.00	2.00	9.50	0.11
11.00	1.00	11.00	0.09	19.00	1.00	19.00	0.05

42.00	1.50	28.00	0.04	8.00	0.50	16.00	0.06
12.00	0.80	15.00	0.07	9.00	0.40	22.50	0.04
26.00	1.30	20.00	0.05	11.00	0.70	15.71	0.06
24.00	1.20	20.00	0.05	6.00	0.50	12.00	0.08
17.00	1.50	11.33	0.09	18.00	1.00	18.00	0.06
29.00	2.00	14.50	0.07	9.00	2.10	4.29	0.23
20.00	1.10	18.18	0.06	13.00	0.70	18.57	0.05
19.00	0.90	21.11	0.05	7.00	0.80	8.75	0.11
16.00	0.80	20.00	0.05	19.00	1.40	13.57	0.07
18.00	1.00	18.00	0.06	11.50	1.60	7.19	0.14
14.00	1.00	14.00	0.07	12.00	0.70	17.14	0.06
18.00	1.00	18.00	0.06	6.00	0.90	6.67	0.15
26.00	1.20	21.67	0.05	13.00	0.80	16.25	0.06
11.00	0.80	13.75	0.07	6.00	0.40	15.00	0.07
21.00	1.20	17.50	0.06	19.00	0.70	27.14	0.04
10.00	1.40	7.14	0.14	23.00	3.00	7.67	0.13
11.00	1.80	6.11	0.16	9.00	1.10	8.18	0.12
31.00	2.00	15.50	0.06	9.00	0.50	18.00	0.06
12.00	1.50	8.00	0.13	9.50	0.60	15.83	0.06
31.00	2.20	14.09	0.07	13.00	1.50	8.67	0.12
25.00	1.00	25.00	0.04	21.00	0.80	26.25	0.04
17.00	1.10	15.45	0.06	22.00	0.80	27.50	0.04
25.00	1.00	25.00	0.04	8.00	1.00	8.00	0.13

Average x/z =	16.63	Average y/z =	14.37
St Deviation x/z =	5.58	St Deviation y/z =	5.95
Average 1/(x/z) =	0.07	Average 1/(y/z) =	0.08
Harmonic mean =	14.62	Harmonic mean =	11.92

HARMONIC: Calculated x/y value 1.23
Calculated K-value 0.08

LOCATION 139: TAKU INLET

x	z	x/z	1/(x/z)	y	z	y/z	1/(y/z)
52.00	9.00	5.78	0.17	23.00	4.10	5.61	0.18
8.00	2.70	2.96	0.34	6.50	2.20	2.95	0.34
4.00	2.00	2.00	0.50	18.00	2.50	7.20	0.14
7.00	3.00	2.33	0.43	6.50	2.00	3.25	0.31
10.00	4.50	2.22	0.45	4.20	2.00	2.10	0.48
16.00	5.50	2.91	0.34	24.50	8.00	3.06	0.33
17.00	6.00	2.83	0.35	13.50	3.00	4.50	0.22
12.00	3.50	3.43	0.29	7.00	1.70	4.12	0.24
19.00	4.50	4.22	0.24	26.00	4.50	5.78	0.17
6.00	2.00	3.00	0.33	21.00	4.00	5.25	0.19
8.00	1.50	5.33	0.19	25.00	4.00	6.25	0.16
11.50	7.00	1.64	0.61	7.50	2.50	3.00	0.33
7.00	2.30	3.04	0.33	9.00	2.00	4.50	0.22
11.00	2.50	4.40	0.23	9.00	2.80	3.21	0.31
6.00	3.00	2.00	0.50	9.00	2.40	3.75	0.27
5.00	2.00	2.50	0.40	17.50	7.50	2.33	0.43
3.00	1.80	1.67	0.60	19.00	7.00	2.71	0.37
17.00	3.00	5.67	0.18	13.50	2.00	6.75	0.15
13.50	3.00	4.50	0.22	30.00	7.00	4.29	0.23
7.00	1.80	3.89	0.26	12.00	3.20	3.75	0.27
6.00	1.00	6.00	0.17	15.00	2.50	6.00	0.17
11.00	4.00	2.75	0.36	4.50	1.20	3.75	0.27
7.50	3.00	2.50	0.40	18.00	2.20	8.18	0.12
10.00	4.50	2.22	0.45	13.00	4.00	3.25	0.31
11.00	8.00	1.38	0.73	12.00	4.50	2.67	0.38
9.50	4.50	2.11	0.47	14.00	1.50	9.33	0.11
22.00	7.50	2.93	0.34	120.00	20.00	6.00	0.17
8.50	2.00	4.25	0.24				
22.50	5.50	4.09	0.24				
6.50	2.00	3.25	0.31				

Average y/z =	3.26	Average x/z =	4.58
St Deviation y/z =	1.29	St Deviation x/z =	1.87
Average 1/(y/z) =	0.36	Average 1/(x/z) =	0.25

Harmonic mean =	2.81		Harmonic mean =		3.94

HARMONIC: Calculated x/y value 1.40
Calculated K- value 0.33

LOCATION 143: TAKU INLET

y	z	y/z	1/(y/z)	x	z	x/z	1/(x/z)
12.00	4.00	3.00	0.33	9.50	5.00	1.90	0.53
12.00	4.70	2.55	0.39	5.00	1.50	3.33	0.30
12.00	2.00	6.00	0.17	9.00	1.50	6.00	0.17
7.00	2.50	2.80	0.36	14.00	2.80	5.00	0.20
14.00	6.00	2.33	0.43	5.50	1.30	4.23	0.24
6.00	1.50	4.00	0.25	14.50	3.50	4.14	0.24
14.00	5.50	2.55	0.39	24.00	6.00	4.00	0.25
6.00	3.00	2.00	0.50	40.00	15.00	2.67	0.38
4.50	2.20	2.05	0.49	7.00	1.80	3.89	0.26
11.00	4.00	2.75	0.36	3.50	1.00	3.50	0.29
12.00	4.50	2.67	0.38	5.50	2.00	2.75	0.36
10.00	3.40	2.94	0.34	4.50	2.50	1.80	0.56
17.00	5.00	3.40	0.29	10.00	2.50	4.00	0.25
8.00	3.50	2.29	0.44	9.00	3.00	3.00	0.33
14.00	4.50	3.11	0.32	19.50	3.50	5.57	0.18
26.50	10.50	2.52	0.40	9.00	3.50	2.57	0.39
174.00	106.00	1.64	0.61	16.00	4.50	3.56	0.28
6.00	2.50	2.40	0.42	11.00	2.00	5.50	0.18
4.00	2.00	2.00	0.50	16.00	2.40	6.67	0.15
5.50	2.80	1.96	0.51	7.50	1.00	7.50	0.13
4.00	1.50	2.67	0.38	9.00	1.00	9.00	0.11
66.00	19.00	3.47	0.29	8.50	3.50	2.43	0.41
9.00	5.00	1.80	0.56	12.50	2.50	5.00	0.20
9.00	4.70	1.91	0.52	19.00	7.20	2.64	0.38
9.00	3.00	3.00	0.33	10.00	2.00	5.00	0.20
18.00	3.20	5.63	0.18	6.50	2.20	2.95	0.34
11.00	2.00	5.50	0.18	7.00	1.50	4.67	0.21
5.50	2.00	2.75	0.36	19.50	9.50	2.05	0.49
15.00	5.00	3.00	0.33	7.50	1.50	5.00	0.20
14.00	7.50	1.87	0.54	8.20	2.00	4.10	0.24
				9.00	4.50	2.00	0.50

Average y/z =	2.89	Average x/z =	4.08
St Deviation y/z =	1.10	St Deviation x/z =	1.70
Average 1/(y/z) =	0.38	Average 1/(x/z) =	0.29
Harmonic mean =	2.60	Harmonic mean =	3.47

HARMONIC: Calculated x/y value 1.33
Calculated K-value 0.30

LOCATION 154: TAKU INLET

x	z	x/z	1/(x/z)	y	z	y/z	1/(y/z)
49.50	41.00	1.21	0.83	5.20	2.50	2.08	0.48
5.00	5.00	1.00	1.00	2.60	1.30	2.00	0.50
3.50	2.20	1.59	0.63	9.50	7.10	1.34	0.75
19.00	16.00	1.19	0.84	13.50	7.50	1.80	0.56
7.00	4.00	1.75	0.57	5.50	3.50	1.57	0.64
5.00	3.00	1.67	0.60	11.20	5.00	2.24	0.45
7.00	2.20	3.18	0.31	6.50	4.00	1.63	0.62
4.00	2.00	2.00	0.50	9.00	7.00	1.29	0.78
20.00	13.00	1.54	0.65	4.00	1.50	2.67	0.38
6.20	3.00	2.07	0.48	16.00	12.00	1.33	0.75
15.00	15.00	1.00	1.00	6.00	2.00	3.00	0.33
8.00	7.50	1.07	0.94	4.50	3.20	1.41	0.71
12.00	11.00	1.09	0.92	11.50	10.00	1.15	0.87
7.00	2.80	2.50	0.40	10.00	7.00	1.43	0.70
6.00	4.00	1.50	0.67	9.00	7.00	1.29	0.78
13.00	5.00	2.60	0.38	7.00	4.80	1.46	0.69
11.50	5.50	2.09	0.48	5.00	3.20	1.56	0.64
20.00	17.00	1.18	0.85	3.50	2.80	1.25	0.80

6.50	4.00	1.63	0.62	61.00	51.00	1.20	0.84
3.80	1.50	2.53	0.39	13.00	7.00	1.86	0.54
4.40	2.60	1.69	0.59	5.00	1.80	2.78	0.36
30.00	18.00	1.67	0.60	3.60	3.40	1.06	0.94
16.00	12.00	1.33	0.75	13.00	3.80	3.42	0.29
23.00	14.00	1.64	0.61	6.70	4.00	1.68	0.60
7.00	3.60	1.94	0.51	5.50	2.50	2.20	0.45
3.40	2.20	1.55	0.65	7.00	4.20	1.67	0.60
8.20	4.00	2.05	0.49	4.60	4.20	1.10	0.91
5.00	2.00	2.50	0.40	6.00	3.00	2.00	0.50
4.00	3.00	1.33	0.75	6.50	3.80	1.71	0.58
2.40	1.00	2.40	0.42	22.30	10.50	2.12	0.47
8.00	3.00	2.67	0.38				
5.50	2.50	2.20	0.45				
12.00	5.50	2.18	0.46				

Average x/z =	1.80	Average y/z =	1.78
St Deviation x/z =	0.55918297	St Deviation y/z =	0.59
Average 1/(x/z) =	0.61	Average 1/(y/z) =	0.62
Harmonic mean =	1.64	Harmonic mean =	1.62

HARMONIC:	Calculated x/y value	1.01
	calculated K-value	0.02

LOCATION 157: TAKU INLET

x	z	x/z	1/(x/z)	y	z	y/z	1/(y/z)
19	4.5	4.22	0.24	3.80	2.2	1.73	0.58
9.5	4	2.38	0.42	9.00	8	1.13	0.89
5	3	1.67	0.6	3.50	2.5	1.4	0.71
8	5	1.6	0.63	3.00	2.5	1.2	0.83
12.5	8	1.56	0.64	3.00	2	1.5	0.67
10.5	6	1.75	0.57	4.20	3	1.4	0.71
13	7	1.86	0.54	4.50	3.2	1.41	0.71
11	6.5	1.69	0.59	7.50	5.8	1.29	0.77
25	19	1.32	0.76	4.20	2.3	1.83	0.55
7	2.5	2.8	0.36	9.00	4.7	1.91	0.52
14	7	2	0.5	6.50	4.5	1.44	0.69
6.5	3	2.17	0.46	6.50	4	1.63	0.62
4.2	2.5	1.68	0.6	3.50	2	1.75	0.57
7	3.5	2	0.5	5.00	3.2	1.56	0.64
8.5	6	1.42	0.71	5.50	2.2	2.5	0.4
5.5	4.5	1.22	0.82	7.00	6.5	1.08	0.93
9.5	6	1.58	0.63	7.00	6	1.17	0.86
15.5	6.5	2.38	0.42	6.00	4	1.5	0.67
9.5	8	1.19	0.84	4.00	2.7	1.48	0.68
10.5	4	2.63	0.38	3.50	2.5	1.4	0.71
12.5	5	2.5	0.4	8.00	4	2	0.5
7.5	5	1.5	0.67	4.50	2.6	1.73	0.58
9	6	1.5	0.67	30.00	16	1.88	0.53
6	4	1.5	0.67	7.00	4	1.75	0.57
7	3	2.33	0.43	3.50	2	1.75	0.57
5.5	4.5	1.22	0.82	3.00	2.2	1.36	0.73
5.5	4.5	1.22	0.82	11.50	8	1.44	0.7
8	3	2.67	0.38	3.00	2.1	1.43	0.7
5.5	3.5	1.57	0.64	5.80	3.6	1.61	0.62
12	9.5	1.26	0.79	8.00	5.7	1.4	0.71

Average x/z =	1.88	Average y/z =	1.55
St Deviation x/z =	0.65	St Deviation y/z =	0.3
Average 1/(x/z) =	0.58	Average 1/(y/z) =	0.66
Harmonic mean =	1.72	Harmonic mean =	1.51

HARMONIC:	Calculated x/y value	1.14
	Calculated K-value	0.32

LOCATION 158: TAKU INLET

y	z	y/z	1/(y/z)	x	z	x/z	1/(x/z)

45	13.5	3.33	0.3	17.00	3.5	4.86	0.21
67	23	2.91	0.34	40.00	8	5	0.2
2.5	5.5	0.45	2.2	15.00	2	7.5	0.13
7.5	3	2.5	0.4	15.00	3	5	0.2
10	2.5	4	0.25	31.00	3.6	8.61	0.12
16.5	4	4.13	0.24	18.00	2	9	0.11
12	5	2.4	0.42	10.00	1.3	7.69	0.13
11	2.5	4.4	0.23	12.50	2.5	5	0.2
24.5	9	2.72	0.37	9.00	1.5	6	0.17
13	1.4	9.29	0.11	12.00	2.5	4.8	0.21
5	1.2	4.17	0.24	16.00	1	16	0.06
17	5.5	3.09	0.32	12.50	1	12.5	0.08
15	4.5	3.33	0.3	16.00	1	16	0.06
7	3.5	2	0.5	12.00	2.2	5.45	0.18
24	8	3	0.33	10.00	1.5	6.67	0.15
13	4.5	2.89	0.35	15.00	4.5	3.33	0.3
10.5	3	3.5	0.29	9.50	2	4.75	0.21
5	3	1.67	0.6	13.50	2	6.75	0.15
8	3	2.67	0.38	9.00	1.6	5.63	0.18
16	2.5	6.4	0.16	9.00	2.5	3.6	0.28
11	4	2.75	0.36	11.00	1.2	9.17	0.11
7	2.5	2.8	0.36	130.00	40	3.25	0.31
6	2	3	0.33	29.00	6.5	4.46	0.22
8.5	2	4.25	0.24	16.00	3	5.33	0.19
9	1.3	6.92	0.14	16.00	3	5.33	0.19
8	3	2.67	0.38	29.00	4.5	6.44	0.16
9	3.5	2.57	0.39	37.00	8	4.63	0.22
14	3	4.67	0.21	20.50	6	3.42	0.29
5.5	2	2.75	0.36	36.00	1.6	22.5	0.04
7.5	6	1.25	0.8	15.00	5	3	0.33
161	80	2.01	0.5				

Average y/z =	3.37	Average x/z =	7.06
St Deviation y/z =	1.7	St Deviation x/z =	4.4
Average 1/(y/z) =	0.4	Average 1/(x/z) =	0.18
Harmonic mean =	2.5	Harmonic mean =	5.57

HARMONIC:

Calculated x/y value	2.23
Calculated K-value	0.87

LOCATION 162: TAKU INLET

Flat Surface :				Vertical Surface :			
x	z	x/z	1/(x/z)	y	z	y/z	1/(y/z)
10	1.4	7.14	0.14	5.00	1.2	4.17	0.24
6	1.4	4.29	0.23	4.50	0.6	7.5	0.13
13	3	4.33	0.23	14.00	4.6	3.04	0.33
40	4.2	9.52	0.11	13.00	2.2	5.91	0.17
12	2.1	5.71	0.18	9.50	1.3	7.31	0.14
10	0.6	16.67	0.06	6.50	2.2	2.95	0.34
45	2	22.5	0.04	15.50	4.2	3.69	0.27
20	1.6	12.5	0.08	7.00	1.4	5	0.2
15	2.3	6.52	0.15	15.00	1.4	10.71	0.09
6	1	6	0.17	23.00	7.8	2.95	0.34
10	2	5	0.2	28.00	9.5	2.95	0.34
8	1.5	5.33	0.19	10.50	2.4	4.38	0.23
6	0.8	7.5	0.13	17.00	2	8.5	0.12
44	4.6	9.57	0.1	15.00	4.4	3.41	0.29
22	1.9	11.58	0.09	17.00	4.3	3.95	0.25
9	2.1	4.29	0.23	11.00	1.7	6.47	0.15
13	1.3	10	0.1	4.00	1.4	2.86	0.35
54.5	2.7	20.19	0.05	8.00	1	8	0.13
21	5.1	4.12	0.24	8.00	1.4	5.71	0.18
30.5	7	4.36	0.23	19.00	3.2	5.94	0.17
15	1	15	0.07	9.00	0.7	12.86	0.08
25	4	6.25	0.16	8.00	2.2	3.64	0.28
19	2.2	8.64	0.12	11.00	2.8	3.93	0.25
6	1	6	0.17	28.00	1.4	20	0.05
24	4	6	0.17	12.00	3.6	3.33	0.3

12	1.8	6.67	0.15	6.50	3.4	1.91	0.52
9	2	4.5	0.22	19.00	4.2	4.52	0.22
21	1.8	11.67	0.09	7.50	1.2	6.25	0.16
13	4	3.25	0.31	15.00	1.4	10.71	0.09
29	7	4.14	0.24	12.00	1.5	8	0.13

Average x/z =	8.31	Average y/z =	6.02
St Deviation x/z =	4.9	St Deviation y/z =	3.77
Average 1/(x/z) =	0.15	Average 1/(y/z) =	0.22
Harmonic mean =	6.47	Harmonic mean =	4.59

HARMONIC:	Calculated x/y value	1.41
	Calculated K-value	0.22

LOCATION 163: TAKU INLET

x	z	x/z	1/(x/z)	y	z	y/z	1/(y/z)
33	4	8.25	0.12	18.00	1.4	12.86	0.08
5.5	0.6	9.17	0.11	6.00	8	0.75	1.33
11	2.2	5	0.2	6.80	1.5	4.53	0.22
12.3	1.7	7.24	0.14	8.00	1.4	5.71	0.18
26	3.2	8.13	0.12	7.20	1.5	4.8	0.21
9	1.5	6	0.17	8.00	2	4	0.25
29	2	14.5	0.07	46.00	5.3	8.68	0.12
23	3.9	5.9	0.17	11.20	2.2	5.09	0.2
33	1.4	23.57	0.04	30.00	2.2	13.64	0.07
38	1.7	22.35	0.04	7.00	5	1.4	0.71
33	4	8.25	0.12	5.00	8	0.63	1.6
15.5	0.3	51.67	0.02	13.50	3	4.5	0.22
8.5	1	8.5	0.12	4.00	1	4	0.25
31.5	1.4	22.5	0.04	7.00	1	7	0.14
8.5	1.4	6.07	0.16	5.50	1	5.5	0.18
19	2	9.5	0.11	24.00	3	8	0.13
16	3	5.33	0.19	5.00	1	5	0.2
22.5	3.2	7.03	0.14	26.00	3.2	8.13	0.12
14.5	3.2	4.53	0.22	32.00	4	8	0.13
19	6	3.17	0.32	8.00	1.2	6.67	0.15
32	1	32	0.03	41.00	6	6.83	0.15
5.5	0.4	13.75	0.07	7.50	3	2.5	0.4
9.5	0.6	15.83	0.06	15.50	2.5	6.2	0.16
15.5	1.9	8.16	0.12	7.60	1	7.6	0.13
5	0.9	5.56	0.18	15.50	1.2	12.92	0.08
14	3	4.67	0.21	30.50	2	15.25	0.07
10.5	4	2.63	0.38	8.60	2.6	3.31	0.3
17	2.6	6.54	0.15	16.50	1.8	9.17	0.11
40	4	10	0.1	9.00	6	1.5	0.67
22	0.7	31.43	0.03	15.00	3	5	0.2

Average x/z =	12.24	Average y/z =	6.31
St Deviation x/z =	10.84	St Deviation y/z =	3.74
Average 1/(x/z) =	0.13	Average 1/(y/z) =	0.29
Harmonic mean =	7.55	Harmonic mean =	3.43

HARMONIC:	Calculated x/y value	2.20
	Calculated K-value	0.64

LOCATION 165: TAKU INLET

x	z	x/z	1/(x/z)	y	z	y/z	1/(y/z)
37	2.5	14.8	0.07	50.00	3.5	14.29	0.07
39	3.5	11.14	0.09	24.00	5.5	4.36	0.23
43	3.2	13.44	0.07	6.50	1.2	5.42	0.18
32	4	8	0.13	16.00	3	5.33	0.19
23	3	7.67	0.13	12.00	1.2	10	0.1
37	1.2	30.83	0.03	36.00	6	6	0.17
23	2.5	9.2	0.11	120.00	5.5	21.82	0.05
27	5	5.4	0.19	42.00	1.5	28	0.04
25	1.3	19.23	0.05	18.00	3	6	0.17
87	3	29	0.03	16.50	1.7	9.71	0.1

18.5	4	4.63	0.22	18.00	1.5	12	0.08
96	4	24	0.04	11.50	3	3.83	0.26
28	3.5	8	0.13	10.00	2.5	4	0.25
22	6	3.67	0.27	30.00	2.5	12	0.08
25.5	6	4.25	0.24	14.00	1	14	0.07
17	2	8.5	0.12	27.00	1.5	18	0.06
23	4.5	5.11	0.2	27.00	2	13.5	0.07
22.5	1.5	15	0.07	20.00	1.2	16.67	0.06
27	1.5	18	0.06	14.00	2	7	0.14
29	13	2.23	0.45	33.00	5.5	6	0.17
18	1.5	12	0.08	8.50	1.2	7.08	0.14
130	15.5	8.39	0.12	32.00	4	8	0.13
23	3	7.67	0.13	22.00	4	5.5	0.18
20	4	5	0.2	43.00	3	14.33	0.07
24	2	12	0.08	47.00	4.5	10.44	0.1
70	17	4.12	0.24	37.00	2	18.5	0.05
36	3.8	9.47	0.11	24.00	1	24	0.04
21	2	10.5	0.1	23.00	3	7.67	0.13
53	4.5	11.78	0.08	7.50	1.8	4.17	0.24
95	2	47.5	0.02	59.00	4	14.75	0.07

Average x/z = 12.35 Average y/z = 11.08
St Deviation x/z = 9.73 St Deviation y/z = 6.38
Average 1/(x/z) = 0.13 Average 1/(y/z) = 0.12
Harmonic mean = 7.81 Harmonic mean = 8.14
NOW = Y/Z NOW = X/Z

HARMONIC MEANS INDICATE INITIAL Y/Z > INITIAL X/Z
THEREFORE INITIAL X/Z = Y/Z ; INITIAL Y/Z = X/Z

HARMONIC: Calculated x/y value 1.04
Calculated K-value 0.02

LOCATION 169: TAKU INLET

y	z	y/z	1/(y/z)	x	z	x/z	1/(x/z)
17	2	8.5	0.12	15.00	1	15	0.07
45	2	22.5	0.04	15.00	1.5	10	0.1
11	6.5	1.69	0.59	15.00	3.6	4.17	0.24
11	4	2.75	0.36	13.00	1.4	9.29	0.11
10	2	5	0.2	19.00	3	6.33	0.16
5	1	5	0.2	15.00	1	15	0.07
4.5	0.8	5.63	0.18	95.00	2.1	45.24	0.02
90	28	3.21	0.31	103.00	2.2	46.82	0.02
12	0.8	15	0.07	4.50	1	4.5	0.22
54	3.5	15.43	0.06	16.00	0.4	40	0.03
11.5	2	5.75	0.17	12.00	1.2	10	0.1
25	4	6.25	0.16	90.00	26	3.46	0.29
5	1.7	2.94	0.34	9.00	2.6	3.46	0.29
9	1.6	5.63	0.18	22.00	1.2	18.33	0.05
8	1	8	0.13	9.00	2.2	4.09	0.24
15	1	15	0.07	28.00	2.5	11.2	0.09
16	1	16	0.06	40.00	1.3	30.77	0.03
20	1	20	0.05	80.00	1.6	50	0.02
25	1.5	16.67	0.06	62.00	4	15.5	0.06
48	6.5	7.38	0.14	26.00	2.7	9.63	0.1
10	0.7	14.29	0.07	23.00	0.8	28.75	0.03
31.5	7	4.5	0.22	36.00	4	9	0.11
9	1.5	6	0.17	20.00	1.5	13.33	0.08
10	3.5	2.86	0.35	74.00	3	24.67	0.04
11	3.5	3.14	0.32	8.00	0.7	11.43	0.09
8	1.7	4.71	0.21	19.00	1.5	12.67	0.08
28	1.5	18.67	0.05	29.00	1.5	19.33	0.05
13	2	6.5	0.15	23.00	1	23	0.04
11	1	11	0.09	13.00	0.7	18.57	0.05
16	1.5	10.67	0.09	5.00	0.7	7.14	0.14

Average y/z = 9.02 Average x/z = 17.36
St Deviation y/z = 5.92 St Deviation x/z = 13.37
Average 1/(y/z) = 0.17 Average 1/(y/z) = 0.1

Harmonic mean =	5.75	Harmonic mean =	9.89

HARMONIC: Calculated x/y value 1.72
Calculated K-value 0.31

LOCATION 170: TAKU INLET

x	z	x/z	1/(x/z)	y	z	y/z	1/(y/z)
16	1.2	13.33	0.08	10.50	1.6	6.56	0.15
20	1.1	18.18	0.06	15.00	1.7	8.82	0.11
37	4	9.25	0.11	12.00	0.9	13.33	0.08
7	1.7	4.12	0.24	28.00	1.5	18.67	0.05
100	2	50	0.02	50.00	4	12.5	0.08
33	2.8	11.79	0.08	40.00	1.5	26.67	0.04
17	1	17	0.06	67.00	4	16.75	0.06
8	1.1	7.27	0.14	24.00	2.5	9.6	0.1
23	1.5	15.33	0.07	24.00	2.2	10.91	0.09
20	2	10	0.1	22.00	1	22	0.05
13	1.6	8.13	0.12	28.00	3	9.33	0.11
20	1.5	13.33	0.08	50.00	6.5	7.69	0.13
60	2.5	24	0.04	16.00	1.5	10.67	0.09
22	2.5	8.8	0.11	14.00	2.5	5.6	0.18
50	3.6	13.89	0.07	14.00	7	2	0.5
23	1.6	14.38	0.07	25.00	1.6	15.63	0.06
28	9	3.11	0.32	20.00	3.5	5.71	0.18
100	5	20	0.05	26.00	2	13	0.08
20	1.7	11.76	0.09				
27	2	13.5	0.07				
54	6.5	8.31	0.12				
43	4.4	9.77	0.1				
13	1	13	0.08				
18	0.6	30	0.03				
20	2	10	0.1				
82	13.5	6.07	0.16				
12.5	1.5	8.33	0.12				
17	1	17	0.06				
24	0.6	40	0.03				
47	7	6.71	0.15				

Average x/z =	14.55	Average y/z =	11.97
St Deviation x/z =	10.14	St Deviation y/z =	6.2
Average 1/(x/z) =	0.1	Average 1/(y/z) =	0.12
Harmonic mean =	10.26	Harmonic mean =	8.42

HARMONIC: Calculated x/y value 1.22
Calculated K-value 0.09

LOCATION 174: TAKU INLET

y	z	y/z	1/(y/z)	x	z	x/z	1/(x/z)
13	6	2.17	0.46	73.00	11	6.64	0.15
12	2.3	5.22	0.19	26.00	1.5	17.33	0.06
15.5	3	5.17	0.19	5.00	1.7	2.94	0.34
6	2.4	2.5	0.4	13.50	3.7	3.65	0.27
3.6	2.8	1.29	0.78	10.50	4	2.63	0.38
15	1	15	0.07	25.00	7.5	3.33	0.3
20	5.5	3.64	0.28	66.00	5	13.2	0.08
44	15	2.93	0.34	13.00	2.1	6.19	0.16
13.5	2.2	6.14	0.16	10.00	8	1.25	0.8
32	1	32	0.03	3.20	2.8	1.14	0.88
8.5	2	4.25	0.24	11.00	2.5	4.4	0.23
12.7	2.5	5.08	0.2	8.50	2	4.25	0.24
25	11.5	2.17	0.46	60.00	1.3	46.15	0.02
19	2.2	8.64	0.12	21.00	4	5.25	0.19
18.5	3.6	5.14	0.19	15.00	0.7	21.43	0.05
8	1.8	4.44	0.23	13.00	4	3.25	0.31
23	2.2	10.45	0.1	31.00	1.1	28.18	0.04
15	2.6	5.77	0.17	17.00	4	4.25	0.24
28	4.5	6.22	0.16				

17.5	2.3	7.61	0.13
6.5	1.6	4.06	0.25
20	5.2	3.85	0.26
11.5	1.3	8.85	0.11
35	6	5.83	0.17
17	3	5.67	0.18
15.5	1	15.5	0.06
13	2.5	5.2	0.19
34	4.5	7.56	0.13
16	2.8	5.71	0.18
36	5.5	6.55	0.15

Average y/z = 6.82
St Deviation y/z = 5.77
Average 1(y/z) = 0.22
Harmonic mean = 4.56
NEW X/Z

Average x/z = 9.75
St Deviation x/z = 11.8
Average 1/(x/z) = 0.26
Harmonic mean = 3.82
NEW Y/Z

HARMONIC MEANS INDICATE: INITIAL X/Z = Y/Z : INITIALY/Z = X/Z

HARMONIC: Calculated x/y value 1.20
Calculated K-value 0.13

LOCATION 175: TAKU INLET

x	z	x/z	1/(x/z)
19.5	1.5	13	0.08
18.5	1.2	15.42	0.06
28	0.7	40	0.03
7	0.7	10	0.1
32	1.3	24.62	0.04
29	5	5.8	0.17
29	0.7	41.43	0.02
13	0.7	18.57	0.05
10	0.5	20	0.05
11	1.5	7.33	0.14
30	1	30	0.03
24	1.5	16	0.06
12.5	0.7	17.86	0.06
7.5	0.7	10.71	0.09
7	0.6	11.67	0.09
21	0.8	26.25	0.04
15	0.8	18.75	0.05
14	1	14	0.07
32	1	32	0.03
35	1.5	23.33	0.04
17.5	0.7	25	0.04
21	0.6	35	0.03
39	1	39	0.03
15	0.8	18.75	0.05
31	1.3	23.85	0.04

Average x/z = 21.53
St Deviation x/z = 10.19
Average 1/(x/z) = 0.06
Harmonic mean = 16.65

LOCATION 183: TAKU INLET

y	z	y/z	1/(y/z)	x	z	x/z	1/(x/z)
60	3	20	0.05	12.50	2	6.25	0.16
24.5	3.5	7	0.14	19.00	1	19	0.05
16.5	1.8	9.17	0.11	8.50	1	8.5	0.12
17.5	1.9	9.21	0.11	17.00	1.1	15.45	0.06
16	1.5	10.67	0.09	16.00	1.2	13.33	0.08
12	2	6	0.17	10.00	1	10	0.1
18	2.2	8.18	0.12	11.50	1.3	8.85	0.11
15.5	2.7	5.74	0.17	22.00	1.1	20	0.05
19	1.6	11.88	0.08	16.00	1	16	0.06

16.5	4	4.13	0.24	35.00	2.5	14	0.07
16	1	16	0.06	21.00	1	21	0.05
10.6	1	10.6	0.09	20.00	1	20	0.05
15	1.3	11.54	0.09	43.00	4	10.75	0.09
16	1.6	10	0.1	8.00	1.6	5	0.2
12.7	2	6.35	0.16	33.50	2	16.75	0.06
26	3.5	7.43	0.13	18.00	1.3	13.85	0.07
46.5	1.2	38.75	0.03	15.00	2	7.5	0.13
11	2.2	5	0.2	25.00	2.5	10	0.1
6.2	2	3.1	0.32	19.00	1.1	17.27	0.06
11	1.5	7.33	0.14	13.00	1	13	0.08
17	1.2	14.17	0.07	11.00	1.8	6.11	0.16
37	3.8	9.74	0.1	40.00	3.5	11.43	0.09
7.5	1	7.5	0.13	30.00	1.3	23.08	0.04
8	1	8	0.13	18.00	1	18	0.06
18	1.6	11.25	0.09	12.00	2.6	4.62	0.22
23	2.8	8.21	0.12	21.00	1.1	19.09	0.05
12	2.5	4.8	0.21	20.00	1.2	16.67	0.06
7.5	2.7	2.78	0.36	17.00	0.5	34	0.03
33	4.5	7.33	0.14				
7	1.2	5.83	0.17				

Average y/z =	9.59	Average x/z =	14.27
St Deviation y/z =	6.65	St Deviation x/z =	6.5
Average 1/(y/z) =	0.14	Average 1/(x/z) =	0.09
Harmonic mean =	7.26	Harmonic mean =	11.35

HARMONIC:	Calculated x/y value	1.56
	Calculated K-value	0.23

LOCATION 190: TAKU INLET

y	z	y/z	1/(y/z)	x	z	x/z	1/(x/z)
12.50	2.50	5.00	0.20	8.50	1.00	8.50	0.12
5.00	0.80	6.25	0.16	30.00	2.70	11.11	0.09
29.00	9.50	3.05	0.33	16.00	0.60	26.67	0.04
16.00	1.80	8.89	0.11	34.00	1.30	26.15	0.04
9.50	1.70	5.59	0.18	84.00	2.00	42.00	0.02
6.50	1.70	3.82	0.26	10.50	1.30	8.08	0.12
5.50	1.10	5.00	0.20	23.00	1.30	17.69	0.06
16.00	2.50	6.40	0.16	62.00	0.80	77.50	0.01
20.00	4.00	5.00	0.20	17.00	1.60	10.63	0.09
13.00	2.20	5.91	0.17	20.00	1.50	13.33	0.08
14.00	2.30	6.09	0.16	13.00	1.20	10.83	0.09
27.00	6.00	4.50	0.22	15.00	1.20	12.50	0.08
23.00	3.50	6.57	0.15	11.50	0.70	16.43	0.06
5.50	1.60	3.44	0.29	20.00	0.60	33.33	0.03
9.00	1.70	5.29	0.19	43.00	1.00	43.00	0.02
12.00	1.50	8.00	0.13	28.00	1.50	18.67	0.05
10.00	0.80	12.50	0.08	52.00	1.30	40.00	0.03
6.50	0.70	9.29	0.11	30.00	3.70	8.11	0.12
11.50	3.00	3.83	0.26	12.00	2.00	6.00	0.17
20.00	5.00	4.00	0.25	27.00	1.60	16.88	0.06
12.00	1.30	9.23	0.11	12.00	2.50	4.80	0.21
8.00	1.50	5.33	0.19	16.00	0.70	22.86	0.04
59.00	6.00	9.83	0.10	5.00	0.70	7.14	0.14
22.50	2.30	9.78	0.10	10.50	1.20	8.75	0.11
11.50	2.00	5.75	0.17	34.00	1.30	26.15	0.04
32.00	2.20	14.55	0.07	7.00	1.10	6.36	0.16
10.00	1.70	5.88	0.17	30.00	2.00	15.00	0.07
7.00	1.70	4.12	0.24	29.00	5.00	5.80	0.17
34.00	1.70	20.00	0.05	14.00	1.50	9.33	0.11
22.50	5.00	4.50	0.22	13.00	2.80	4.64	0.22

Average y/z =	6.91	Average x/z =	18.61
St Deviation y/z =	3.67	St Deviation x/z =	15.81
Average 1/(y/z) =	0.17	Average 1/(x/z) =	0.09
Harmonic mean =	5.73	Harmonic mean =	11.33

HARMONIC: Calculated x/y value 1.98
Calculated K-value 0.39

LOCATION 193: TAKU INLET

y	z	y/z	1/(y/z)	x	z	x/z	1/(x/z)
8.50	1.80	4.72	0.21	36.00	1.60	22.50	0.04
7.00	2.00	3.50	0.29	20.00	10.50	1.90	0.53
14.30	2.80	5.11	0.20	17.00	1.60	10.63	0.09
8.00	1.10	7.27	0.14	14.00	1.50	9.33	0.11
12.50	2.00	6.25	0.16	7.50	1.80	4.17	0.24
10.50	1.80	5.83	0.17	16.00	1.80	8.89	0.11
9.00	1.50	6.00	0.17	57.00	5.40	10.56	0.09
26.00	2.50	10.40	0.10	150.00	4.00	37.50	0.03
12.00	1.50	8.00	0.13	57.00	2.30	24.78	0.04
22.00	3.00	7.33	0.14	10.00	1.00	10.00	0.10
12.00	2.80	4.29	0.23	10.00	1.00	10.00	0.10
5.50	2.50	2.20	0.45	58.00	4.00	14.50	0.07
9.50	1.50	6.33	0.16	28.00	2.00	14.00	0.07
9.00	3.00	3.00	0.33	12.00	1.00	12.00	0.08
22.00	4.50	4.89	0.20	24.00	1.00	24.00	0.04
14.50	1.50	9.67	0.10	14.00	2.00	7.00	0.14
13.00	2.50	5.20	0.19	31.00	2.50	12.40	0.08
9.00	2.50	3.60	0.28	14.00	1.50	9.33	0.11
10.50	2.00	5.25	0.19	51.00	1.00	51.00	0.02
20.00	6.00	3.33	0.30	110.00	4.00	27.50	0.04
14.50	3.50	4.14	0.24	20.00	3.00	6.67	0.15
4.50	3.50	1.29	0.78	21.00	1.50	14.00	0.07
8.00	1.00	8.00	0.13	12.00	1.00	12.00	0.08
13.00	2.00	6.50	0.15	20.00	1.50	13.33	0.08
17.50	4.00	4.38	0.23	60.00	5.00	12.00	0.08
12.00	2.20	5.45	0.18	44.00	2.00	22.00	0.05
10.50	2.50	4.20	0.24	34.00	1.20	28.33	0.04
6.50	1.00	6.50	0.15	61.00	0.90	67.78	0.01
14.00	3.00	4.67	0.21	42.00	0.70	60.00	0.02
6.00	1.50	4.00	0.25	70.00	0.60	116.67	0.01

Average y/z =	5.38	Average x/z =	22.49
St Deviation y/z =	2.04	St Deviation x/z =	23.88
Average 1/(y/z) =	0.22	Average 1/(x/z) =	0.09
Harmonic mean =	4.48	Harmonic mean =	11.03

HARMONIC: Calculated x/y value 2.46
Calculated K-value 0.60

LOCATION 216: MENDENHALL GLACIER

y	z	y/z	1/(y/z)
140	2.2	63.64	0.02
56	1	56	0.02
150	0.5	300	0
41	1	41	0.02
76	1	76	0.01
126	2.1	60	0.02
210	1	210	0
51	0.8	63.75	0.02
250	1	250	0
205	2.5	82	0.01

OTHER XENOLITHS TOO LONG TO MEASURE

Average 1/(y/z) =	0.01
Harmonic mean =	78.27

LOCATION 222: MENDENHALL GLACIER

y	z	y/z	1/(y/z)	x	z	x/z	1/(x/z)
20	1.7	11.76	0.09	40	2	20	0.05
5.5	1	5.5	0.18	50	13.5	3.7	0.27

12.1	1.6	7.56	0.13	17	1.5	11.33	0.09
10	2.2	4.55	0.22	7.7	0.7	11	0.09
7.6	1.6	4.75	0.21	12	2	6	0.17
8	0.4	20	0.05	60	0.7	85.71	0.01
6.5	1.1	5.91	0.17	11.5	1.1	10.45	0.1
5.2	1.5	3.47	0.29	15	2.5	6	0.17
21.6	1.5	14.4	0.07	8	1.1	7.27	0.14
3.2	1.9	1.68	0.59	25	1.3	19.23	0.05
6	0.7	8.57	0.12	20	2	10	0.1
				13	0.7	18.57	0.05
				10	1.5	6.67	0.15
				15.5	1.2	12.92	0.08
				15	3.1	4.84	0.21
				24	2.1	11.43	0.09
				11	2	5.5	0.18
				11.5	2	5.75	0.17
				27	4	6.75	0.15
				26	1.2	21.67	0.05
				20.5	1.5	13.67	0.07
				8.5	0.8	10.63	0.09
				19.5	1.6	12.19	0.08
				11	2	5.5	0.18
				12	2.3	5.22	0.19
				11	1.5	7.33	0.14

Average y/z =	8.01	Average x/z =	13.05
St Deviation y/z =	5.41	St Deviation x/z =	13.32
Average 1/(y/z) =	0.19	Average 1/(x/z) =	0.12
Harmonic mean =	5.2	Harmonic mean =	8.35

HARMONIC:	Calculated x/y value	1.61
	Calculated K-value	0.29

LOCATION 227

y	z	y/z	1/(y/z)
8	1	8	0.13
10.5	0.7	15	0.07
25	1.9	13.16	0.08
11.5	1	11.5	0.09
10	0.8	12.5	0.08
12	0.5	24	0.04
10	0.4	25	0.04
20.5	0.6	34.17	0.03
7	0.3	23.33	0.04
16.5	0.5	33	0.03
10	1.1	9.09	0.11
10	1	10	0.1
7	0.7	10	0.1
1.7	1.2	1.42	0.71
12	1.5	8	0.13
9.5	1	9.5	0.11
9	0.7	12.86	0.08
14	6	2.33	0.43
8	1	8	0.13
14	0.7	20	0.05
19	0.5	38	0.03
6	0.5	12	0.08
6.5	0.7	9.29	0.11
9	0.8	11.25	0.09
15	1	15	0.07
10	0.4	25	0.04
5.5	1.4	3.93	0.25
11.5	0.7	16.43	0.06
7	1.3	5.38	0.19
12	1.4	8.57	0.12

Average y/z =	14.52	Average1/(y/z) =	0.12
St Deviation y/z =	9.35	Harmonic mean =	8.39

HARMONIC MEAN (X/Z) = 8.21 HARMONIC MEAN (Y/Z) = 5.80

X/Y = 1.42

K = LOG10(X/Y)/LOG10(Y/Z)
K = 0.20

LOCATION 256 PORT SNETTISHAM

X	Z	X/Z	1/(X/Z)	Y	Z	Y/Z	1/(Y/Z)
37.00	1.00	37.00	0.03	126.00	2.00	63.00	0.02
37.00	0.60	61.67	0.02	100.00	2.00	50.00	0.02
30.00	1.30	23.08	0.04	34.00	1.00	34.00	0.03
100.00	2.00	50.00	0.02	42.00	0.40	105.00	0.01
70.00	0.70	100.00	0.01	54.00	0.40	135.00	0.01
80.00	1.70	47.06	0.02	62.00	0.40	155.00	0.01
85.00	1.30	65.38	0.02	130.00	1.80	72.22	0.01
90.00	1.30	69.23	0.01	19.00	1.00	19.00	0.05
80.00	1.10	72.73	0.01	37.00	1.30	28.46	0.04
41.00	0.40	102.50	0.01	38.00	2.00	19.00	0.05
25.00	0.30	83.33	0.01	30.00	0.80	37.50	0.03
35.00	0.80	43.75	0.02	58.00	2.00	29.00	0.03
26.00	1.50	17.33	0.06	52.00	2.20	23.64	0.04
66.00	1.00	66.00	0.02	35.00	1.10	31.82	0.03
55.00	0.80	68.75	0.01	62.00	2.50	24.80	0.04
43.00	0.50	86.00	0.01	125.00	2.50	50.00	0.02
76.00	0.60	126.67	0.01	54.00	1.50	36.00	0.03
70.00	3.50	20.00	0.05	90.00	1.50	60.00	0.02
43.00	0.80	53.75	0.02	110.00	1.20	91.67	0.01
87.00	1.80	48.33	0.02	70.00	1.50	46.67	0.02
84.00	1.50	56.00	0.02	24.00	0.60	40.00	0.03
100.00	2.10	47.62	0.02	28.00	0.60	46.67	0.02
147.00	7.50	19.60	0.05	100.00	1.50	66.67	0.02
201.00	4.50	44.67	0.02	80.00	1.80	44.44	0.02
25.00	0.80	31.25	0.03				
21.00	0.80	26.25	0.04				
100.00	1.80	55.56	0.02				

MEAN(1/X/Z) = 0.02 MEAN(1/(Y/Z)) = 0.02

HARMONIC MEAN (X/Z) = 43.37 HARMONIC MEAN(Y/Z) = 40.08

CALCULATION OF X/Y :
X/Y = (X/Z)/(Y/Z)
X/Y = 1.08

CALCULATION OF K - VALUE :
K = LOG10(X/Y)/LOG10(Y/Z)
K = 0.02

TRACY ARM LOCATION #1
PHOTOGRAPH: measurements in millimetres

X	Z	X/Z	1/(X/Z)
14.88	2.64	5.64	0.18
11.34	1.84	6.16	0.16
24.11	2.06	11.70	0.09
20.92	9.62	2.17	0.46
8.00	1.56	5.13	0.20
9.44	1.62	5.83	0.17
11.00	1.86	5.91	0.17
5.18	1.28	4.05	0.25
5.30	1.38	3.84	0.26
14.06	2.44	5.76	0.17
9.18	2.12	4.33	0.23
5.52	1.68	3.29	0.30
5.46	1.06	5.15	0.19
11.88	2.48	4.79	0.21
13.20	3.40	3.88	0.26
8.40	0.94	8.94	0.11
8.92	1.38	6.46	0.15

XENOLITH DATA COLLECTED IN 1991

LOCATION 254 PORT SNETTISHAM

X	Z	X/Z	1/(X/Z)
22.00	7.50	2.93	0.34
7.00	1.80	3.89	0.26
9.50	1.70	5.59	0.18
6.50	0.70	9.29	0.11
10.50	2.30	4.57	0.22
5.00	1.90	2.63	0.38
7.50	1.70	4.41	0.23
9.00	2.20	4.09	0.24
7.00	2.50	2.80	0.36
5.00	1.50	3.33	0.30
12.00	2.50	4.80	0.21
4.40	1.20	3.67	0.27
6.00	1.70	3.53	0.28
15.00	3.20	4.69	0.21
23.00	4.00	5.75	0.17
19.00	3.70	5.14	0.19
10.00	2.80	3.57	0.28
11.00	4.30	2.56	0.39
11.00	2.00	5.50	0.18

MEAN(1/(X/Z) = 0.25

HARMONIC MEAN = 3.95

LOCATION 255 PORT SNETTISHAM

X	Z	X/Z	1/(X/Z)	Y	Z	Y/Z	1/(Y/Z)
20.00	2.00	10.00	0.10	23.00	2.50	9.20	0.11
20.00	1.75	11.43	0.09	12.00	1.50	8.00	0.13
27.00	3.50	7.71	0.13	18.00	5.00	3.60	0.28
30.00	2.00	15.00	0.07	8.50	4.00	2.13	0.47
10.00	2.00	5.00	0.20	40.00	7.00	5.71	0.18
7.00	0.50	14.00	0.07	20.00	3.50	5.71	0.18
8.00	0.70	11.43	0.09	5.00	1.50	3.33	0.30
8.00	2.00	4.00	0.25	38.00	1.20	31.67	0.03
7.00	2.50	2.80	0.36	26.00	6.00	4.33	0.23
10.00	0.70	14.29	0.07	6.00	2.00	3.00	0.33
5.50	0.40	13.75	0.07	6.00	1.50	4.00	0.25
15.00	2.10	7.14	0.14	18.00	1.20	15.00	0.07
17.00	2.00	8.50	0.12	10.00	2.00	5.00	0.20
15.00	2.70	5.56	0.18	9.00	1.00	9.00	0.11
39.00	2.20	17.73	0.06	19.00	2.00	9.50	0.11
17.00	2.50	6.80	0.15	11.00	2.20	5.00	0.20
24.00	3.00	8.00	0.13	19.00	3.50	5.43	0.18
20.00	2.30	8.70	0.12	10.00	1.20	8.33	0.12
10.00	1.80	5.56	0.18	25.00	1.30	19.23	0.05
9.50	0.70	13.57	0.07	69.00	8.00	8.63	0.12
18.00	2.00	9.00	0.11	20.00	1.50	13.33	0.08
28.00	1.80	15.56	0.06	31.00	1.50	20.67	0.05
28.00	3.00	9.33	0.11	18.00	8.00	2.25	0.44
14.00	1.00	14.00	0.07	23.00	4.00	5.75	0.17
16.00	2.10	7.62	0.13	20.00	1.80	11.11	0.09
13.00	1.50	8.67	0.12	11.00	1.20	9.17	0.11
18.00	1.80	10.00	0.10	41.00	3.50	11.71	0.09
15.00	1.50	10.00	0.10				
14.00	1.50	9.33	0.11				
32.00	3.80	8.42	0.12				

MEAN 1/(X/Z) = 0.12 MEAN(1/(Y/Z) = 0.17

20.56	1.10	18.69	0.05
10.00	1.22	8.20	0.12
9.88	1.22	8.10	0.12

MEAN 1/(X/Z) = 0.19

HARMONIC MEAN = 5.18

TRACY ARM LOCATION #2
PHOTOGRAPH: measurements in millimetres

X	Z	X/Z	1/(X/Z)
6.60	2.06	3.20	0.31
5.10	1.24	4.11	0.24
8.10	1.82	4.45	0.22
6.70	3.48	1.93	0.52
9.38	3.50	2.68	0.37
3.56	0.76	4.68	0.21
5.22	1.08	4.83	0.21
5.28	1.44	3.67	0.27
8.94	0.52	17.19	0.06
13.46	1.80	7.48	0.13
12.60	1.76	7.16	0.14
4.38	1.00	4.38	0.23
6.78	1.04	6.52	0.15
24.72	2.56	9.66	0.10
11.02	4.06	2.71	0.37
9.20	4.04	2.28	0.44
36.18	4.68	7.73	0.13
6.82	2.06	3.31	0.30
15.28	1.00	15.28	0.07
14.62	1.34	10.91	0.09
9.00	2.82	3.19	0.31
7.12	2.00	3.56	0.28
9.20	3.54	2.60	0.38
16.04	1.20	13.37	0.07
6.16	1.22	5.05	0.20
37.56	2.86	13.13	0.08
10.00	2.56	3.91	0.26
12.14	2.08	5.84	0.17
10.52	1.14	9.23	0.11
7.82	1.34	5.84	0.17
6.58	1.79	3.68	0.27
35.36	2.92	12.11	0.08
42.52	1.64	25.93	0.04
13.26	1.48	8.96	0.11
5.08	1.10	4.62	0.22
5.32	1.74	3.06	0.33
7.82	2.24	3.49	0.29
7.70	2.90	2.66	0.38
7.38	2.04	3.62	0.28
9.54	1.52	6.28	0.16
5.00	1.48	3.38	0.30
6.96	1.26	5.52	0.18

MEAN 1/(X/Z) = 0.22

HARMONIC MEAN = 4.55

TRACY ARM LOCATION #3
PHOTOGRAPH: measurements in millimetres

X	Z	X/Z	1/(X/Z)
3.64	1.52	2.39	0.42
8.40	2.34	3.59	0.28
4.66	1.44	3.24	0.31

6.08	1.62	3.75	0.27
12.34	3.74	3.30	0.30
5.10	1.54	3.31	0.30
7.48	1.92	3.90	0.26
6.60	2.51	2.63	0.38
5.08	1.88	2.70	0.37
7.28	2.46	2.96	0.34
11.64	2.30	5.06	0.20
6.48	2.20	2.95	0.34
5.14	1.22	4.21	0.24
5.58	1.66	3.36	0.30
17.92	4.33	4.14	0.24
7.47	2.18	3.43	0.29
10.10	3.68	2.74	0.36

MEAN 1/(X/Z) = 0.31

HARMONIC MEAN = 3.27

TRACY ARM LOCATION #4

PHOTOGRAPH: measurements in millimetres

X	Z	X/Z	1/(X/Z)
10.57	2.78	3.80	0.26
10.62	3.58	2.97	0.34
20.20	3.94	5.13	0.20
26.18	8.48	3.09	0.32
16.10	5.61	2.87	0.35
7.92	1.67	4.74	0.21
7.35	1.52	4.84	0.21
9.18	1.29	7.12	0.14
4.77	1.44	3.31	0.30
3.70	1.50	2.47	0.41
5.90	2.30	2.57	0.39
13.07	5.69	2.30	0.44
29.54	9.04	3.27	0.31
4.86	2.32	2.09	0.48
5.83	2.96	1.97	0.51
9.51	3.26	2.92	0.34
7.68	3.47	2.21	0.45
3.74	1.25	2.99	0.33
4.48	1.08	4.15	0.24
7.04	1.80	3.91	0.26
11.60	3.28	3.54	0.28
5.17	1.30	3.98	0.25
4.38	1.89	2.32	0.43

MEAN 1/(X/Z) = 0.32

HARMONIC MEAN = 3.09

TRACY ARM LOCATION #5

PHOTOGRAPH: measurements in millimetres

X	Z	X/Z	1\(X/Z)
6.88	1.46	4.71	0.21
8.12	1.92	4.23	0.24
12.83	2.20	5.83	0.17
14.42	3.08	4.68	0.21
12.58	2.30	5.47	0.18
12.10	2.58	4.69	0.21
21.82	2.11	10.34	0.10
11.10	1.14	9.74	0.10
12.80	1.57	8.15	0.12
6.80	1.13	6.02	0.17
14.00	1.05	13.33	0.08

18.32	1.40	13.09	0.08
12.16	0.75	16.21	0.06
14.42	1.58	9.13	0.11
10.91	1.20	9.09	0.11
5.00	1.52	3.29	0.30
8.78	1.92	4.57	0.22
7.46	1.48	5.04	0.20
26.25	3.54	7.42	0.13
18.26	2.48	7.36	0.14
8.00	2.18	3.67	0.27
11.06	0.80	13.83	0.07
8.25	0.92	8.97	0.11
16.48	1.98	8.32	0.12
14.08	0.63	22.35	0.04
18.40	1.32	13.94	0.07
4.60	0.62	7.42	0.13
15.70	0.78	20.13	0.05
8.82	0.86	10.26	0.10
7.11	0.86	8.27	0.12

MEAN 1/(X/Z) = 0.14

HARMONIC MEAN = 7.08

LOCATION 258 FORD'S TERROR INLET

X	Z	X/Z	1/(X/Z)	Y	Z	Y/Z	1/(Y/Z)
6.20	0.70	8.86	0.11	18.00	2.10	8.57	0.12
11.00	0.40	27.50	0.04	7.50	2.60	2.88	0.35
28.00	7.50	3.73	0.27	13.00	3.70	3.51	0.28
20.00	4.00	5.00	0.20	15.00	0.50	30.00	0.03
30.00	2.20	13.64	0.07	11.50	2.50	4.60	0.22
6.00	0.50	12.00	0.08	11.00	1.60	6.88	0.15
13.00	2.50	5.20	0.19	5.00	1.00	5.00	0.20
8.00	1.80	4.44	0.23	3.70	2.10	1.76	0.57
19.00	1.90	10.00	0.10	8.00	2.10	3.81	0.26
18.00	2.60	6.92	0.14	6.00	1.30	4.62	0.22
15.00	3.80	3.95	0.25	7.00	1.00	7.00	0.14
11.00	1.90	5.79	0.17	60.00	3.50	17.14	0.06
15.00	1.30	11.54	0.09	14.00	1.20	11.67	0.09
22.00	2.70	8.15	0.12	10.00	0.80	12.50	0.08
38.00	9.00	4.22	0.24	7.00	1.00	7.00	0.14
27.00	5.40	5.00	0.20	5.50	1.30	4.23	0.24
23.00	5.20	4.42	0.23	11.50	2.10	5.48	0.18
7.00	1.20	5.83	0.17	6.50	1.00	6.50	0.15
26.00	2.20	11.82	0.08	7.50	1.10	6.82	0.15
19.00	0.80	23.75	0.04	8.00	1.60	5.00	0.20
40.00	2.80	14.29	0.07	7.00	1.10	6.36	0.16
12.00	2.30	5.22	0.19	13.50	1.20	11.25	0.09
9.00	2.30	3.91	0.26	8.00	1.50	5.33	0.19
8.50	1.80	4.72	0.21	12.00	0.90	13.33	0.08
10.00	1.30	7.69	0.13	34.00	2.00	17.00	0.06
7.50	2.60	2.88	0.35	8.50	1.40	6.07	0.16
34.00	4.50	7.56	0.13	11.50	0.60	19.17	0.05
15.00	5.50	2.73	0.37	11.60	1.90	6.11	0.16
6.00	0.90	6.67	0.15	39.00	3.70	10.54	0.09
8.50	1.90	4.47	0.22	22.00	1.00	22.00	0.05
8.00	1.00	8.00	0.13	12.00	2.50	4.80	0.21
9.00	1.80	5.00	0.20	21.00	0.90	23.33	0.04
				20.00	1.80	11.11	0.09
MEAN (1/(X/Z)) =			0.17	8.50	1.20	7.08	0.14
				8.50	0.50	17.00	0.06
HARMONIC MEAN(X/Z) =			5.89	10.20	0.40	25.50	0.04
				16.00	4.40	3.64	0.28
				MEAN(1/(Y/Z)) =			0.16

HARMONIC MEAN(Y/Z) = 6.42

SWAP AXES :

NEW Y/Z = 5.89

NEW X/Z = 6.42

CALCULATION OF X/Y :

X/Y = (X/Z)/(Y/Z)

X/Y = 1.09

CALCULATION OF K - VALUE :

K - VALUE = 0.05

LOCATION 262 FORD'S TERROR INLET

X	Z	X/Z	1/(X/Z)
50.00	4.00	12.50	0.08
90.00	4.50	20.00	0.05
64.00	5.30	12.08	0.08
30.00	3.00	10.00	0.10
110.00	2.00	55.00	0.02
16.00	1.20	13.33	0.08
20.00	1.80	11.11	0.09
7.50	1.10	6.82	0.15
80.00	7.30	10.96	0.09
79.00	7.20	10.97	0.09
180.00	12.50	14.40	0.07
69.00	4.20	16.43	0.06
22.00	2.00	11.00	0.09
20.00	2.20	9.09	0.11
76.00	4.50	16.89	0.06
40.00	1.70	23.53	0.04
80.00	4.30	18.60	0.05
36.00	1.70	21.18	0.05
17.00	1.00	17.00	0.06
16.00	0.80	20.00	0.05
21.00	1.20	17.50	0.06
30.00	1.30	23.08	0.04
20.00	0.60	33.33	0.03
42.00	1.30	32.31	0.03
20.00	1.00	20.00	0.05
11.00	1.70	6.47	0.15
42.00	3.00	14.00	0.07
20.00	2.10	9.52	0.11
26.50	2.50	10.60	0.09
126.00	8.00	15.75	0.06
33.00	2.50	13.20	0.08
59.00	4.40	13.41	0.07
26.00	2.10	12.38	0.08
37.00	2.70	13.70	0.07
37.50	2.70	13.89	0.07
32.00	1.80	17.78	0.06

X/Z	FREQUENCY
0 -5	0
6 - 10	5
11 - 15	15
16 - 20	9
21 - 25	3
26 - 30	0
31 - 35	2
36 - 40	0
41 - 45	0
46 - 50	0
51 - 55	1

MEAN (1/(X/Z)) = 0.07

HARMONIC MEAN(X/Z) = 13.84

LOCATION #1: FORD'S TERROR INLET

PHOTOGRAPH: measurements in millimetres

X	Z	X/Z	1/(X/Z)
10.00	4.40	2.27	0.44
8.20	4.00	2.05	0.49
6.80	1.90	3.58	0.28
9.40	4.80	1.96	0.51
7.30	3.90	1.87	0.53
12.20	2.80	4.36	0.23
18.20	4.40	4.14	0.24
4.30	1.40	3.07	0.33
7.00	0.60	11.67	0.09

5.10	1.80	2.83	0.35
12.60	2.40	5.25	0.19
6.00	1.30	4.62	0.22
6.00	2.00	3.00	0.33
6.50	1.40	4.64	0.22
13.30	6.20	2.15	0.47
15.50	1.70	9.12	0.11
5.20	1.60	3.25	0.31
12.20	2.20	5.55	0.18
18.00	1.90	9.47	0.11
6.30	2.40	2.63	0.38
11.60	2.30	5.04	0.20
8.30	1.40	5.93	0.17
8.70	2.20	3.95	0.25
7.90	2.60	3.04	0.33
14.50	5.10	2.84	0.35
8.80	3.20	2.75	0.36
16.80	7.20	2.33	0.43
20.50	3.30	6.21	0.16

MEAN 1/(X/Z) = 0.29

HARMONIC MEAN = 3.39

LOCATION #2: FORD'S TERROR INLET
PHOTOGRAPH: measurements in millimetres

X	Z	X/Z	1/(X/Z)
12.00	2.70	4.44	0.23
7.10	1.30	5.46	0.18
17.60	2.50	7.04	0.14
10.60	2.50	4.24	0.24
23.60	1.40	16.86	0.06
7.60	0.90	8.44	0.12
18.20	2.90	6.28	0.16
4.30	1.70	2.53	0.40
8.00	1.50	5.33	0.19
14.00	2.20	6.36	0.16
10.30	1.30	7.92	0.13
15.30	2.60	5.88	0.17
12.10	1.90	6.37	0.16
16.80	4.80	3.50	0.29
9.00	2.80	3.21	0.31
36.20	3.20	11.31	0.09
10.10	2.50	4.04	0.25
6.30	2.10	3.00	0.33

MEAN 1/(X.Z) = 0.20

HARMONIC MEAN = 5.02

LOCATION #3: FORD'S TERROR INLET
PHOTOGRAPH: measurements in millimetres

X	Z	X/Z	1/(X/Z)
10.60	1.50	7.07	0.14
34.90	10.00	3.49	0.29
27.70	3.70	7.49	0.13
12.40	1.70	7.29	0.14
70.60	5.10	13.84	0.07
9.80	1.40	7.00	0.14
12.40	1.90	6.53	0.15
56.80	1.00	56.80	0.02
10.30	1.10	9.36	0.11
9.00	1.20	7.50	0.13
26.40	1.30	20.31	0.05
21.50	2.60	8.27	0.12

22.20	1.20	18.50	0.05
29.30	2.10	13.95	0.07
8.90	0.70	12.71	0.08
18.80	2.00	9.40	0.11
13.20	2.30	5.74	0.17
19.60	2.30	8.52	0.12
21.60	1.80	12.00	0.08
24.60	1.40	17.57	0.06
8.20	1.10	7.45	0.13
6.20	1.50	4.13	0.24
10.20	2.10	4.86	0.21
39.90	4.50	8.87	0.11
25.00	2.00	12.50	0.08
21.30	2.30	9.26	0.11
20.40	2.10	9.71	0.10
38.80	2.00	19.40	0.05

MEAN 1/(X/Z) = 0.12

HARMONIC MEAN = 8.55

LOCATION #4: FORD'S TERROR INLET
PHOTOGRAPH: measurements in millimetres

X	Z	X/Z	1/(X/Z)
8.30	1.30	6.38	0.16
13.00	2.50	5.20	0.19
17.70	1.50	11.80	0.08
49.20	2.80	17.57	0.06
30.00	2.00	15.00	0.07
11.80	1.20	9.83	0.10
12.00	1.60	7.50	0.13
11.00	2.20	5.00	0.20
17.60	6.40	2.75	0.36
14.60	6.10	2.39	0.42
14.30	2.10	6.81	0.15
11.90	1.80	6.61	0.15
6.80	0.90	7.56	0.13
9.20	0.70	13.14	0.08
10.40	7.90	1.32	0.76
9.20	0.70	13.14	0.08
10.20	1.30	7.85	0.13
7.90	0.80	9.88	0.10
10.30	1.50	6.87	0.15
7.10	0.80	8.88	0.11
14.30	2.90	4.93	0.20
15.10	2.60	5.81	0.17
17.50	1.00	17.50	0.06
12.30	1.20	10.25	0.10
17.50	3.30	5.30	0.19
8.00	1.70	4.71	0.21
6.50	0.60	10.83	0.09

MEAN 1/(X/Z) = 0.17

HARMONIC MEAN = 5.84

LOCATION 302: BURROUGHS BAY

X	Z	X/Z	1/(X/Z)	Y	Z	Y/Z	1/(Y/Z)
20.00	2.00	10.00	0.10	20.00	1.50	13.33	0.08
11.00	1.20	9.17	0.11	10.50	1.60	6.56	0.15
29.00	1.40	20.71	0.05	17.00	2.50	6.80	0.15
32.00	3.70	8.65	0.12	9.00	3.60	2.50	0.40
38.00	3.00	12.67	0.08	7.00	1.40	5.00	0.20
38.00	6.40	5.94	0.17	18.00	7.20	2.50	0.40
22.50	3.30	6.82	0.15	8.00	1.20	6.67	0.15

MEAN 1/(X/Z) = 0.11

HARMONIC MEAN (X/Z) = 9.13

CALCULATED X/Y = 1.99

K - VALUE = 0.45

MEAN 1/(Y/Z) = 0.22

HARMONIC MEAN (Y/Z) = 4.59

LOCATION 303: BURROUGHS BAY

X	Z	X/Z	1/(X/Z)
19.00	3.20	5.94	0.17
8.00	2.50	3.20	0.31
12.00	2.00	6.00	0.17
12.00	2.10	5.71	0.18
10.00	2.70	3.70	0.27
18.00	0.80	22.50	0.04
27.00	1.60	16.88	0.06

MEAN 1/(X/Z) = 0.17

HARMONIC MEAN (X/Z) = 5.85

LOCATION 304: BURROUGHS BAY

X	Z	X/Z	1/(X/Z)
19.00	2.00	9.50	0.11
20.00	5.50	3.64	0.28
20.00	1.20	16.67	0.06
10.00	2.00	5.00	0.20
18.00	0.50	36.00	0.03
12.00	1.60	7.50	0.13
15.00	3.20	4.69	0.21
9.00	1.10	8.18	0.12
21.00	2.00	10.50	0.10
20.00	1.50	13.33	0.08
20.00	0.50	40.00	0.03
23.00	0.70	32.86	0.03
40.00	3.20	12.50	0.08
31.00	3.30	9.39	0.11

MEAN 1/(X/Z) = 0.11

HARMONIC MEAN (X/Z) = 9.04

LOCATION 306 BURROUGHS BAY

X	Z	X/Z	1/(X/Z)	Y	Z	Y/Z	1/(Y/Z)
46.00	6.00	7.67	0.13	61.00	14.50	4.21	0.24
17.00	3.00	5.67	0.18	24.00	3.10	7.74	0.13
26.00	3.00	8.67	0.12	11.00	4.00	2.75	0.36
26.00	4.00	6.50	0.15	8.50	2.20	3.86	0.26
69.00	5.00	13.80	0.07				
10.00	2.00	5.00	0.20		MEAN 1/(Y/Z) =		0.25

MEAN 1/(X/Z) = 0.14 HARMONIC MEAN Y/Z = 4.04

HARMONIC MEAN(X/Z) = 7.07

X/Y = (X/Z)/(Y/Z)

X/Y = 1.75

K - VALUE = 0.40

LOCATION 308: BURROUGHS BAY

X	Z	X/Z	1/(X/Z)
17.00	3.00	5.67	0.18
8.00	3.00	2.67	0.38
6.00	1.50	4.00	0.25
13.50	5.00	2.70	0.37

MEAN (X/Z) = 0.29

HARMONIC MEAN (X/Z) = 3.41

LOCATION 318: WALKER COVE

Y	Z	Y/Z	1/(Y/Z)
42.00	3.70	11.35	0.09
30.00	1.70	17.65	0.06
11.50	3.20	3.59	0.28
14.50	2.10	6.90	0.14
15.00	1.60	9.38	0.11
38.00	4.00	9.50	0.11
15.00	3.50	4.29	0.23
32.50	2.20	14.77	0.07
1.80	3.00	0.60	1.67
11.00	1.80	6.11	0.16
12.00	1.40	8.57	0.12
12.00	1.30	9.23	0.11
9.50	2.10	4.52	0.22
31.00	6.30	4.92	0.20
19.00	3.20	5.94	0.17

MEAN 1/(Y/Z) = 0.25

HARMONIC MEAN (Y/Z) = 4.02

HERBERT GLACIER LOCATION 322

Y	Z	Y/Z	1/(Y/Z)
7.50	1.80	4.17	0.24
33.50	3.40	9.85	0.10
10.00	2.00	5.00	0.20
6.00	1.70	3.53	0.28
8.00	2.10	3.81	0.26
10.00	2.50	4.00	0.25
6.00	1.70	3.53	0.28
5.50	1.30	4.23	0.24
6.00	0.80	7.50	0.13
9.00	1.60	5.63	0.18
23.00	3.00	7.67	0.13
4.70	1.60	2.94	0.34
6.00	1.00	6.00	0.17
20.00	2.00	10.00	0.10
15.00	1.80	8.33	0.12

MEAN 1/(Y/Z) = 0.20

HARMONIC MEAN = 4.96

LOCATION 328: LEMON CREEK GLACIER

X	Z	X/Z	1.(X/Z)
17.00	1.10	15.45	0.06
36.00	1.70	21.18	0.05
20.00	1.70	11.76	0.09
29.00	4.00	7.25	0.14
12.00	1.80	6.67	0.15
9.00	1.80	5.00	0.20
17.00	2.00	8.50	0.12
18.00	2.10	8.57	0.12

34.00	2.50	13.60	0.07
4.00	5.20	0.77	1.30
19.00	1.70	11.18	0.09
32.00	2.60	12.31	0.08
25.00	2.50	10.00	0.10
36.00	3.40	10.59	0.09
18.00	1.00	18.00	0.06
15.00	1.90	7.89	0.13
10.50	1.20	8.75	0.11
7.00	1.20	5.83	0.17

MEAN 1 (X/Z) = 0.17

HARMONIC MEAN (X/Z) = 5.76

LOCATION 338: WEST MENDENHALL GLACIER

X	Z	X/Z	1/(X/Z)
43.00	0.90	47.78	0.02
30.00	0.80	37.50	0.03
5.50	0.50	11.00	0.09
29.00	1.70	17.06	0.06

MEAN 1/(X/Z) = 0.05

HARMONIC MEAN (X/Z) = 20.29

LOCATION 348: GRANITE CREEK TRAIL

X	Y	X/Y	1/(X/Y)
11.50	5.20	2.21	0.45
16.50	7.00	2.36	0.42
9.50	4.40	2.16	0.46
8.50	3.40	2.50	0.40
9.50	3.00	3.17	0.32
8.00	4.00	2.00	0.50
13.30	5.00	2.66	0.38
12.00	9.50	1.26	0.79
13.00	9.50	1.37	0.73
11.00	7.50	1.47	0.68

MEAN 1 (X/Y) = 0.51

HARMONIC MEAN (X/Y) = 1.95

LOCATION 360: HERBERT GLACIER

X	Z	X/Z	1/(X/Z)	Y	Z	Y/Z	1.(Y/Z)
7.50	1.90	3.95	0.25	9.00	1.30	6.92	0.14
10.00	1.60	6.25	0.16	8.00	1.30	6.15	0.16
54.00	3.20	16.88	0.06	4.50	0.80	5.63	0.18
57.00	2.50	22.80	0.04	17.50	7.50	2.33	0.43
14.00	0.90	15.56	0.06	14.50	2.00	7.25	0.14
10.00	0.80	12.50	0.08	12.20	1.80	6.78	0.15
20.00	2.00	10.00	0.10	5.50	0.80	6.88	0.15
9.50	1.00	9.50	0.11	1.00	1.00	1.00	1.00
13.00	2.00	6.50	0.15	5.00	0.70	7.14	0.14
7.00	0.80	8.75	0.11	18.00	1.50	12.00	0.08
10.00	1.00	10.00	0.10	9.50	1.00	9.50	0.11
23.00	0.60	38.33	0.03	7.00	0.60	11.67	0.09
21.00	1.10	19.09	0.05	9.00	0.90	10.00	0.10
16.00	1.10	14.55	0.07	4.50	0.50	9.00	0.11
36.00	0.50	72.00	0.01	16.00	4.30	3.72	0.27
5.00	0.40	12.50	0.08	17.00	4.00	4.25	0.24
11.50	1.90	6.05	0.17	11.00	2.00	5.50	0.18
17.00	1.50	11.33	0.09	6.50	1.60	4.06	0.25
17.50	0.90	19.44	0.05	5.00	1.30	3.85	0.26

18.00	1.00	18.00	0.06	22.00	11.00	2.00	0.50
20.00	0.80	25.00	0.04	7.00	1.10	6.36	0.16
9.00	1.10	8.18	0.12	8.00	2.50	3.20	0.31
13.00	0.40	32.50	0.03	8.00	1.80	4.44	0.23
				15.00	2.50	6.00	0.17
				6.50	2.10	3.10	0.32
				9.00	0.90	10.00	0.10
				8.00	3.50	2.29	0.44
				44.00	7.00	6.29	0.16
				16.00	3.00	5.33	0.19
				12.00	1.70	7.06	0.14
				16.00	3.70	4.32	0.23
				10.00	2.00	5.00	0.20

MEAN 1/(X/Z) =	0.09	MEAN 1.(Y/Z) =	0.23
STD DEVIATION =	0.06	STD DEVIATION =	0.17
HARMONIC MEAN (X/Z) =	11.34	HARMONIC MEAN (Y/Z) =	4.38

X/Y = 2.58 K = 0.64

LOCATION 390: CAMP 17, LEMON CREEK GLACIER

X	Z	X/Z	1/(X/Z)	Y	Z	Y/Z	1/(Y/Z)
62.00	2.00	31.00	0.03	35.00	2.50	14.00	0.07
74.00	5.50	13.45	0.07	15.00	1.40	10.71	0.09
46.00	1.60	28.75	0.03	9.50	1.20	7.92	0.13
52.00	1.80	28.89	0.03	19.00	2.70	7.04	0.14
36.00	1.00	36.00	0.03	26.00	2.50	10.40	0.10
75.00	1.30	57.69	0.02	26.00	1.90	13.68	0.07
72.00	2.00	36.00	0.03	20.00	4.00	5.00	0.20
53.00	3.50	15.14	0.07	24.50	3.50	7.00	0.14
33.00	3.50	9.43	0.11	16.00	1.50	10.67	0.09
27.00	1.20	22.50	0.04	25.00	3.00	8.33	0.12
50.00	1.00	50.00	0.02	44.00	2.30	19.13	0.05
60.00	1.00	60.00	0.02	26.00	2.50	10.40	0.10
87.00	1.90	45.79	0.02	17.00	1.00	17.00	0.06
90.00	6.50	13.85	0.07	40.00	2.00	20.00	0.05
26.00	2.70	9.63	0.10	19.00	1.70	11.18	0.09
32.00	1.00	32.00	0.03	23.00	1.30	17.69	0.06
20.00	1.20	16.67	0.06	15.00	2.50	6.00	0.17
44.00	0.90	48.89	0.02	24.00	2.70	8.89	0.11
38.00	1.80	21.11	0.05	12.00	1.50	8.00	0.13
36.00	2.20	16.36	0.06	57.00	4.00	14.25	0.07
20.00	1.50	13.33	0.08	40.00	1.90	21.05	0.05
19.00	3.50	5.43	0.18	18.00	1.60	11.25	0.09
37.00	1.50	24.67	0.04	46.00	1.00	46.00	0.02
15.50	1.60	9.69	0.10	23.00	1.70	13.53	0.07
12.00	1.00	12.00	0.08	22.50	1.30	17.31	0.06
39.00	2.00	19.50	0.05	18.00	2.10	8.57	0.12
46.00	2.10	21.90	0.05	20.00	1.40	14.29	0.07
29.00	1.70	17.06	0.06	24.00	2.00	12.00	0.08
13.00	0.70	18.57	0.05	14.50	0.40	36.25	0.03
				35.00	1.40	25.00	0.04
				26.00	2.00	13.00	0.08
				10.00	1.40	7.14	0.14
				34.00	1.30	26.15	0.04
				13.50	1.80	7.50	0.13
				17.50	1.80	9.72	0.10
				8.50	1.70	5.00	0.20
				24.00	3.40	7.06	0.14
				12.00	1.70	7.06	0.14
				21.00	2.50	8.40	0.12
				14.00	1.30	10.77	0.09

MEAN 1/(X/Z) =	0.06	MEAN 1/(Y/Z) =	0.10
STD DEVIATION 1/(X/Z) =	0.04	STD DEVIATION 1/(Y/Z) =	0.04
HARMONIC MEAN (X/Z) =	17.95	HARMONIC MEAN (Y/Z) =	10.39

X./Y = 1.73 K = 0.23

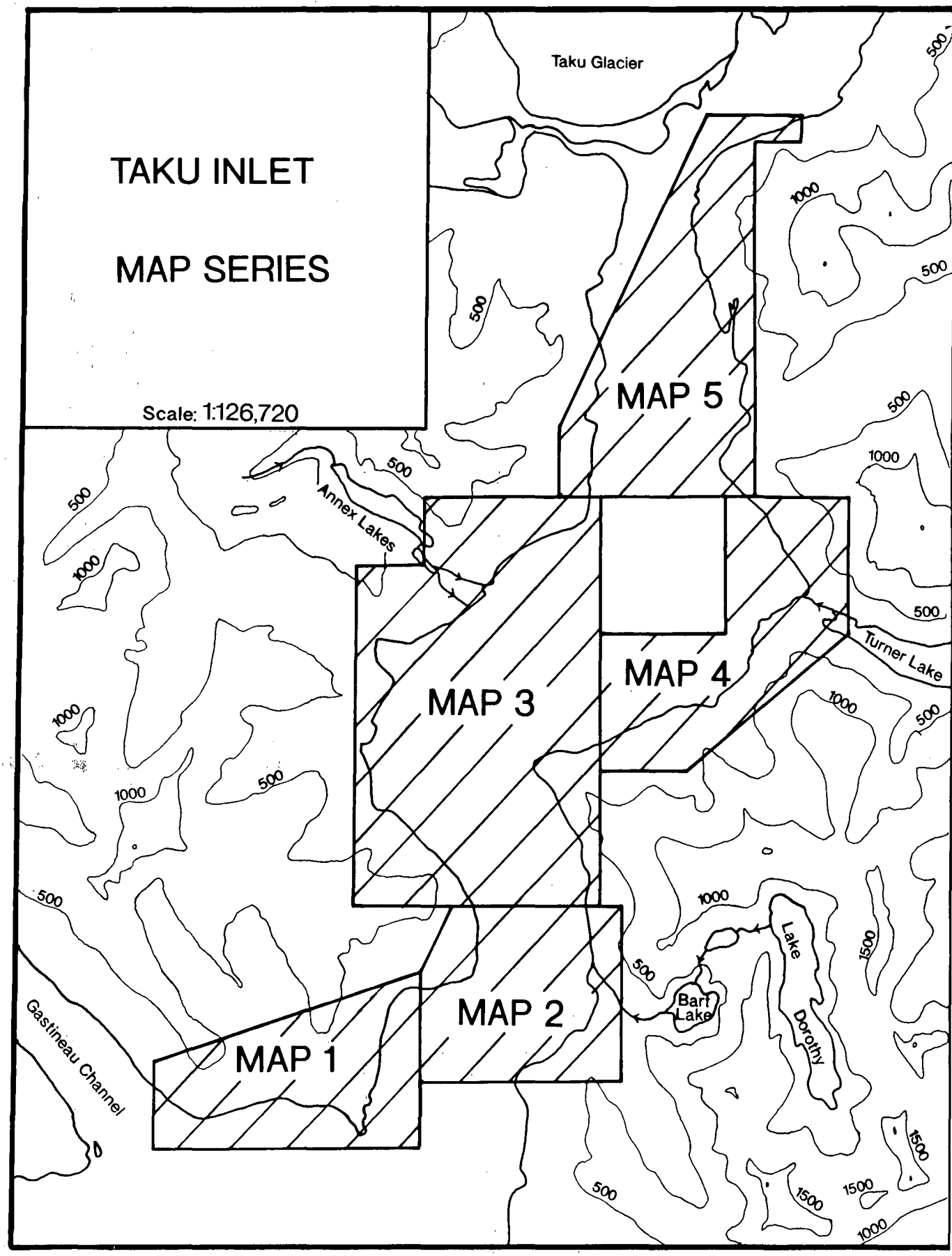

TAKU POINT / TAKU INLET

(MAP 5)

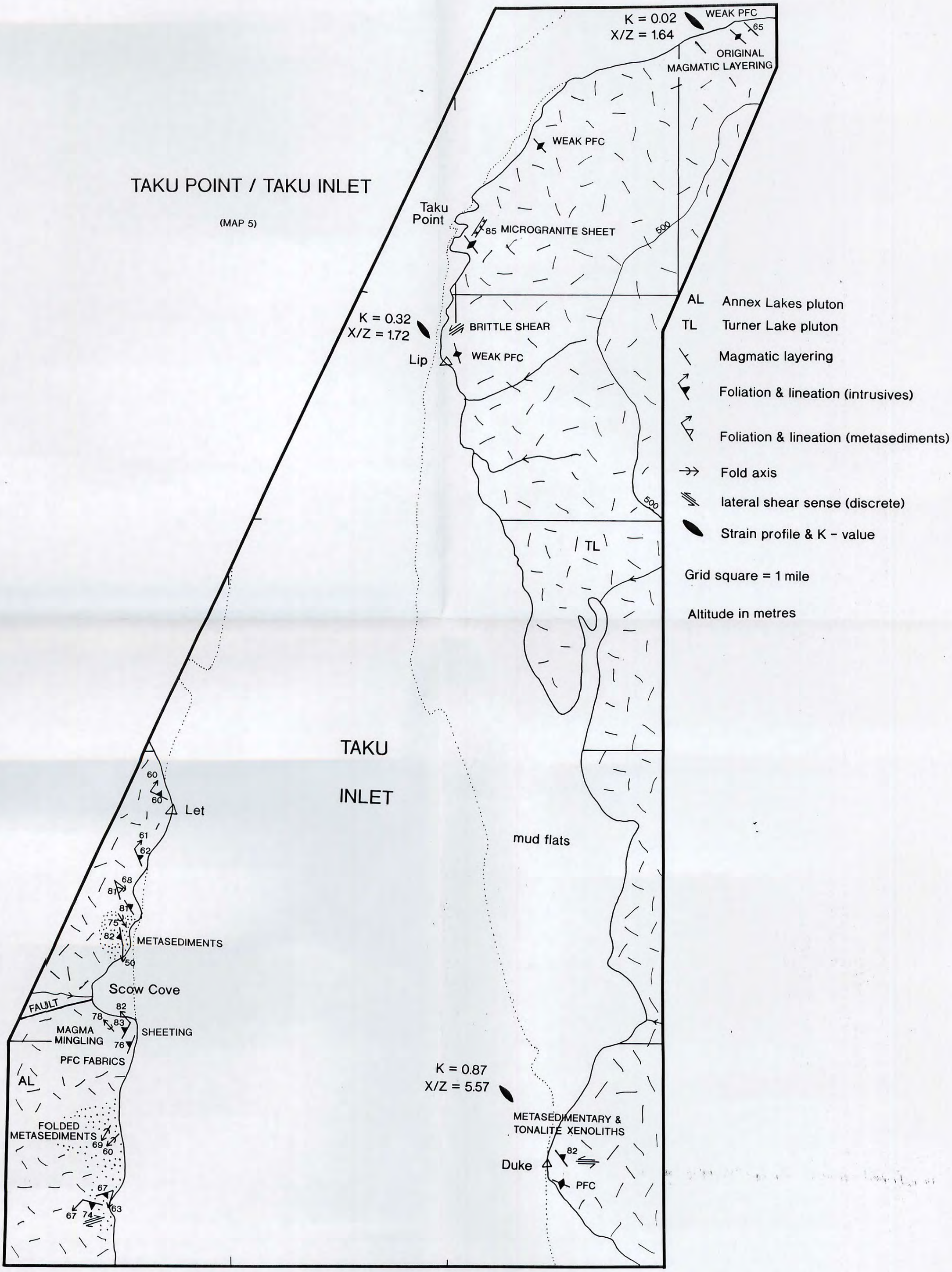

MENDENHALL GLACIER

MENDENHALL LAKE

Gridl Square = 1 kilometre

Altitude in metres

0 1/2 1 Km

KEY

T	Mendenhall Glacier pluton. Tonalite.
gns	Gneiss of sedimentary origin. Migmatite.
mca	Metamorphosed calcareous rocks.
vch	Volcanics + intrusives: hornblende schist (pyroclastics), amphibolite.

Metasediment / migmatite foliation+lineation.

Igneous rock foliation.

Bedding; foliation parallel.

Normal fault ; oblique.

Shear sense.

Pre-full crystallization fabric+lineation.

Taku Inlet

(MAP 3)

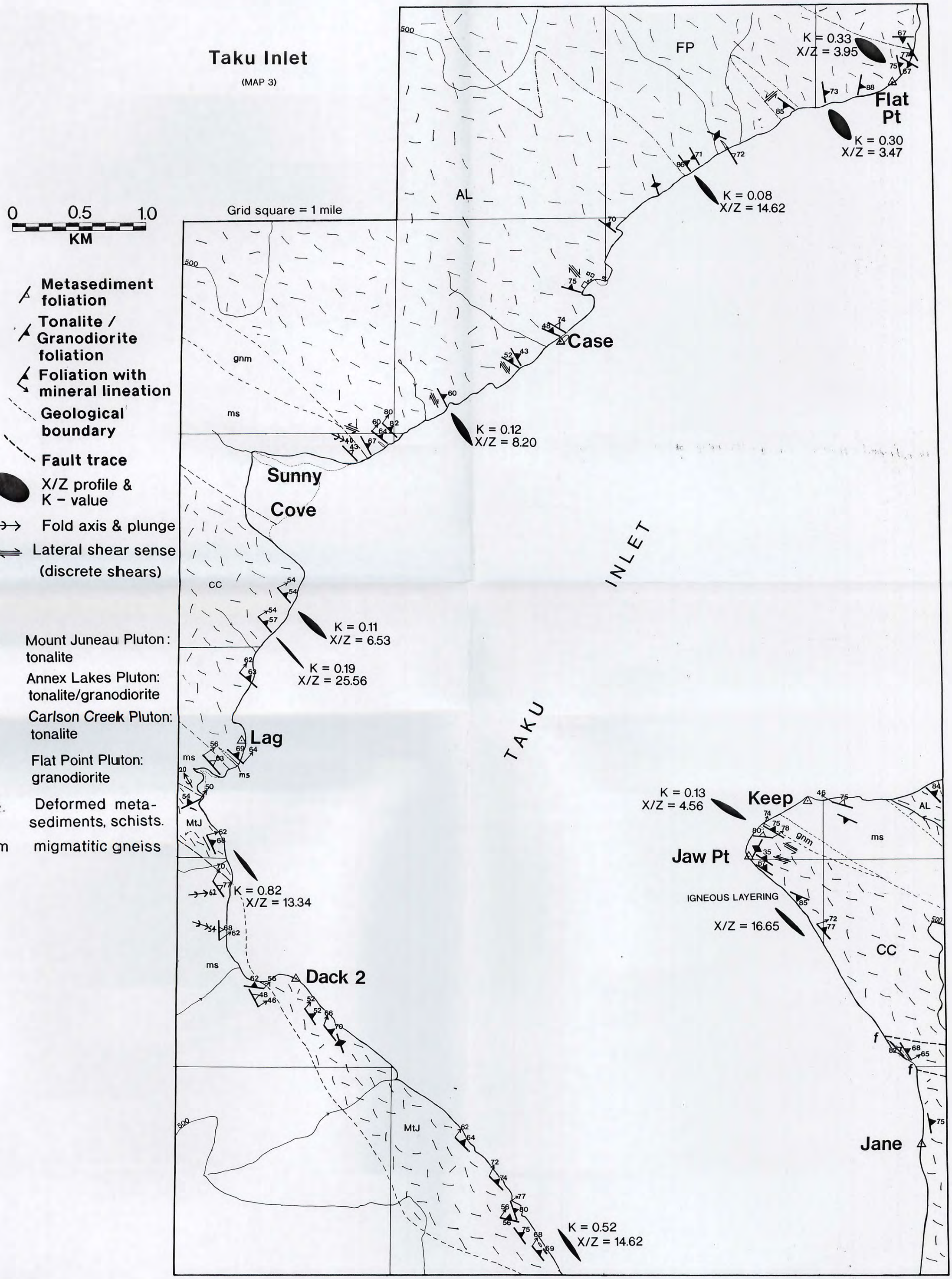

COOPER POINT/TAKU INLET

(MAP 2)

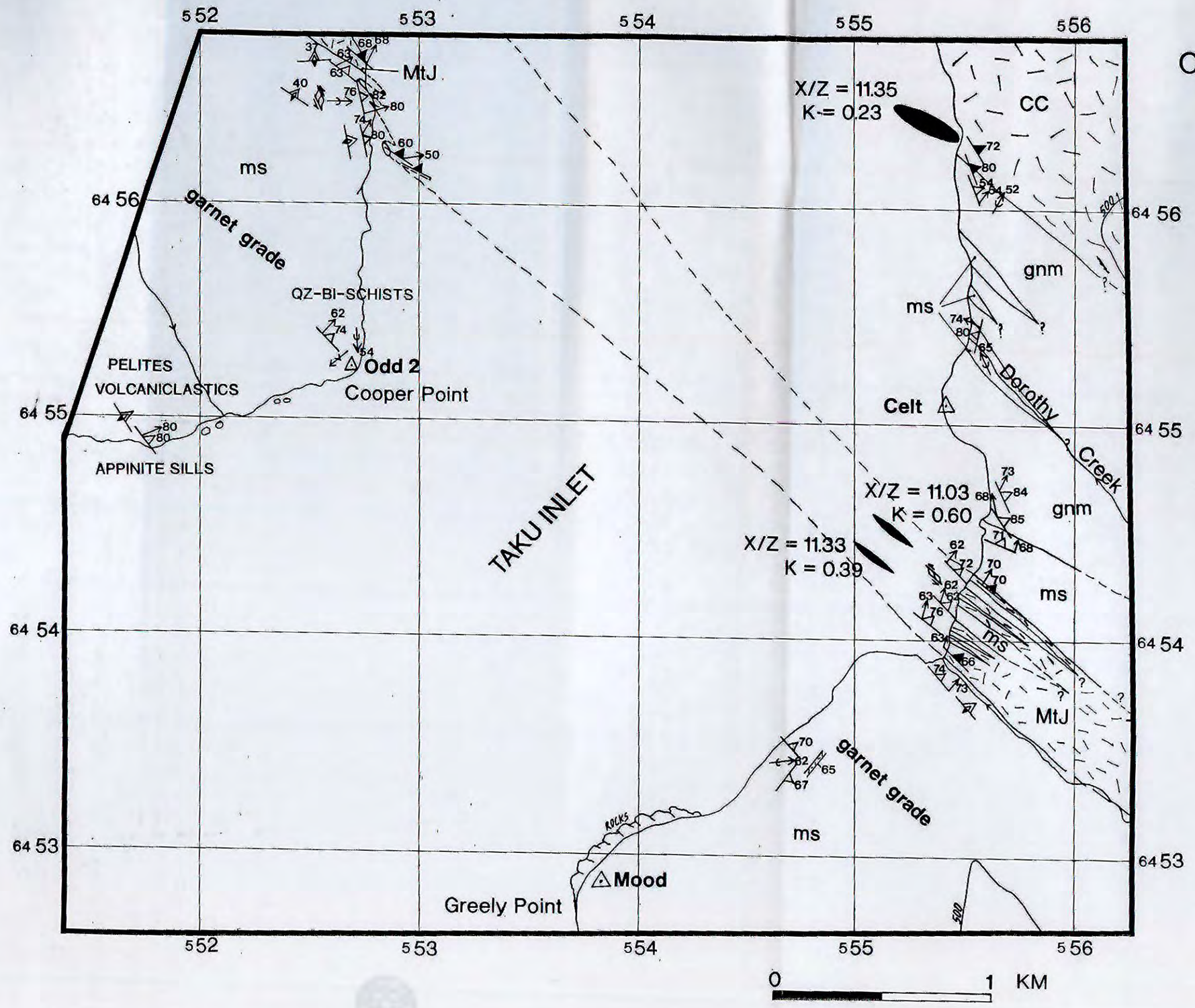

MtJ Mount Juneau pluton.

CC Carlson Creek pluton

gnm migmatitic gneiss.

ms Deformed metasediments. Pelitic schists and metavolcanics.

Metasediment/migmatite foliation and lineation.

Igneous rock foliation and lineation.

Pre-full crystallization fabric and lineation.

Fold axis.

Vergence.

Horizontal shear sense.

X/Z strain profile and k-value.

Thin granite sheet.

Geological boundary.

Inferred boundary.

Vertical shear sense. Double triangle points down dip. Small solid triangle indicates hanging-wall transport.

BISHOP POINT / TAKU INLET

(MAP 1)

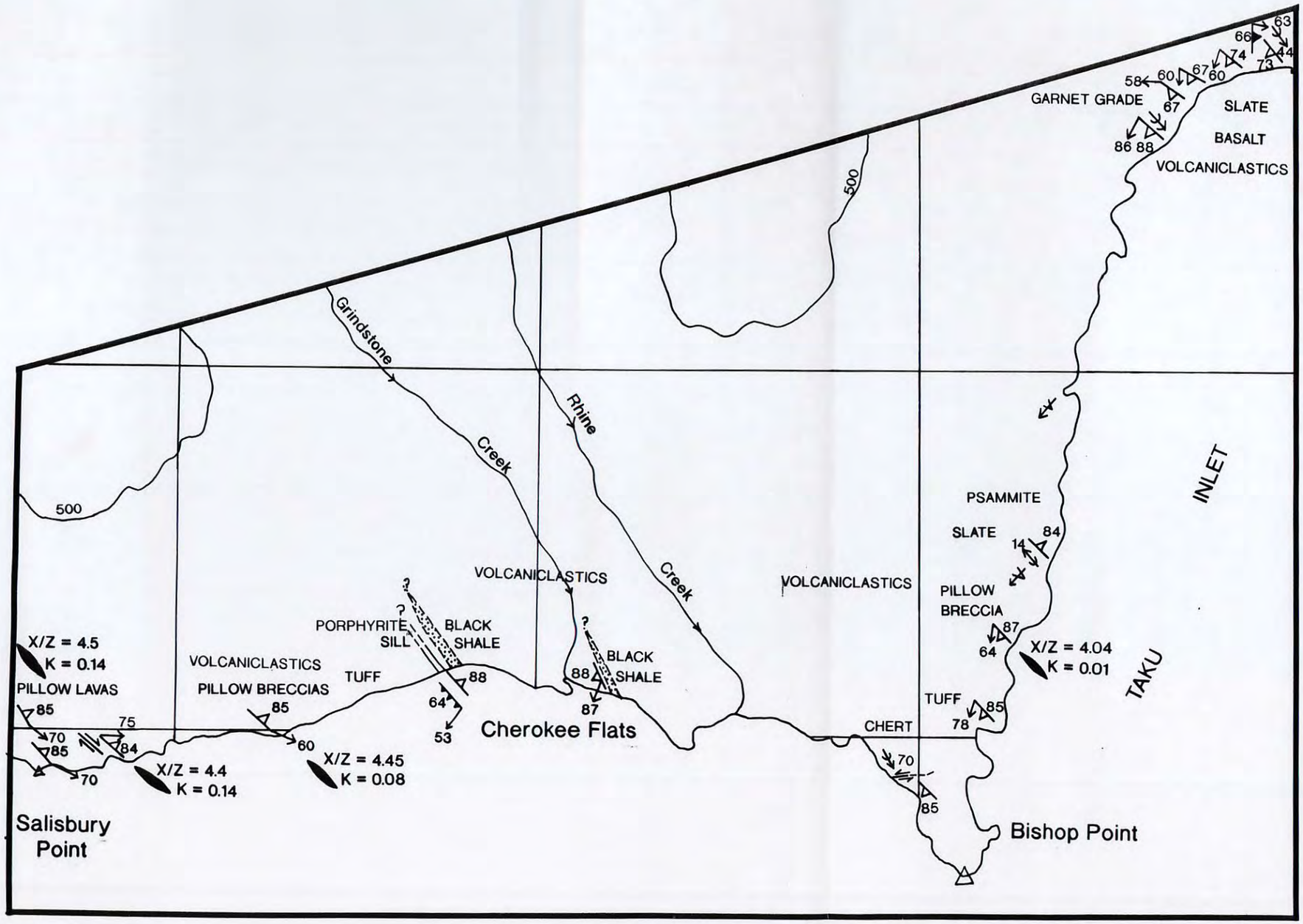

- metasediment/metavolcanic foliation & lineation
- Foliation and lineation in intrusives
- Lateral shear sense
- Fold axis & plunge
- Vergence direction
- Thrust plane & lineation
- X/Z profile & K – value

Altitude in metres

Grid square = 1 mile

TURNER LAKE / TAKU INLET

(MAP 4)

Foliation & lineation (intrusives)

Foliation & lineation (metasediments/metavolcanics)

Lateral shear sense

Strain profile & K – value

Lithological boundary/inferred

Grid square = 1 mile

Altitude in metres